

Climate driven shifts in benthic habitat composition as a potential demographic bottleneck for Western Rock Lobster

Understanding the role of recruitment habitats to better predict the under-size lobster population for fishery sustainability

**Stanley Mastrantonis¹, Tim Langlois^{*1}, Sharyn Hickey¹, Ben Radford²,
Claude Spencer¹ and Simon de Lestang³**

¹The University of Western Australia, ²Australian Institute of Marine Science,

³Department of Primary Industries and Regional Development,

^{*}Communicating author

May 2025



© 2025 Fisheries Research and Development Corporation.

All rights reserved.

**Climate driven shifts in benthic habitat composition as a potential demographic bottleneck for Western Rock Lobster
FRDC 2019-099**

Ownership of Intellectual property rights

Unless otherwise noted, copyright (and any other intellectual property rights, if any) in this publication is owned by the Fisheries Research and Development Corporation.

Unless otherwise noted, this publication should be attributed to **Mastrantonis, S., Langlois, T., Hickey, S., Radford, B., Spencer, C., de Lestang, S. The University of Western Australia, 2024. Climate driven shifts in benthic habitat composition as a potential demographic bottleneck for Western Rock Lobster. Perth, August. CC BY 3.0**

Creative Commons licence

All material in this publication is licensed under a Creative Commons Attribution 3.0 Australia Licence, save for content supplied by third parties, logos and the Commonwealth Coat of Arms.



Creative Commons Attribution 3.0 Australia Licence is a standard form licence agreement that allows you to copy, distribute, transmit and adapt this publication provided you attribute the work. A summary of the licence terms is available from

<https://creativecommons.org/licenses/by/3.0/au/>. The full licence terms are available from <https://creativecommons.org/licenses/by-sa/3.0/au/legalcode>.

Inquiries regarding the licence and any use of this document should be sent to: frdc@frdc.com.au

Disclaimer

The authors do not warrant that the information in this document is free from errors or omissions. The authors do not accept any form of liability, be it contractual, tortious, or otherwise, for the contents of this document or for any consequences arising from its use or any reliance placed upon it. The information, opinions and advice contained in this document may not relate, or be relevant, to a readers particular circumstances. Opinions expressed by the authors are the individual opinions expressed by those persons and are not necessarily those of the publisher, research provider or the FRDC.

The Fisheries Research and Development Corporation plans, invests in and manages fisheries research and development throughout Australia. It is a statutory authority within the portfolio of the federal Minister for Agriculture, Fisheries and Forestry, jointly funded by the Australian Government and the fishing industry.

Researcher Contact Details

Name: Tim Langlois
Address: 35 Stirling Highway
Crawley WA 6009
Phone: 0423 708 312
Email: tim.langlois@uwa.edu.au

FRDC Contact Details

Address: 25 Geils Court
Deakin ACT 2600
Phone: 02 6122 2100
Email: frdc@frdc.com.au
Web: www.frdc.com.au

In submitting this report, the researcher has agreed to FRDC publishing this material in its edited form.

Contents

Tables	vi
Figures	vii
Acknowledgments.....	xi
Executive Summary.....	xi
General Introduction	13
Objectives of the project.....	13
Studies	14
References	15
Study 1 - Benthic Observation Survey System (BOSS) to survey marine benthic habitats	16
Preface	16
Benthic Observation Survey System (BOSS) to survey marine benthic habitats.....	17
Abstract.....	19
Introduction.....	20
Design and methods	22
Conclusion	27
Acknowledgements	28
References	29
Supporting Information	31
Camera and photogrammetry.....	31
Metadata format and file organisation.....	33
Synchronisation diode.....	34
Effect of increasing number of fields of view on habitat observations and cost of data collection.....	36
References used in Supporting Information	37
Study 2 - A novel method for robust marine habitat mapping.....	39
Preface	39
A novel method for robust marine habitat mapping using a kernelised aquatic vegetation index	40
Abstract.....	41
Introduction.....	42
Methods	43
Results	48
Discussion.....	52
Conclusions	53
Author responsibilities	54
Declaration of Competing Interest.....	54
Acknowledgments	54
Data availability	54
References	54
Supplementary Material.....	59
Study 3 - Revealing the impact of spatial bias in survey design for habitat mapping.....	67
Preface	67
Revealing the impact of spatial bias in survey design for habitat mapping: a tale of two sampling designs.....	68

Abstract.....	69
Introduction.....	70
Methods	71
Study Sites.....	71
Survey designs.....	72
Results	75
Discussion.....	80
Conclusion	81
Acknowledgments	82
References	83
Study 4: Observations of the association by early-juvenile Western Rock Lobster with seagrass assemblages	88
Preface	88
Observations of the association by early-juvenile Western Rock Lobster <i>Panulirus cygnus</i> George, 1962 with seagrass assemblages (Decapoda: Achelata: Palinuridae).....	89
Abstract.....	90
Introduction.....	91
Methods	93
Collection and housing of early-juvenile lobsters	93
Collection and housing of seagrass assemblage	93
Mesocosm aquaria.....	94
Y-maze	97
Results	98
<i>Amphibolis</i> and <i>Posidonia</i> assemblages	98
Density of <i>Amphibolis</i> stems	99
Microhabitats within <i>Amphibolis</i>	102
Y-maze olfaction trials between <i>Amphibolis</i> assemblage components	103
Discussion.....	104
How microhabitat association varied with seagrass density	106
Y-maze	107
Acknowledgements	108
References	109
Supplementary materials	115
Study 5 - Disconnect between settlement and fishery recruitment driven by decadal changes in nearshore habitats	117
Preface	117
Disconnect between settlement and fishery recruitment driven by decadal changes in nearshore habitats	118
Abstract.....	119
Introduction.....	120
Methods and Materials	124
Study Location.....	124
Survey designs.....	126
Remote sensing imagery, climate and SAV classification.....	127
Puerulus Index.....	128
Undersize lobster catch rate index	128

Multiple regression and change analysis	128
Results	130
SST & Submerged Aquatic Vegetation	130
Puerulus Index & multiple regression analysis	132
Change analysis	136
Discussion.....	138
Conclusion	140
Acknowledgements	140
References	140
Supplementary material	145
Project Conclusions	147
The need for continuous monitoring of habitat.....	147
Recommendations	147
Further development and future studies	147
References	148
Project Communication	148
Workshops, research updates and assessment.....	148
Project media coverage	149
Watching coastal habitats for the impact of the Ningaloo Niño	149

Tables

Table 1. Validation statistics (kappa) for select feature sets and cross-validation methods. For the independent site cross-validation (Site-CV) Fold-1 through Fold-5 represents Two Rocks, Lancelin, Cervantes, Jurien Bay, and Freshwater, respectively. The overall best-performing model is indicated with an asterisk..... 49

Table 2. Estimated area of SAV in square kilometers for the kNDAVI and NDAVI models for each site. Numbers in brackets represent the predicted percentage of SAV at each site for the respective model.... 52

Table 3. Estimated area of SAV in square kilometers for each model and site. Numbers in brackets represent the predicted percentage of SAV at each site for the respective model..... 76

Table 4. Validation metrics of different models and designs..... 76

Table 5 Generalised linear mixed-effects model (GLMM) results for the probability of early-juvenile *Panulirus cygnus* associating with habitat types (*Amphibolis* assemblages, bare sand, or limestone crevices) in response to fixed factors (*Amphibolis* stem density and alternate habitats), random factor (mesocosm Tank) and their interactions. Significant terms ($P < 0.05$) are shown in bold. Coefficients express the difference between each factor level and the intercept. S.E, standard error; *, interaction between the factors..... 101

Table 6. Generalised linear mixed-effects model (GLMM) results for the probability of early-juvenile *Panulirus cygnus* found in either bare sand or limestone crevices in response to fixed factor (alternate habitats), random factor (mesocosm Tank) and their interactions. Significant terms ($P < 0.05$) are shown in bold. Coefficients express the difference between each factor level and the intercept. S.E., standard error. 102

Table 7. Results of paired t-test testing choices of early-juvenile *Panulirus cygnus* for a chemical stimulus using scents of fronds vs. rhizomes of *Amphibolis* (A), epifauna vs. epiphytes (B), and *Amphibolis* without epiphytes vs. with additional epiphytes (C). 104

Table 8 Global undersize Catch Model Comparison. Numbers outside the brackets represent the effect sizes, while bracketed numbers represent the error estimates. Significant effects are represented by star symbols. 135

Table 9 Undersize catch models at each location. Numbers outside the brackets represent the effect sizes, while bracketed numbers represent the error estimates. Significant effects are represented by star symbols. 135

Table 10 : Global undersize Catch Model Comparison. Numbers outside the brackets represent the effect sizes, while bracketed numbers represent the error estimates. Significant effects are represented by star symbols. 136

Figures

Figure 1 Sites across the mid-west coast of Western Australia where habitat and fishery populations parameters were monitored as part of this project. The red polygons represent surveyed and mapped regions, while the green points represent established post-larval (puerulus) settlement monitoring stations.	14
Figure 2 BOSS workflow for benthic composition ground truthing and production of predictive spatial models. a) Spatially balanced design with inclusion probability, b)	21
Figure 3 BOSS design. a) stereo configuration with camera pairs mounted on internal base bar cassette, showing camera housings (grey) and lights (black), b) specifications of the stereo camera separation and angle of convergence, c) overhead field of view showing the wide 270° field of view, and d) lighter weight mono configuration.....	23
Figure 4 BOSS equipment required for deployment. a) Stereo camera frame with an additional downward facing camera mounted in buoyancy compartment, b) rope and floats, c) synchronisation diodes, d) detachable ballast and gloves, e) lights and batteries, f) cameras, battery packs, SD cards and spare O-rings, g) field metadata sheet, whiteboard and marker, h) charging equipment and downloading footage, and i) tools including silicone grease.	24
Figure 5 Lighter weight mono-configuration wide-field drop camera system being deployed by hand (top) and stereo-configuration wide-field drop camera system deployed from a commercial fishing vessel fitted with a 'pot tipper' (bottom).....	25
Figure 6 Synchronised and composited imagery from four horizontal cameras.	26
Figure 7 Study sites (blue) span the midwest region of Western Australia. Bathymetry (m) data were sourced from Geoscience Australia's Bathymetry and Topography Grid (Whiteway, 2009). Contour lines represent 30m depth intervals.	44
Figure 8 Habitat summaries from the BOSS the underwater image annotations obtained within this study. The percent values represent annotations for each habitat in all images for the corresponding site.	45
Figure 9 The Sentinel-2 composite images of the five study sites. Panels A-E represent Two Rocks, Lancelin, Cervantes, Jurien and Freshwater, respectively. The sample ground truthing points of the underwater imagery and their corresponding habitat type have been overlaid on the composites for reference. Subplot labels (A-E) correspond to the sites depicted in Figure 7.	46
Figure 10 Box plots showing the response of the kNDAVI (panel A) and NDAVI (panel B) index for submerged aquatic vegetation (SAV; green) and non-vegetated (beige) ground truthing points for all sites combined and for each site individually. Due to the tangent function, kNDAVI ranges between 0 and 1 and shows clear distinction between habitat types, while NDAVI range between -1 and 0 and exhibits much less separability between habitat types.....	50
Figure 11 The probability of SAV presence for the five study sites with the kNDAVI and SDB model. Panels A-E represent Two Rocks, Lancelin, Cervantes, Jurien and Freshwater, respectively.	51
Figure 12 The classification of SAV for the five study sites with the kNDAVI and SDB model. Panels A-E represent Two Rocks, Lancelin, Cervantes, Jurien and Freshwater, respectively. The sample ground truthing points of the underwater imagery and their corresponding habitat type have been overlaid for reference.....	51

Figure 13 Study sites (blue) span the midwest region of Western Australia. Bathymetry (m) data were sourced from Geoscience Australia's Bathymetry and Topography Grid (Whiteway 2009). Contour lines represent 30m depth intervals. 72

Figure 14 Habitat summaries of the preferential (Panel A) and balanced (Panel B) underwater image annotations for all study sites. The percent values represent annotations for each habitat in all images for the corresponding site. 74

Figure 15 Sentinel-2 composite image, habitat probability estimates and habitat classification using the preferential survey design data and the kNDAVI remotely sensed index. The point data represents the ground control sample points where green is 'SAV' and tan is 'Other' benthic habitat. Panel A represents the model outcomes for the Freshwater site. Panel B represents the model outcomes for the Jurien site. Panel C represents the model outcomes for the Lancelin site. Panel D represents the model outcomes for the Two Rocks site. 78

Figure 16 Sentinel-2 composite image, habitat probability estimates and habitat classification using the spatially balanced survey design data and the kNDAVI remotely sensed index. The point data represents the ground control sample points where green is 'SAV' and tan is 'Other' benthic habitat. Panel A represents the model outcomes for the Freshwater site. Panel B represents the model outcomes for the Jurien site. Panel C represents the model outcomes for the Lancelin site. Panel D represents the model outcomes for the Two Rocks site. 79

Figure 17 Summary visualisation of model outcomes. Each model with the type of sampling design and predictor variable is shown on the left y-axis, while sites are depicted on the top x-axis. The colour hue of each circle represents the kappa statistic for each model, while the size of the circle represents the percent of SAV in each site area predicted by each model. 80

Figure 18 Experimental setup of mesocosm aquaria with *Amphibolis antarctica* and *Posidonia australis* assemblages (A), *Amphibolis* and bare sand (B), and *Amphibolis* and limestone crevices (C) as stimuli to test habitat associations of early-juvenile *Panulirus cygnus*. Setups B and C were conducted under changing *Amphibolis* stem densities. Habitat choices for *Amphibolis* were defined as within the patch (dark green) and associated with patch habitat (light green). Habitat choices for bare sand or limestone crevices were defined when early-juveniles were not found within patches of *Amphibolis* assemblages. Photo of mesocosm setup with *Amphibolis* and limestone crevices (D). 95

Figure 19 Experimental setup of the Y-maze seen from top (A) and side (B) views, with modified design adapted from Kenning et al. (2015). All walls of the Y-maze were made of PVC except a mesh screen (red line) providing a rough filter for the outflow. Yellow bars indicate perforated PVC sheets to allow water to flow through. 97

Figure 20 Mean number of early-juvenile *Panulirus cygnus* found in *Amphibolis* and *Posidonia* assemblages, or having no association with either seagrass assemblages, after 24 h in mesocosm trials (N = 6). Dots represent data points. Each box represents the interquartile range (IQR) and length of whiskers is restricted to maximum of 1.5 times of IQR. Dots outside of whiskers interval are outliers. Bold line in each box and the red star represents the median and mean, respectively. 99

Figure 21 Mean number of early-juvenile *Panulirus cygnus* found in bare sand or *Amphibolis* assemblages (A), limestone crevices or *Amphibolis* assemblages (B), or having no association with habitat types, across four experimental densities of *Amphibolis* in mesocosm trials (N = 6 each treatment) (BS, bare sand; A, *Amphibolis* assemblages; C, limestone crevices; NA, no association). Dots represent data points. Each box represents the interquartile range (IQR) and length of whiskers is restricted to maximum of 1.5 times of IQR. Dots outside of whiskers interval are outliers. Bold line in each box and the red star represents the median and mean respectively. 100

Figure 22 Mean number of early-juvenile *Panulirus cygnus* found in four *Amphibolis* microhabitats across four experimental densities of *Amphibolis* stems in mesocosm trials (F, fronds; St, stems; D, debris; S, *Amphibolis*-associated sand; B, bare sand; NA, no association). Dotted line represents the habitat choices between bare sand (left of line) and the *Amphibolis* assemblage (right). Dots represent data points. Each box represents the interquartile range (IQR) and length of whiskers is restricted to maximum of 1.5 times of IQR. Dots outside of whiskers interval are outliers. Bold line in each box and the red star represents the median and mean respectively. 103

Figure 23 Choices for early-juvenile *Panulirus cygnus* for a chemical stimulus, as defined by total time spent at the end of a chosen Y-maze when presented with scents of habitat assemblages of *Amphibolis* fronds and rhizomes (A), common prey item epifauna and epiphytes (B), *Amphibolis* without and with additional epiphytes (C). Each box represents the interquartile range (IQR) and length of whiskers is restricted to maximum of 1.5 times of IQR. Black dots outside of whiskers interval are outliers. Bold line in each box and the red cross represents the median and mean respectively. 104

Figure 24 Sea Surface Temperature anomalies (SSTa) for Port Gregory, Freshwater, Jurien, Lancelin, and Mandurah sites from 1987 to 2023. The orange region represents the 2010-/11 Marine Heatwave (MHW). Sea Surface Temperature Anomalies were sourced from NOAA OISST..... 122

Figure 25 The puerulus Index (PI; blue) and the undersize catch rate with a four-year lag (orange) for Port Gregory, Freshwater, Jurien, Lancelin, and Mandurah from 1968 to 2023. The orange region represents the 2010/11 Marine Heatwave (MHW). 123

Figure 26 Study locations span the midwest region of Western Australia. Study locations have been shown with 0-5m regions, 5-15m, and 15-30m extents. Bathymetry (m) data were sourced from Geoscience Australia's Bathymetry and Topography Grid (Whiteway, 2009). Contour lines represent 30m depth intervals. 125

Figure 27 Habitat summaries of the underwater image annotations for each of the study locations. The percent values represent annotations for each habitat in all images for the corresponding location, with the total number of sample points depicted on the x-axis. The stacked bar of 'All locations' represents the average composition of all locations. 127

Figure 28 Percent Submerged Aquatic Vegetation (%SAV) for Port Gregory, Freshwater, Jurien, Lancelin, and Mandurah from 1987 to 2023. The %SAV has been depicted for the 15-30m extent (Blue), and for the depth intervals of 5-15 m (orange) and 0-5 m (Green). The pale orange region represents the 2010-2011 Marine Heatwave (MHW), and the grey bars represent years where remote sensing imagery was unavailable..... 131

Figure 29 The %SAV five years before and after the 2010-2011 MHW event for Mandurah, Lancelin, Jurien and Freshwater in 0-5 m of water. Port Gregory was not included due to a lack of data, and Mandurah represents the 15-30m depth range as there were few regions at the site shallower than 5m..... 132

Figure 30 Relative residuals (i.e., the observed undersize catch subtracted from predicted undersize catch and divided by the maximum of the observed catch) between Puerulus-only model predictions and observed undersize WRL catch rates for Port Gregory, Freshwater, Jurien, Lancelin, and Mandurah from 1987 to 2023. The orange region represents the 2010-2011 Marine Heatwave (MHW). 133

Figure 31 The response of undersize Western Rock Lobster (WRL) catch rates to the percent Submerged Aquatic Vegetation (SAV) with a two-year lag (t-2) at each of the locations. These relationships are representative of the SAV at the 0-15 m depth intervals. Residual points are coloured by the distance to the regression line, where blue is close to the line of best fit and red is far. 134

Figure 32 Change Vector Analysis (CVA) results for historical Landsat imagery (1987-2022) for the five regions that have experienced a high magnitude of change for the study period are represented in yellow, while blue represents regions that have remained stable for the study period..... 137

Figure 33 Local Indicators of Spatial Autocorrelation (LISA) results for historical Landsat imagery (1987-2022) for the five locations..... 138

Acknowledgments

The authors acknowledge the Traditional Custodians of the country throughout Australia and their connections to the land, sea and community. We pay our respects to their Elders past and present and extend that respect to all Aboriginal and Torres Strait Islander peoples. This research was supported by the Fisheries Research and Development Corporation (FRDC Project Number 2019-099) on behalf of the Australian Government. The research is part of the ICoAST collaborative project and acknowledges support from the Indian Ocean Marine Institute Research Centre collaborative research fund and partner organisations AIMS, CSIRO, DPIRD and UWA.

Executive Summary

The West Coast Rock Lobster Managed Fishery (WCRLMF) is one of the most valuable and sustainable single-species fisheries in Australia. WCRLMF is managed, in part, using larval (puerulus) settlement indices obtained from artificial seagrass stations that are continuously monitored at eight locations throughout the shallow coastal habitats of the Western Bioregion of Western Australia. The settlement indices correlate to subsequent catch rates of the Western Rock Lobster (WRL) and are used to predict catch into the WCRLMF in typically 3-4 years times. Recently, the relationship of the settlement indices to catch have become less evident in some parts of the fishery, particularly after the marine heatwave that occurred in Western Australia in 2011. Since the heatwave reportedly impacted habitats, these ocean climate mitigated changes WRL recruitment habitats, such as seagrasses and macroalgae, are hypothesised to be the source of increased unexplained variation in the WRL population, but causal links remain unclear.

Modelling and tracking the changes in coastal habitat in space and time has become an important aspect of managing our environments more generally. This project set out to investigate if including measures of recruitment habitat into the WCRLMF stock assessment will improve management of the fishery.

The overall objective of the project was to evaluate the implications of habitat change for the WCRLMF by determining the relative importance of habitat in the survivorship and growth of early juvenile WRL. This information could then be used to assess how accurately existing settlement metrics may relate to recruitment to the fishery, when habitat change is also occurring. Four linked objectives were originally proposed within this project:

1. Synthesise evidence of habitat change: use novel and historical habitat imagery and other remote sensing datasets to determine the spatial extent of habitat loss and recovery, either attributed to 2011/2012 marine heat wave or changes in coastal processes.
2. Investigate fine-scale correlations in anomalies between predicted and observed undersize catch rate index and areas of habitat loss and recovery, either attributed to 2011/2012 marine heat waves or changes in coastal Processes.
3. Evaluate evidence of essential benthic habitat for juvenile lobster, by measuring how habitat quality (cover and composition) influences lobster survival.
4. Create a spatial index of essential habitats to inform the interpretation of existing settlement and recruitment metrics.

These objectives were achieved, and results have been published or are currently under review at Q1 journals. To achieve these objectives, we strategically built complementary parts of the project until the key objectives could be addressed.

Initially we developed a novel method to robustly ground truth remotely sensed imagery, across the WCRLMF (objective 4). Ground truthing was achieved using a newly designed drop camera system, optimised to be rapidly deployed and retrieved from commercial lobster fishing boats. The wide panoramic field of view of this camera system, for the first time in a marine sampling context, provided ground truthing imagery at a comparable scale to the resolution of remotely sensed imagery.

Next, we developed a novel spatial index to map and monitor recruitment habitat from space, with robust ground truthing, across the WCRLMF (objective 4). This remotely sensed vegetation index provides a significant advancement for mapping and monitoring submerged aquatic vegetation (i.e., seagrasses and macroalgae) at regional scales, and these methods are applicable globally. This vegetation index is created by extracting the maximum amount of spectral information from satellite products while also calibrating measurements in space and time. In addition to this approach and to inform future survey designs, we also published a complimentary study that demonstrate how bias is created in habitat mapping when samples are taken from preferential designs as opposed to spatially balanced designs. We found models using preferential designs can overestimate submerged vegetation extent by 25% resulting in low model accuracy. Prior to this work all previous publications on sampling design have been theoretical and relied on simulated data for inference. We have demonstrated sampling design theory explicitly using two different datasets across the WCRLMF.

These three publications provide practical methods and best practices for monitoring important fishery habitat from space.

To understand the importance of recruitment habitat for the WRL (objective 3), we built on previous aquarium experiments, that demonstrated a chemosensory preference for seagrass assemblages by early juvenile WRL, by determining the influence of seagrass density and physical complexity. In a published study we demonstrated that both density and physical complexity increase the likelihood of early juvenile WRL associating with seagrass assemblages, and in particular with wireweed species (i.e. *Amphibolis* spp). These findings and of WRL recruitment habitats were critical to fundamentally understand the relationships between habitat and WRL population dynamics at a much broader scale.

To achieve the stated objectives (1) and (2), we integrated the remote sensing index and the findings from the aquarium experiments to interpret modern and historical observations across the fishery, in a final publication. We successfully reconstructed time-series change in habitat extents for five key sites across the WCRLMF from 1987 to 2024. We used this habitat time series with ocean climate data, including sea surface temperature anomalies and Degree Heating Weeks, to investigate the relationship between variation in indexes of WRL settlement and recruitment, and both habitat and climate change. Sites with complete data for remote sensing imagery and recruitment data, in the form of juvenile catch rate, demonstrated that habitat in previous years can significantly and positively affected juvenile catch, and likely recruitment into the fishery, in subsequent years. Moreover, including habitat measures into the predictive model improved model fits.

This project has demonstrated the importance of including habitat extent into fishery prediction models, the importance of spatially balanced sampling designs for habitat mapping and further informed our understanding the likely preferential recruitment habitats of the WRL.

Keywords

Western Rock Lobster, fisheries ecology, catch rate, remote sensing, sampling design, puerulus settlement.

General Introduction

Despite robust and sustainable management of the West Coast Rock Lobster Managed Fishery (WCRLMF) and, since 2009, relatively consistent larval settlement of Western Rock Lobster (WRL, Kolbusz et al. 2022) previously observed correlations between the puerulus index and undersize catch rates in the fishery (de Lestang et al. 2015) have become more uncertain since the marine heat wave of 2010/11. Habitat change and climate anomalies may explain the variation in WRL larval settlement and catch rates. However, mapping marine habitats, particularly through time, is complex, even with contemporary satellite platforms. Moreover, remote sensing of marine habitats requires representative ground truth data to calibrate and validate mapping models (Mastrantonis et al., 2024). Assessing the effects of habitat change and climate requires novel remote sensing techniques that can be applied to historical imagery catalogues, such as Landsat, to accurately track changes in WRL habitat extents and climate anomalies into the past. By reconstructing multi-decadal habitat extents and temperature anomalies for the WCRLMF, we can understand potential drivers and interactions of larval settlement and juvenile catch rates.

Objectives of the project

The objectives of this project were to:

1. Synthesise evidence of habitat change: use novel and historical habitat imagery and other remote sensing datasets to determine the spatial extent of habitat loss and recovery, either attributed to 2011/2012 marine heat wave or changes in coastal processes.
2. Investigate fine-scale correlations in anomalies between predicted and observed undersize catch rate index and areas of habitat loss and recovery, either attributed to 2011/2012 marine heat waves or changes in coastal Processes.
3. Evaluate evidence of essential benthic habitat for juvenile lobster, by measuring how habitat quality (cover and composition) influences lobster survival.
4. Create a spatial index of essential habitats to inform the interpretation of existing settlement and recruitment metrics.

This project set out to meet these objectives with a collaborative process informed by the results of prior studies and expert fisher knowledge and expertise from The University of Western Australia (UWA), the Australian Institute of Marine Science (AIMS) and Department of Primary Industries and Regional Development (DPIRD). This approach generated a series of complementary studies which are detailed below.

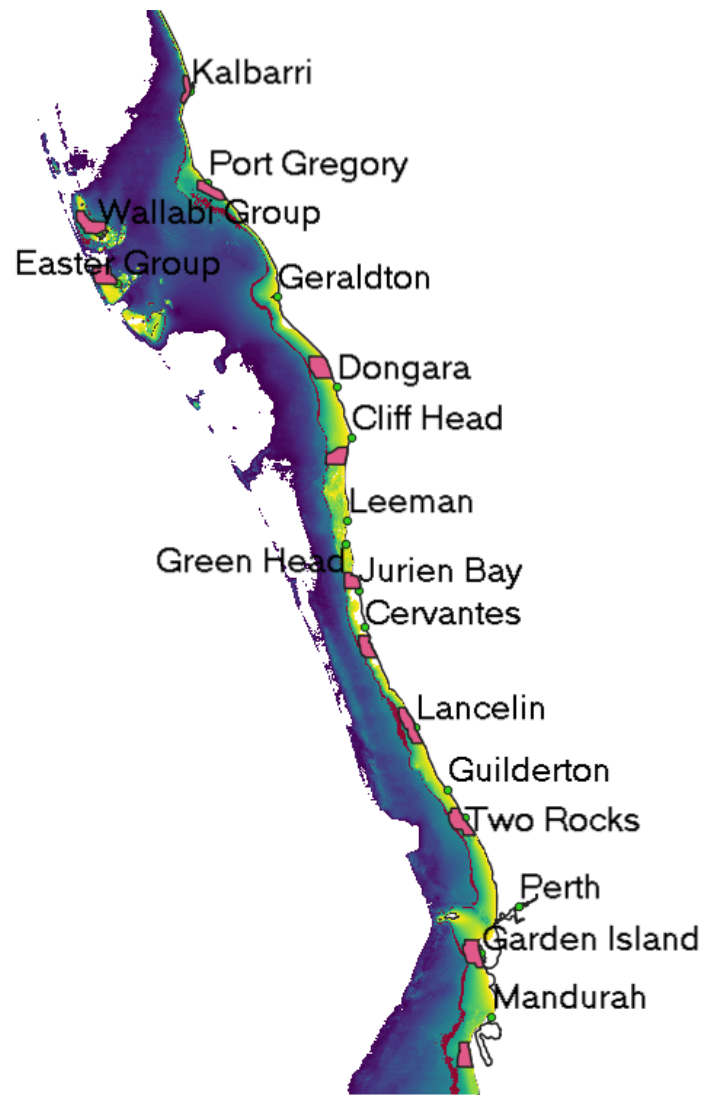


Figure 1 Sites across the mid-west coast of Western Australia where habitat and fishery populations parameters were monitored as part of this project. The red polygons represent surveyed and mapped regions, while the green points represent established post-larval (puerulus) settlement monitoring stations.

Studies

A combination of complementary studies was used to address the project objectives, building upon one another until the key objectives could be addressed. Study 1 presents a new underwater camera system for sampling and ground truthing benthic environments (Objective 4).

5. [Study 1](#) - Benthic Observation Survey System (BOSS) to survey marine benthic habitats.

Study 2 presents a novel vegetation index for mapping submerged aquatic vegetation and Study 3 presents the contrasting results of habitat mapping using two different sampling designs (Objective 4).

6. [Study 2](#) - A novel method for robust marine habitat mapping using a kernelised aquatic vegetation index.
7. Study 3 - Revealing the impact of spatial bias in survey design for habitat mapping: a tale of two sampling designs.

Study 4 presents the results of aquaria experiment on preferential habitat for the WRL (Objective 3)

8. [Study 4](#) - Observations of the association by early-juvenile Western Rock Lobster *Panulirus cygnus* with seagrass assemblages (Decapoda: Achelata: Palinuridae)

Study 5 reconstructs time-series of habitat extents for the WCRLMF, and we use this multi-decadal data to determine the importance of habitat on the recruitment of the WRL (Objective 1 and 2)

9. [Study 5](#) - Reconstruction of decadal changes in essential recruitment habitats across a fishery.

For each study, it is indicated where these studies are published or in preparation for submission for publication. A conclusion section then provides a summary of lessons learned and future recommendations for future informing our understanding of the fisheries ecology of the Western Rock Lobster.

References

Lestang, Simon de, Nick Caputi, Ming Feng, Ainslie Denham, James Penn, Dirk Slawinski, Alan Pearce, and Jason How. 2015. "What Caused Seven Consecutive Years of Low Puerulus Settlement in the Western Rock Lobster Fishery of Western Australia?" *ICES Journal of Marine Science: Journal Du Conseil* 72 (suppl_1): i49–58.

Kolbusz, Jessica, Tim Langlois, Charitha Pattiaratchi, and Simon de Lestang. 2022. "Using an Oceanographic Model to Investigate the Mystery of the Missing Puerulus." *Biogeosciences* 19 (2): 517–39.

Mastrantonis, Stanley, Ben Radford, Tim Langlois, Claude Spencer, Simon de Lestang, and Sharyn Hickey. 2024. "A Novel Method for Robust Marine Habitat Mapping Using a Kernelised Aquatic Vegetation Index." *ISPRS Journal of Photogrammetry and Remote Sensing: Official Publication of the International Society for Photogrammetry and Remote Sensing* 209 (March):472–80.

Study 1 - Benthic Observation Survey System (BOSS) to survey marine benthic habitats

Preface

This study presents a standard operating procedure for the Benthic Observation Survey System (BOSS). The BOSS provides an efficient and robust method for observing seabed habitats, designed to be deployed and retrieved in a similar way to lobster pots. We propose demonstrate how this is useful for calibrating habitat and remote sensing models. The BOSS was critical in generating the remotely sensed habitat index developed in [Study 2](#), testing the outcomes of sampling plans in [Study 3](#), and developing the long-term habitat time series we related to fisheries management presented in [Study 5](#).

Benthic Observation Survey System (BOSS) to survey marine benthic habitats

Published in: *Methods in Ecology and Evolution*

<https://doi.org/10.1111/2041-210X.70010>

Authors and affiliations

Tim Langlois^{1,2}, Claude Spencer^{1,2}, Brooke A Gibbons^{1,2}, Kingsley J Griffin^{1,2}, Kye Adams³, Charlotte Aston^{1,2}, Neville Barrett⁴, Ashlee Bastiaansen⁴, Donna Beach⁵, Ant Bernard⁶, Todd Bond^{1,2,7}, Genevieve R Carey⁵, Jenn Caselle⁸, Katie Cieri⁹, Gabrielle Cummins^{1,2}, Katherine Cure¹⁰, Simon de Lestang¹¹, John Fitzhardinge¹², Anita Giraldo-Ospina^{1,8}, Gretchen Grammer¹³, David R Guilfoyle⁵, Christopher Henderson¹⁴, Sharyn Hickey^{2,15}, Jamie Hicks¹⁶, Renae Hovey^{1,2}, Charlie Huveneers¹⁷, Daniel Ierodiaconou¹⁸, John Keesing^{2,19,20}, Nathan Knott²¹, Jennifer L Lavers⁵, Steve Lindfield²², James Lindholm⁹, Stanley Mastrantonis^{1,15}, Kinsey Matthews⁹, Matthew L Navarro^{1,2}, Julian Partridge², Dominique Pellieter²³, Camilla Piggott²⁴, Rachel Przeslawski²¹, Ben Radford^{2,10,15}, Matt Rees²¹, Ron Reynolds⁵, Fernanda A Rolim²⁵, Adam Smith²⁶, Felix Spencer¹², Rick Starr⁹, Samuel Thompson^{1,2,20}, Iszaac Webb²⁷, Wayne Webb²⁷, Sasha Whitmarsh¹⁸, Joel Williams⁴, Jacquomo Monk⁴

1 School of Biological Sciences, The University of Western Australia, Crawley, WA 6009, Australia

2 UWA Oceans Institute, The University of Western Australia, Crawley, WA 6009, Australia

3 Department of Biodiversity, Conservation and Attractions, Kensington, WA 6151, Australia

4 University of Tasmania, Hobart, TAS, 7005, Australia

5 Esperance Tjaltjraak Native Title Aboriginal Corporation, 11A Shelden Road, Esperance, WA 6450, Australia

6 South African Institute for Aquatic Biodiversity, Grahamstown, 6140, South Africa

7 Minderoo-UWA Deep-Sea Research Centre, The University of Western Australia, Crawley, WA 6009, Australia

8 University of California Santa Barbara, Santa Barbara, CA 93106, United States

9 MOSS Landing Marine Laboratories, CA 95039, United States

10 Australian Institute of Marine Science, Crawley, WA 6009, Australia

11 Department of Primary Industries and Regional Development, Hillarys, WA 6025, Australia

12 Southerly Designs, Port Denison, WA 6525, Australia

13 South Australian Research and Development Institute (SARDI, Aquatic Sciences), West Beach, SA 5024, Australia

14 School of Science, Technology and Engineering, University of the Sunshine Coast, Sippy Downs, QLD

15 School of Agriculture Geography and Environmental Sciences, The University of Western Australia, Crawley, WA 6009, Australia

16 Department for Environment and Water, Marine Science, 81-95 Waymouth Street, Adelaide, SA, 5000, Australia

17 College of Science and Engineering, Flinders University, Adelaide, SA, 5042, Australia

18 School of Life and Environmental Science, Deakin University, Warrnambool, Victoria

19 CSIRO Environment, Indian Ocean Marine Research Centre, Fairway, Crawley, WA, 6009, Australia

20 School of Molecular and Life Sciences, Curtin University, Hayman Road, Bentley, WA, 6102, Australia

- 21 NSW Department of Primary Industries, Fisheries Research, 4 Woollamia Rd, Huskisson
2540 NSW
- 22 University of Technology Sydney, Ultimo, NSW 2007, Australia
- 23 UMR DECOD, French Institute for the Exploitation of the Sea (Ifremer), Lorient, France
- 24 Environment Agency, Sir John Moore House, Bodmin, Cornwall, PL31 1EB, United
Kingdom.
- 25 Laboratorio de Ecologia e Conservacao Marinha, Universidade Federal de Sao Paulo
(UNIFESP), Santos, SP, 11070-102, Brazil
- 26 School of Mathematical and Computational Sciences, Massey University, Auckland
0745, New Zealand
- 27 Undalup Association Incorporated, PO Box 985, Margaret River, WA 6285, Australia



Sebastian Gundling and John Fitzhardinge of Dongara Marine prototyping the Benthic Observation Survey System (BOSS). Photograph by Tim Langlois.

Abstract

Most platforms for collecting images to characterise marine benthic habitats involve a downward-facing field of view that is relatively constrained ($\sim 70^\circ$), covering only a small area of benthos ($\sim 1 \text{ m}^2$). Here we propose the use of a four-camera platform having a wide combined field of view ($\sim 270^\circ$), covering a much greater area (up to 100 m^2). We also present a stereo-camera configuration which has the added benefit of being able to accurately measure sample area and dimensions of benthic biota. The design proposed is robust and self-righting, facilitating rapid deployment and retrieval from a range of vessels, depths, and environments. We present an exemplar workflow to generate a habitat map ($\sim 100 \text{ km}^2$) within a no-take National Park Zone within the South-west Corner Marine Park, Australia and demonstrate the benefit of increasing the field of view to estimate habitat heterogeneity. The relatively broad sample unit of this wide-field drop camera is well suited to estimating coverage (e.g. of a seagrass bed) and habitat mapping. It is time-efficient in the field enabling spatially balanced sampling designs to acquire ground-truthing data for medium- to large-scale habitat mapping projects. This platform is a practical tool to track changes in marine environments and undertake environmental impact assessments, in particular for offshore energy or fisheries that may alter the seabed.

Introduction

Marine benthic images are commonly used to quantify habitat composition, ground-truth remote data and predict the extent of habitat types (Pelletier et al., 2020). Such imagery is now widely used to calibrate spatial analyses such as distribution models and change-over-time mapping (Mastrantonis et al., 2024). Benthic images captured by platforms such as divers, drop cameras, towed-video, Remotely Operated Video (ROV), and Autonomous Underwater Video (AUV) are generally acquired from downward-facing cameras, with a field of view that is relatively constrained ($\sim 70^\circ \times \sim 40^\circ$) and covers a small area per sample unit ($\sim 1 \text{ m}^2$, Bennett et al., 2016; Sheehan et al., 2016). Horizontal-facing images, using the same field of view, have a larger area ($\sim 25 \text{ m}^2$) and are useful in a variety of situations and ecosystems (Bennett et al., 2016). Downward-facing images generally provide higher taxonomic resolution for sessile assemblages and sub-canopy species than horizontal-facing images, and improved estimates of mobile invertebrate numbers (Perkins et al., 2020). However, the larger area per sample unit of horizontal-facing images better aligns with resolutions of remote sensing products such as bathymetric LiDAR (Light Detection and Ranging; $\sim 25 \text{ m}^2$) and optical remote sensing platforms ($\sim 100 \text{ m}^2$). Obtaining ground truthing data at a commensurate scale to remotely sensed products is an important consideration when modelling extent or assemblage composition (Mastrantonis et al. in review). Horizontal-facing imagery is also more effective for monitoring the cover of erect habitats including canopy algae and corals (Bennett et al., 2016; Vergés et al., 2016), particularly if stereo images are captured allowing the dimensions of biota to be measured (Langlois et al., 2021). Stereo images further allow the sample unit to be standardised across varying visibility (Broad et al. 2023; McLean et al. 2016). The structural dimensions (i.e. height) of benthic biota can be an indicator of anthropogenic and environmental impacts, with imagery from Baited Remote Underwater stereo-Video (stereo-BRUV) surveys being successfully used to measure the recovery of soft-coral height after the cessation of trawling across an area of continental shelf (Langlois et al., 2021), and the impacts of marine heat waves on macroalgal canopy height (Vergés et al., 2016).

Spatially-balanced survey designs can increase sampling efficiency by evenly spreading samples in space and across the range of covariates of interest (e.g., depth and relief) (Robertson et al., 2013). Typical platforms for collecting benthic images (i.e. divers, towed-video, ROV, and AUV) have logistical constraints that result in them generally being deployed along transects, or in discrete patches or mosaics (Sheehan et al., 2016). By contrast, drop cameras provide point-samples, providing a more spatially independent method of gathering benthic data (Robertson et al., 2013). Where rapid repeated deployments are possible, drop cameras are suited to ground-truthing relatively large spatial areas (Pelletier et al., 2020) and sites requiring validation can be chosen based on covariates of interest (Mastrantonis et al., 2024). Transect-based sampling can also be used in a spatially balanced manner, but care must be taken to account for spatial dependence within transects and clusters of transects (Foster et al., 2020). Regardless, transect-based and locally-dense sampling can introduce clusters of samples within similar environmental settings, or spatial bias, that can weaken subsequent statistical analyses (Robertson et al., 2013). While drop cameras have clear logistical and efficiency advantages for sampling larger areas, due mainly to the brevity of their deployments and relative ease of obtaining independent observation units, deeper water environments ($>200 \text{ m}$) increase time for deployment and create logistical challenges. Below these depths, multi-platform swarms, either of AUVs and ROVs conducting transects, are likely to be more cost-effective (Liu et al., 2023).

We have developed a remote wide-field drop camera system, called the Benthic Observation Survey System (BOSS), with a combined field of view of approximately 270° (Figs 2-3), amenable to stereo- or mono-camera configurations (Fig. 4). The design originated from an integrated fibre-optic camera system developed by Rick Starr at Moss Landing Laboratories for

sampling demersal fish assemblages, that developed from rotating stereo-video landers (Starr et al., 2016). The system was adapted to be able to be rapidly deployed and retrieved from a variety of vessels into water depths of 2 to 200 m and is self-righting on the seabed (Figs 2-4), with a single deployment in 30 m of water taking just 8 minutes with a 5-minute bottom time. This tool is suited to the collection of widespread georeferenced point samples, enabling the cost-effective sampling of broad areas using spatially-balanced sampling designs, to produce benthic habitat coverage predictions (Fig. 2) or inform other environmental assessments (i.e. benthic biota dimensions). We demonstrate this method through a project led by Traditional Owners of the south-west of Australia to characterise the habitats associated with ancient submerged coastline features across the continental shelf, to inform further detailed analysis (Langlois et al. in review). We provide a standard operating protocol (SOP) for the BOSS with information on system design, field operation, image annotation, data validation, and examples of a workflow to generate a habitat map product (Fig. 2). We highlight the benefits of using multiple horizontal fields of view to characterise benthic habitat heterogeneity but also suggest that future studies should investigate the potential of collecting demersal fish assemblage information comparable to Starr et al. (2016).

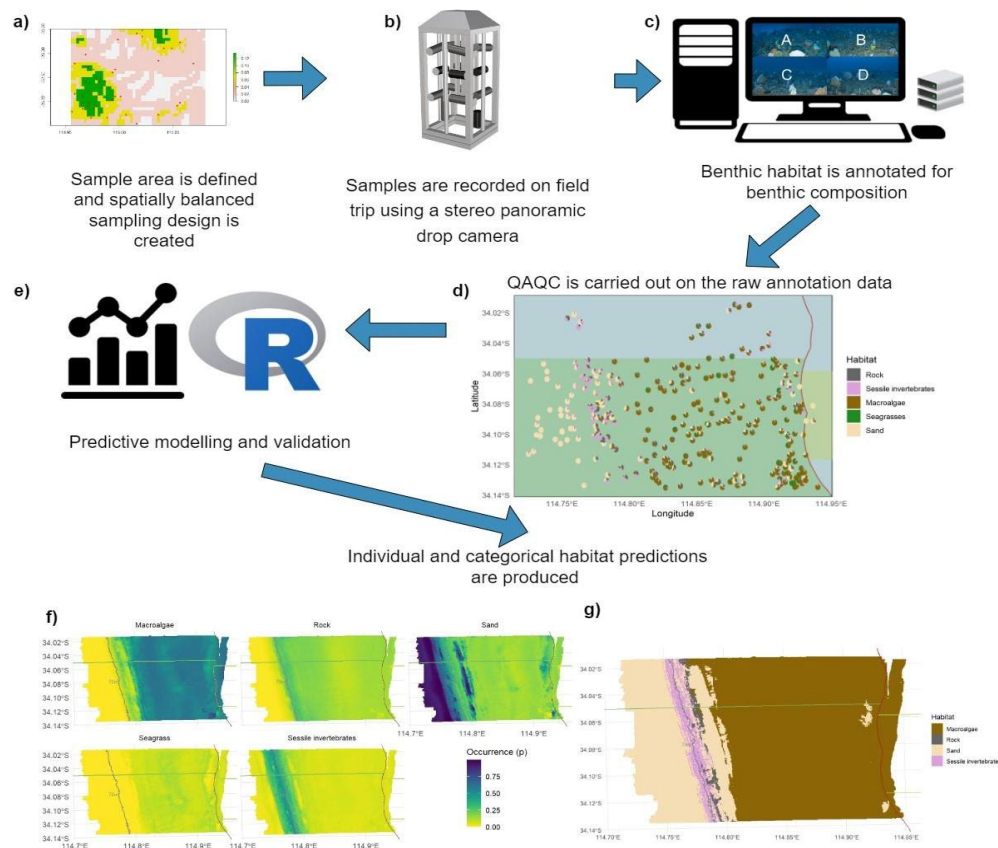


Figure 2 BOSS workflow for benthic composition ground truthing and production of predictive spatial models. a) Spatially balanced design with inclusion probability, b) BOSS workflow for benthic composition ground truthing and production of predictive spatial models, c) imagery annotation, d) quality control, e) predictive modelling and validation to produce f) probabilities of occurrence for individual habitat classes and g) categorical habitat predictions.

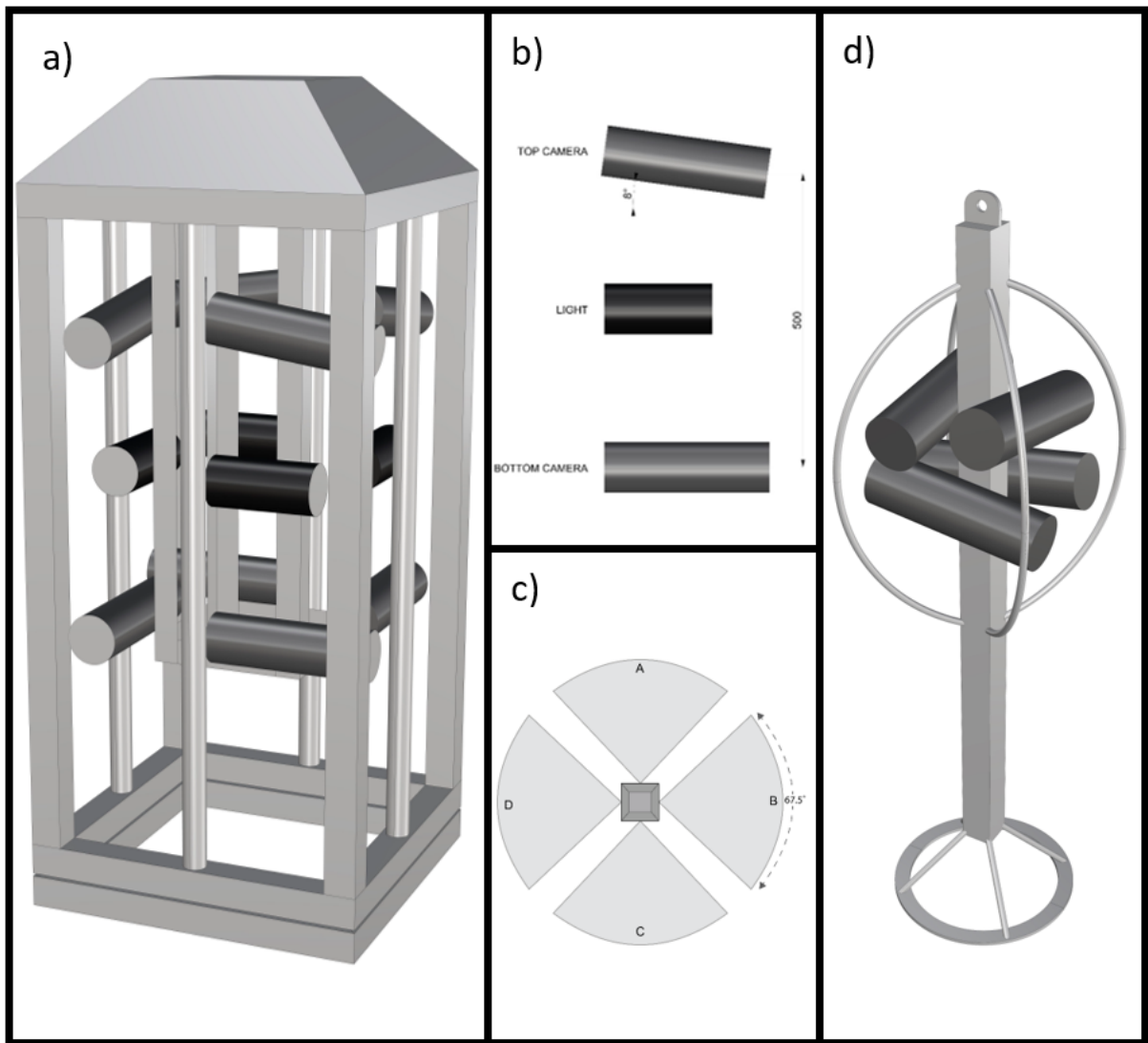
Design and methods

SOP development

The development of the SOP followed the approach described in Przeslawski et al. (2023). Briefly, experts and users in marine imagery and habitat classification were invited to join a working group and contribute to the content of the SOP. The SOP will be maintained as part of a broader suite of sampling methods used for marine monitoring established by the Australian Government's National Environmental Science Program (marine-sampling-field-manual.github.io).

System design

The BOSS has two variants: a stereo system (Fig. 3) and a lighter-weight mono system (Fig. 4). Both consist of a sturdy aluminium frame to secure and protect the camera equipment, a flotation compartment at the top and a bolt-on base weight. The buoyancy and weighting counteract to create a self-righting action, with flotation provided by compression-resistant syntactic foam or subsurface floats. The weighting and compression-resistant buoyancy means that no adjustments are necessary to work, up to the limits of the camera housings and buoyancy (i.e. 1,000 m). When weights are removed, either system can be safely carried by two people (i.e. <35 kg). In the stereo version, eight horizontally-facing cameras are secured to brackets aligned in four stereo pairs at 90-degree intervals (Fig. 3c), and an optional downward-facing camera can be mounted within the buoyancy compartment to collect more traditional imagery (Fig. 5a). Brackets are provided for four lights. In the stereo version, camera brackets are secured to a common central column (Fig. 4a and 5a) and removed from the outer frame to reduce the risk of any physical impacts on the outer frame compromising the stereo calibration. By using small-form action cameras with external battery packs and large capacity memory cards, it is possible to film continuously for 12 hours and not require the camera housings to be opened until the end of the day, thus reducing risks to equipment, calibration stability, and substantially increasing efficiency in the field. Further information on cameras and photogrammetry are provided in Supporting Information 1. In the stereo system, each pair of cameras is separated by 500 mm, with the top camera in each pair angled 8 degrees downward and the bottom camera horizontal (Fig. 2) to provide adequate separations and overlap of imagery (Langlois et al. 2020).



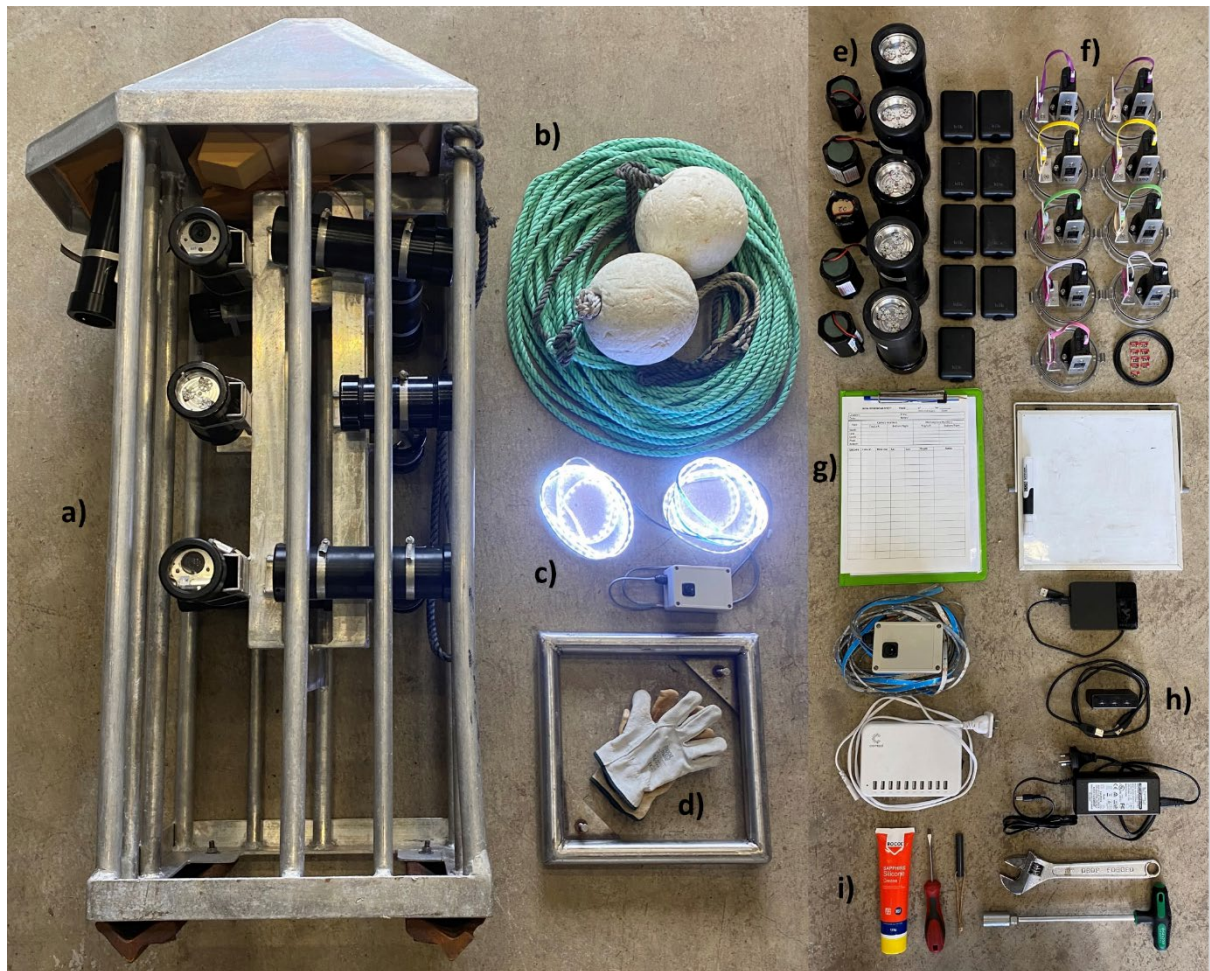


Figure 4 BOSS equipment required for deployment. a) Stereo camera frame with an additional downward facing camera mounted in buoyancy compartment, b) rope and floats, c) synchronisation diodes, d) detachable ballast and gloves, e) lights and batteries, f) cameras, battery packs, SD cards and spare O-rings, g) field metadata sheet, whiteboard and marker, h) charging equipment and downloading footage, and i) tools including silicone grease.

Sampling design

Using sampling strategies appropriate for the study objectives will allow valid inferences, interpretations, and generalisation of resulting data (Robertson et al., 2013). For surveys of habitat composition to ground-truth remote sensed data or existing spatial predictive models, we recommend spatially balanced *a priori* stratification of survey locations as per Balanced Acceptance Sampling (BAS) or Generalised Randomised Tessellation Structures (GRTS) (Robertson et al., 2013). BAS and GRTS approaches can be implemented using R packages ‘MBHdesign’ (Foster et al., 2020) or ‘spsurvey’ respectively (Kincaid et al., 2007). Resampling and spatial coverage can be minimised by separating individual samples in space. Minimum separation distance is dependent on the spatial heterogeneity in the acquired data and should be tested during statistical analysis with spatial variograms, and any significant autocorrelation taken into account (Robertson et al., 2013).

Field logistics

We recommend the drop camera be deployed for a standard duration, with trials indicating five minutes bottom time allows any sediment suspended during the landing to settle, resulting in clear footage of the habitat. Shorter deployments may be sufficient for areas with limited

sediment, and the ideal deployment length should be determined based on study objectives. Local fishing vessels fitted with trap retrieval equipment such as a swinging davit arm or a 'pot-tipper' and winch are ideal for deploying and retrieving both the stereo and mono-video systems, especially in deeper waters (Fig. 4). These vessels are usually suited to the local sea conditions, and the involvement of experienced commercial skippers may provide valuable logistical and local knowledge. Due to the weight of the stereo-system with weights attached (~50 kg), we strongly encourage the engagement of commercial fishers and deckhands who are experienced at deploying weighted traps and their expertise will be beneficial and likely result in better Occupational Health and Safety outcomes. A field deployment checklist is provided in Supporting Information 2.



Figure 5 Lighter weight mono-configuration wide-field drop camera system being deployed by hand (left) and stereo-configuration wide-field drop camera system deployed from a commercial fishing vessel fitted with a 'pot tipper' (right).

Metadata collection

Metadata should be collected to ensure that imagery can be georeferenced and needs to be maintained throughout the planning, fieldwork, imagery download, and annotation phases to ensure data quality. Examples of metadata requirements are provided in Supporting Information 3.

Image synchronisation, compositing and stereo calibration

To ensure that the imagery from each camera can be effectively composited to be viewed simultaneously, both the lightweight mono-video and the larger stereo-video drop camera systems require synchronisation. In particular, for stereo-video imagery, we recommend a minimum of four intermittent synchronisations should be done throughout the day. We propose the use of a flexible strip of waterproof LED lights, for synchronisation, to generate a simultaneous flash in the fields of view of all eight or four horizontally facing cameras (Fig. 3c). We provide wiring diagrams for this synchronisation hardware in Supporting Information 4. Video from each set of four horizontally facing cameras must be synchronised and composited into a single video stream (Fig. 6). We recommend using VidComp software which is freely available

from seagis.com.au. For the stereo-video version of this platform, the use of a video composite is formed from standard fields of view, to minimise barrel distortion, rather than the typical 360° image which is formed using ‘fish-eye’ or ‘omnidirectional’ lenses. Standard lenses result in a less distorted image that is more suitable for stereo-calibration. For the stereo-video calibration procedures, we recommend the widely used and supported SeaGIS CAL (seagis.com.au/bundle.html) software and recommend calibrating cameras frequently, before and after each field campaign (e.g every two weeks or 300 deployments). Frequent calibration will ensure against loss of stereo capability which could come from camera misalignment or swapping of cameras (i.e. optical properties vary within camera models).

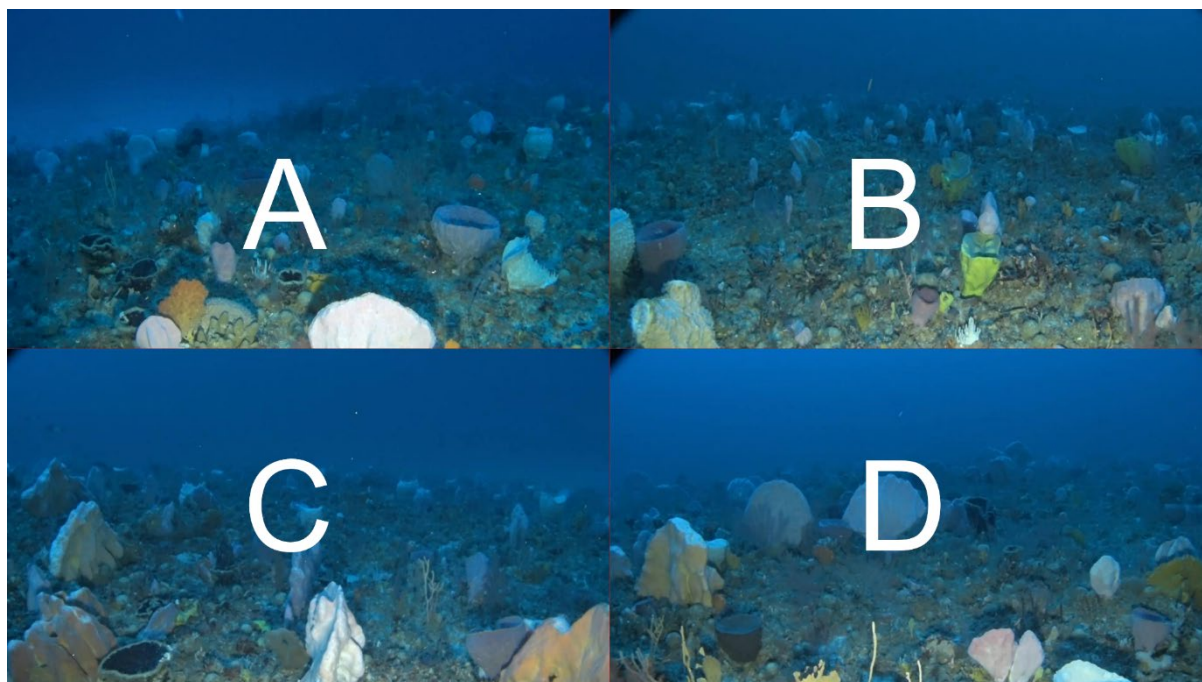


Figure 6 Synchronised and composited imagery from four horizontal cameras.

Annotation software

There is a range of readily available image annotation software and platforms available such as TransectMeasure (www.seagis.com.au/transect.html), Squidle+ (squidle.org), CoralNet (coralnet.ucsd.edu), Benthobox (benthobox.com), and ReefCloud (reefcloud.ai), all of which are suitable for mono video annotation. For stereo-video annotation, we have used SeaGIS EventMeasure (seagis.com.au/event.html) and recommend this as a widely used and well-supported software workflow for stereo-annotation and measurement.

Image annotation

For horizontally facing wide-field imagery, we recommend annotating 20 random points assigned to the lower 50% of each image. We provide example annotation and quality control workflows (globalarchivemanual.github.io/CheckEM/). A simulation study of point annotation of downward-facing imagery found that 20 points would provide an adequate estimate of variance in benthic assemblage composition whereas 80 points would provide a highly consistent estimate (Dumas et al. 2009). Similarly, for the horizontal-facing images collected by the BOSS, we explored the implication of annotating one field of view, using 20 points, to up to four fields of view, a total of 80 points, across multiple independent tropical, subtropical, and temperate locations (Supporting Information 5, code publicly available at github.com/UWA-Marine-Ecology-Group-projects/paper-boss-habitat/). We found generally more precise estimates of

habitat composition using 40 to 80 points, annotating two to four fields of view, justifying our recommendation to annotate the combined field of view (~270°) of the four cameras, to characterise benthic composition (Supporting Information 5).

For annotation of benthic composition, we recommend the CATAMI classification schema (Althaus et al., 2015), which classifies habitats into morphological groups. This schema is also recommended for similar marine sampling protocols for towed video, ROVs, AUVs (Przeslawski et al., 2023) and benthic composition from BRUV (Langlois et al., 2020). We provide a controlled repository of CATAMI formatted for use in TransectMeasure available at github.com/GlobalArchiveManual/annotation-schema, which also includes species-specific annotation for certain common and easily identifiable taxa from the CAAB classification schema relevant to Australia (Rees et al., 1999). Also included is an annotation schema for visual estimates of structural complexity or relief (see Langlois et al., 2020).

Quality control and data curation

Quality control and data curation workflows are vital to ensure data is findable, accessible, interoperable and reusable (FAIR, Wilkinson et al., 2016). All corrections should be made within the original annotation files to ensure data consistency over time. We recommend the following approaches to ensure quality control:

- Annotators should complete small identical ‘training’ image sets where habitat classes are known, to assess competency and benchmark accuracy.
- Quality assurance should be carried out by a senior analyst and involves a randomised review of 10% of annotated images and data within a project. If accuracy is below 95% for all identifications, imagery should be re-annotated.
- All annotators should meet periodically as a group to discuss image classification to ensure that consistency is maintained throughout the project.

We propose a series of simple visual quality control plots to identify outliers and provide examples of these in the annotation guide (globalarchivemanual.github.io/CheckEM/, Fig. 2).

Conclusion

The need for marine spatial planning and concerns about the environmental impacts of anthropogenic activities (including climate change, pollution and offshore industries) has led to a growing requirement for large-scale habitat characterisation to inform management, through mapping or environmental assessments. The drop camera system described here is robust, wide-field, and horizontal-facing, in either the stereo or mono-video variations. It is specifically designed for rapidly collecting benthic habitat composition and has been demonstrated to improve habitat quantification across a range of depths from 2 - 220 m. The system is ideal for collecting spatially balanced point samples over large areas, which can be logistically restrictive for other survey platforms, either due to their long deployment times (e.g. stereo-BRUVs), limit on number of ascents (e.g. scuba) or need to be tethered or supported along transects with a finite time underwater (e.g. ROV, AUV), which typically lead to nested or spatially constrained sampling (Monk et al., 2018; Shortis et al., 2008). The optional use of stereo-cameras enables the usable area of the image and range of observation to be quantified and included as an offset in analysis (e.g. when turbidity varies among sites, Broad et al., 2023). Photogrammetry of stereo images also enables the measurement of additional metrics such as algal canopy height or the dimension of benthic biota (Langlois et al., 2021; Vergés et al., 2016). These data are highly amenable for medium to large-scale habitat mapping of marine parks (Leleu et al., 2012), detection of recovery in benthic biota after trawling (Langlois et al., 2021), and environmental impact assessments of emerging industries such as offshore renewables (LaFrance et al., 2014).

Acknowledgements

The authors would like to thank James Seager (SeaGIS.com.au) for support with software and both James Seager and Ray Scott for stereo equipment and advice. The design was inspired by the work of Rick Starr and adapted with the expertise of John Fitzhardinge. Syntactic foam was donated by Total Marine Technology. Cultural guidance in trialling this method on Wadandi Sea Country was provided by Dr Wayne Webb and Iszaac Webb, and on Wudjari Sea Country by Dr Doc Reynolds and Donna Beach respectively. Collaboration with Traditional Owner Rangers to deploy this *Boordiya* camera system and annotate the imagery provided feedback to optimise the workflows presented here. Nicole Middleton and Darren Phillips of Parks Australia provided advice and encouragement. David Hannen and Chris Biessel completed design improvements and fabrication, with technical drawings made by Felix Spencer. The initial development of the camera system was supported by the Fisheries Research and Development Corporation (Project Number 2019-099). Data collection and Standard Operating Protocol workshop was supported with funding from the Australian Government through the NESP Marine and Coastal Hub and Parks Australia.

References

- Althaus, F., Hill, N., Ferrari, R., Edwards, L., Przeslawski, R., Schönberg, C. H. L., Stuart-Smith, R., Barrett, N., Edgar, G., Colquhoun, J., Tran, M., Jordan, A., Rees, T., & Gowlett-Holmes, K. (2015). A Standardised Vocabulary for Identifying Benthic Biota and Substrata from Underwater Imagery: The CATAMI Classification Scheme. *PloS One*, 10(10), e0141039.
- Bennett, K., Wilson, S. K., Shedrawi, G., McLean, D. L., & Langlois, T. J. (2016). Can diver operated stereo-video surveys for fish be used to collect meaningful data on benthic coral reef communities? In *Limnology and Oceanography: Methods* (Vol. 14, Issue 12, pp. 874–885). <https://doi.org/10.1002/lom3.10141>
- Boutros, N., Shortis, M. R., & Harvey, E. S. (2015). A comparison of calibration methods and system configurations of underwater stereo-video systems for applications in marine ecology. In *Limnology and Oceanography: Methods* (Vol. 13, Issue 5, pp. 224–236). <https://doi.org/10.1002/lom3.10020>
- Broad, A., Rees, M., Knott, N., Swadling, D., Hammond, M., Ingleton, T., Morris, B., & Davis, A. R. (2023). Anchor scour from shipping and the defaunation of rocky reefs: A quantitative assessment. *The Science of the Total Environment*, 863, 160717.
- Foster, S. D., Hosack, G. R., Monk, J., Lawrence, E., Barrett, N. S., Williams, A., & Przeslawski, R. (2020). Spatially balanced designs for transect-based surveys. *Methods in Ecology and Evolution / British Ecological Society*, 11(1), 95–105.
- Kincaid, T., Olsen, T., Kincaid, M. T., & Imports, M. (2007). The spsurvey Package. <http://ftp.uni-bayreuth.de/math/statlib/R/CRAN/doc/packages/spsurvey.pdf>
- LaFrance, M., King, J. W., Oakley, B. A., & Pratt, S. (2014). A comparison of top-down and bottom-up approaches to benthic habitat mapping to inform offshore wind energy development. *Continental Shelf Research*, 83, 24–44.
- Langlois, T. J., Goetze, J., Bond, T., Monk, J., Abesamis, R. A., Asher, J., Barrett, N., Bernard, A. T. F., Bouchet, P. J., Birt, M. J., Cappo, M., Currey-Randall, L. M., Driessen, D., Fairclough, D. V., Fullwood, L. A. F., Gibbons, B. A., Harasti, D., Heupel, M. R., Hicks, J., ... Harvey, E. S. (2020). A field and video annotation guide for baited remote underwater stereo-video surveys of demersal fish assemblages. *Methods in Ecology and Evolution / British Ecological Society*, 11(11), 1401–1409.
- Langlois, T. J., Wakefield, C. B., Harvey, E. S., Boddington, D. K., & Newman, S. J. (2021). Does the benthic biota or fish assemblage within a large targeted fisheries closure differ to surrounding areas after 12 years of protection in tropical northwestern Australia? *Marine Environmental Research*, 170, 105403.
- Leleu, K., Remy-Zephir, B., Grace, R., & Costello, M. J. (2012). Mapping habitats in a marine reserve showed how a 30-year trophic cascade altered ecosystem structure. *Biological Conservation*, 155, 193–201.
- Liu, G., Chen, L., Liu, K., & Luo, Y. (2023). A swarm of unmanned vehicles in the shallow ocean: A survey. *Neurocomputing*, 531, 74–86.
- Mastrantonis, Stanley, Ben Radford, Tim Langlois, Claude Spencer, Simon de Lestang, and Sharyn Hickey. 2024. "A Novel Method for Robust Marine Habitat Mapping Using a Kernelised Aquatic Vegetation Index." *ISPRS Journal of Photogrammetry and Remote Sensing: Official*

Monk, J., Barrett, N. S., Peel, D., Lawrence, E., Hill, N. A., Lucieer, V., & Hayes, K. R. (2018). An evaluation of the error and uncertainty in epibenthos cover estimates from AUV images collected with an efficient, spatially-balanced design. *PloS One*, 13(9), e0203827.

Pelletier, D., Selmaoui-Folcher, N., Bockel, T., & Schohn, T. (2020). A regionally scalable habitat typology for assessing benthic habitats and fish communities: Application to New Caledonia reefs and lagoons. *Ecology and Evolution*, 10(14), 7021–7049.

Perkins, N. R., Hosack, G. R., Foster, S. D., Monk, J., & Barrett, N. S. (2020). Monitoring the resilience of a no-take marine reserve to a range extending species using benthic imagery. *PloS One*, 15(8), e0237257.

Przeslawski, R., Barrett, N., Carroll, A., Foster, S., Gibbons, B., Jordan, A., Monk, J., Langlois, T., Lara-Lopez, A., Pearlman, J., Picard, K., Pini-Fitzsimmons, J., van Ruth, P., & Williams, J. (2023). Developing an ocean best practice: A case study of marine sampling practices from Australia. *Frontiers in Marine Science*, 10. <https://doi.org/10.3389/fmars.2023.1173075>

Rees, A. J. J., Yearsley, G. K., Gowlett-Holmes, K., & Pogonoski, J. (1999). CSIRO National Collections and Marine Infrastructure (formerly CSIRO Marine and Atmospheric Research). CAAB - Codes for Australian Aquatic Biota. <https://www.marine.csiro.au/data/caab/>

Robertson, B. L., Brown, J. A., McDonald, T., & Jaksons, P. (2013). BAS: Balanced Acceptance Sampling of Natural Resources. In *Biometrics* (Vol. 69, Issue 3, pp. 776–784). <https://doi.org/10.1111/biom.12059>

Sheehan, E. V., Vaz, S., Pettifer, E., Foster, N. L., Nancollas, S. J., Cousens, S., Holmes, L., Facq, J.-V., Germain, G., & Attrill, M. J. (2016). An experimental comparison of three towed underwater video systems using species metrics, benthic impact and performance. *Methods in Ecology and Evolution / British Ecological Society*, 7(7), 843–852.

Shortis, Seager, & Williams. (2008). Using stereo-video for deep water benthic habitat surveys. *Marine Technology*. https://www.researchgate.net/profile/Mark-Shortis/publication/233526348_Using_Stereo-Video_for_Deep_Water_Benthic_Habitat_Surveys/links/0deec52b3521743ce4000000/Using-Stereo-Video-for-Deep-Water-Benthic-Habitat-Surveys.pdf

Starr, R. M., Gleason, M. G., Marks, C. I., Kline, D., Rienecke, S., Denney, C., Tagini, A., & Field, J. C. (2016). Targeting Abundant Fish Stocks while Avoiding Overfished Species: Video and Fishing Surveys to Inform Management after Long-Term Fishery Closures. *PloS One*, 11(12), e0168645.

Vergés, A., Doropoulos, C., Malcolm, H. A., Skye, M., Garcia-Pizá, M., Marzinelli, E. M., Campbell, A. H., Ballesteros, E., Hoey, A. S., Vila-Concejo, A., Bozec, Y.-M., & Steinberg, P. D. (2016). Long-term empirical evidence of ocean warming leading to tropicalization of fish communities, increased herbivory, and loss of kelp. *Proceedings of the National Academy of Sciences of the United States of America*, 113(48), 13791–13796.

Wilkinson, M. D., Dumontier, M., Aalbersberg, I. J. J., Appleton, G., Axton, M., Baak, A., Blomberg, N., Boiten, J.-W., da Silva Santos, L. B., Bourne, P. E., Bouwman, J., Brookes, A. J., Clark, T., Crosas, M., Dillo, I., Dumon, O., Edmunds, S., Evelo, C. T., Finkers, R., ... Mons, B. (2016). The FAIR Guiding Principles for scientific data management and stewardship. *Scientific Data*, 3, 160018.

Supporting Information

Camera and photogrammetry

Camera specifications can influence the accuracy of taxonomic identification, and stereo-measurements require careful adherence to camera alignment and calibration protocols. In our system, we record video with Sony FDR-X3000 cameras filming at 1920 x 1080 pixels, a frame rate of 60 frames per second and using the ‘medium’ field of view setting (~67.5 °). We recommend the use of cameras with a minimum resolution of 1920 × 1080 pixels (Langlois et al. 2020; Harvey et al. 2010) and a minimum capture rate of 30 frames per second, with all settings standardised across cameras. Higher camera resolution will generally improve taxonomic identification, but all systems should be thoroughly tested before deployment for overheating issues or write speed limitations at higher-quality settings.

To maintain stereo-calibrations, cameras must have video stabilisation disabled, and a fixed focal length can allow measurements both close to and far from the camera when correctly calibrated (Boutros, Shortis, and Harvey 2015; Shortis, Harvey, and Abdo 2009). Field of view settings should be chosen to limit distortion in the image rather than maximise the field of view. White lights (550 - 560 nm) are recommended for low-light conditions (Birt et al. 2019). We recommend seeking manufacture and calibration advice for the frame from recognised providers, to ensure that the tight tolerances for effective stereo-vision are met. Each housing and camera set should be uniquely identified to ensure that individual cameras are used only in the housing they are calibrated in. Any changes to camera positions (e.g. if a camera is dismounted during battery replacement) will disrupt the calibration, increasing error in length measurements.

Video cameras can skip or lose frames, disrupting synchronisation among cameras and requiring the use of manual reference points such as a clapper board shown at the start of each take. The wide-field stereo-video drop camera system is designed to record many successive deployments but requires manual synchronisation at regular intervals. We use a flexible strip of waterproof LED lights to generate a simultaneous flash at all nine cameras. The chosen camera model should be tested to determine how often resynchronisation needs to occur to maintain accurate stereo measurements.

Field Deployment Checklist

We provide here a series of checklists that ensure that all data is collected consistently in the field.

Pre-field work

Supporting Table 1. Pre-fieldwork checklist.

Step	Action
1	Check equipment as shown in Fig. 3.
2	Conduct 3D calibration of stereo-camera pairs following (Boutros, Shortis, and Harvey 2015). We recommend an enclosed pool environment with good visibility. This must be repeated at the end of the field campaign, or if any camera or housing positions have changed.

- 3 Ensure sampling design can be imported to the research vessel navigation system or bring a standalone navigation and depth sounding system for the skipper.
- 4 Ensure sufficient data storage capacity for downloading all video imagery collected, and for back-up copies.
- 5 Ensure sufficient spares for the wide-field drop camera and check the condition of o-rings (Fig. 3).
- 6 Create a camera metadata sheet or preferably use a capture device (e.g. Collector for ArcGIS, tablet computer with GIS) to record the sample and memory card unique identifier (Supporting Table 6). Prepare a field metadata sheet to record unique sample identifiers, time, GPS coordinates and other necessary metadata entries (Supporting Table 7).

Pre-deployment

Supporting Table 2 Pre-deployment checklist.

Step	Action
1	Set up the wide-field stereo-video drop camera frame, including ropes and floats (if necessary).
2	Check all camera batteries are charged and memory cards are formatted.
3	Check the light batteries and synchronising device battery.
4	Discuss deployment, retrieval procedures and safety with the skipper and crew.

Deployment

Supporting Table 3 Deployment checklist.

Step	Action
1	Turn on all cameras and synchronise together. Turn on all battery packs and check that cameras are charging (if applicable).
2	Check camera settings are consistent.
3	Film the metadata sheet with the information of each camera to attribute this to the recorded video footage.
4	Check the camera housings are dry and clean before aligning and inserting cameras. Check o-rings are not pinched or dirty.
5	Turn on all exterior lights.
6	Once on site, and at the command of the master of the vessel, experienced personnel or deck hands should physically deploy the drop camera and ropes clear of the vessel. At this point a GPS mark should be recorded.
7	The vessel should remain directly on the site whilst deploying the drop camera. During the settlement time on the seabed, contact between the vessel and camera system can be maintained with the drop camera via the ropes, however no tension should be held on the ropes to ensure that the drop camera is not moved from the sampling location. Alternatively, the rope with floats attached can be dropped and retrieved once the sample time has elapsed.

Retrieval

Supporting Table 4 Retrieval checklist.

Step	Action
1	Once the deployment time is complete, the vessel should remain directly on top of the sampling location while the drop camera is retrieved.
2	Once the drop camera has been retrieved, it should remain on the deck or securely fastened to the pot tipper or davit arm as the vessel transits to the next sampling location. The upcoming unique sample code should be shown to all cameras. Frequent checking and resynchronisation of cameras should occur to ensure that all cameras are recording, lights are turned on and any issues with loss of stereo calibration due to dropped frames are accounted for. If any cameras stop recording during the recording period, then all cameras should be restarted to maintain synchronicity.

End of day checks

Supporting Table 5 End of day checklist.

Step	Action
1	Once the drop camera is on the deck at the end of the day's sampling, dry the housings and remove cameras, battery packs and memory cards.
2	Review, download and backup all footage at the end of each day, using clear naming conventions for filenames and folder structure (Supporting Fig. 4.1).
3	Ensure all metadata is backed up and set all equipment to charge for the next day's sampling.

Metadata format and file organisation

We provide templates for metadata (Supporting Tables 3.1-3.3) and file organisation (Supporting Fig. 3.1) here.

Supporting Table 6. Example of a completed camera metadata

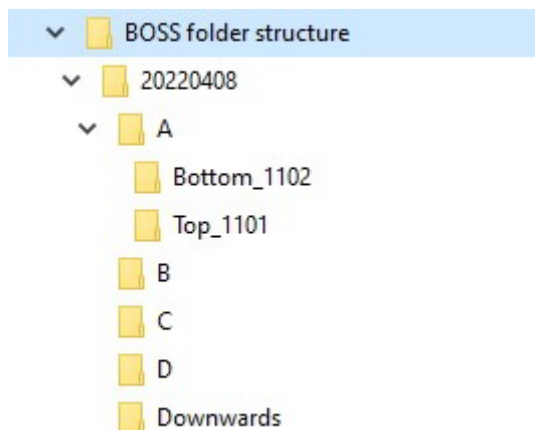
Date	Face	Top camera	Top SD card	Bottom camera	Bottom SD card
20220408	A	1101	200	1102	201
20220408	B	1103	202	1104	203
20220408	C	1105	204	1106	205
20220408	D	1107	206	1108	207
20220408	Downwards	1109	208	NA	

Supporting Table 7. Example of a completed field metadata sheet.

Sample	Date	Time	Longitude	Latitude	Depth	Notes
MEG001	20220408	10:01	113.15	-34.05	24.1	
MEG002	20220408	10:05	113.16	-34.06	24.7	
MEG003	20220408	10:08	113.17	-34.07	24.3	Checked all cameras
MEG004	20220408	10:12	113.18	-34.08	22.8	
MEG005	20220408	10:16	113.19	-34.09	21.9	

Supporting Table 8. Example of completed annotation metadata columns, to join to field metadata.

Status	Annotation.date.completed	Observer	Video.notes
Fished	20220408	Tim	
Fished	20220408	Tim	check octocoral
No-take	20220408	Tim	
No-take	20220408	Tim	
No-take	20220408	Tim	



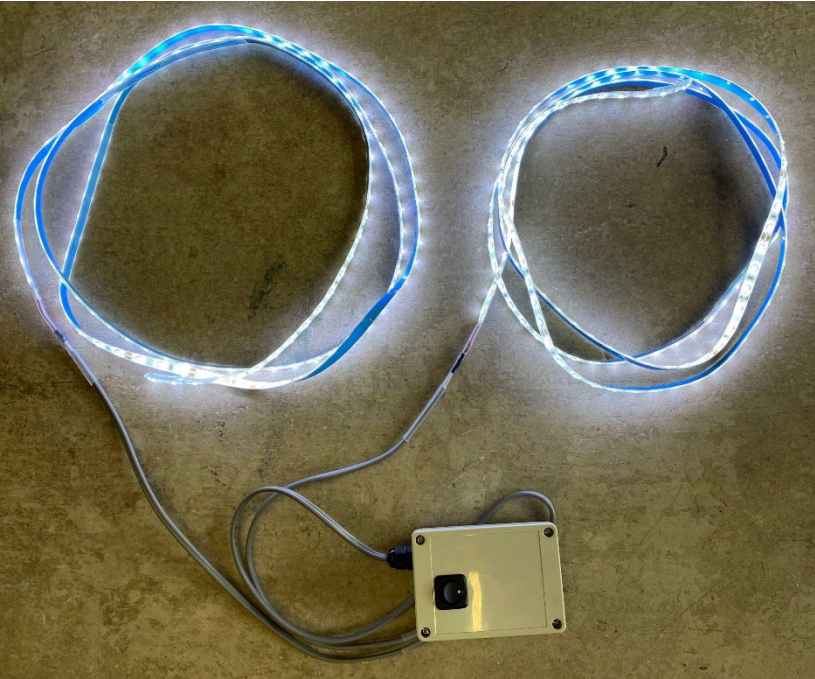
Supporting Figure 1. Folder structure for downloaded footage. Footage is stored in a parent folder indicating the date the footage was recorded on, with separate folders for each of the eight stereo cameras and the downwards camera.

Synchronisation diode

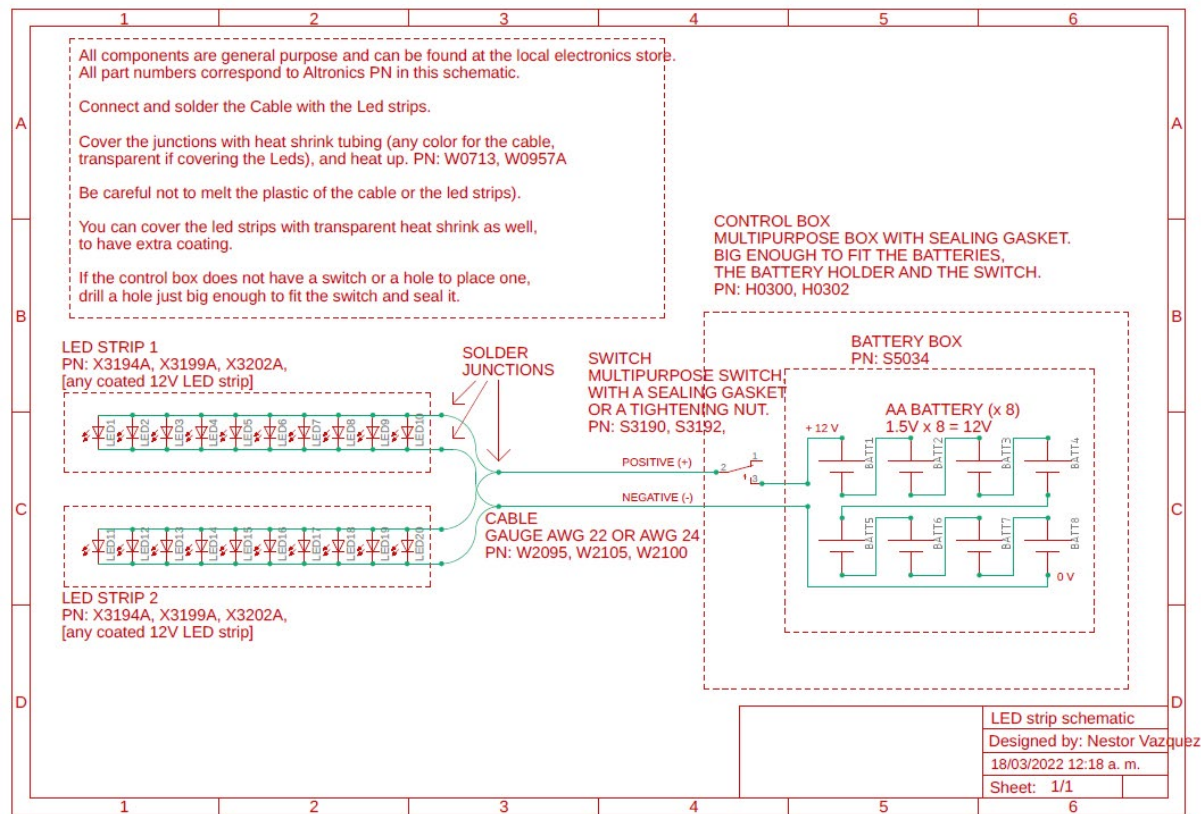
We recommend that video rather than still imagery is collected and by using action cameras with external battery packs and large capacity memory cards, it is possible to record video for the whole day of field work and not require the camera housings to be opened until the end of the day.

However, to ensure that the imagery from each camera can be synchronised, both the lightweight mono-video and the larger stereo-video wide-field drop camera systems will require intermittent synchronisation with diodes, out of the water, throughout field deployment to enable imagery to be composited (see below for Image compositing).

For stereo-video imagery, we recommend intermittent with a minimum of four synchronisations should be done throughout the day. We propose the use of a flexible strip of waterproof LED lights, as synchronisation diodes, to generate a simultaneous flash in all eight or four horizontally facing cameras (Supporting Fig. 4.1) and provide wiring diagrams for this synchronisation diode (Supporting Fig. 4.2).



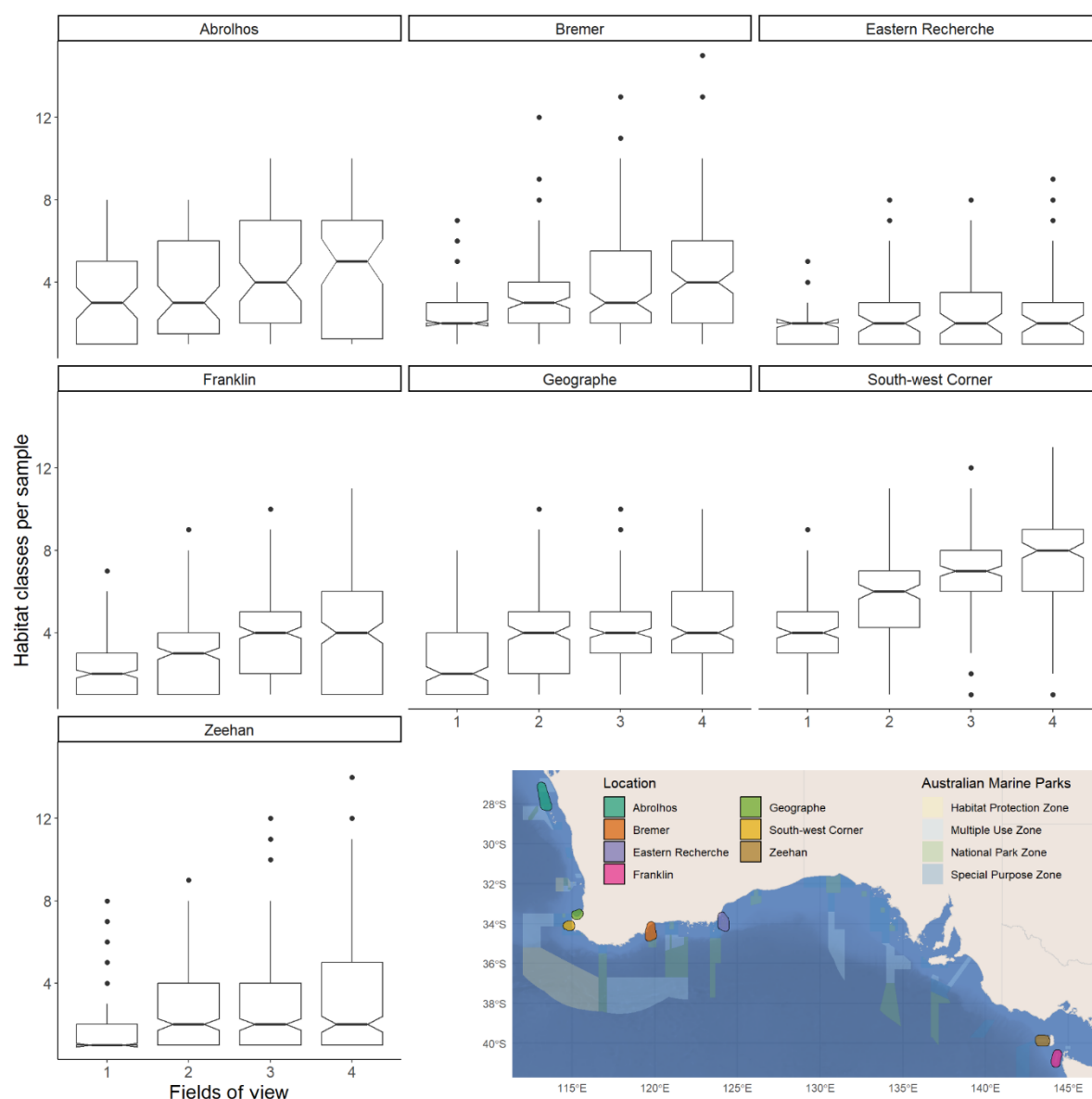
Supporting Figure 2 Synchronisation diode.



Supporting Figure 3 Schematic diagram of synchronisation diode wiring.

Effect of increasing number of fields of view on habitat observations and cost of data collection

The benefits of using wide-field or 360-degree cameras has been demonstrated when quantifying fish assemblages (Whitmarsh, Huveneers, and Fairweather 2018; Pelletier et al. 2021), but is also beneficial when characterising benthic habitats (Mallet et al. 2021; Pelletier et al. 2020). A wide-field of view, made up of multiple composited views, reduces issues with observation direction in single view systems, where at habitat edges or in high-relief environments where the dominant seascape feature may be missed (Mallet et al. 2021). We further demonstrate the value of additional fields of view (Supporting Fig. 3.1), by showing that habitat heterogeneity per sample increases as the number of fields of view increases, each of approximately 70° wide, across seven locations from the subtropical Abrolhos Marine Park (Western Australia) to the temperate Franklin Marine Park (Tasmania). The code and data are publicly available at github.com/UWA-Marine-Ecology-Group-projects/paper-boss-habitat/. The increase in effort to annotate this additional imagery is minor (1-2 minutes) and the field time required to deploy a single view versus multiple view system is the same. The relative increase in habitat classes varied across marine parks surveyed from a limited increase (e.g. Eastern Recherche Marine Park) to a two-fold increase in the number of habitats identified (South-west Corner Marine Park, Supporting Fig. 4.1). At least two fields of view provide a consistent benefit to sampling habitat heterogeneity, and up to four fields of view can be beneficial at some locations, with minimum increases in annotation costs. Having more information on habitat heterogeneity better informs any habitat distribution modelling and mapping, thereby justifying the use of additional fields of view.



Supporting Figure 4. Relationship between number of fields of view and number of habitat classes detected across seven continental shelf locations within the Australian Marine Parks.

References used in Supporting Information

Birt, Matthew J., Marcus Stowar, Leanne M. Currey-Randall, Dianne L. McLean, and Karen J. Miller. 2019. "Comparing the Effects of Different Coloured Artificial Illumination on Diurnal Fish Assemblages in the Lower Mesophotic Zone." *Marine Biology* 166 (12): 154.

Boutros, Nader, Mark R. Shortis, and Euan S. Harvey. 2015. "A Comparison of Calibration Methods and System Configurations of Underwater Stereo-Video Systems for Applications in Marine Ecology." *Limnology and Oceanography: Methods*. <https://doi.org/10.1002/lom3.10020>.

Harvey, Euan S., Jordan Goetze, Bryce McLaren, Tim Langlois, and Mark R. Shortis. 2010. "Influence of Range, Angle of View, Image Resolution and Image Compression on Underwater Stereo-Video Measurements: High-Definition and Broadcast-Resolution Video Cameras Compared." *Marine Technology Society Journal*. <https://doi.org/10.4031/mts.44.1.3>.

Langlois, Tim J., Jordan Goetze, Todd Bond, Jacquomo Monk, Rene A. Abesamis, Jacob Asher, Neville Barrett, et al. 2020. "A Field and Video Annotation Guide for Baited Remote Underwater Stereo-video Surveys of Demersal Fish Assemblages." *Methods in Ecology and Evolution* / British Ecological Society 11 (11): 1401–9.

Mallet, Delphine, Marion Olivry, Sophia Ighiouer, Michel Kulbicki, and Laurent Wantiez. 2021. "Nondestructive Monitoring of Soft Bottom Fish and Habitats Using a Standardized, Remote and Unbaited 360 Video Sampling Method." *Fishes of Sahul: Journal of the Australia New Guinea Fishes Association* 6 (4): 50.

Pelletier, Dominique, David Roos, Marc Bouchoucha, Thomas Schohn, William Roman, Charles Gonson, Thomas Bockel, et al. 2021. "A Standardized Workflow Based on the STAVIRO Unbaited Underwater Video System for Monitoring Fish and Habitat Essential Biodiversity Variables in Coastal Areas." *Frontiers in Marine Science* 8.
<https://doi.org/10.3389/fmars.2021.689280>.

Pelletier, Dominique, Nazha Selmaoui-Folcher, Thomas Bockel, and Thomas Schohn. 2020. "A Regionally Scalable Habitat Typology for Assessing Benthic Habitats and Fish Communities: Application to New Caledonia Reefs and Lagoons." *Ecology and Evolution* 10 (14): 7021–49.

Shortis, Mark, Euan Harvey, and Dave Abdo. 2009. "A Review Of Underwater Stereo-Image Measurement For Marine Biology And Ecology Applications." *Oceanography and Marine Biology*.
<https://doi.org/10.1201/9781420094220.ch6>.

Whitmarsh, Sasha K., Charlie Huveneers, and Peter G. Fairweather. 2018. "What Are We Missing? Advantages of More than One Viewpoint to Estimate Fish Assemblages Using Baited Video." *Royal Society Open Science* 5 (5): 171993.

Study 2 - A novel method for robust marine habitat mapping

Preface

This study presents a new habitat index to map and monitor submerged aquatic vegetation from satellite imagery. This index extracts the maximum available information from optical remote sensing platforms and allows for better standardisation of spectral characteristic over space and time. This index was calibrated using images of the seabed habitat collected with the BOSS system presented in [Study 1](#) and was fundamental for generating habitat time-series for the WA coast and informing fisheries management, as presented in [Study 5](#).

A novel method for robust marine habitat mapping using a kernelised aquatic vegetation index

Published in: *ISPRS Journal of Photogrammetry and Remote Sensing*

<https://doi.org/10.1016/j.isprsjprs.2024.02.015>

Authors and affiliations:

Stanley Mastrantonis^{1,2,3,5}, Ben Radford^{1,2,3,4}, Tim Langlois^{3,5}, Claude Spencer^{3,5}, Simon de Lestang^{5,6} and Sharyn Hickey^{1,2,3}

¹ School of Agriculture and Environment, The University of Western Australia, Crawley, WA, Australia

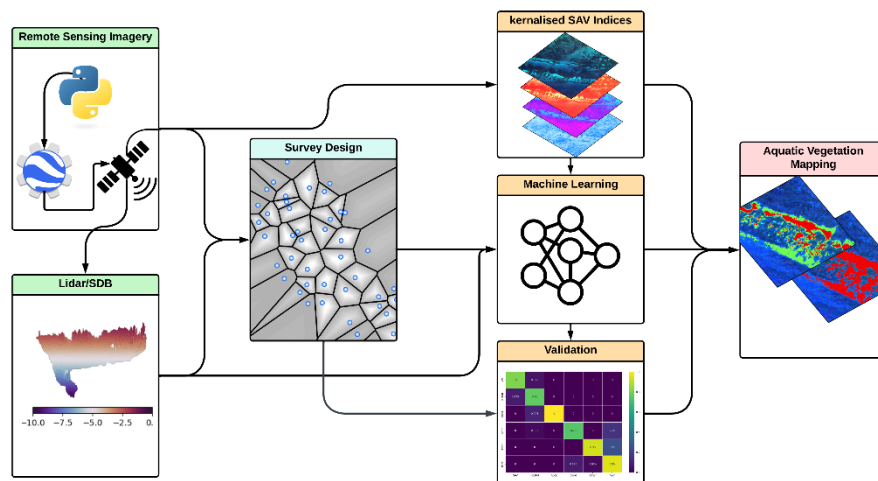
² Centre for Water and Spatial Science, The University of Western Australia, Crawley, WA, Australia

³ UWA Oceans Institute, The University of Western Australia, Crawley, WA, Australia

⁴ Australian Institute of Marine Science, 39 Fairway, Crawley, Western Australia, Australia.

⁵ School of Biological Sciences, The University of Western Australia, Crawley, WA, Australia

⁶ Western Australian Fisheries and Marine Research Laboratories, Department of Primary Industries and Regional Development, North Beach, WA, Australia



Abstract

Efficient and timely mapping and monitoring of marine vegetation are becoming increasingly important as coastal habitats have experienced significant declines in spatial extent due to climate change. Recent advances in machine learning and cloud computing, such as Google Earth Engine, have demonstrated that online analysis platforms make global-scale habitat mapping and monitoring possible. However, the mapping and monitoring of marine ecosystems with remote sensing is challenging, and we lack reliable, generalisable and scalable indices such as normalised difference vegetation index (NDVI) to assess spatiotemporal change in marine habitats. Here, we present a novel method for mapping coastal marine habitats using a kernelised aquatic vegetation index (kNDAVI) with spatially balanced in-water ground truthing, acquired with the BOSS camera system, and compare it to existing indices and mapping approaches. The kernelised vegetation index provides a simple, consistent, scalable and accurate method for mapping shallow marine vegetation across ~400 km of coastline along mid-west Australia (31.58°S - 29.56°S). This region has significant coastal macroalgae cover that provides critical recruitment habitat for many invertebrates, including commercially valuable fisheries, and has experienced significant loss due to climate-induced heatwaves. We extensively validate kNDAVI and satellite-derived covariates for their utility in mapping submerged aquatic vegetation (SAV) using three approaches 1] cross-validation, 2] block cross-validation and 3] site validation. Habitat models that included the kernelised vegetation index achieved excellent agreement (Accuracy > 0.90 and Cohen's kappa > 0.80) for classifying submerged vegetation. We demonstrate that the kNDAVI index has considerable potential for large-scale vegetation monitoring and provides an applicable metric to map spatiotemporal dynamics and more effectively manage these changing coastal habitats.

Introduction

Submerged aquatic vegetation (SAV) refers to plants that obligately grow underwater and are critical components of marine ecosystems (Rowan and Kalacska, 2021). Here, SAV relates to coastal macroalgae and seagrass (Rowan and Kalacska, 2021). SAV provides various ecosystem services, including habitat and food for marine fauna supporting recreational and commercial fishing (Hughes et al., 2009; Massicotte et al., 2015; Silberstein et al., 1986). SAV improves coastal resilience, nutrient cycling (de los Santos et al., 2020; Garden and Smith, 2011; Griffiths et al., 2020) and carbon storage (Macreadie et al., 2021), yet SAV is declining globally. Seagrass is estimated to have disappeared at a rate of 110 km² yr⁻¹ since 1980 (Waycott et al., 2009), and global kelp distributions have reduced by 0.018% annually in the last half a century (Krumhansl et al., 2016). A 2011 marine heatwave resulted in the loss of approximately 2,300 km² of kelp along the southern Australian coastline. This event led to a contraction of kelp ranges by 100 km² and triggered a phase shift towards assemblage-wide tropicalisation, significantly impacting ecological processes (Wernberg et al., 2016). Given the declining trends in SAV globally, monitoring the dynamics and establishing the drivers of these habitats at applicable geographic and temporal scales is a priority for management (Duffy et al., 2019). Thus, spatial and temporal information on the extent, conditions and trends of SAV are required to assess past and future changes and inform management decisions (Brisset et al., 2021; Duffy et al., 2013).

Over 100 major programs worldwide undertake repeated measurements of SAV at local and regional scales (Cavanaugh et al., 2021; Duffy et al., 2019). These programs employ continuous manual sampling, remote sensing (from satellites, crewed and uncrewed aerial vehicles), remote underwater imagery or a combination of these methods to quantify and track SAV extent dynamics (Cavanaugh et al., 2021; Carter et al., 2021; Zoffoli et al., 2020; Roelfsema et al., 2015; Duffy et al., 2019). In-situ monitoring of SAV can be costly and laborious, and the extent and frequency of mapping and monitoring can be limited when compared to remote sensing methods, which have the potential to provide frequent measurements of SAV extent and dynamics across regional and global scales (Traganos et al., 2018). Remote sensing is time-efficient and affordable and is increasingly used to map SAV, often in combination with machine learning (Brown et al., 2022; Rowan and Kalacska, 2021; Traganos et al., 2018). However, remote sensing without ground truthing and proper calibrations can be unreliable for detecting changes in SAV. Previous research has suggested that without ground truthing, seagrass monitoring can underestimate the extent of change by 30-50% (Schultz et al., 2015). Thus, the accuracy ability to detect changes in SAV can vary greatly depending on the ground truthing strategy (or absence thereof), and remote sensing should be complemented by ground truthing to map SAV at scale.

Mapping SAV with remote sensing is further complicated by factors such as oceanographic changes (Yuan and Yamagata, 2015), clouds (Mateo-García et al., 2018), water clarity (Dierssen et al., 2019) and sunglint (Traganos et al., 2018). Additional radiometric corrections, such as atmospheric correction, depth invariant indices and sunglint corrections, are commonly applied to standardise and calibrate imagery across scenes and through time (Rowan and Kalacska, 2021). The choice of modelling framework is also an important consideration for habitat mapping (i.e., decision trees, support vector machines or neural networks), but map accuracy will be influenced more by the representativeness of ground truthing and imagery derivatives, such as vegetation indices, rather than modelling framework (Jamali, 2019; Maxwell et al., 2018; Sonobe et al., 2018).

Typically, satellite remote sensing relies on spectral band vegetation indices (VIs) to detect vegetation extent and change. These indices allow change detection using a single range of values while also controlling for differences in solar irradiance through scaling and normalising

the contrasting spectral responses, maximising the information relating to vegetation cover and structure. The normalised difference vegetation index (NDVI), an index that contrasts the red and near-infrared (NIR) bands, is widely used for the terrestrial environment. Similar VIs exist for the marine environment, such as the normalised difference aquatic vegetation index (NDAVI) or the water-adjusted vegetation index (WAVI), which have been demonstrated to map SAV extents effectively at local scales. Recently, NASA has used NDAVI to monitor multi-decadal seagrass changes across the Chandeleur Sound (ARSET, 2022). However, VIs are limited because the spectral relationships to vegetation biophysical properties and photosynthetic pigments are non-linear and can saturate across bands, meaning that as reflectance in one band increases, the other band may remain fully absorbed.

Recent terrestrial remote sensing studies have used kernelised VIs to improve VI limitations with non-linear spectral relationships and address complexities in sensing vegetation dynamics and phenologies. Typical VIs only account for first-order relationships between the spectral bands, kernelised VIs can account for all the higher-order relationships and summarise all monomials of the differences (i.e., {NIR-red, (NIR-red)², (NIR-red)³, ...}) in a single scalar. Kernelised VIs have several use cases for monitoring vegetation traits and provide better estimates of gross primary production, leaf chlorophyll, leaf area index and photosynthetically active radiation for broadacre crops while reducing error propagation for leaf trait estimation (Wang et al., 2023). Kernelised VIs have also been shown to provide better estimates of latent heat fluxes computed over flux networks and better estimates of carbon content for forest biomes (Wang et al., 2023). Though kernelised VIs were proposed for explicitly monitoring the terrestrial environment (e.g., for monitoring fluxes in gross primary production), we explore if kernelised VIs can be applied for mapping SAV areal extent in shallow coastal regions.

This study investigates the effectiveness of a kernelised VI, kNDAVI, for modelling SAV across a broad geographic region (31.58°S - 29.56°S). We test and validate the performance of the models using three methods: 1] cross-validation, 2] block cross-validation and 3] site validation. In doing so, we compare the predictive accuracy of kNDAVI to an established SAV index and other band and depth combinations. We explore the differences in the areal extent of habitat across the various models and provide suggestions for the best practice for future research of mapping and monitoring of SAV at regional scales. Finally, we present this novel index as a simple, scalable and reliable method to map and monitor SAV at regional and global scales, bridging the gap between the limitations of geographic scale and effective global habitat monitoring.

Methods

Study area

Five study sites on the mid-west coast of Australia were selected as they represent an important fishery zone for the Western Rock lobster fishery and are actively monitored with in situ sampling. The sites spanned from Two Rocks as the southernmost site (115.56°E 31.51°S) to Freshwater as the northernmost site (114.92°E 29.61°S), with Lancelin (115.29°E 31.01°S), Cervantes (115.07°E 30.60°S) and Jurien Bay (114.99°E 30.26°S), in-between (Fig. 7). The sites range in depth from zero to 30 m below sea level and are broadly dominated by brown macroalgae *Ecklonia radiata* and unconsolidated (sandy) substrate, with seagrasses, such as *Posidonia spp.* and *Amphibolis spp.*, sponges and stony corals also present in lower abundance at the sites (Fig. 8).

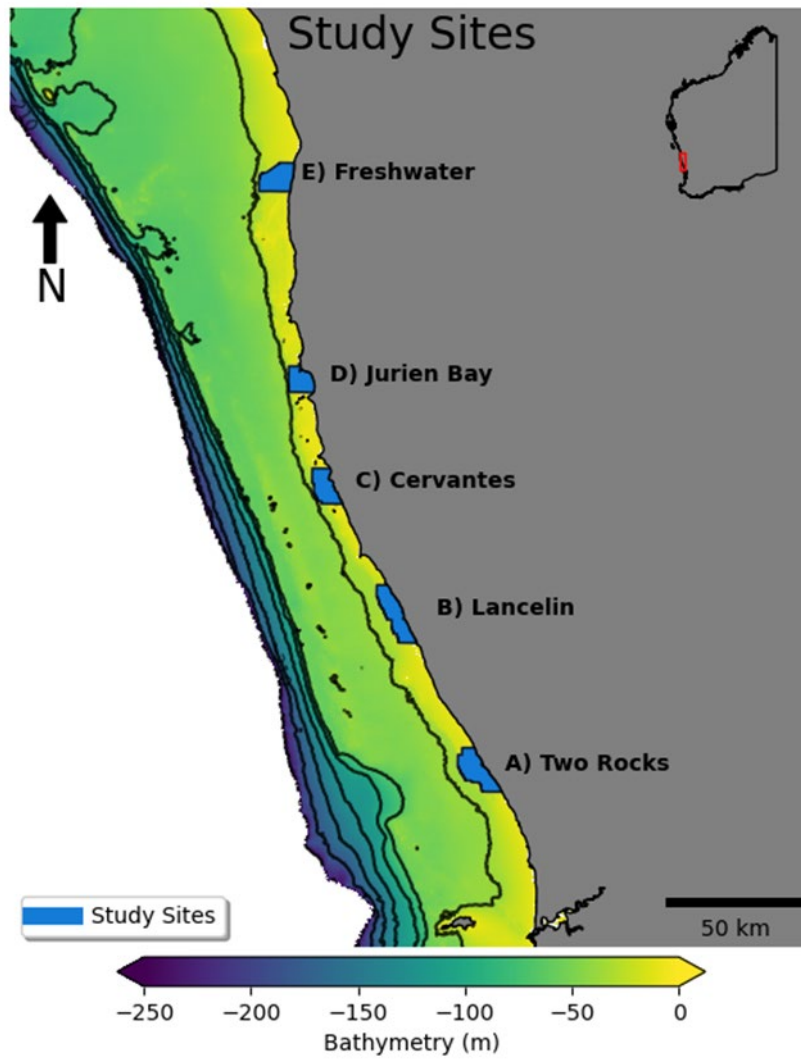


Figure 7 Study sites (blue) span the midwest region of Western Australia. Bathymetry (m) data were sourced from Geoscience Australia's Bathymetry and Topography Grid (Whiteway, 2009). Contour lines represent 30m depth intervals.

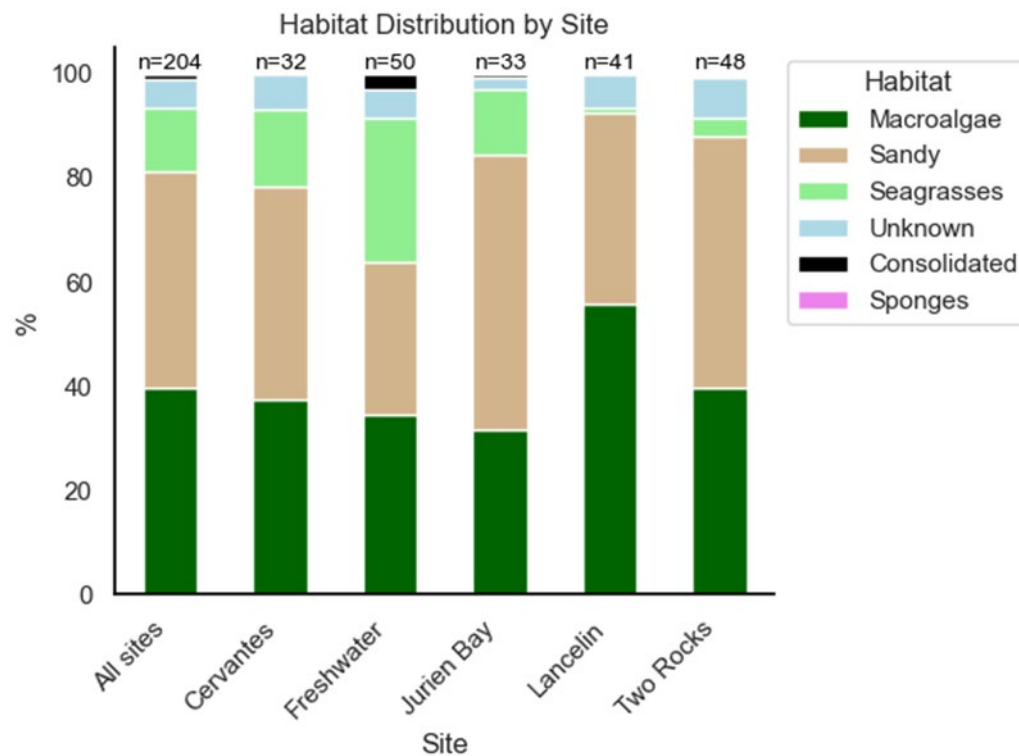


Figure 8 Habitat summaries from the BOSS the underwater image annotations obtained within this study. The percent values represent annotations for each habitat in all images for the corresponding site.

Remote sensing imagery and bathymetry

Google Earth Engine (GEE) and its Python API were utilised to access the Sentinel-2 image library (Gorelick et al., 2017; Wu, 2020). An image collection for April 2021 was sourced from the harmonised Sentinel-2 surface reflectance product (S2SR) for the extent of our study sites (Fig. 7). The S2SR collection was cloud and shadow-masked using the Sentinel-2 QA bands and bitwise operators and subsequently reduced into minimum-value rasters (Fig. 9). A sunglint correction to the mosaic using the methods outlined in Hedley et al. (2005) and Traganos et al. (2018), using a linear correction of each composite band, where bands are adjusted by the spectral range of the near-infrared band was applied at all sites (see section S1). A 10-metre resolution land mask was generated using a Normalised Difference Water Index (NDWI; Fisher et al., 2016), and the image collections were masked to exclude any land within the imagery.

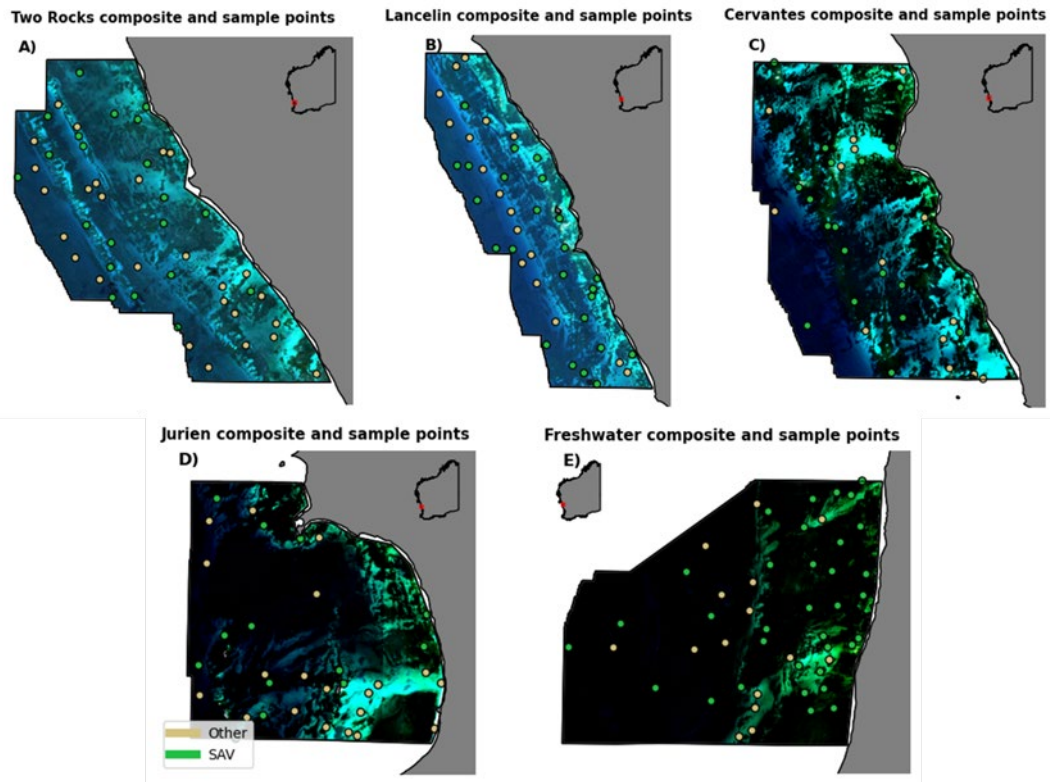


Figure 9 The Sentinel-2 composite images of the five study sites. Panels A-E represent Two Rocks, Lancelin, Cervantes, Jurien and Freshwater, respectively. The sample ground truthing points of the underwater imagery and their corresponding habitat type have been overlaid on the composites for reference. Subplot labels (A-E) correspond to the sites depicted in Figure 7.

Fine-resolution (5m) LiDAR, captured in 2019 and sourced from the West Australian Department of Transport (DoT), provided bathymetric coverage for most of our study sites. LiDAR was unavailable for small portions of the Two Rocks, Cervantes and Freshwater sites (see sections S2). Additionally, we generated Satellite Derived Bathymetry (SDB) for the extent of the study sites using multiple linear regression of the blue and green bands from the S2SR collection, where model coefficients were derived using the site-specific DoT LiDAR data (see section S2; Lyzenga, 1985). As the S2SR product provides imagery at 10m resolution, the DoT LiDAR was resampled to 10m, and the SDB was modelled at the same resolution where SDB is defined as:

$$z = h_0 + h_i X_i + h_j Y_j$$

Where z is the satellite-derived bathymetry, h_0 , h_i , and h_j are the coefficients (intercept and slopes), and X_j and Y_j are the independent variables (the reflectance in the blue and green bands, respectively). As the LiDAR data was captured in 2019, an S2SR image collection was sourced from GEE for modelling for the same year. Thus, the LiDAR and SDB represent coastal depth ranges two years prior to the in-water sampling.

Coastal submerged aquatic vegetation ground truthing surveys

Spatially balanced survey designs were employed to sample the five coastal sites (Stevens and Olsen, 2004). Using an initial K-means unsupervised classification, the sites were stratified with the Sentinel-2 imagery (coastal blue, blue, green and red) and LiDAR (see section S3). We chose the number of centres for the K-means clustering by minimising the within-cluster residual distances (Chiang and Mirkin, 2010). Spectral curves for each cluster were visually assessed, and clusters were grouped based on spectral similarity (see section S3), forming the stratifications for the spatially balanced sampling. We applied Generalized Random Tessellation Stratified (GRTS) design from the R software library 'spsurvey' library (Kincaid et al., 2015) to these unsupervised clustering results to create the spatially balanced survey designs (see section S3). Following the site designs, sites were surveyed between April 7 and 24, 2021, and each sample point represents a unique Ground Truthing Point (GTP) that would subsequently be used for model calibration and validation. Sites were surveyed using the BOSS drop camera system (see [Study 1](#) and section S4). The cameras are horizontally facing and are deployed at each sample location for 1-5 minutes to allow any suspended sediment to settle for clear footage of the sea floor. Imagery is assigned an ordinal rank (very poor, poor, moderate and good) depending on how much of the imagery was obscured; this study restricted use to those images assigned moderate or good. Annotation was confined to the lower 50% of each image to avoid open water (Langlois et al., 2020). The imagery was annotated with 80 randomly allocated points following the Collaborative and Annotation Tools for Analysis of Marine Imagery and Video (CATAMI) classification scheme (Althaus et al., 2015). The classified annotations were split into feature labels using a hierarchical clustering algorithm (see section S4). Clusters were separated based on the proportion of each CATAMI class for all the underwater imagery, resulting in two distinct classes: Submerged Aquatic Vegetation (SAV) and 'other', which comprised unconsolidated (sandy) and consolidated substrate and stony corals and sponges (Fig. 3).

Aquatic vegetation indices

From the S2SR collection, we generated the normalised difference aquatic vegetation index (NDAVI) index $((X_{nir} - X_{blue}) / (X_{nir} + X_{blue}))$ and also the kernelised NDAVI (kNDAVI), which is defined as:

$$kNDAVI = \tanh\left(\left(\frac{X_{nir} - X_{blue}}{2\sigma}\right)^2\right) \quad (1)$$

Where X_{nir} and X_{blue} represent the near-infrared and blue bands of the S2SR collection and σ is the kernel similarity measure representing the mean spectral difference between the blue and NIR bands of each site (N) where σ is defined as:

$$\sigma = N^{-1} \sum_i^N |X_{nir_i} - X_{blue_i}| \quad (2)$$

The sigma value was calculated following the recommendation of Wang et al (2023) and Camps-Valls et al (2021) and represented the mean absolute difference between the NIR and blue bands for each of the five study sites. The σ value for the Two Rocks, Lancelin, Cervantes, Jurien Bay and Freshwater, was computed to be 0.017, 0.021, 0.011, 0.005 and 0.001, respectively.

SAV Classification and Validation

The spectral bands, indices and bathymetry were extracted at each drop camera location as predictors for random forest (RF) models (Breiman, 2001). We tested 12 combinations of optical bands (coastal blue, blue, green and red), calculated indices (NDAVI and kNDAVI) and

bathymetry (SDB and LiDAR) feature sets for the models (see S5 for all model combinations). The RF models were parameterised with 1000 trees and a maximum splitting depth of 4 nodes to avoid overfitting. These models were used to classify SAV and predict the probability of SAV presence at each site. The RF models were validated with three approaches: 1] BlockCV, spatial cross-validation using the 'blockCV' package (Valavi et al., 2018), where the survey data is split into five cross-validation folds and 21 spatial blocks. Block sizes were informed using 'spatialAutoRange' function from the package, and blocks were nested within folds across the study region for training and independent testing and validation; 2] Randomised 5-fold cross-validation (Ramezan et al., 2019), where the data points in each fold were randomly sampled from the survey dataset (see section S6); and 3] Site validation (Cunningham et al., 2009; Lawley et al., 2016), where each site is independently held-out for testing and the remaining four sites are used for training (see section S6). The predictions from each iteration were then independently validated on the ground truth data at the respective hold-out site. The Receiver Operating Characteristic (ROC) curves and Area Under the Curve (AUC) values for each RF model for each validation approach were calculated for model comparison (see section S5).

Results

Model Validations

For all three validation approaches (i.e., cross-validation, block cross-validation and site validation), models with kNDAVI consistently performed better than standard NDAVI or other optical band combinations (Table 1). The RF model trained using kNDAVI and SDB, validated using site folds, performed the best, achieving an average Cohen's kappa score of 0.87 and an AUC of 0.93 (Table 1). Models that used the kNDAVI index performed better than models that included all optical bands. We observed good performance of models using all optical bands instead of a single index, but these models resulted in lower model parsimony due to increased training features. For models that were trained using the optical band features, the blue band (B2) was consistently the most important predictor, except when kNDAVI was also included. There was also a much wider range of variation in NDAVI model performance across sites compared to the kNDAVI models, which performed more consistently across the range of sites (Table 1). Models that included SDB as a depth feature performed marginally better than those that instead included LiDAR (Table 1), with the caveat that SDB was generated using the blue and green optical bands and the coefficients derived from the site DoT LiDAR data. The blue and green bands will interact and reflect the submerged vegetation before interacting with the seafloor. Thus, the SDB product captures the structure and height of the submerged vegetation, likely improving the classification of vegetated benthos. Except where models included kNDAVI, our results show that models tested with site validation (where each site is independently held out from training) performed worse than those tested with block cross-validation or cross-validation.

Model predictions

For each site across the study area, the probability estimates of SAV presence (Fig. 11) and the classifications of SAV (Fig. 12) have been visualised for the best-performing model (kNDAVI and SDB). For each model, we calculate the area and percentage SAV for each site (Table. 2). The kNDAVI and SDB model indicate that Two Rocks, Lancelin, Cervantes, Jurien and Freshwater sites contained 48km², 59km², 50km², 42km² and 76km² of SAV, respectively, with a total extent of 277km². The percentage of SAV at each site was 46%, 56%, 64%, 69% and 86%, respectively, while the percentage of SAV at each site increased with an equatorward gradient (Fig. 12). For all model outputs, Freshwater was consistently predicted to contain the highest

proportion of SAV (>85%), while Two Rocks and Cervantes had the lowest amount of SAV proportionally. The models trained using the kNDAVI and SDB features showed comparable results in terms of SAV area for all sites but also within sites, though the area estimates for the models trained using NDAVI and SDB were varied overall and within sites (Table 2).

Table 1. Validation statistics (kappa) for select feature sets and cross-validation methods. For the independent site cross-validation (Site-CV) Fold-1 through Fold-5 represents Two Rocks, Lancelin, Cervantes, Jurien Bay, and Freshwater, respectively. The overall best-performing model is indicated with an asterisk.

Feature Set	Method	Fold-1	Fold-2	Fold-3	Fold-4	Fold-5	Mean
kNDAVI	Block-CV	0.78	0.78	0.94	0.94	0.82	0.853
NDAVI	Block-CV	0.63	0.69	0.60	0.80	0.61	0.665
kNDAVI + SDB	Block-CV	0.76	0.81	0.91	0.92	0.86	0.856
NDAVI + SDB	Block-CV	0.70	0.87	0.69	0.92	0.71	0.778
kNDAVI	CV	0.77	0.85	0.81	0.83	0.94	0.839
NDAVI	CV	0.74	0.64	0.78	0.60	0.71	0.696
kNDAVI + SDB	CV	0.79	0.79	0.80	0.86	0.94	0.841
NDAVI + SDB	CV	0.85	0.66	0.86	0.70	0.83	0.780
kNDAVI	Site-CV	0.83	0.85	0.94	0.88	0.81	0.863
NDAVI	Site-CV	0.60	0.56	0.69	0.70	0.79	0.668
kNDAVI + SDB	Site-CV	0.85	0.85	0.94	0.88	0.81	0.867*
NDAVI + SDB	Site-CV	0.67	0.66	0.69	0.79	0.77	0.714

* Overall best-performing model.

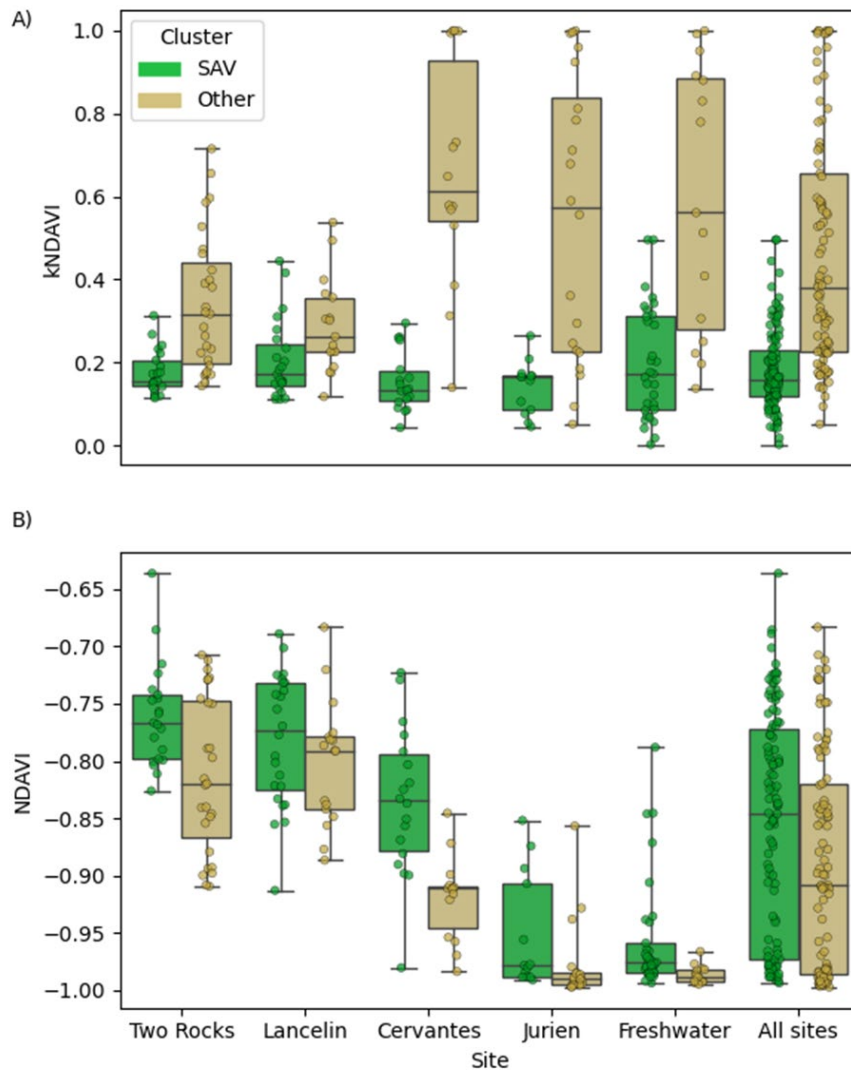


Figure 10 Box plots showing the response of the kNDAVI (panel A) and NDAVI (panel B) index for submerged aquatic vegetation (SAV; green) and non-vegetated (beige) ground truthing points for all sites combined and for each site individually. Due to the tangent function, kNDAVI ranges between 0 and 1 and shows clear distinction between habitat types, while NDAVI range between -1 and 0 and exhibits much less separability between habitat types.

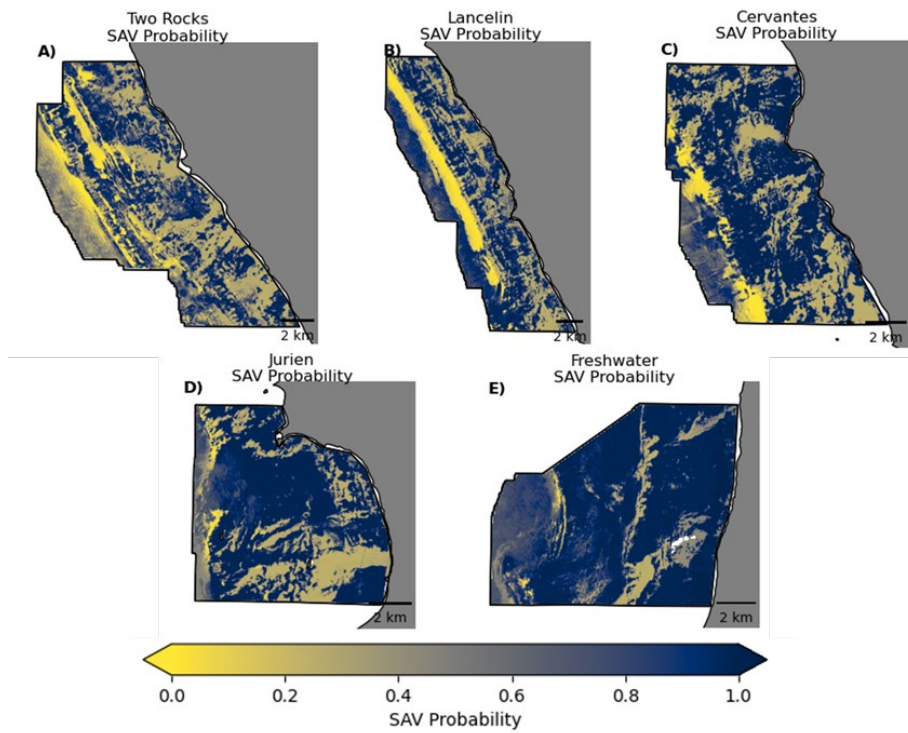


Figure 11 The probability of SAV presence for the five study sites with the kNDAVI and SDB model. Panels A-E represent Two Rocks, Lancelin, Cervantes, Jurien and Freshwater, respectively.

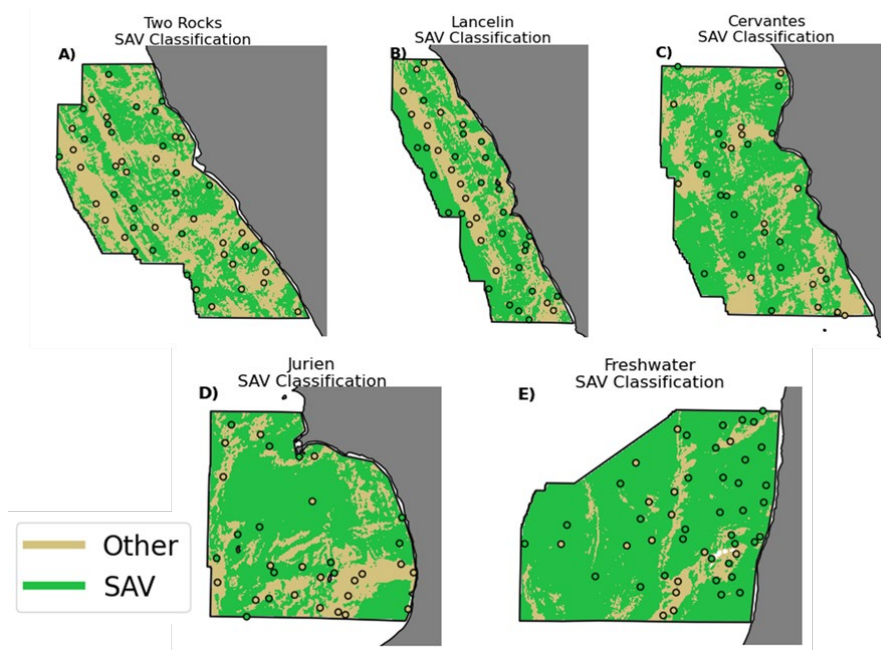


Figure 12 The classification of SAV for the five study sites with the kNDAVI and SDB model. Panels A-E represent Two Rocks, Lancelin, Cervantes, Jurien and Freshwater, respectively. The sample ground truthing points of the underwater imagery and their corresponding habitat type have been overlaid for reference.

Table 2. Estimated area of SAV in square kilometers for the kNDAVI and NDAVI models for each site. Numbers in brackets represent the predicted percentage of SAV at each site for the respective model.

Model	Two Rocks	Lancelin	Cervantes	Jurien	Freshwater	All
kNDAVI	55.8 (53%)	60.5 (57%)	50.7 (65%)	44.7 (73%)	76.6 (87%)	288.3
kNDAVI + SDB	48.6 (46%)	59.8 (56%)	50.0 (64%)	42.7 (69%)	76.0 (86%)	277.1
NDAVI	44.3 (42%)	43.3 (41%)	19.8 (25%)	36.7 (60%)	78.9 (89%)	223.1
NDAVI + SDB	72.6 (68%)	78.9 (74%)	47.4 (61%)	49.6 (80%)	86.3 (97%)	334.8

Discussion

We have demonstrated a novel marine vegetation index, adopted from comparable terrestrial development, for accurately mapping SAV in the midwest coastal region of Western Australia over five disjunct and independent sites covering 400 km of coastline. We tested the models using cross-validation, block cross-validation and site cross-validation. In all cases, the kNDAVI index achieved high accuracy and agreement ($\kappa > 0.80$; McHugh, 2012) for the classification of SAV. The adoption of this novel index for SAV remote sensing studies has considerable potential to facilitate computationally efficient, large-scale, repeatable and cost-effective monitoring of shallow water marine vegetation extents. Moreover, we have shown the effectiveness of balanced sampling designs for mapping habitats across regional spatial scales. The spatially balanced designs, combined with in-water sampling, provide a better representation of heterogeneous benthic habitats with a relatively low amount of ground truthing. For the 433 km² of coastline modelled in this study, only 204 GTPs were required to produce accurate extents of SAV, equating to roughly one sample point per 0.5 km².

Increased sensitivity of kNDAVI to detect SAV

The performance of this novel index, particularly when compared to other aquatic vegetation indices, can be attributed to two factors: 1] the increased sensitivity of the spectrally kernelised bands, and 2] the kernel similarity parameter (σ ; Wang et al., 2023). The increased sensitivity of kNDAVI, is due to the application of the kernel function (the hyperbolic tangent function), which assists in retrieving the maximum information possible from remotely sensed reflectance (Wang et al., 2023). The kernel function enables the detection of higher-order relationships between the near-infrared (NIR) and blue reflectance while being simple to express and practical to apply. The increased sensitivity of kNDAVI to detect SAV is then partly due to the response of the contrasting NIR and blue band to aquatic vegetation, water and substrate. Typically, the NIR signal (800nm to 2500nm) exhibits greater reflectance for plants with high chlorophyll content, but the NIR signal is rapidly absorbed through the water column (Pegau et al., 1997). Conversely, the blue signal (440nm to 500nm) is absorbed by healthy vegetation but has better transmission through the water column (Markager and Vincent, 2000). Established aquatic vegetation indices (i.e., NDAVI and WAVI (Villa et al., 2014a) exploit these contrasting differences between the blue and NIR bands to detect SAV at the spatial scales provided by the remote sensing platforms (Rowan and Kalacska, 2021; Villa et al., 2014b). kNDAVI exploits the same relationship between chlorophyll and the blue band while maximising sensitivity to the marginal differences between the NIR and blue bands. Though the NIR band is fully absorbed in the water column within the first 5m of depth, the spectral information of the NIR band is useful for mapping shallow SAV

such as seagrasses (Villa et al., 2014a). The NIR band further contributes to mapping SAV by correcting for inter-site noise and standardising surface irradiance within the σ parameter. This enables more appropriate inputs into predictive machine learning models across space, resulting in a clear distinction of habitats across spectra and better classification of SAV (Fig. 10).

The sigma parameter (σ) used in kNDAVI varies by an order of magnitude for each site. Thus, σ is an important parameter to consider when applying kNDAVI across varying depths and habitat compositions, at different spatial and temporal scales and when using different types of remote sensing data (either as individual images or image composites). Models without appropriate spatiotemporal calibration are unlikely to be accurate or generalisable (Tsai et al., 2021). This will be particularly true where there is limited training data (as is the case with this study and marine remote sensing in general), models may overfit data, capture localised noise, or be required to predict into space or time that is out of range of the training data (Mizukami et al., 2017; Owens et al., 2013). In this study, we have optimised kNDAVI and (σ) by using multiple locations to explore how habitat composition and depth profiles affect kNDAVI, and by extensively validating model outputs using a range of cross-validation methods to ensure robust parameterisation. Remote sensing can be complex due to space and time variability in imagery, such as tidal changes, wind, wave dynamics, coastal discharge, sediment re-suspension and cloud cover. kNDAVI can be sensitive to these factors that affect image quality and can be influenced by image corrections and image compositions. Nevertheless, we have demonstrated that kNDAVI, with appropriate σ calibration, maximises the spectral information available to map SAV. With proper care taken to calibrate and test models with field data, kNDAVI could be applied to other marine vegetative habitats at multiple sites and scales. It is also computationally efficient and easily scalable via cloud-based remote sensing platforms such as Google Earth Engine. While we have provided a foundational case study on kNDAVI for use in mapping, its wider application to monitoring will benefit from additional case studies and research, which should also be extended to other remote sensing data types and platforms.

Management applicability and considerations

Given the importance of SAV for coastal ecosystems and the declining trends of SAV globally (Rowan and Kalacska, 2021), coupled with increasing trends in increased marine temperatures or heatwaves altering the extents of SAV (Strydom et al., 2020), managing and monitoring coastal ecosystems through reliable mapping is a priority. A critical aspect of environmental management is understanding the drivers of change and quantifying those changes into a narrative for decision-makers (Kilminster et al., 2015). Despite recent advances in in-water and remote sensing habitat monitoring, synthesised approaches for monitoring changes in SAV extents are still lacking. A unified aquatic vegetation index, such as kNDAVI and similar vegetation indices, are a useful tool to address the limitations of shallow water SAV mapping limitations. kNDAVI provides an accessible, reliable and spatially optimised means to establish baseline extents of SAV, with the potential to continuously monitor changes in SAV extent as new imagery or ground-truth data is generated. Indeed, the reliability and sensitivity of kNDAVI to classify SAV across regional geographic domains provide an opportunity SAV change detection and better management of these habitats (Kilminster et al., 2015).

Conclusions

In this study, we have tested and applied a novel remote sensing index, kNDAVI, for mapping SAV across a region of coastal waters along the western coast of Australia. We establish accurate extents of SAV for the region, which could be used to monitor and quantify changes in the future. Our results indicate that kNDAVI effectively distinguishes between aquatic vegetation

and other habitats, even when projecting into sites where training data was withheld, with much higher levels of accuracy than NDAVI and band combinations. kNDAVI achieves this by exploiting substantially more information across the available blue and infrared spectra in remote sensing imagery while including spatial calibration. In the current study, we derived kNDAVI with Sentinel-2 imagery, but it is transferable across many other Earth observation platforms, such as the Landsat inventory, and very high-resolution instruments, such as Worldview and PlanetLabs. Future work could assess the applicability of kNDAVI to create long-term hindcasts of SAV with Landsat imagery and its effectiveness when applied with very-high-resolution sensors. Previous studies have suggested that multispectral platforms like Sentinel-2 do not have the spectral and spatial resolution to distinguish between these SAV habitats (such as seagrass and macroalgae; Rowan and Kalacska, 2021). Future work in marine habitat remote sensing should test indices such as kNDAVI to distinguish between the different habitat types and classes of aquatic vegetation.

Author responsibilities

SM: Conceptualization, Methodology, Software, Formal analysis, Writing – original draft, Writing – review & editing. BR: Conceptualization, Methodology, Data Acquisition, Writing, Funding acquisition. TL: Conceptualisation, Methodology, Data Acquisition, Writing, Funding acquisition. CS: Methodology, Data Acquisition. SD: Methodology, Data Acquisition, Funding acquisition. SH: Conceptualization, Methodology, Data Acquisition, Writing, Funding acquisition.

Declaration of Competing Interest

The authors declare that they have no known competing financial interests or personal relationships that could have appeared to influence the work reported in this paper.

Acknowledgments

The authors acknowledge the Traditional Custodians of the land, the Noongar peoples, and their connections to the land, sea and community. We pay our respects to their Elders past and present and extend that respect to all Aboriginal and Torres Strait Islander peoples. The research as part of the ICoAST collaborative project and acknowledges support from the Indian Ocean Marine Institute Research Centre collaborative research fund and partner organisations AIMS, CSIRO, DPIRD and UWA.

Data availability

Code and imagery to calculate the kNDAVI index is available at the authors GitHub page: <https://github.com/StanleyMastrantonis/kNDAVI>

References

Althaus, F., Hill, N., Ferrari, R., Edwards, L., Przeslawski, R., Schönberg, C.H.L., Stuart-Smith, R., Barrett, N., Edgar, G., Colquhoun, J., Tran, M., Jordan, A., Rees, T., Gowlett-Holmes, K., 2015. A Standardised Vocabulary for Identifying Benthic Biota and Substrata from Underwater Imagery: The CATAMI Classification Scheme. *PLoS One* 10, e0141039.

- ARSET, 2022. Monitoring Aquatic Vegetation with Remote Sensing. NASA Applied Remote Sensing Training Program. <http://appliedsciences.nasa.gov/join-mission/training/english/arset-monitoring-aquatic-vegetation-remote-sensing>
- Breiman, L., 2001. Random Forests. *Mach. Learn.* 45, 5–32.
- Brisset, M., Van Wynsberge, S., Andréfouët, S., Payri, C., Soulard, B., Bourassin, E., Gendré, R.L., Coutures, E., 2021. Hindcast and Near Real-Time Monitoring of Green Macroalgae Blooms in Shallow Coral Reef Lagoons Using Sentinel-2: A New-Caledonia Case Study. *Remote Sensing* 13, 211.
- Brown, C.F., Brumby, S.P., Guzder-Williams, B., Birch, T., Hyde, S.B., Mazzariello, J., Czerwinski, W., Pasquarella, V.J., Haertel, R., Ilyushchenko, S., Schwehr, K., Weisse, M., Stolle, F., Hanson, C., Guinan, O., Moore, R., Tait, A.M., 2022. Dynamic World, Near real-time global 10 m land use land cover mapping. *Scientific Data* 9, 1–17.
- Camps-Valls, G., Campos-Taberner, M., Moreno-Martínez, Á., Walther, S., Duveiller, G., Cescatti, A., Mahecha, M.D., Muñoz-Marí, J., García-Haro, F.J., Guanter, L., Jung, M., Gamon, J.A., Reichstein, M., Running, S.W., 2021. A unified vegetation index for quantifying the terrestrial biosphere. *Sci Adv* 7. <https://doi.org/10.1126/sciadv.abc7447>
- Cavanaugh, K.C., Bell, T., Costa, M., Eddy, N.E., Gendall, L., Gleason, M.G., Hessing-Lewis, M., Martone, R., McPherson, M., Pontier, O., Reshitnyk, L., Beas-Luna, R., Carr, M., Caselle, J.E., Cavanaugh, K.C., Flores Miller, R., Hamilton, S., Hedy, W.N., Hirsh, H.K., Hohman, R., Lee, L.C., Lorda, J., Ray, J., Reed, D.C., Saccomanno, V.R., Schroeder, S.B., 2021. A Review of the Opportunities and Challenges for Using Remote Sensing for Management of Surface-Canopy Forming Kelps. *Frontiers in Marine Science* 8. <https://doi.org/10.3389/fmars.2021.753531>
- Chiang, M.M.-T., Mirkin, B., 2010. Intelligent Choice of the Number of Clusters in K-Means Clustering: An Experimental Study with Different Cluster Spreads. *J. Classification* 27, 3–40.
- Cunningham, S.C., Mac Nally, R., Read, J., Baker, P.J., White, M., Thomson, J.R., Griffioen, P., 2009. A Robust Technique for Mapping Vegetation Condition Across a Major River System. *Ecosystems* 12, 207–219.
- de los Santos, C.B., Olivé, I., Moreira, M., Silva, A., Freitas, C., Araújo Luna, R., Quental-Ferreira, H., Martins, M., Costa, M.M., Silva, J., Cunha, M.E., Soares, F., Pousão-Ferreira, P., Santos, R., 2020. Seagrass meadows improve inflowing water quality in aquaculture ponds. *Aquaculture* 528, 735502.
- Dierssen, H.M., Bostrom, K.J., Chlus, A., Hammerstrom, K., Thompson, D.R., Lee, Z., 2019. Pushing the Limits of Seagrass Remote Sensing in the Turbid Waters of Elkhorn Slough, California. *Remote Sensing* 11, 1664.
- Duffy, J.E., Amaral-Zettler, L.A., Fautin, D.G., Paulay, G., Ryneerson, T.A., Sosik, H.M., Stachowicz, J.J., 2013. Envisioning a Marine Biodiversity Observation Network. *Bioscience* 63, 350–361.
- Duffy, J.E., Benedetti-Cecchi, L., Trinanes, J., Muller-Karger, F.E., Ambo-Rappe, R., Boström, C., Buschmann, A.H., Byrnes, J., Coles, R.G., Creed, J., Cullen-Unsworth, L.C., Diaz-Pulido, G., Duarte, C.M., Edgar, G.J., Fortes, M., Goni, G., Hu, C., Huang, X., Hurd, C.L., Johnson, C., Konar, B., Krause-Jensen, D., Krumhansl, K., Macreadie, P., Marsh, H., McKenzie, L.J., Mieszkowska, N., Miloslavich, P., Montes, E., Nakaoka, M., Norderhaug, K.M., Norlund, L.M., Orth, R.J., Prathep, A., Putman, N.F., Samper-Villarreal, J., Serrao, E.A., Short, F., Pinto, I.S., Steinberg, P., Stuart-Smith,

R., Unsworth, R.K.F., van Keulen, M., van Tussenbroek, B.I., Wang, M., Waycott, M., Weatherdon, L.V., Wernberg, T., Yaakub, S.M., 2019. Toward a Coordinated Global Observing System for Seagrasses and Marine Macroalgae. *Frontiers in Marine Science* 6. <https://doi.org/10.3389/fmars.2019.00317>

Fisher, A., Flood, N., Danaher, T., 2016. Comparing Landsat water index methods for automated water classification in eastern Australia. *Remote Sens. Environ.* 175, 167–182.

Garden, C.J., Smith, A.M., 2011. The role of kelp in sediment transport: Observations from southeast New Zealand. *Mar. Geol.* 281, 35–42.

Gorelick, N., Hancher, M., Dixon, M., Ilyushchenko, S., Thau, D., Moore, R., 2017. Google Earth Engine: Planetary-scale geospatial analysis for everyone. *Remote Sens. Environ.* 202, 18–27.

Griffiths, L.L., Connolly, R.M., Brown, C.J., 2020. Critical gaps in seagrass protection reveal the need to address multiple pressures and cumulative impacts. *Ocean Coast. Manag.* 183, 104946.

Gu, Y., Wylie, B.K., Howard, D.M., Phuyal, K.P., Ji, L., 2013. NDVI saturation adjustment: A new approach for improving cropland performance estimates in the Greater Platte River Basin, USA. *Ecol. Indic.* 30, 1–6.

Hedley, J.D., Harborne, A.R., Mumby, P.J., 2005. Technical note: Simple and robust removal of sunglint for mapping shallow-water benthos. *Int. J. Remote Sens.* 26, 2107–2112.

Hughes, A.R., Williams, S.L., Duarte, C.M., Heck, K.L., Jr, Waycott, M., 2009. Associations of concern: declining seagrasses and threatened dependent species. *Front. Ecol. Environ.* 7, 242–246.

Jamali, A., 2019. Evaluation and comparison of eight machine learning models in land use/land cover mapping using Landsat 8 OLI: a case study of the northern region of Iran. *SN Applied Sciences* 1, 1448.

Kilminster, K., McMahon, K., Waycott, M., Kendrick, G.A., Scanes, P., McKenzie, L., O'Brien, K.R., Lyons, M., Ferguson, A., Maxwell, P., Glasby, T., Udy, J., 2015. Unravelling complexity in seagrass systems for management: Australia as a microcosm. *Sci. Total Environ.* 534, 97–109.

Kincaid, T., Olsen, T., Stevens, D., Platt, C., White, D., Remington, R., Kincaid, M.T., 2015. Package "spsurvey."

Krumhansl, K.A., Okamoto, D.K., Rassweiler, A., Novak, M., Bolton, J.J., Cavanaugh, K.C., Connell, S.D., Johnson, C.R., Konar, B., Ling, S.D., Micheli, F., Norderhaug, K.M., Pérez-Matus, A., Sousa-Pinto, I., Reed, D.C., Salomon, A.K., Shears, N.T., Wernberg, T., Anderson, R.J., Barrett, N.S., Buschmann, A.H., Carr, M.H., Caselle, J.E., Derrien-Courtet, S., Edgar, G.J., Edwards, M., Estes, J.A., Goodwin, C., Kenner, M.C., Kushner, D.J., Moy, F.E., Nunn, J., Steneck, R.S., Vásquez, J., Watson, J., Witman, J.D., Byrnes, J.E.K., 2016. Global patterns of kelp forest change over the past half-century. *Proc. Natl. Acad. Sci. U. S. A.* 113, 13785–13790.

Langlois, T., Goetze, J., Bond, T., Monk, J., Abesamis, R.A., Asher, J., Barrett, N., Bernard, A.T.F., Bouchet, P.J., Birt, M.J., Cappo, M., Currey-Randall, L.M., Driessen, D., Fairclough, D.V., Fullwood, L.A.F., Gibbons, B.A., Harasti, D., Heupel, M.R., Hicks, J., Holmes, T.H., Huveneers, C., Ierodiaconou, D., Jordan, A., Knott, N.A., Lindfield, S., Malcolm, H.A., McLean, D., Meekan, M., Miller, D., Mitchell, P.J., Newman, S.J., Radford, B., Rolim, F.A., Saunders, B.J., Stowar, M., Smith, A.N.H., Travers, M.J., Wakefield, C.B., Whitmarsh, S.K., Williams, J., Harvey, E.S., 2020. A

field and video annotation guide for baited remote underwater stereo-video surveys of demersal fish assemblages. *Methods Ecol. Evol.* 11, 1401–1409.

Lawley, V., Lewis, M., Clarke, K., Ostendorf, B., 2016. Site-based and remote sensing methods for monitoring indicators of vegetation condition: An Australian review. *Ecol. Indic.* 60, 1273–1283.

Lyzenga, D.R., 1985. Shallow-water bathymetry using combined lidar and passive multispectral scanner data. *Int. J. Remote Sens.* 6, 115–125.

Macreadie, P.I., Costa, M.D.P., Atwood, T.B., Friess, D.A., Kelleway, J.J., Kennedy, H., Lovelock, C.E., Serrano, O., Duarte, C.M., 2021. Blue carbon as a natural climate solution. *Nature Reviews Earth & Environment* 2, 826–839.

Markager, S., Vincent, W.F., 2000. Spectral light attenuation and the absorption of UV and blue light in natural waters. *Limnol. Oceanogr.* 45, 642–650.

Massicotte, P., Bertolo, A., Brodeur, P., Hudon, C., Mingelbier, M., Magnan, P., 2015. Influence of the aquatic vegetation landscape on larval fish abundance. *J. Great Lakes Res.* 41, 873–880.

Mateo-García, G., Gómez-Chova, L., Amorós-López, J., Muñoz-Marí, J., Camps-Valls, G., 2018. Multitemporal Cloud Masking in the Google Earth Engine. *Remote Sensing* 10, 1079.

Maxwell, A.E., Warner, T.A., Fang, F., 2018. Implementation of machine-learning classification in remote sensing: an applied review. *Int. J. Remote Sens.* 39, 2784–2817.

McHugh, M.L., 2012. Interrater reliability: the kappa statistic. *Biochem. Med.* 22, 276–282.

Mizukami, N., Clark, M.P., Newman, A.J., Wood, A.W., Gutmann, E.D., Nijssen, B., Rakovec, O., Samaniego, L., 2017. Towards seamless large-domain parameter estimation for hydrologic models. *Water Resour. Res.* 53, 8020–8040.

Owens, H.L., Campbell, L.P., Dornak, L.L., Saupe, E.E., Barve, N., Soberón, J., Ingenloff, K., Lira-Noriega, A., Hensz, C.M., Myers, C.E., Peterson, A.T., 2013. Constraints on interpretation of ecological niche models by limited environmental ranges on calibration areas. *Ecol. Modell.* 263, 10–18.

Pegau, W.S., Gray, D., Zaneveld, J.R., 1997. Absorption and attenuation of visible and near-infrared light in water: dependence on temperature and salinity. *Appl. Opt.* 36, 6035–6046.

Ramezan, C., Warner, T., Maxwell, A., 2019. Evaluation of Sampling and Cross-Validation Tuning Strategies for Regional-Scale Machine Learning Classification. *Remote Sensing* 11, 185.

Roelfsema, C., Lyons, M., Dunbabin, M., Kovacs, E.M., Phinn, S., 2015. Integrating field survey data with satellite image data to improve shallow water seagrass maps: the role of AUV and snorkeller surveys? *Remote Sens. Lett.* 6, 135–144.

Rowan, G.S.L., Kalacska, M., 2021. A Review of Remote Sensing of Submerged Aquatic Vegetation for Non-Specialists. *Remote Sensing* 13, 623.

Schultz, S.T., Kruschel, C., Bakran-Petricioli, T., Petricioli, D., 2015. Error, Power, and Blind Sentinels: The Statistics of Seagrass Monitoring. *PLoS One* 10, e0138378.

- Shi, X., Qin, T., Nie, H., Weng, B., He, S., 2019. Changes in Major Global River Discharges Directed into the Ocean. *Int. J. Environ. Res. Public Health* 16. <https://doi.org/10.3390/ijerph16081469>
- Silberstein, K., Chiffings, A.W., McComb, A.J., 1986. The loss of seagrass in cockburn sound, Western Australia. III. The effect of epiphytes on productivity of *Posidonia australis* Hook. *F. Aquat. Bot.* 24, 355–371.
- Sonobe, R., Yamaya, Y., Tani, H., Wang, X., Kobayashi, N., Mochizuki, K.-I., 2018. Crop classification from Sentinel-2-derived vegetation indices using ensemble learning. *JARS* 12, 026019.
- Stevens, D.L., Olsen, A.R., 2004. Spatially Balanced Sampling of Natural Resources. *J. Am. Stat. Assoc.* 99, 262–278.
- Strydom, S., Murray, K., Wilson, S., Huntley, B., Rule, M., Heithaus, M., Bessey, C., Kendrick, G.A., Burkholder, D., Fraser, M.W., Zdunic, K., 2020. Too hot to handle: Unprecedented seagrass death driven by marine heatwave in a World Heritage Area. *Glob. Chang. Biol.* 26, 3525–3538.
- Traganos, D., Aggarwal, B., Poursanidis, D., Topouzelis, K., Chrysoulakis, N., Reinartz, P., 2018. Towards Global-Scale Seagrass Mapping and Monitoring Using Sentinel-2 on Google Earth Engine: The Case Study of the Aegean and Ionian Seas. *Remote Sensing* 10, 1227.
- Tsai, W.-P., Feng, D., Pan, M., Beck, H., Lawson, K., Yang, Y., Liu, J., Shen, C., 2021. From calibration to parameter learning: Harnessing the scaling effects of big data in geoscientific modeling. *Nat. Commun.* 12, 5988.
- Valavi, R., Elith, J., Lahoz-Monfort, J.J., Guillera-Aroita, G., 2018. blockCV: an R package for generating spatially or environmentally separated folds for k-fold cross-validation of species distribution models. *bioRxiv*. <https://doi.org/10.1101/357798>
- Villa, P., Bresciani, M., Braga, F., Bolpagni, R., 2014a. Comparative Assessment of Broadband Vegetation Indices Over Aquatic Vegetation. *IEEE Journal of Selected Topics in Applied Earth Observations and Remote Sensing* 7, 3117–3127.
- Villa, P., Mousivand, A., Bresciani, M., 2014b. Aquatic vegetation indices assessment through radiative transfer modeling and linear mixture simulation. *Int. J. Appl. Earth Obs. Geoinf.* 30, 113–127.
- Wang, Q., Moreno-Martínez, Á., Muñoz-Marí, J., Campos-Taberner, M., Camps-Valls, G., 2023. Estimation of vegetation traits with kernel NDVI. *ISPRS J. Photogramm. Remote Sens.* 195, 408–417.
- Waycott, M., Duarte, C.M., Carruthers, T.J.B., Orth, R.J., Dennison, W.C., Olyarnik, S., Calladine, A., Fourqurean, J.W., Heck, K.L., Jr, Hughes, A.R., Kendrick, G.A., Kenworthy, W.J., Short, F.T., Williams, S.L., 2009. Accelerating loss of seagrasses across the globe threatens coastal ecosystems. *Proc. Natl. Acad. Sci. U. S. A.* 106, 12377–12381.
- Wernberg, T., Bennett, S., Babcock, R.C., de Bettignies, T., Cure, K., Depczynski, M., Dufois, F., Fromont, J., Fulton, C.J., Hovey, R.K., Harvey, E.S., Holmes, T.H., Kendrick, G.A., Radford, B., Santana-Garcon, J., Saunders, B.J., Smale, D.A., Thomsen, M.S., Tuckett, C.A., Tuya, F., Vanderklift, M.A., Wilson, S., 2016. Climate-driven regime shift of a temperate marine ecosystem. *Science* 353, 169–172.

Whiteway, T., 2009. Australian Bathymetry and Topography Grid, June 2009.
<https://doi.org/10.4225/25/53D99B6581B9A>

Wu, Q., 2020. geemap: A Python package for interactive mapping with Google Earth Engine. *J. Open Source Softw.* 5, 2305.

Yuan, C., Yamagata, T., 2015. Impacts of IOD, ENSO and ENSO Modoki on the Australian Winter Wheat Yields in Recent Decades. *Sci. Rep.* 5, 17252.

Zeng, Y., Hao, D., Huete, A., Dechant, B., Berry, J., Chen, J.M., Joiner, J., Frankenberg, C., Bond-Lamberty, B., Ryu, Y., Xiao, J., Asrar, G.R., Chen, M., 2022. Optical vegetation indices for monitoring terrestrial ecosystems globally. *Nature Reviews Earth & Environment* 3, 477–493.

Zoffoli, M.L., Gernez, P., Rosa, P., Le Bris, A., Brando, V.E., Barillé, A.-L., Harin, N., Peters, S., Poser, K., Spaias, L., Peralta, G., Barillé, L., 2020. Sentinel-2 remote sensing of *Zostera noltei*-dominated intertidal seagrass meadows. *Remote Sens. Environ.* 251, 112020.

Supplementary Material

S1 Sunlint correction

The sunglint correction of the Sentinel-2 imagery follows the methods outlined in Hedley et al (2005). Each of the Sentinel-2 optical bands is included in a multiple linear regression of near-infrared (NIR; B8) reflectance against the optical band reflectance. Let the slope of the regression line for band i be b_i , then all the pixels in the image can be deglinted in band i by the application of the following equation:

$$R'_i = R_i - b_i(R_{B8} - Min_{B8})$$

This reduces the pixel value in band i (R_i) by the product of regression slope (b_i) and the difference between the B8 pixel value (R_{B8}) and the ambient NIR reflectance (Min_{B8}). This gives the sun-glint corrected pixel reflectance in band i essentially represents the NIR reflectance of a pixel with no sunglint and is the minimum NIR value found in the whole image.

S2 Satellite Derived Bathymetry model

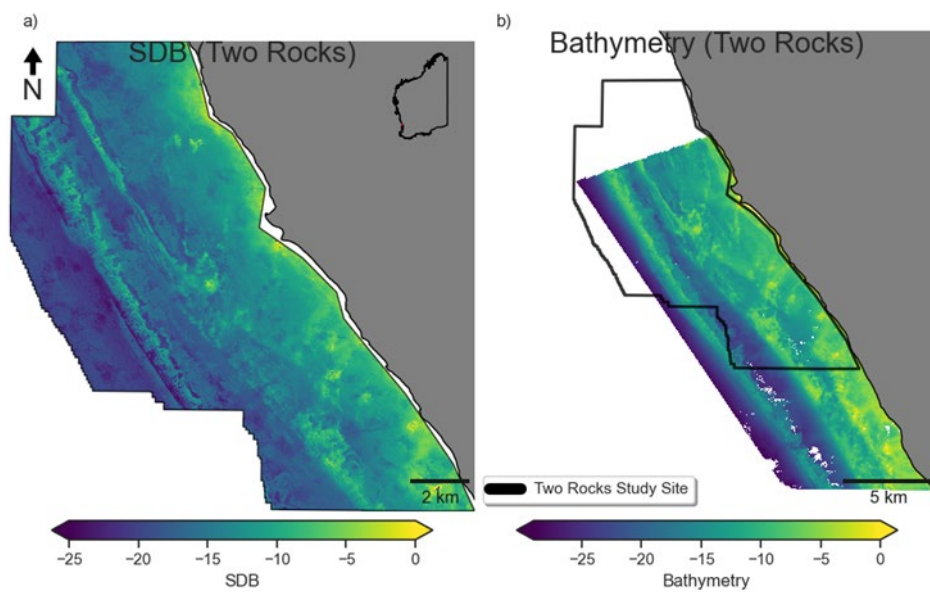
The Satellite Derived Bathymetry model was generated following the methods in Lyzenga (1985). The model is expressed as:

$$z = h_0 + h_i X_j + h_i Y_j$$

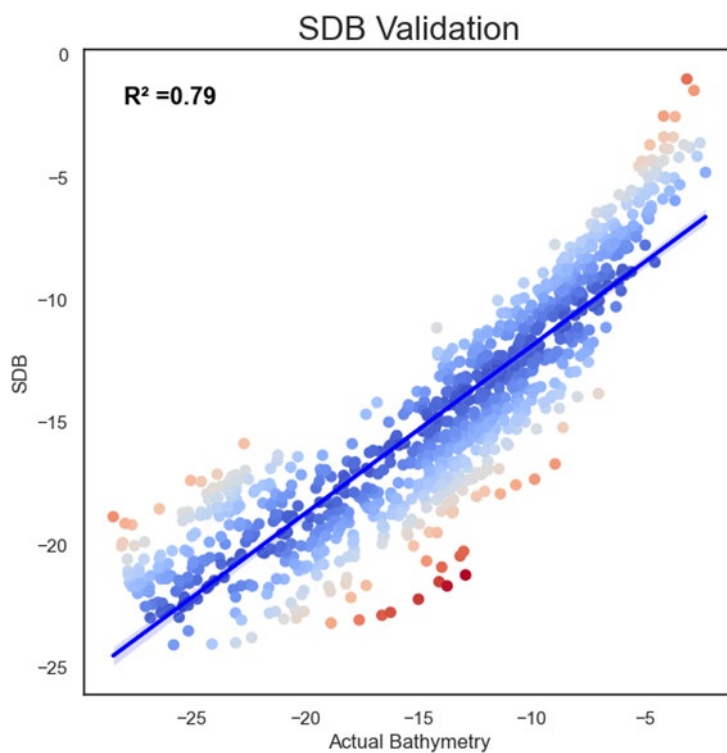
Where z is the satellite-derived bathymetry, h_0 , h_i , and h_i are the coefficients (intercept and slopes), and X_j and Y_j are the independent variables (the reflectance in the blue and green bands, respectively). The R^2 of the model was 0.79 and takes the form:

$$z = -20.97 + 43.17B2 - 38.84B3$$

The coefficients were determined using the Department of Transport LiDAR for each site (Whiteway, 2009).

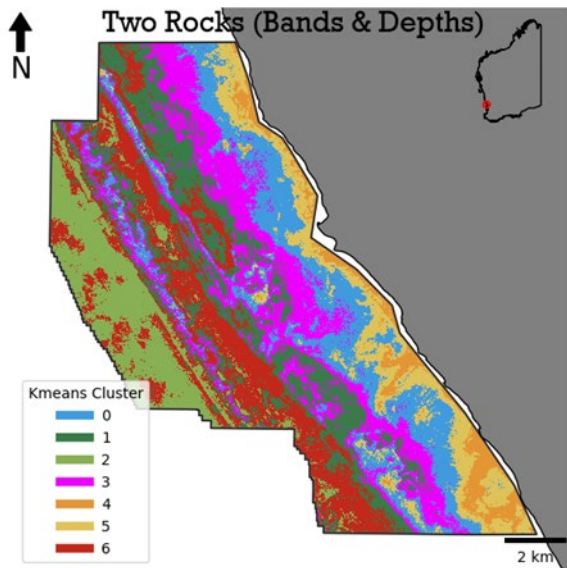


Supporting figure 5: The SDB model (Panel a) and LiDAR dataset (Panel b). Visualised for the two Rocks site.

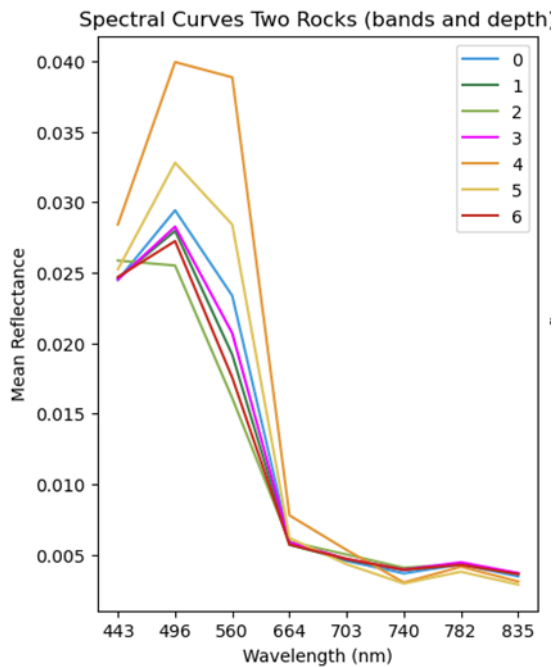


Supporting figure 6: Validation plots (R^2) of the LiDAR (x-axis) against image-derived bathymetries (y-axis) at the Two-Rocks site.

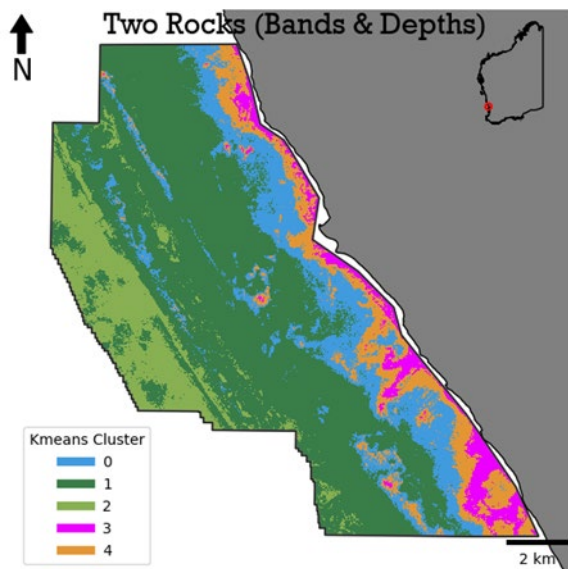
S3 GRTS sampling



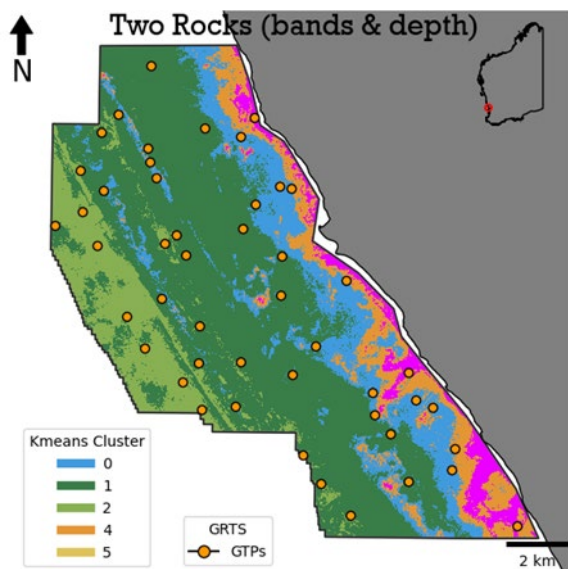
Supporting figure 7: The initial K-means clustering of the Sentinel-2 image composites and depth for the Two Rocks Site.



Supporting figure 8: The spectral curves of mean reflectance for each cluster across the range of wavelengths for the Sentinel-2 imagery.

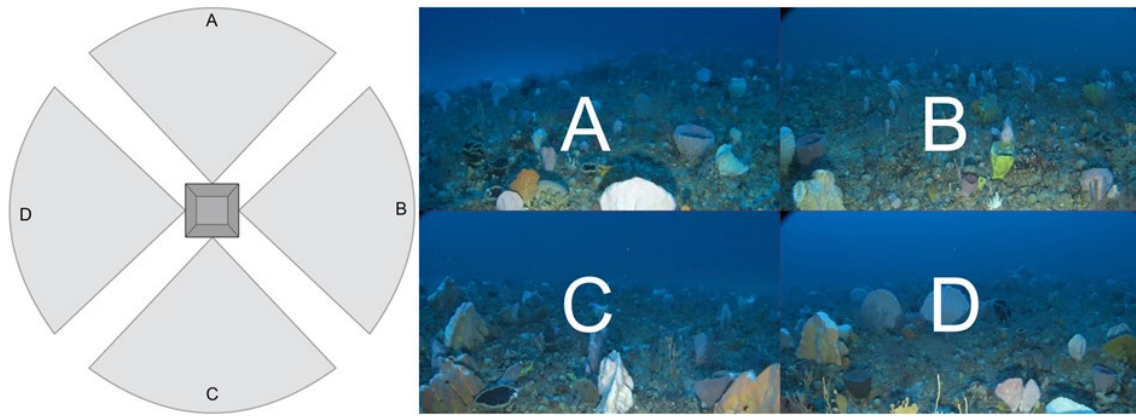


Supporting figure 9: The results of grouping the K-means clustering informed by the spectral curves.

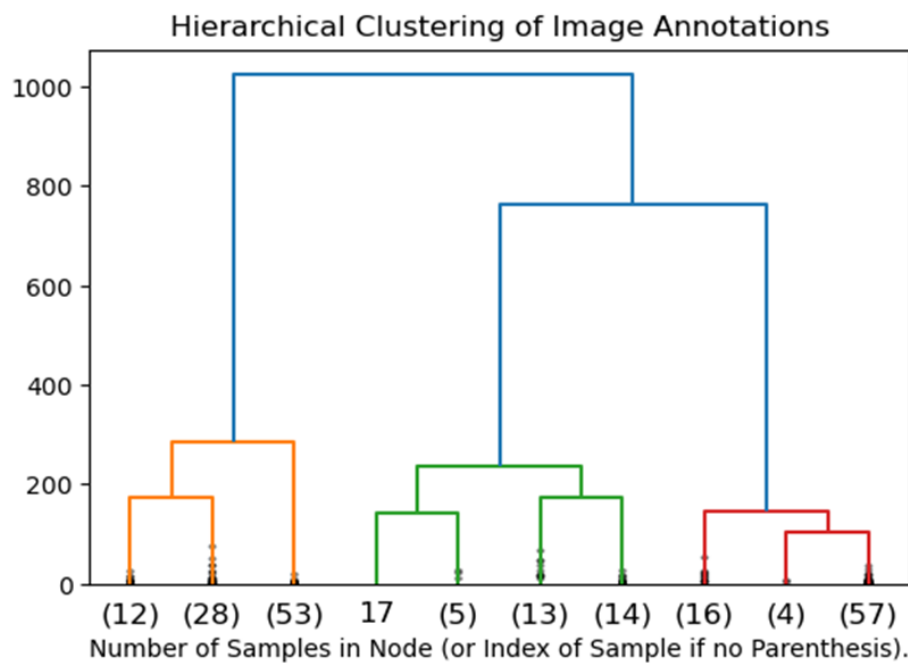


Supporting figure 10: The Generalised Random Tessellation Stratified (GRTS) design for the Two Rocks. The yellow points represent the Ground Truthing Points (GTPs) used for model calibration and validation

S4 Underwater imagery hierarchical clustering

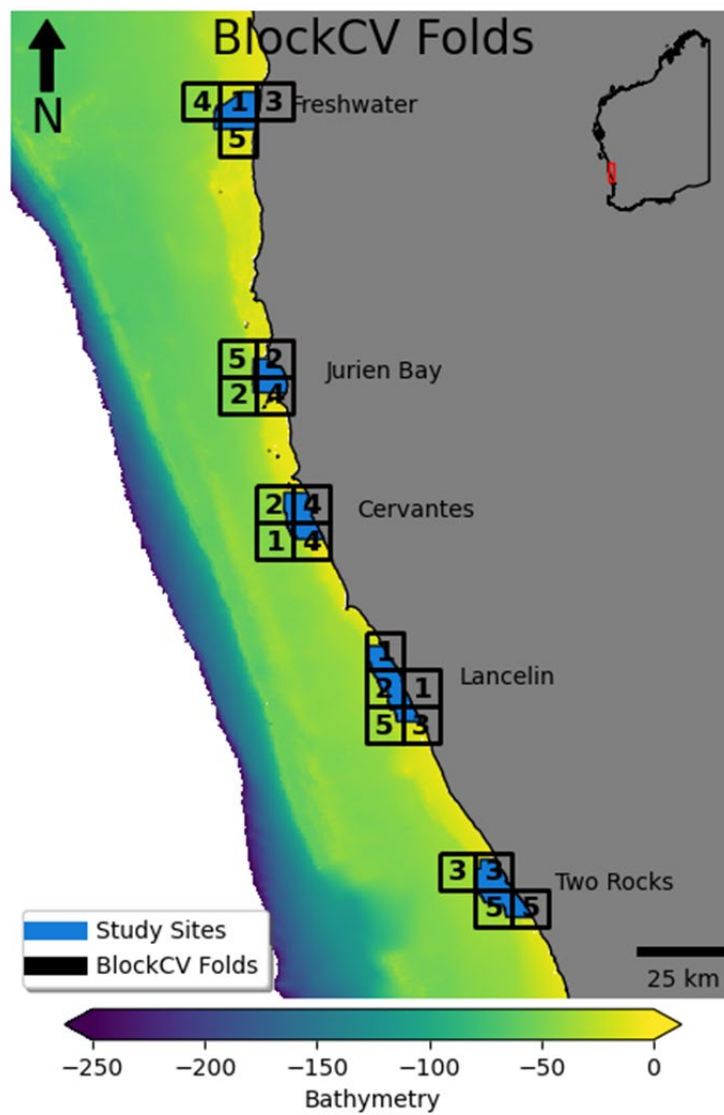


Supporting figure 11: Diagram of the stereo drop-camera imagery and corresponding FOV angles used for the in-water surveys.

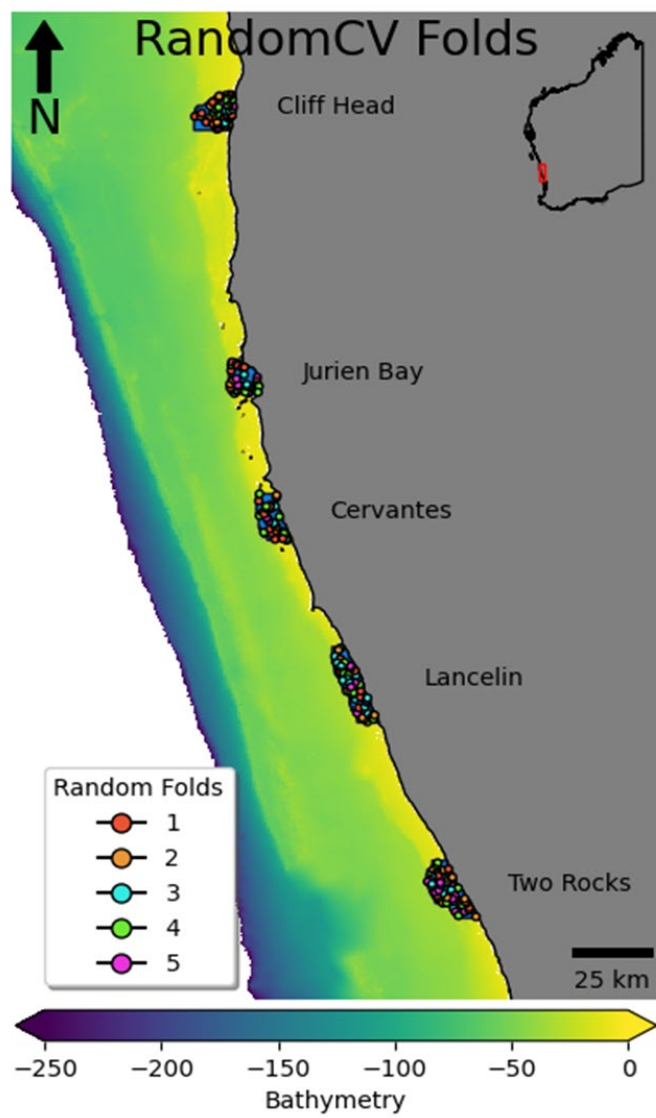


Supporting figure 12: Hierarchical clustering of the annotated underwater imagery. The orange, green and red groups represent unconsolidated, seagrass and macroalgae habitats, respectively. The first group separation was used to label imagery as ‘other’ and Submerged Aquatic Vegetation (SAV).

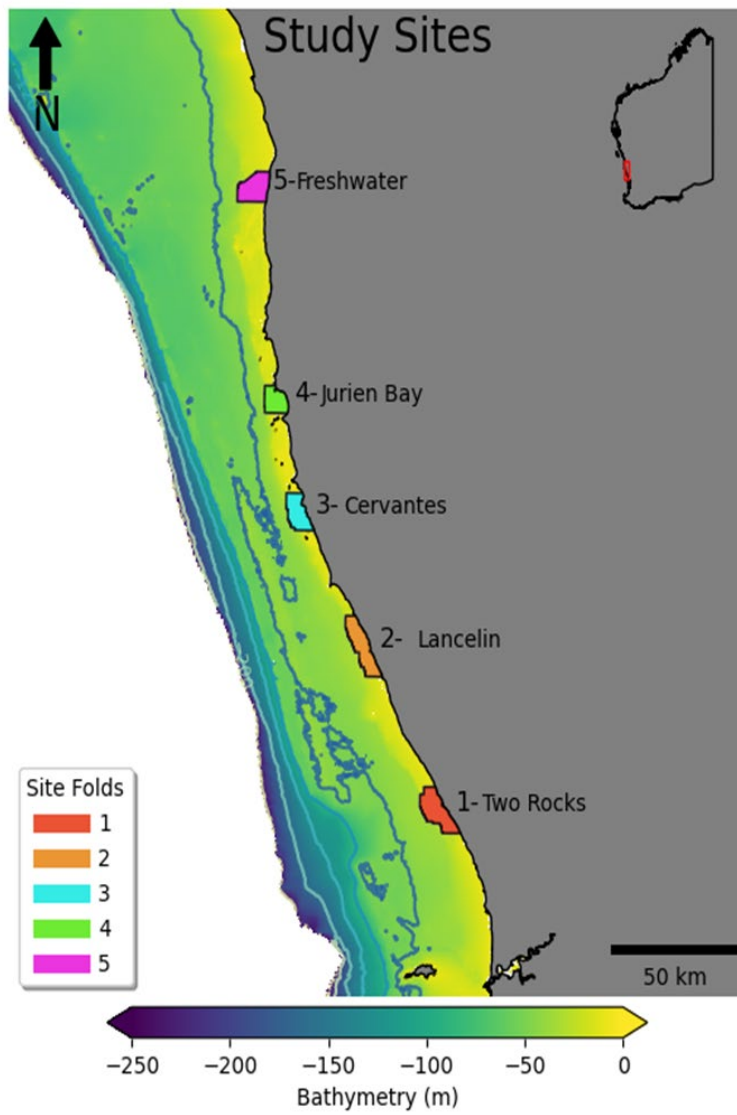
S5 Block-CV, Random-CV and Site-CV Folds



Supporting figure 13: The spatial blocks and folds used for spatial cross-validation. Block sizes and folds were informed and generated using the 'blockCV' package (Valavi et al., 2018).



Supporting figure 14: The randomised folds used for the random 5-fold cross-validation.



Supporting figure 15: The independent site folds used for the 5-fold cross-validation. Ground truth data at each site was iteratively held out of training, and the Random Forest models were trained on the remaining four sites. The predictions from each iteration were then independently validated on the ground truth data at the respective held-out site.

Study 3 - Revealing the impact of spatial bias in survey design for habitat mapping

Preface

This study tests the habitat mapping outcomes between preferential and spatially balanced survey designs. The findings presented here are critical for the future monitoring of seabed habitats that maybe important to the WRLMF and other fisheries around the world. Future studies intending to map and monitor habitat change should employ balanced designs for robust outcomes, similar to hydrographic surveys of water depth.

Revealing the impact of spatial bias in survey design for habitat mapping: a tale of two sampling designs

Published in: Remote Sensing Applications: Society and Environment

<https://doi.org/10.1016/j.rsase.2024.101327>

Authors and affiliations:

Stanley Mastrantonis^{1,2,3,5}, Tim Langlois^{3,5}, Ben Radford^{1,2,3,4}, Claude Spencer^{3,5}, Simon de Lestang^{5,6} and Sharyn Hickey^{1,2,3}

¹ School of Agriculture and Environment, The University of Western Australia, Crawley, WA, Australia

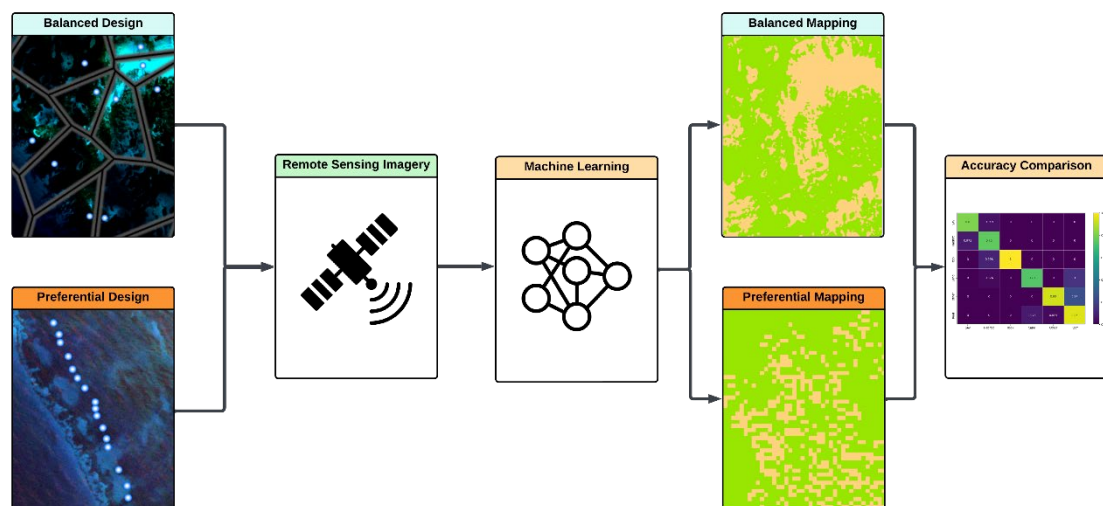
² Centre for Water and Spatial Science, The University of Western Australia, Crawley, WA, Australia

³ UWA Oceans Institute, The University of Western Australia, Crawley, WA, Australia

⁴ Australian Institute of Marine Science, 39 Fairway, Crawley, Western Australia, Australia.

⁵ School of Biological Sciences, The University of Western Australia, Crawley, WA, Australia

⁶ Western Australian Fisheries and Marine Research Laboratories, Department of Primary Industries and Regional Development, North Beach, WA, Australia



Abstract

Submerged aquatic vegetation, referring to benthic macroalgae and plants that obligately grow underwater, are critical components of marine ecosystems and are frequently found to provide preferential recruitment habitats. The mapping and monitoring of aquatic vegetation through remote sensing and machine learning is becoming an important aspect of managing coastal environments at scale. Accurate mapping and monitoring require robust sampling and occurrence data to assess predictive error and quantify submerged vegetation extents. The form of ground truthing survey design (preferential, random, grid-based or spatially balanced) could significantly influence predictive model outcomes and the overall accuracy of mapping and monitoring. Here, we test and contrast mapping aquatic vegetation extent ground-truthed using two different sampling designs: we used both preferential and spatially balanced sampling designs across four coastal sites along the midwest of Australia. We validate the map outcomes using spatial cross-validation and demonstrate that spatially balanced ground truthing significantly outperforms preferential sampling designs regarding modelled extent and map accuracy. In our comparison, we found that, on average, preferential designs overestimated vegetation extent by 25 percent compared to balanced designs and achieved an average kappa statistic, F1 score and Area under the Curve of 0.48, 0.615 and 0.517, respectively, whereas balanced designs achieved a kappa statistic, F1 score and AUC of 0.84, 0.85 and 0.83 respectively. We strongly recommend that sampling designs for remote sensing-derived habitat models be spatially balanced where habitat extent is proposed as a metric for monitoring.

Introduction

Benthic marine habitats are under increasing pressure from climate change (Strydom et al. 2020; Hickey et al. 2020), and accurate methods for monitoring and mapping habitat extent change are imperative for management (Mastrantonis et al. 2024; Arenas-Castro and Sillero 2021). Effective mapping of habitat extents relates ground-truthing data to environmental predictors through statistical or machine-learning approaches (Hirzel and Guisan 2002; Martínez et al. 2012; Wisz et al. 2013; Waśniewski, Hościło, and Aune-Lundberg 2023). Reliable ground-truthing data can be challenging to collect, and field-based sampling is time-consuming and costly, particularly across a large spatial scale (i.e., region) or in heterogeneous landscapes and seascapes (Kéry et al. 2010; Pennino et al. 2019; Christianson and Kaufman 2016). Ground truthing data may be collected in situ based on predetermined designs, such as random, regular or spatially balanced designs (Pennino et al. 2019; Hirzel and Guisan 2002; Mannino, Borfecchia, and Micheli 2021; Kermorvant et al. 2019). However, ground truth data often originates from opportunistic sampling scenarios, such as observing habitats that are known to support a species of interest or in regions deemed likely to yield results. These instances exemplify preferential sampling and are common practice due to their perceived cost-effectiveness (Conn, Thorson, and Johnson 2017; Pennino et al. 2019). In many studies that collect data using preferential sampling, such ground-truthing data often violates the assumptions of independence for geostatistical models, does not cover the range of environmental predictors, and ultimately leads to biased estimates and predictions (Diggle, Menezes, and Su 2010; Conn, Thorson, and Johnson 2017).

To achieve less biased estimates within spatial models, the spatial pattern of the sampling should reflect the spatial heterogeneity of the surveyed habitat. Therefore, an effective sampling strategy is to spread the sampling effort evenly over the habitat, otherwise referred to as spatially balanced designs (Kermorvant et al. 2019). The most popular framework for spatially balanced designs is Generalized Random Tessellation Stratified (GRTS; Stevens and Olsen 2004; Grafström and Tillé 2013). GRTS uses systematic sampling, reverse hierarchical ordering and random permutation of grid cells across a given sampling frame (i.e., study site) to ensure a design that is spatially balanced (Stevens and Olsen 2004). The primary advantage of GRTS is that it allows for a priori stratification of the sampling frame based on background environmental information, such as climate, topography or even stratified remotely sensed data (Lv et al. 2021; Eagleston and Marion 2020; Kermorvant et al. 2019; Mastrantonis et al. 2024). Samples are allocated across each stratum, avoiding over-coverage or under-coverage of any particular stratum, which can happen with preferential or even totally spatially balanced designs (Christianson and Kaufman 2016; Li et al. 2021).

Stratified spatially balanced designs have become increasingly popular for surveying and monitoring benthic habitats (Foster 2021; Foster et al. 2020; Van Hoey et al. 2019). Balanced designs can address challenges associated with marine surveys by optimising sample effort across depth or spectral gradients, providing more information per sampling unit, a better representation of the benthos and ultimately, a more cost-effective design (Foster 2021; Sward, Monk, and Barrett 2022). Recent work has shown the efficacy of using spatially balanced designs in combination with contemporary remote sensing products to accurately map submerged aquatic vegetation at regional (400km of coastline) geographic scales (Mastrantonis et al. 2024).

Critical components of marine ecosystems, macroalgae and seagrass are also referred to as Submerged Aquatic Vegetation (SAV; Rowan and Kalacska 2021). SAV are declining globally (Waycott et al. 2009; Krumhansl et al. 2016), and the global trends of declining SAV are also apparent in Australia, where significant losses to seagrass extents have occurred at the Shark Bay World Heritage Area due to marine heatwaves (Strydom et al. 2020). Given the global

decline in SAV, monitoring and mapping its dynamics and identifying drivers of change at relevant spatiotemporal scales is critical for effective management (Duffy et al. 2019).

With the advent of remote sensing, machine learning and cloud technologies, it has become possible to map SAV at moderate to fine resolutions (10m - 30m) at large, potentially global, geographic scales (Traganos et al. 2018; Duffy et al. 2019; López de Olmos Reyes et al. 2023). Remote sensing for mapping habitats and land cover is time efficient and affordable and is becoming increasingly more accessible through online platforms such as Google Earth Engine (Brown et al. 2022; Gorelick et al. 2017). However, remote sensing alone is insufficient for accurately mapping SAV; without appropriate ground truthing data for model training and validation, mapping SAV can misestimate extents by 30%-50% (Schultz et al. 2015).

Choosing an appropriate sampling design for a particular study is challenging, and there is no ideal design for all research questions (Stehman 2009; Kiefer et al. 2015). Previous research has focused on comparing model outcomes based on the number of samples within the design, the combination of environmental predictors used for modelling, and the parametrisation of models (Emeric Thibaud, Blaise Petitpierre, Olivier Broennimann, Anthony C. Davison, Antoine Guisan 2014). Thibaud et al. found that most of the variation in predictive accuracy was due to sample size and modelling technique and that spatial autocorrelation has marginal impacts, but these findings were based on a 'virtual ecologist' framework where data were simulated (Aubry, Francesiaz, and Guillemain 2024). Other studies have explored methods to account for and correct for bias in preferential survey designs by including bias covariate correction (i.e., constants such as zero or mean values of environmental data) in predictive models (Chauvier et al. 2021). Moreover, many studies have based their conclusions and recommendations on simulated sampling designs (Emeric Thibaud, Blaise Petitpierre, Olivier Broennimann, Anthony C. Davison, Antoine Guisan 2014; Conn, Thorson, and Johnson 2017; Pennino et al. 2019; Hirzel and Guisan 2002; Geiziane Tessarolo, Thiago F. Rangel, Miguel B. Araújo, Joaquín Hortal 2014; Christianson and Kaufman 2016).

Here, we combine a unique dataset of benthic ground truthing data from both preferential and spatially balanced survey designs across the same spatiotemporal range to map SAV across the west coast of Australia. We use environmental predictors, including bathymetric LiDAR, optical remote sensing and an aquatic vegetation index derived from Sentinel-2, to test model outcomes between the two survey designs. We demonstrate significant differences in mapping outcomes between preferential and spatially balanced designs and discuss the importance of balanced designs when instituting habitat mapping studies.

Methods

Study Sites

Four study locations were selected along the mid-west coast of Australia, representing a crucial zone for the Western Rock Lobster fishery. These sites cover a 2-degree latitudinal range from Two Rocks in the south (115.56°E 31.58°S) and Freshwater in the North (114.92°E 29.55°S; Fig. 13). Water depth in the study sites ranges from 0 - 30m, with habitat dominated by macroalgae and unconsolidated (sandy) substrate. Additionally, seagrasses such as *Posidonia* spp. and *Amphibolis* spp., sponges and stony corals are present but in comparatively lower abundance (Fig. 14).

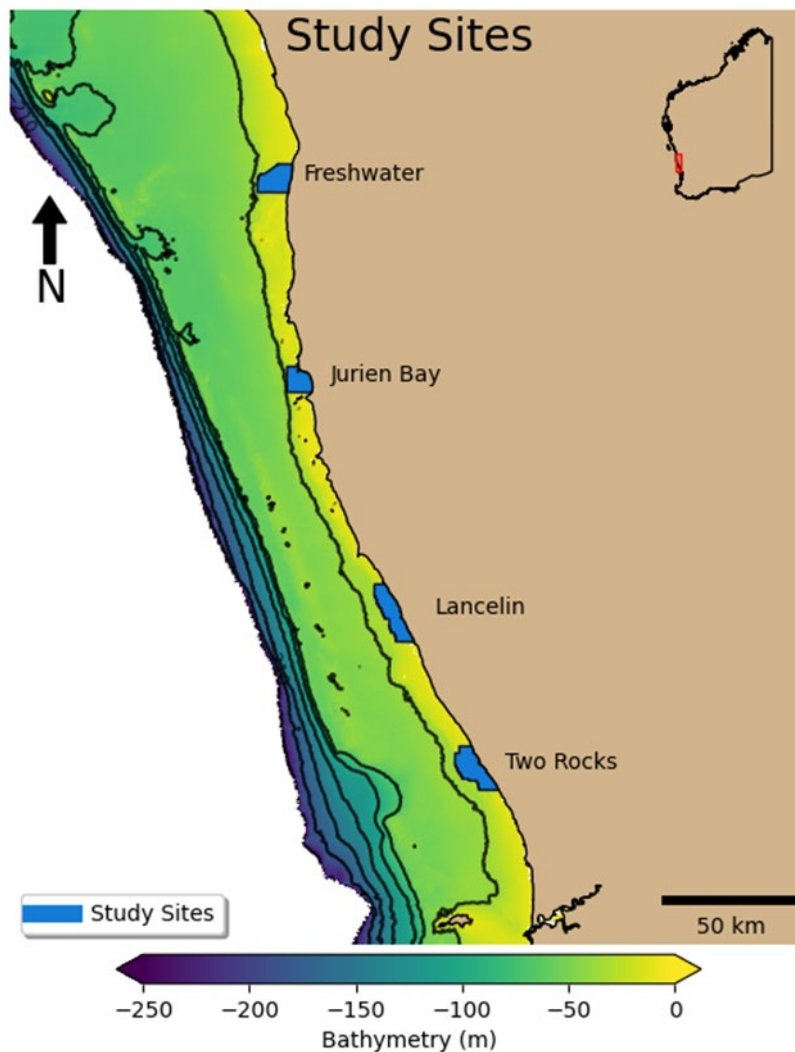


Figure 13 Study sites (blue) span the midwest region of Western Australia. Bathymetry (m) data were sourced from Geoscience Australia's Bathymetry and Topography Grid (Whiteway 2009). Contour lines represent 30m depth intervals.

Survey designs

Two contrasting survey designs were used to compare mapping outcomes for the study sites: a spatially balanced design and a preferential design. The spatially balanced design was prepared and sampled using the BOSS system ([Study 1](#)) and the preferential sampling design was originally designed to provide fishery-independent data for undersize Western Rock Lobster.

Spatially balanced designs

Spatially balanced survey designs were employed to collect SAV occurrence data for the four coastal sites (Stevens and Olsen 2004). Using K-means unsupervised classification, the sites were stratified based on Sentinel-2 imagery and LiDAR data. The number of cluster centres was informed by minimising within-cluster residual distances (Chiang and Mirkin 2010). Spectral curves for each cluster were visually assessed, and clusters were grouped based on spectral similarity. A GRTS design, implemented via the 'spsurvey' library in R (Kincaid et al. 2015), was

used to allocate samples within each stratum, where each sample represents a unique Ground Truthing Point (GTP) for model training and testing.

Surveys were conducted between April 7th and 24th, 2021 at the four sites. A Benthic Observation Survey System (BOSS, see [Study 1](#)), mounted on an aluminium frame, was used for site surveys (<https://drop-camera-field-manual.github.io/>). Four cameras were each positioned for horizontal footage, providing a wide-field (~2700) of view, and the frame was deployed at each GTP for 1-5 minutes to ensure that any suspended sediment settled for clear footage. The imagery was ranked ordinally (very poor, poor, moderate, and good) based on the level of obstruction within the image, with this study only using imagery ranked as moderate or good. Image annotation was confined to the lower 50% of each image to avoid open water (Langlois et al. 2020). For each image, 80 randomly allocated points were annotated using a modified version of the Collaborative and Annotation Tools for Analysis of Marine Imagery and Video (CATAMI) classification scheme (Althaus et al. 2015; Fig. 14).

The annotated imagery was classified into feature labels using a hierarchical clustering algorithm using the 'Scikit-Learn' library (Kramer 2016). These clusters were delineated by the proportion of each CATAMI class in all underwater imagery, resulting in two distinct classes: 'Submerged Aquatic Vegetation (SAV)' and 'other', which includes unconsolidated and consolidated substrate, stony corals, and sponges.

Preferential designs

The preferential SAV occurrence data was derived from the Department of Primary Industries and Regional Developments (DPIRD) Independent Shallow Survey (ISS) programme. The ISS survey is designed to monitor the nearshore regions with reduced catch rates, which were historically productive shallow fishing grounds. The survey revisits areas that have been surveyed since 2019, and the precise sample locations have been determined with input from more than 30 coastal fishers and represent areas for each location that commercial fishers associate with juvenile Western Rock Lobster populations. It is important to note that ISS is designed to monitor localised changes in juvenile Western Rock Lobster populations over time and not for explicitly mapping habitats in space and time.

The ISS surveys were conducted between August 14th 2020, and August 4th 2021. The camera systems, image annotations and classification were similar to the methods outlined for the spatially balanced occurrence data.

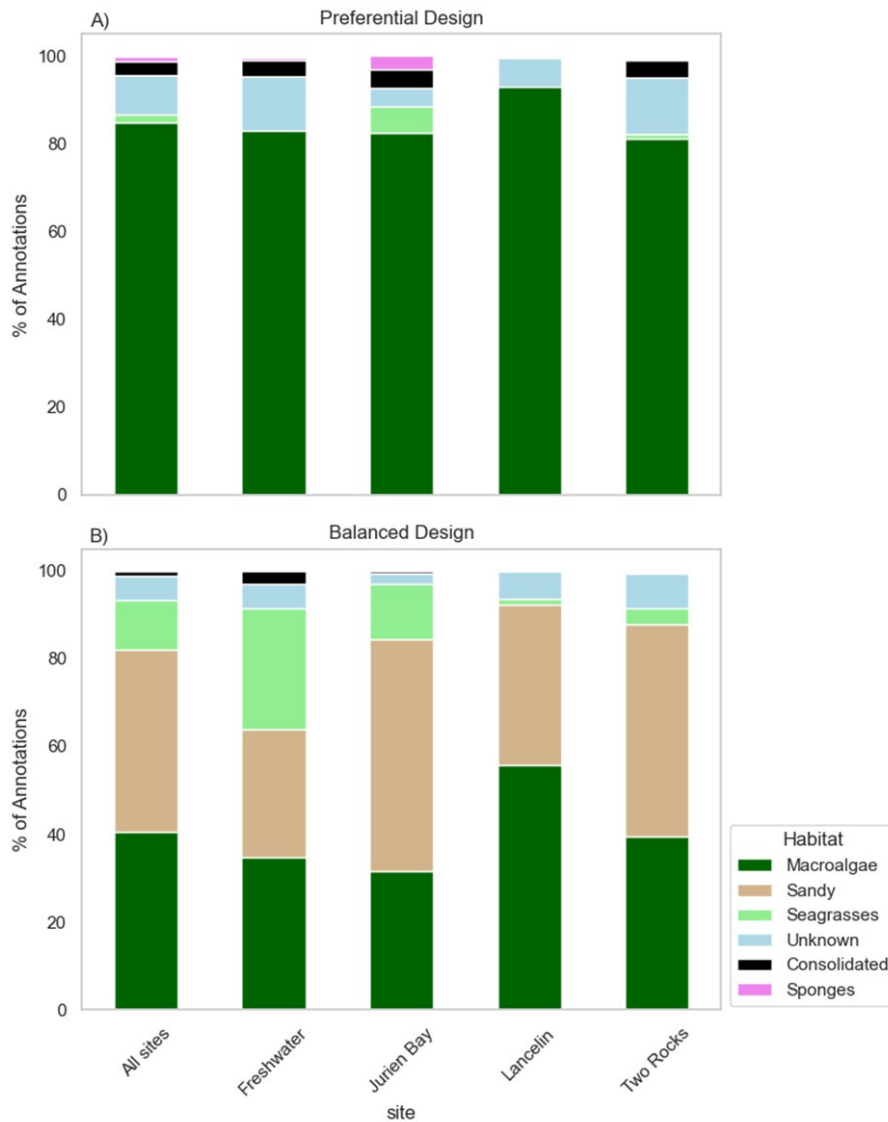


Figure 14 Habitat summaries of the preferential (Panel A) and balanced (Panel B) underwater image annotations for all study sites. The percent values represent annotations for each habitat in all images for the corresponding site.

Remote sensing imagery and bathymetry

The Sentinel-2 image library was accessed using Google Earth Engine (GEE) and its Python API (Gorelick et al. 2017; Wu 2020). An image collection for April 2021 was retrieved from the harmonised Sentinel-2 surface reflectance product (S2SR) within the scope of our study sites. The S2SR collection was cloud and shadow masked using Sentinel-2 QA bands and bitwise operators, and the collection was reduced into minimum-value rasters. A sunglint correction was applied to the rasters (Hedley, Harborne, and Mumby 2005). This correction linearly adjusts the S2SR colour bands based on the spectral range of the near-infrared band, correcting sunglint-affected pixels. A 10-meter resolution land mask was generated using the Normalised Difference Water Index (NDWI; Fisher, Flood, and Danaher 2016), and the rasters were then masked to the seaward extent of each study site. The blue band (B2) from the S2SR raster was used as an environmental predictor for SAV extent modelling.

High-resolution (5m) LiDAR data obtained from the West Australian Department of Transport (DoT) was accessible for all study sites but data was unavailable for certain portions of the Two

Rocks and Freshwater sites. The LiDAR data was used as an environmental predictor for the SAV extent models.

Aquatic vegetation Indices

The kernalised Normalised Difference Aquatic Vegetation Index (kNDAVI) was derived from the S2SR rasters (see [Study 2](#)). kNDAVI is defined as:

$$kNDAV = \tanh\left(\left(\frac{X_{nir} - X_{blue}}{2\sigma}\right)^2\right)$$

Where X_{nir} and X_{blue} represent the near-infrared and blue bands of the S2SR raster and is the kernel similarity measure representing the mean spectral difference between the blue and NIR bands of each site (N), where $\sigma = N - 1 \sum_i^N |X_{nir} - X_{blue}_i|$

The sigma value was calculated following the recommendation of Wang et al. (2023) and Camps-Valls et al. (2021) and represented the mean absolute difference between the NIR and blue bands for each of the four study sites.

SAV Classification and Validation

The values of the blue band, kNDAVI and bathymetry were extracted at the GTP locations of both survey designs to serve as environmental predictors for Random Forest (RF) models (Breiman 2001). To prevent overfitting, RF models were parameterised with 1000 trees and a maximum splitting depth of 4 nodes. These models were used to classify SAV and predict the probability of SAV presence at each site for the spatially balanced and ISS occurrence data.

We used each of the four sites to create spatial cross-validation folds. In other words, the GTPs from each site were iteratively held-out from model training, the model was fit on the remaining three sites, and each site was classified into ‘SAV’ or ‘other’. The classifications were then validated on the held-out site GTPs based on the kappa statistics, F1 scores and Area Under the Curve (AUC; Wardhani et al. 2019).

Results

For mapping SAV, preferential designs overestimated SAV by 25.25%, 21.5% and 5.5% for the kNDAVI, Blue Band and LiDAR models, respectively (Table 3). The significant differences between the predicted extent and probability of SAV between the preferential and balanced kNDAVI models have been visualised for the four coastal sites (Figs. 15 - 16). Regarding map accuracy validation, preferential designs using the kNDAVI predictor achieved an average kappa, F1 score and AUC of 0.489, 0.615 and 0.517, respectively (Table 4). Balanced designs using the kNDAVI predictor achieved an average kappa, F1 score and AUC of 0.853, 0.853 and 0.835, respectively (Table 3). Preferential designs using the blue band achieved an average kappa, F1 score and AUC of 0.608, 0.746 and 0.670, respectively (Table 3). Balanced designs using the blue band achieved an average kappa, F1 score and AUC of 0.679, 0.705 and 0.667, respectively (Table 3). Preferential designs using the LiDAR data achieved an average kappa, F1 score and AUC of 0.548, 0.682 and 0.551, respectively (Table 3). Balanced designs using the LiDAR data achieved an average kappa, F1 score and AUC of 0.679, 0.705 and 0.667, respectively. Generally, models that were trained using balanced ground truth data achieved higher validation metrics when compared to models trained using preferential data, and this is true even when accounting for class imbalances in the RF models (Table 3).

Table 3. Estimated area of SAV in square kilometers for each model and site. Numbers in brackets represent the predicted percentage of SAV at each site for the respective model.

Model	Design	Freshwater	Jurien	Lancelin	Two Rocks
kNDAVI	Preferential	87.34 (99%)	56.12 (92%)	93.12 (89%)	93.18 (90%)
kNDAVI	Balanced	76.66 (87%)	44.53 (73%)	59.62 (57%)	54.87 (53%)
B2	Preferential	86.36 (98%)	54.29 (89%)	97.30 (93%)	76.61 (74%)
B2	Balanced	87.54 (99%)	54.90 (90%)	27.20 (26%)	53.83 (53%)
LiDAR	Preferential	53.75 (61%)	53.68 (88%)	77.43 (74%)	76.62 (74%)
LiDAR	Balanced	60.80 (69%)	40.26 (66%)	77.42 (74%)	68.33 (66%)

Table 4. Validation metrics of different models and designs

Statistic	Model	Design	Two Rocks (n=48)	Lancelin (n=41)	Jurien (n=33)	Freshwater (n=48)	Mean
Kappa	kNDAVI	Balanced	0.833	0.854	0.879	0.812	0.845
F1	kNDAVI	Balanced	0.826	0.857	0.857	0.873	0.853
AUC	kNDAVI	Balanced	0.841	0.875	0.887	0.736	0.835
Kappa	B2	Balanced	0.729	0.634	0.667	0.688	0.679
F1	B2	Balanced	0.755	0.545	0.703	0.815	0.705
AUC	B2	Balanced	0.754	0.688	0.725	0.500	0.667
Kappa	LiDAR	Balanced	0.729	0.634	0.667	0.688	0.679
F1	LiDAR	Balanced	0.755	0.545	0.703	0.815	0.705
AUC	LiDAR	Balanced	0.754	0.688	0.725	0.501	0.667
Statistic	Model	Design	Two Rocks (n=80)	Lancelin (n=59)	Jurien Bay (n=96)	Freshwater (n=100)	Mean
Kappa	kNDAVI	Preferential	0.412	0.576	0.438	0.53	0.489
F1	kNDAVI	Preferential	0.584	0.699	0.491	0.685	0.615
AUC	kNDAVI	Preferential	0.505	0.597	0.493	0.478	0.517
Kappa	B2	Preferential	0.413	0.763	0.698	0.56	0.608
F1	B2	Preferential	0.582	0.663	0.72	0.718	0.670
AUC	B2	Preferential	0.504	0.494	0.491	0.5	0.496
Kappa	LiDAR	Preferential	0.408	0.492	0.729	0.56	0.548
F1	LiDAR	Preferential	0.584	0.583	0.843	0.712	0.682
AUC	LiDAR	Preferential	0.503	0.706	0.500	0.501	0.551
Statistic	Model (class weights)	Design	Two Rocks (n=80)	Lancelin (n=59)	Jurien Bay (n=96)	Freshwater (n=100)	Mean
Kappa	kNDAVI	Preferential	0.412	0.797	0.500	0.540	0.562

F1	kNDAVI	Preferential	0.584	0.880	0.586	0.685	0.683
AUC	kNDAVI	Preferential	0.500	0.619	0.512	0.492	0.530
Kappa	B2	Preferential	0.411	0.831	0.698	0.56	0.625
F1	B2	Preferential	0.582	0.707	0.825	0.718	0.708
AUC	B2	Preferential	0.500	0.480	0.491	0.5	0.492
Kappa	LiDAR	Preferential	0.408	0.525	0.729	0.56	0.556
F1	LiDAR	Preferential	0.586	0.622	0.846	0.716	0.692
AUC	LiDAR	Preferential	0.500	0.725	0.500	0.501	0.556

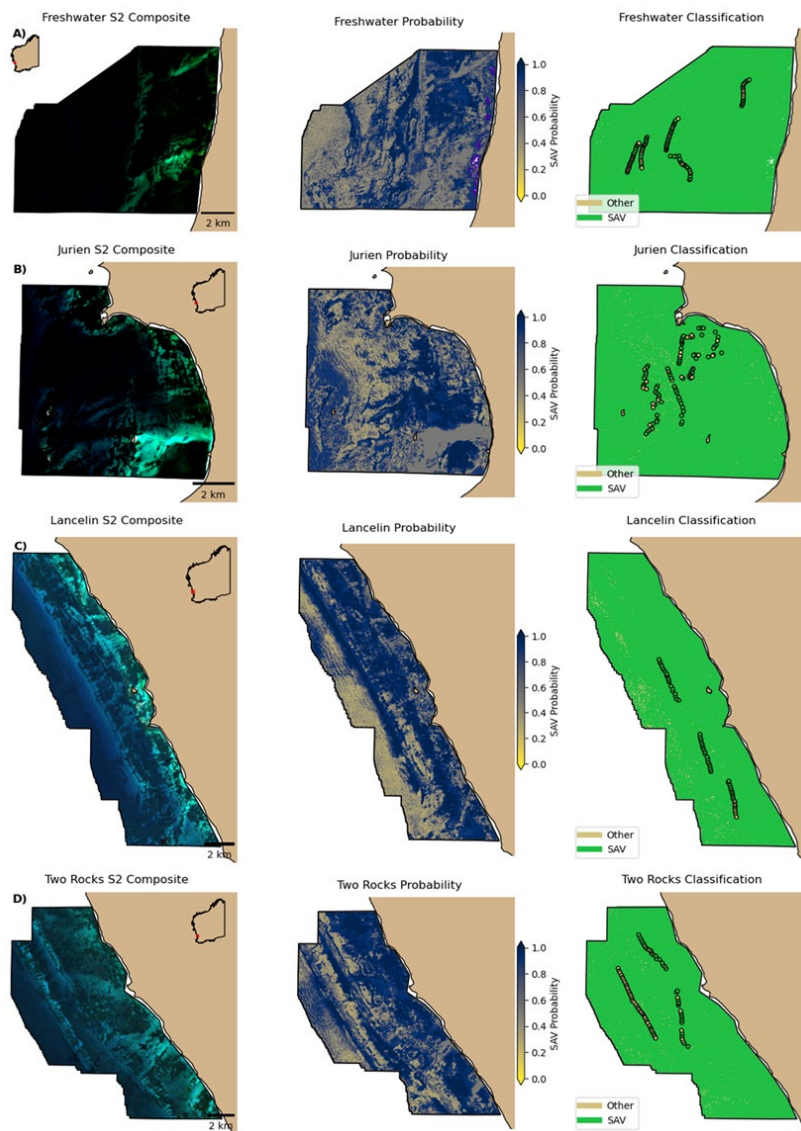


Figure 15 Sentinel-2 composite image, habitat probability estimates and habitat classification using the preferential survey design data and the kNDAVI remotely sensed index. The point data represents the ground control sample points where green is 'SAV' and tan is 'Other' benthic habitat. Panel A represents the model outcomes for the Freshwater site. Panel B represents the model outcomes for the Jurien site. Panel C represents the model outcomes for the Lancelin site. Panel D represents the model outcomes for the Two Rocks site.

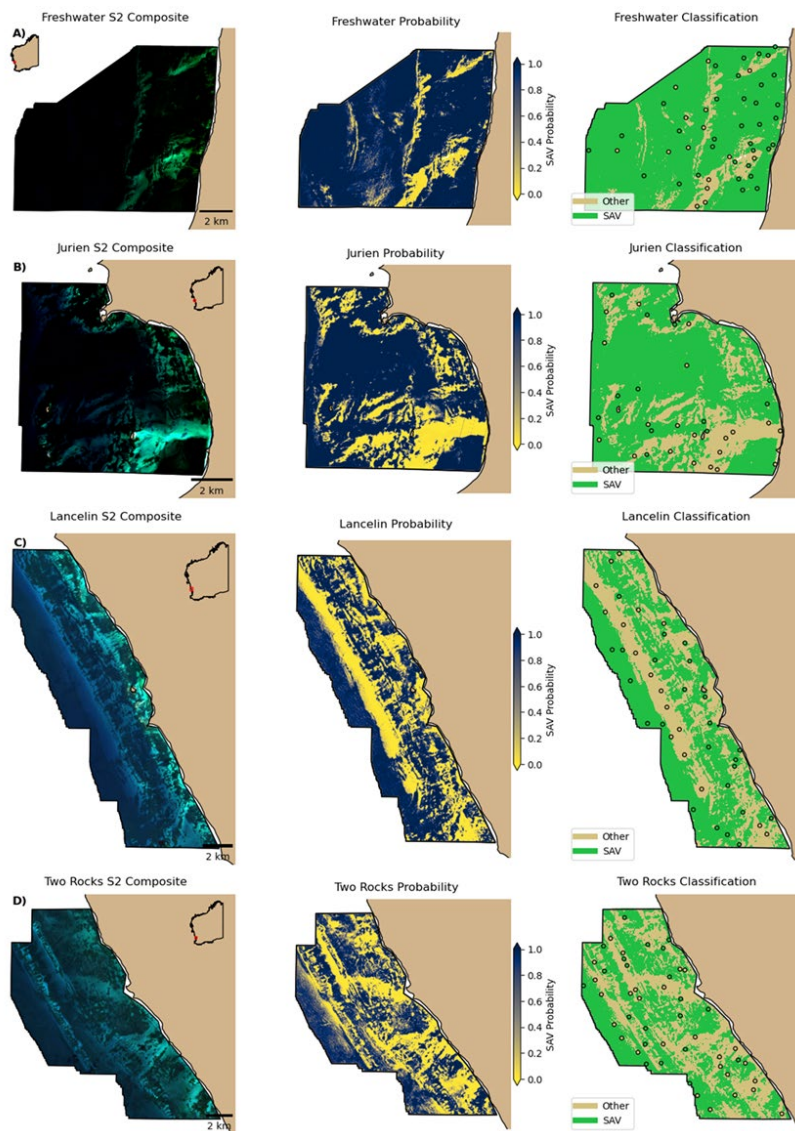


Figure 16 Sentinel-2 composite image, habitat probability estimates and habitat classification using the spatially balanced survey design data and the kNDAVI remotely sensed index. The point data represents the ground control sample points where green is 'SAV' and tan is 'Other' benthic habitat. Panel A represents the model outcomes for the Freshwater site. Panel B represents the model outcomes for the Jurien site. Panel C represents the model outcomes for the Lancelin site. Panel D represents the model outcomes for the Two Rocks site.

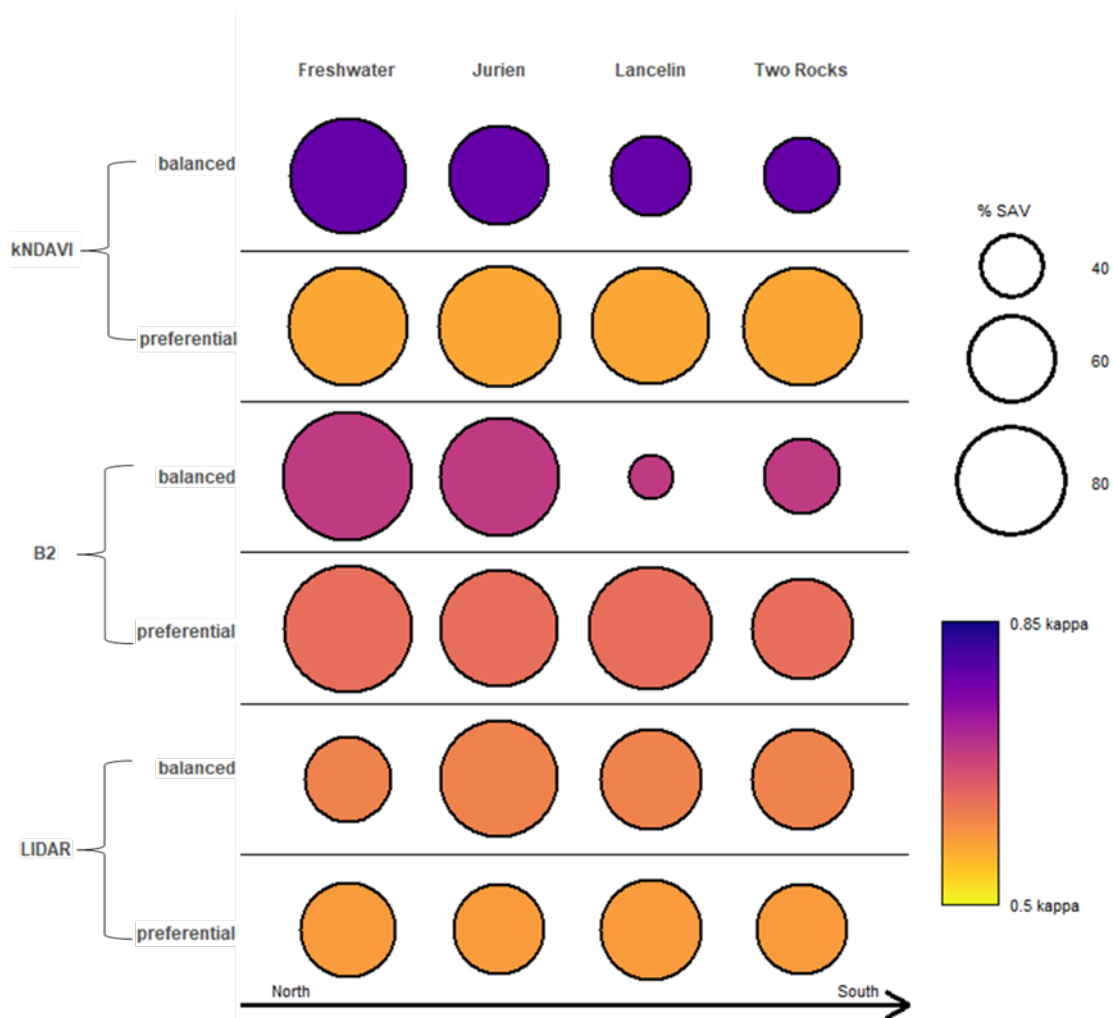


Figure 17 Summary visualisation of model outcomes. Each model with the type of sampling design and predictor variable is shown on the left y-axis, while sites are depicted on the top x-axis. The colour hue of each circle represents the kappa statistic for each model, while the size of the circle represents the percent of SAV in each site area predicted by each model.

Discussion

Habitat extent data derived from preferential designs significantly overestimates SAV and results in poor model and map accuracy. The overestimation of SAV extent is predominantly due to the unbalanced occurrence data inherent with the preferential designs. The preferential design included 335 GTPs, with over 90% of these annotations being macroalgae (Fig. 14). In contrast, the balanced design included only 172 GTPs, with 42% of these annotations being macroalgae. Despite being common in remote sensing studies, unbalanced training data is a significant problem for machine learning classification, and previous research has suggested addressing unbalanced training data within ensemble models (Chen, Liaw, and Breiman 2004; Mellor et al. 2015). It is important to note that we attempted to address the training data imbalance by including ensemble weightings in the RF models. Still, these models resulted in negligible improvements in accuracy (Table 4).

Generally, more training data results in better outcomes for mapping and monitoring habitats, but there are clear trade-offs between sampling effort and sample quality and the accuracy of models (Maccherini et al. 2020; Del Vecchio et al. 2019). The results presented here clearly indicate that balanced survey designs significantly improve habitat mapping outcomes even with fewer samples. This finding is somewhat counter-intuitive, where the preferential surveys are

designed to monitor WRL and their localised habitat use but result in poor accuracy and mapping of that habitat at scale. Conversely, here the balanced design allocated substantially less sampling effort across the habitat of interest but resulted in much better outcomes for mapping that habitat. Thus, accurate mapping of habitats, particularly SAV, should always be instigated with a sampling plan representative of all the ecological gradients in the sampling frame rather than just the habitat of interest.

The type of predictor data used also affects the accuracy and predictions of SAV extents, albeit to a much lesser degree than the survey design. The balanced design using the kNDAVI predictor performed the best, achieving almost perfect agreement for classifying SAV (McHugh 2012). The accuracy of the kNDAVI predictor is due to the spectral calibration of the RS imagery across the four sites, where any inter-site variability is accounted for with the sigma hyperparameter. However, this is not the case for the preferential model, where the kNDAVI model only achieved moderate agreement for classifying SAV. As kNDAVI classifies vegetation and other benthic classes at the extreme ranges of the index, an imbalance in ground truth data towards vegetation restricts the spectral range of predictor data and limits habitat classification. Thus, balanced ground truth data appropriately allocated across the sampling frame remains necessary even when spatially calibrating RS imagery. The blue band achieved substantial agreement for SAV classification for both the preferential and balanced design models. Still, the balanced models performed better and did not overestimate SAV extent (Fig. 17). The LiDAR models achieved similar accuracies for mapping SAV, with the balanced design performing better (Table 3).

Despite the stark difference in SAV mapping between the preferential and balanced designs, it should be noted that the Independent Shallow Survey for the Western Rock Lobster fishery, our case study for this paper, was not established to map habitat extents across geographic scales. Instead, the Independent Shallow Survey is designed to monitor localised changes in juvenile Western Rock Lobster populations over time. Nevertheless, the benthic ground truthing data, concurrently collected from the Independent Shallow Survey provided a unique opportunity to explicitly show the differences between preferential and spatially balanced habitat mapping in a real-world context. Samples from both designs were collected within the same spatiotemporal range and processed with a similar methodology, which is a key strength of this study compared to other sampling design comparisons conducted using simulated designs across resources that have already been modelled and mapped (Emeric Thibaud, Blaise Petitpierre, Olivier Broennimann, Anthony C. Davison, Antoine Guisan 2014; Conn, Thorson, and Johnson 2017; Pennino et al. 2019; Hirzel and Guisan 2002; Geiziane Tessarolo, Thiago F. Rangel, Miguel B. Araújo, Joaquín Hortal 2014; Christianson and Kaufman 2016).

Conclusion

Preferential sampling designs are inadequate for accurately mapping habitats and their extent, particularly benthic habitats, which are challenging to map using remotely sensed data. Preferential designs result in unbalanced ground truthing data, leading to biased model estimates toward the habitat of interest and resulting in low accuracy and significant overestimation of habitat extents. Though methods exist to account for unbalanced data, in the current study they were found to be insufficient for correcting the limitations of skewed sampling. A spatially balanced approach that allocates representative samples across ecological gradients is critical for accurate habitat mapping, even when attempting to map a single ecological feature (i.e., vegetation). Future habitat mapping studies, particularly remote sensing studies, should plan to balance samples appropriately before in situ data collection to achieve accurate and ecologically sound outcomes.

Acknowledgments

The authors acknowledge the Traditional Custodians of the land, and their connections to the land, sea and community. We pay our respects to their Elders past and present and extend that respect to all Aboriginal and Torres Strait Islander peoples. This research was supported by the Fisheries Research and Development Corporation (FRDC Project Number 2019-099) on behalf of the Australian Government. The research as part of the ICoAST collaborative project and acknowledges support from the Indian Ocean Marine Institute Research Centre collaborative research fund and partner organisations AIMS, CSIRO, DPIRD and UWA.

References

- Althaus, Franziska, Nicole Hill, Renata Ferrari, Luke Edwards, Rachel Przeslawski, Christine H. L. Schönberg, Rick Stuart-Smith, et al. 2015. "A Standardised Vocabulary for Identifying Benthic Biota and Substrata from Underwater Imagery: The CATAMI Classification Scheme." *PloS One* 10 (10): e0141039.
- Arenas-Castro, Salvador, and Neftalí Sillero. 2021. "Cross-Scale Monitoring of Habitat Suitability Changes Using Satellite Time Series and Ecological Niche Models." *The Science of the Total Environment* 784 (August): 147172.
- Aubry, Philippe, Charlotte Francesiaz, and Matthieu Guillemain. 2024. "On the Impact of Preferential Sampling on Ecological Status and Trend Assessment." *Ecological Modelling* 492 (June): 110707.
- Breiman, Leo. 2001. "Random Forests." *Machine Learning* 45 (1): 5–32.
- Brown, Christopher F., Steven P. Brumby, Brookie Guzder-Williams, Tanya Birch, Samantha Brooks Hyde, Joseph Mazzariello, Wanda Czerwinski, et al. 2022. "Dynamic World, Near Real-Time Global 10 M Land Use Land Cover Mapping." *Scientific Data* 9 (1): 1–17.
- Camps-Valls, Gustau, Manuel Campos-Taberner, Álvaro Moreno-Martínez, Sophia Walther, Grégory Duveiller, Alessandro Cescatti, Miguel D. Mahecha, et al. 2021. "A Unified Vegetation Index for Quantifying the Terrestrial Biosphere." *Science Advances* 7 (9). <https://doi.org/10.1126/sciadv.abc7447>.
- Chavier, Yohann, Niklaus E. Zimmermann, Giovanni Poggiato, Daria Bystrova, Philipp Brun, and Wilfried Thuiller. 2021. "Novel Methods to Correct for Observer and Sampling Bias in Presence-only Species Distribution Models." *Global Ecology and Biogeography: A Journal of Macroecology* 30 (11): 2312–25.
- Chen, C., A. Liaw, and L. Breiman. 2004. "Using Random Forest to Learn Imbalanced Data." University of California, Berkeley, Wellness Letter.
- Chiang, Mark Ming-Tso, and Boris Mirkin. 2010. "Intelligent Choice of the Number of Clusters in K-Means Clustering: An Experimental Study with Different Cluster Spreads." *Journal of Classification* 27 (1): 3–40.
- Christianson, Danielle S., and Cari G. Kaufman. 2016. "Effects of Sample Design and Landscape Features on a Measure of Environmental Heterogeneity." *Methods in Ecology and Evolution / British Ecological Society* 7 (7): 770–82.
- Conn, Paul B., James T. Thorson, and Devin S. Johnson. 2017. "Confronting Preferential Sampling When Analysing Population Distributions: Diagnosis and Model-based Triage." *Methods in Ecology and Evolution / British Ecological Society* 8 (11): 1535–46.
- Del Vecchio, Silvia, Edy Fantinato, Giulia Silan, and Gabriella Buffa. 2019. "Trade-Offs between Sampling Effort and Data Quality in Habitat Monitoring." *Biodiversity and Conservation* 28 (1): 55–73.
- Diggle, Peter J., Raquel Menezes, and Ting-Li Su. 2010. "Geostatistical Inference under Preferential Sampling." *Journal of the Royal Statistical Society. Series C, Applied Statistics* 59 (2): 191–232.

Duffy, J. Emmett, Lisandro Benedetti-Cecchi, Joaquin Trinanes, Frank E. Muller-Karger, Rohani Ambo-Rappe, Christoffer Boström, Alejandro H. Buschmann, et al. 2019. "Toward a Coordinated Global Observing System for Seagrasses and Marine Macroalgae." *Frontiers in Marine Science* 6. <https://doi.org/10.3389/fmars.2019.00317>.

Eagleston, Holly, and Jeffrey L. Marion. 2020. "Application of Airborne LiDAR and GIS in Modeling Trail Erosion along the Appalachian Trail in New Hampshire, USA." *Landscape and Urban Planning* 198 (June): 103765.

Emeric Thibaud, Blaise Petitpierre, Olivier Broennimann, Anthony C. Davison, Antoine Guisan. 2014. "Measuring the Relative Effect of Factors Affecting Species Distribution Model Predictions." *Methods in Ecology and Evolution* 5 (9): 947–55.

Fisher, Adrian, Neil Flood, and Tim Danaher. 2016. "Comparing Landsat Water Index Methods for Automated Water Classification in Eastern Australia." *Remote Sensing of Environment* 175 (March): 167–82.

Foster, Scott D. 2021. "MBHdesign: An R-package for Efficient Spatial Survey Designs." *Methods in Ecology and Evolution / British Ecological Society* 12 (3): 415–20.

Foster, Scott D., Geoffrey R. Hosack, Jacquomo Monk, Emma Lawrence, Neville S. Barrett, Alan Williams, and Rachel Przeslawski. 2020. "Spatially Balanced Designs for Transect-based Surveys." *Methods in Ecology and Evolution / British Ecological Society* 11 (1): 95–105.

Geiziane Tessarolo, Thiago F. Rangel, Miguel B. Araújo, Joaquín Hortal. 2014. "Uncertainty Associated with Survey Design in Species Distribution Models." *Diversity and Distributions* 20 (11): 1258–69.

Gorelick, Noel, Matt Hancher, Mike Dixon, Simon Ilyushchenko, David Thau, and Rebecca Moore. 2017. "Google Earth Engine: Planetary-Scale Geospatial Analysis for Everyone." *Remote Sensing of Environment* 202 (December): 18–27.

Grafström, Anton, and Yves Tillé. 2013. "Doubly Balanced Spatial Sampling with Spreading and Restitution of Auxiliary Totals." *Environmetrics* 24 (2): 120–31.

Hedley, J. D., A. R. Harborne, and P. J. Mumby. 2005. "Technical Note: Simple and Robust Removal of Sunlint for Mapping Shallow-water Benthos." *International Journal of Remote Sensing* 26 (10): 2107–12.

Hickey, Sharyn M., Ben Radford, Chris M. Roelfsema, Karen E. Joyce, Shaun K. Wilson, Daniel Marrable, Kathryn Barker, et al. 2020. "Between a Reef and a Hard Place: Capacity to Map the Next Coral Reef Catastrophe." *Frontiers in Marine Science* 7. <https://doi.org/10.3389/fmars.2020.544290>.

Hirzel, Alexandre, and Antoine Guisan. 2002. "Which Is the Optimal Sampling Strategy for Habitat Suitability Modelling." *Ecological Modelling* 157 (2): 331–41.

Kermorvant, Claire, Frank D'Amico, Noëlle Bru, Nathalie Caill-Milly, and Blair Robertson. 2019. "Spatially Balanced Sampling Designs for Environmental Surveys." *Environmental Monitoring and Assessment* 191 (8): 524.

Kéry, Marc, J. Andrew Royle, Hans Schmid, Michael Schaub, Bernard Volet, Guido Häfliger, and Niklaus Zbinden. 2010. "Site-Occupancy Distribution Modeling to Correct Population-Trend Estimates Derived from Opportunistic Observations." *Conservation Biology: The Journal of the Society for Conservation Biology* 24 (5): 1388–97.

- Kiefer, Isabel, Daniel Odermatt, Orlane Anneville, Alfred Wüest, and Damien Bouffard. 2015. "Application of Remote Sensing for the Optimization of in-Situ Sampling for Monitoring of Phytoplankton Abundance in a Large Lake." *The Science of the Total Environment* 527-528 (September): 493–506.
- Kincaid, Tom, Tony Olsen, Don Stevens, Christian Platt, Denis White, Richard Remington, and Maintainer Tom Kincaid. 2015. "Package 'spsurvey.'" *Journal of Statistical Software* 61: 1–10.
- Kramer, Oliver. 2016. "Scikit-Learn." In *Machine Learning for Evolution Strategies*, edited by Oliver Kramer, 45–53. Cham: Springer International Publishing.
- Krumhansl, Kira A., Daniel K. Okamoto, Andrew Rassweiler, Mark Novak, John J. Bolton, Kyle C. Cavanaugh, Sean D. Connell, et al. 2016. "Global Patterns of Kelp Forest Change over the Past Half-Century." *Proceedings of the National Academy of Sciences of the United States of America* 113 (48): 13785–90.
- Langlois, Tim, Jordan Goetze, Todd Bond, Jacquomo Monk, Rene A. Abesamis, Jacob Asher, Neville Barrett, et al. 2020. "A Field and Video Annotation Guide for Baited Remote Underwater Stereo-video Surveys of Demersal Fish Assemblages." *Methods in Ecology and Evolution* / British Ecological Society 11 (11): 1401–9.
- Li, Jian, Liqiao Tian, Yihong Wang, Shuanggen Jin, Tingting Li, and Xuejiao Hou. 2021. "Optimal Sampling Strategy of Water Quality Monitoring at High Dynamic Lakes: A Remote Sensing and Spatial Simulated Annealing Integrated Approach." *The Science of the Total Environment* 777 (July): 146113.
- López de Olmos Reyes, Yasser Said, Margarita Elizabeth Gallegos Martínez, Rainer Andreas Ressler, and Gilberto Hernández Cárdenas. 2023. "Changes in Submerged Aquatic Vegetation Cover off the Northern Yucatán Peninsula Detected with Sentinel-2 Imagery Using a Fuzzy Classification System." *Remote Sensing Applications: Society and Environment* 32 (November): 101008.
- Lv, Tingting, Xiang Zhou, Zui Tao, Xiaoyu Sun, Jin Wang, Ruoxi Li, and Futai Xie. 2021. "Remote Sensing-Guided Spatial Sampling Strategy over Heterogeneous Surface Ground for Validation of Vegetation Indices Products with Medium and High Spatial Resolution." *Remote Sensing* 13 (14): 2674.
- Maccherini, Simona, Giovanni Bacaro, Enrico Tordoni, Andrea Bertacchi, Paolo Castagnini, Bruno Foggi, Matilde Gennai, Michele Mugnai, Simona Sarmati, and Claudia Angiolini. 2020. "Enough Is Enough? Searching for the Optimal Sample Size to Monitor European Habitats: A Case Study from Coastal Sand Dunes." *Diversity* 12 (4): 138.
- Mannino, Anna Maria, Flavio Borfecchia, and Carla Micheli. 2021. "Tracking Marine Alien Macroalgae in the Mediterranean Sea: The Contribution of Citizen Science and Remote Sensing." *Journal of Marine Science and Engineering* 9 (3): 288.
- Martínez, Brezo, Rosa M. Viejo, Francisco Carreño, and Silvia C. Aranda. 2012. "Habitat Distribution Models for Intertidal Seaweeds: Responses to Climatic and Non-climatic Drivers." *Journal of Biogeography* 39 (10): 1877–90.
- Mastrantonis, Stanley, Ben Radford, Tim Langlois, Claude Spencer, Simon de Lestang, and Sharyn Hickey. 2024. "A Novel Method for Robust Marine Habitat Mapping Using a Kernelised Aquatic Vegetation Index." *ISPRS Journal of Photogrammetry and Remote Sensing: Official*

Publication of the International Society for Photogrammetry and Remote Sensing 209 (March): 472–80.

McHugh, Mary L. 2012. "Interrater Reliability: The Kappa Statistic." *Biochemia Medica: Casopis Hrvatskoga Drustva Medicinskih Biokemicara / HDMB* 22 (3): 276–82.

Mellor, Andrew, Samia Boukir, Andrew Haywood, and Simon Jones. 2015. "Exploring Issues of Training Data Imbalance and Mislabelling on Random Forest Performance for Large Area Land Cover Classification Using the Ensemble Margin." *ISPRS Journal of Photogrammetry and Remote Sensing: Official Publication of the International Society for Photogrammetry and Remote Sensing* 105 (July): 155–68.

Pennino, Maria Grazia, Iosu Paradinas, Janine B. Illian, Facundo Muñoz, José María Bellido, Antonio López-Quílez, and David Conesa. 2019. "Accounting for Preferential Sampling in Species Distribution Models." *Ecology and Evolution* 9 (1): 653–63.

Rowan, Gillian S. L., and Margaret Kalacska. 2021. "A Review of Remote Sensing of Submerged Aquatic Vegetation for Non-Specialists." *Remote Sensing* 13 (4): 623.

Schultz, Stewart T., Claudia Kruschel, Tatjana Bakran-Petricioli, and Donat Petricioli. 2015. "Error, Power, and Blind Sentinels: The Statistics of Seagrass Monitoring." *PLoS One* 10 (9): e0138378.

Stehman, Stephen V. 2009. "Sampling Designs for Accuracy Assessment of Land Cover." *International Journal of Remote Sensing* 30 (20): 5243–72.

Stevens, Don L., and Anthony R. Olsen. 2004. "Spatially Balanced Sampling of Natural Resources." *Journal of the American Statistical Association* 99 (465): 262–78.

Strydom, Simone, Kathy Murray, Shaun Wilson, Bart Huntley, Michael Rule, Michael Heithaus, Cindy Bessey, et al. 2020. "Too Hot to Handle: Unprecedented Seagrass Death Driven by Marine Heatwave in a World Heritage Area." *Global Change Biology* 26 (6): 3525–38.

Sward, Darryn, Jacquomo Monk, and Neville Scott Barrett. 2022. "Regional Estimates of a Range-extending Ecosystem Engineer Using Stereo-imagery from ROV Transects Collected with an Efficient, Spatially Balanced Design." *Remote Sensing in Ecology and Conservation* 8 (1): 105–18.

Traganos, Dimosthenis, Bharat Aggarwal, Dimitris Poursanidis, Konstantinos Topouzelis, Nektarios Chrysoulakis, and Peter Reinartz. 2018. "Towards Global-Scale Seagrass Mapping and Monitoring Using Sentinel-2 on Google Earth Engine: The Case Study of the Aegean and Ionian Seas." *Remote Sensing* 10 (8): 1227.

Van Hoey, Gert, Julia Wischniewski, Johan Craeymeersch, Jennifer Dannheim, Lisette Enserink, Laurent Guerin, Francisco Marco-Rius, et al. 2019. "Methodological Elements for Optimising the Spatial Monitoring Design to Support Regional Benthic Ecosystem Assessments." *Environmental Monitoring and Assessment* 191 (7): 423.

Wang, Qiang, Álvaro Moreno-Martínez, Jordi Muñoz-Marí, Manuel Campos-Taberner, and Gustau Camps-Valls. 2023. "Estimation of Vegetation Traits with Kernel NDVI." *ISPRS Journal of Photogrammetry and Remote Sensing: Official Publication of the International Society for Photogrammetry and Remote Sensing* 195 (January): 408–17.

Wardhani, Ni Wayan Surya, Masithoh Yessi Rochayani, Atiek Iriany, Agus Dwi Sulistyono, and Prayudi Lestantyo. 2019. "Cross-Validation Metrics for Evaluating Classification Performance

on Imbalanced Data.” In 2019 International Conference on Computer, Control, Informatics and Its Applications (IC3INA), 14–18. IEEE.

Waśniewski, Adam, Agata Hościło, and Linda Aune-Lundberg. 2023. “The Impact of Selection of Reference Samples and DEM on the Accuracy of Land Cover Classification Based on Sentinel-2 Data.” *Remote Sensing Applications: Society and Environment* 32 (November): 101035.

Waycott, Michelle, Carlos M. Duarte, Tim J. B. Carruthers, Robert J. Orth, William C. Dennison, Suzanne Olyarnik, Ainsley Calladine, et al. 2009. “Accelerating Loss of Seagrasses across the Globe Threatens Coastal Ecosystems.” *Proceedings of the National Academy of Sciences of the United States of America* 106 (30): 12377–81.

Whiteway, T. 2009. “Australian Bathymetry and Topography Grid, June 2009.” <https://doi.org/10.4225/25/53D99B6581B9A>.

Wisn, Mary Susanne, Julien Pottier, W. Daniel Kissling, Loïc Pellissier, Jonathan Lenoir, Christian F. Damgaard, Carsten F. Dormann, et al. 2013. “The Role of Biotic Interactions in Shaping Distributions and Realised Assemblages of Species: Implications for Species Distribution Modelling.” *Biological Reviews of the Cambridge Philosophical Society* 88 (1): 15–30.

Wu, Qiusheng. 2020. “Geemap: A Python Package for Interactive Mapping with Google Earth Engine.” *Journal of Open Source Software* 5 (51): 2305.

Study 4: Observations of the association by early-juvenile Western Rock Lobster with seagrass assemblages

Preface

This study examines habitat associations of early-juvenile lobsters in relation to seagrass density and type, particularly with ‘wire-weed’ *Amphibolis* assemblages. Our findings suggest that juvenile lobsters actively select these habitats, with further research needed to understand the cues driving these choices and their impact on subsequent recruitment into the fishery.

Observations of the association by early-juvenile Western Rock Lobster *Panulirus cygnus* George, 1962 with seagrass assemblages (Decapoda: Achelata: Palinuridae)

Published in: Journal of Crustacean Biology

<https://doi.org/10.1093/jcbiol/ruad045>

Authors and affiliations:

Daphne Oh¹, Tim Langlois¹, Michael Brooker¹, Hugo Salinas⁶, Jason How² and Simon de Lestang²

¹ School of Biological Sciences and the UWA Oceans Institute, The University of Western Australia, Crawley, WA 6009, Australia

² Western Australian Fisheries and Marine Research Laboratories, Department of Primary Industries and Regional Development, Government of Western Australia, North Beach, WA 6920, Australia

Abstract

The fishery of the Western Rock Lobster, *Panulirus cygnus* George, 1962, is Australia's most valuable wild-caught single-species fishery. Recruitment in some regions of the fishery was observed to be significantly lower than expected after the 2010/2011 West Australian marine heatwave that caused extensive disturbance of dominant coastal habitats. This event generated interest in the study of the factors influencing survival and recruitment of post-larval benthic *P. cygnus* after settlement. The habitat associations of the highly cryptic post-settlement early-juveniles were previously unknown, with only anecdotal observations of individuals within limestone crevices in nearshore habitats. Our study used early-juveniles derived from ongoing monitoring of puerulus settlement to examine their habitat association mechanism in aquaria experiments. Comparison of common nearshore habitat assemblages (bare sand, limestone crevices, and seagrasses (*Posidonia* and *Amphibolis*) at varying seagrass densities) found that most early-juveniles associated strongly with *Amphibolis* assemblages at high stem densities (~2,100 stems m⁻²). A shift in association between *Amphibolis* fronds and stems at high stem density to *Amphibolis*-shaded sand and leaf debris at low stem density indicated active habitat selection by early-juveniles. Habitat choices were tested with the scents of prey items and habitat types within *Amphibolis* assemblages using Y-maze bioassays. No significant olfactory choices were found, suggesting that habitat associations may be driven by multiple cues. Our study provides new laboratory-based insights into the habitat association of early-juvenile *P. cygnus* and suggests changes in seagrass assemblage identity and density are likely to be important. Further experimentation is needed to define the cues driving these patterns. The impact of habitat change on recruitment in this important fishery remains unknown and should be an objective of future research.

Introduction

Many marine organisms with separate juvenile and adult life stages often rely on refugia in their early life stages, presumably to avoid predators and to find food (Wahle & Steneck, 1992; Cowen et al., 2006). Identifying the nature, qualities, and availability of refugia habitats for benthic juveniles is crucial as it may explain the processes that underpin the structures of adult populations (Cowen et al., 2007; Pineda et al., 2007). With marine ecosystems experiencing rapid changes in nearshore habitats due to climate change and anthropogenic impacts (Jordà et al., 2012; Koch et al., 2013; Koenigstein et al., 2016), understanding the impact of change in such habitats on the recruitment of commercially important species is important to inform fisheries science and subsequent management.

The Western Rock Lobster (*Panulirus cygnus* George, 1962) is distributed along the mid-lower west coast of Western Australia (WA), supporting Australia's largest single-species, wild-capture commercial fishery worth over AUD\$400 million annually (Kennington et al., 2013; de Lestang et al., 2016). The lobster has an extended pelagic larval phase of 9 to 11 m, during which the larvae disperse over 1,500 km offshore (Phillips et al., 1979). As larvae are carried shoreward by ocean currents, they metamorphose into a nektonic puerulus stage that more closely resembles the adult form (Phillips & McWilliam, 2009). Using a combination of vertical migration and active swimming, pueruli actively migrate towards the coast where the majority are thought to settle in nearshore habitats (Jefferies et al., 2005; Feng et al., 2011). Puerulus settlement has been sampled using artificial seagrass collectors at eight locations along the WA coast since the 1960s (Phillips, 1986; de Lestang et al., 2009). This settlement index has been the basis of the management of the Western Rock Lobster fishery over the last 30+ yr (de Lestang et al., 2009). The index has historically been a reliable predictor of sub-legal catches 2 to 3 y later and recruitment to the fishery 3 to 4 y later, enabling fisheries managers to adapt management accordingly by anticipating years of high or low catch per unit effort (de Lestang et al., 2009; Reid et al., 2013).

After settlement, *P. cygnus* moult into a benthic post-puerulus form (0+ yr post-settlement, 10–20 mm carapace length (CL)), also known as an early-juvenile *P. cygnus* (Bellchambers et al., 2012). This life stage is highly cryptic in the wild. Little is therefore known about its ecology, an issue common in palinurid (family Palinuridae) and homarid (family Nephropidae) lobsters (van der Meeren & Woll, 2019). No methods or surveys have successfully monitored the abundance and distribution of post-settlement early-juvenile *P. cygnus* with substantial numbers of individuals only appearing in fisheries meshed trap-based surveys as undersized *P. cygnus* juveniles. The minimum size of lobsters typically caught in these meshed trap-based surveys is 40 mm CL, which is likely 1 to 2 y post settlement (Miller et al., 2023). Early-juveniles have been anecdotally observed, typically as solitary individuals and as small as 7 mm CL, in limestone crevices via intensive diver-based searches (Jernakoff, 1990). Larger juveniles (0+ yr, 10–20 mm CL) have also been found by diver-based surveys to be gregarious and closely associated with seagrass and macroalgal assemblages (Edgar, 1990a; Jernakoff, 1990). Seagrass and macroalgal meadows are commonly distributed in shallow-nearshore habitats throughout the distribution of the fishery of the Western Rock Lobster (Bellchambers et al., 2012). These diver surveys, however, were highly intensive and found the abundance of lobsters to be highly variable (Jernakoff, 1990). The fishery is considered to be one of the most well researched and managed fisheries in the world, yet there is still remarkably little knowledge about the recruitment ecology of early-juvenile *P. cygnus* due to their highly cryptic behaviour.

In the austral summer of 2010/2011, an extreme marine heatwave (MHW) affected > 2,000 km of coastline in mid-western WA, with warming anomalies of 2–4 °C (Wernberg et al., 2013; Pearce & Feng, 2013). The MHW led to extensive changes in dominant shallow-nearshore

habitats such as canopy-forming seagrass species *Amphibolis antarctica* and *Posidonia australis* (Thomson et al., 2015; Fraser et al., 2015; Kendrick et al., 2019) and macroalgae (Wernberg et al., 2013; Smale & Wernberg, 2013). Extensive defoliation of *Amphibolis* was observed immediately after the MHW in Shark Bay, WA, with little documentation of recovery several years after the impact (Kendrick et al., 2019; Strydom et al., 2020). While *Posidonia* meadows showed better immediate resilience to the 2010/2011 MHW compared to *Amphibolis* meadows (Kendrick et al., 2019; Strydom et al., 2020), low levels of *Posidonia* seed production and recovery were also observed five years post-MHW (Kendrick et al., 2019). The central and northern part of the Western Rock Lobster fishery in Kalbarri, WA experienced an extensive decrease in coverage and density of previously dominant seagrass meadows, which are a more complex habitat likely to be ideal for the settlement of lobster, and an increase in turf-dominated habitats, which are a much simpler habitat, as a result of the heatwave (Wernberg et al., 2016; Caputi et al., 2019). Two years after the MHW, the abundance of undersized *P. cygnus* (~68–75 mm CL) in Kalbarri was observed to be well below predicted abundance based on the puerulus settlement index from 3 to 4 y ago (Caputi et al., 2019). This disjunction between previous puerulus settlement indices and abundance of undersized lobsters was the strongest in nearshore shallow waters of Kalbarri, corresponding with where their habitats were suspected to be most impacted in the geographical centre of the 2010/2011 MHW event (Smale et al., 2017). The observed disjunction may be a result of increased mortality in early-juvenile lobsters after the MHW due to the loss of habitat and/or food assemblages. With extreme MHWs projected to occur more frequently and intensively in the future (Oliver et al., 2018; Babcock et al., 2019), understanding suitable habitat requirements of early-juvenile *P. cygnus* is important to inform fisheries science and to better understand the implications of potential habitat change.

There remains limited knowledge on the suitable habitats of the cryptic yet crucial life stages of the early-juvenile *P. cygnus*. There are only a handful of in-situ anecdotal detections (Jernakoff, 1990) and laboratory-based inferences of the possible natural habitats (Phillips et al., 1977; Brooker et al., 2022), a case which parallels the early life stages of the European lobster *Homarus gammarus* (Linnaeus, 1758), where there are no published observations of wild juveniles (van der Meeren & Woll, 2019). Early-juveniles of the Caribbean spiny lobster *Panulirus argus* (Latreille, 1804), however, have been observed to settle onto vegetated habitats such as dense beds of the red macroalgae *Laurencia* spp. (Behringer et al., 2009) and seagrass meadows (Briones-Fourzán & Lozano-Álvarez 2013). The success in finding the habitats of early-juvenile *P. argus* has led to further investigations (Marx & Herrnkind, 1985; Childress & Herrnkind, 2001), including understanding the relationship between recruitment and fishery stocks in the economically important fishery species (Baeza et al., 2018).

Existing laboratory-based research on early-juvenile *P. cygnus* revealed their general habitat preferences for seagrass assemblages, where they were shown to actively select *Amphibolis* and *Posidonia* assemblages using chemotaxis (Brooker et al., 2022). *Amphibolis* and *Posidonia* are dominant seagrass habitats that occupy a large portion of shallow coastal habitats along the southern and south-western coast of Australia (Kilminster et al., 2018). These benthic habitats are also typical of the nearshore area that occurs over most of the distribution of the Western Rock Lobster, where sub-adults have been found to be closely associated with (Jernakoff, 1987; Edgar, 1990a, b; Jernakoff et al., 1993). It is thus hypothesized that seagrass meadows are likely to be important habitats for the successful recruitment of the species.

Both *Amphibolis* and *Posidonia* are habitat-forming seagrasses that can form extensive meadows (Walker et al., 1988), which creates a highly complex canopy, likely providing early-juveniles with protection from predators and with food such as epifauna and epiphytes (Edgar 1990b). A stronger preference by the early-juveniles of *P. cygnus* for complex *Amphibolis* and *Posidonia* assemblages over the less complex *Halophila/Zostera* seagrass species had been described (Brooker et al., 2022). It is noteworthy that there was only some evidence of early-

juveniles choosing the scents of *Amphibolis* over *Posidonia* assemblages (Brooker et al., 2022). Early-juveniles *P. argus* reportedly use a combination of chemical, sound, and conspecific cues to navigate and select suitable microhabitats within the intricate branches of dense, erect red macroalgae (Baeza et al., 2018; Briones-Fourzán & Lozano-Álvarez, 2019). It is therefore possible for early-juveniles of *P. cygnus* to prefer the scents of *Amphibolis* over *Posidonia* assemblages due to the variation in canopy complexities where the branches of *Amphibolis* provide interstitial microhabitats and additional prey species unlike the ribbon-like leaves of *Posidonia* assemblages (Edgar 1990b; Gartner et al., 2013).

We aimed to refine the knowledge gaps in the habitat associations, specifically for seagrass assemblages, and requirements of post-settlement early-juvenile *P. cygnus*. Our study built on the novel findings of a previous chemosensory study, which demonstrated early-juvenile *P. cygnus* displaying a strong preference for the scents of *Amphibolis* over *Posidonia* assemblages (Brooker et al., 2022). We used early-juvenile *P. cygnus* (0+ yr, 10–20 mm CL) obtained from puerulus collectors to examine their habitat associations using physical structures of various habitats. We used controlled mesocosms to compare the degree of habitat association between dominant coastal habitats, such as bare sand, limestone crevices, and *Posidonia* and *Amphibolis* seagrass assemblages of varying densities, which are present in the biogeographic centre of the *P. cygnus* distribution. We hypothesized that early-juveniles demonstrate a stronger association with 1) seagrasses, especially for *Amphibolis* assemblages, and 2) seagrasses of higher stem density. We also used two-chambered Y-maze bioassays to investigate potential chemical signals within *Amphibolis* assemblages that may influence active habitat selection in early-juvenile *P. cygnus*. We compared choices between two chemical stimuli of fine-scale components of *Amphibolis* assemblages and choices between habitat types (*Amphibolis* fronds vs. rhizomes assemblages) (see Edgar, 1990b), habitat structure where *Amphibolis* fronds and rhizomes were cleaned of both epiphytes and epifauna, and common prey items such as the assemblages of epiphytes and epifauna. We hypothesised that early-juveniles would associate with the olfactory cue of *Amphibolis* fronds more frequently, as they would be an indicator of the presence of a favourable habitat (Jernakoff, 1987, 1990).

Methods

Collection and housing of early-juvenile lobsters

We collected early-juveniles of *P. cygnus* (0+ yr, 10–20 mm CL) monthly around the full moon along the Western Australian (WA) coastline from pre-established artificial puerulus collectors (Phillips, 1972). A total of 230 individuals were collected from August 2019 to January 2020. The early-juveniles were transported in an aerated transport canister to the Indian Ocean Marine Research Centre (IOMRC) laboratory in Watermans, WA within 24 hr of collection. The early-juveniles were kept communally in holding tanks due to insufficient aquaria space for individual housings, where they acclimated for 5–7 d before they were used in trials. Artificial habitat made from plastic meshes and green nylon scourer pads was provided as shelter in the tanks to control for any habitat bias during trials. Constant flows of filtered (100 µm) seawater at 125 l h⁻¹ and ambient ocean-water temperatures (16.3–23.6 °C) and salinity (35.5–36.0‰) were maintained in the holding tanks for six months. The lighting in the aquaria room was on a normal daylight cycle following an astronomical clock under LED white and blue lights.

Collection and housing of seagrass assemblage

Seagrass assemblages were sampled at two coastal sites representative of the biogeographic centre of the distribution of *P. cygnus* (Phillips, 1972). The sites were Seven Mile Beach (29°11'S, 114°53'E) and Cliff Head (29°31'S, 114°59'E) near Dongara, WA. The sites were

dominated by benthic habitats typical of the nearshore area where settlement and recruitment are suspected to be greatest (see Jernakoff et al., 1994). Both sites faced west and were located 30 km apart. Meadows of the seagrass *Amphibolis* spp. dominate limestone reefs and are patchily distributed within 400 m of the shore at Seven Mile Beach, and on a few heavily dissected rock outcrops and limestone reefs at Cliff Head. The seafloor of Cliff Head is also extensively colonized by the seagrass *Posidonia* spp.

A seagrass assemblage sample is characterised by a dominant seagrass species and its associated macrofaunal assemblages. *Amphibolis antarctica* (hereinafter *Amphibolis*) assemblage samples were collected at both sites with *Posidonia australis* (hereinafter *Posidonia*) assemblages sampled at Cliff Head. These two seagrass assemblages have considerable differences in their physical structural complexity, their diversity and abundance of associated macrofaunal species (Edgar, 1990b). The seagrass assemblage samples were collected mostly during low tide at both sites. Assemblages were sampled by placing the open face of a 25 × 15 cm plastic container over the sandy substratum, cutting around the edges of the container to the bedrock with a shovel, and levering the core into the container with minimal disturbance to the rhizomes and sediments (see Edgar, 1990b). Assemblage samples were placed into 70 l heavy-duty plastic tubs filled to the top with fresh seawater and placed under constant aeration. The seagrass assemblage samples were then transported back to the IOMRC laboratory, Watermans WA within 10 h of collection and housed in the same holding room as the early-juveniles. Assemblage samples were used in trials as soon as possible after collection to minimise any changes from being sampled and confined within mesocosms.

Mesocosm aquaria

We used mesocosm aquaria to observe the habitat associations of *P. cygnus* early-juveniles. Trials were conducted in three 100 l glass aquaria (L 60 × W 45 × H 45 cm) with running (125 l h⁻¹) aerated, filtered seawater from Watermans Bay Beach. An air stone was placed into the centre of each aquarium. Water temperatures (21.4–24.2 °C) and salinity (35.7–36.0 ‰) of the glass aquaria reflected that of ambient seawater from when the trials occurred. The lighting system of the holding room was used during the trials. Beach sand provided a 15–20 cm layer of natural substratum for the habitat samples. Treatment combinations consisted of two habitat types, each as a single block, with the combinations alternated between the three mesocosms to account for positional bias (Fig. 18). The early-juveniles were randomly transferred to one of three mesocosm tanks to reduce any effects associated with the aquaria. No food was provided during the trials. The position of each early-juveniles within the mesocosm was recorded and photographed after 24 h (see Herrnkind & Butler, 1986).

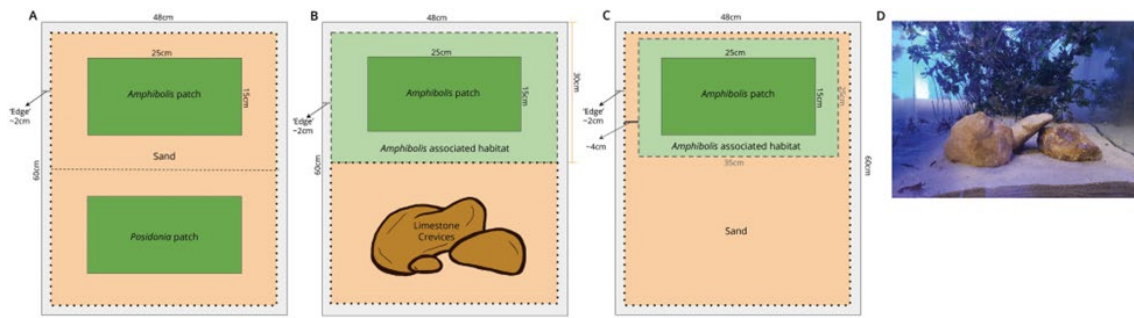


Figure 18 Experimental setup of mesocosm aquaria with *Amphibolis antarctica* and *Posidonia australis* assemblages (A), *Amphibolis* and bare sand (B), and *Amphibolis* and limestone crevices (C) as stimuli to test habitat associations of early-juvenile *Panulirus cygnus*. Setups B and C were conducted under changing *Amphibolis* stem densities. Habitat choices for *Amphibolis* were defined as within the patch (dark green) and associated with patch habitat (light green). Habitat choices for bare sand or limestone crevices were defined when early-juveniles were not found within patches of *Amphibolis* assemblages. Photo of mesocosm setup with *Amphibolis* and limestone crevices (D).

Due to the limited number of individuals from the puerulus collectors, 160 early-juveniles were used across three treatment combinations of the mesocosm trials. We conducted visual assessments before the start of every trial to ensure only early-juveniles of similar size class (10–20 mm CL) with no obvious physical damage (i.e., no missing legs or antennae) were used. Within the same treatment combination, early-juveniles were used up to three times total with a rest period of at least 48 h before they were haphazardly selected for subsequent trials. Early-juveniles were moved to a different holding tank containing only used individuals after each trial, depending on how many times they had been used. Those that were used three times were held in separate tanks from those that were used once and two times, respectively. There was a rest period of at least 24 h for each glass tank between trials to account for a random effect of mesocosm tank identity.

The association of early-juvenile *P. cygnus* with either *Amphibolis*, *Posidonia* assemblages or no association to a given habitat types was examined first. Habitat patches were created by burying the rhizomes of *Amphibolis* and *Posidonia* samples under sediment within a 25 × 15 cm area each (Fig. 18A). At least 10 cm of sediment surrounded each seagrass-assemblage to segregate the two seagrass patches and the surrounding walls of the mesocosm. We conducted six replicate trials (N of early-juveniles = 15 each) from 17–21 December 2019 (water temperature 21.4–21.9 °C). Ninety early-juveniles, 30 collected in November 2019 and 60 in December 2019, were used in these experiments. Early-juveniles had not been used prior to this treatment combination. Those found within 2 cm of mesocosm walls (edge) were recorded as ‘no association’ with any given habitat types due to potential influence of artificial structure (the wall). *Amphibolis* assemblages were then compared against bare sand and limestone crevices based on the stronger association with the seagrass-assemblage by early-juveniles (see results for *Amphibolis* and *Posidonia* trials). Limestone crevices and bare sand were used as alternate habitat choices because they are the other dominant habitats in the nearshore areas of Seven Mile Beach and Cliff Head (Edgar & Robertson, 1992). The limestone crevices used in the trials consisted of limestone rock piled together, forming holes to simulate crevices in limestone reefs. The densities of *Amphibolis* stems in the trials were manipulated to examine the habitat associations of early-juveniles when the density of seagrasses changed. Each alternate-habitat choice trial was replicated six times (N = 10 each) with four treatment levels of *Amphibolis* stem density. All four density levels were compared to limestone crevices and bare sand separately. Each trial started with a maximum test density of 80 *Amphibolis* stems, which simulated dense *Amphibolis* meadows at Seven Mile and Cliff Head. Rhizomes were buried within an area of 25 × 15 cm with a stock estimate of ~2,100 stems m⁻². Densities of *Amphibolis* were decreased three

times by haphazardly cutting 20 stems, reducing approximately 500 stems m^{-2} each time. The lowest *Amphibolis* stem density tested was ~ 600 stems m^{-2} .

In the *Amphibolis* assemblage vs. bare sand trials, *Amphibolis*-associated habitat was defined by one body length (~ 2 cm) of an early-juvenile *P. cygnus* from the seagrass patch (Fig. 18B). If an early-juvenile was found on the edge of *Amphibolis*-associated habitats, its position would be recorded as bare sand. Early-juveniles found within the edge of the mesocosms were recorded as no association with habitat types. The trials for *Amphibolis* assemblage against bare sand were conducted from 18–26 January 2020 (water temperature 21.7–23.6°C). We used 84 early-juveniles in these trials, with 78 collected in January 2020 and 8 in December 2019. Only individuals collected in January 2020 were reused for a second time in these trials. The microhabitat occurrences of early-juveniles within *Amphibolis* habitats were also investigated under changing stem density. Initially, pooled together as *Amphibolis* assemblage, the microhabitat positions were analysed as a supplement to the main comparison between the *Amphibolis* assemblages and bare sand. Choices for *Amphibolis* microhabitat types were recorded using four categories: 1) sand edges of *Amphibolis* patch, 2) debris, 3) *Amphibolis* stems and 4) *Amphibolis* fronds (Supporting Table 9).

In the *Amphibolis* assemblage vs. limestone crevices trials, the two habitat patches were separated at the halfway point of the aquaria (Fig. 18C, D). Associations with the *Amphibolis* assemblage were instead defined by the position of each early-juvenile within the *Amphibolis* patch or seagrass-associated habitat. The latter was defined by sandy boundaries around the *Amphibolis* patch that had some shelter provided by overhanging seagrass fronds and underlying debris. The areas of *Amphibolis*-associated habitats between the two trial types were defined differently due to varying lengths of *Amphibolis* stems between the seagrass samples. Early-juveniles found on open sand were likely associated with limestone crevices as indicated by the halfway point. The trials were conducted 10–20 March 2020 (water temperature 22.6–24.2 °C) with 120 early-juveniles of similar size class (10–20 mm CL). Sixty individuals collected in January 2020, and 60 from November and December 2019 combined. All early-juveniles had been used twice. Those found within the edge of the mesocosms were recorded as no association with habitat types.

All statistical analyses were conducted in R (R Core Team, 2021). A goodness-of-fit chi-squared test was applied to assess the frequency of early-juvenile *P. cygnus* observed between *Amphibolis*, *Posidonia* assemblages, and no association, and a uniform distribution of early-juveniles across the three habitat types (Fig. 18A).

In the *Amphibolis* stem density trials (Fig. 18B, C), generalised linear mixed-effects models (GLMM) were fitted to test if *Amphibolis* stem density (2,100, 1,600, 1,100, and 600 stems m^{-2} , fixed) and alternate habitat (limestone crevices and bare sand, or no association; fixed) influenced the probabilities of early-juveniles occurring in alternate habitats. Mesocosm tanks were treated as a random factor in the models. GLMMs were fitted using the binomial family with a logistic link function using functions from the lme4 package (Bates et al., 2015).

The effect of *Amphibolis* stem density (2,100, 1,600, 1,100. and 600 stems m^{-2}) on the frequencies of early-juveniles associating with microhabitats (fronds, stems, debris, sand edges of *Amphibolis* patch, bare sand, and no association) was assessed using a chi-square test of independence. The P-values were computed with Monte-Carlo simulations for 8,000 replicates (Hope, 1968). If the test was significant ($P < 0.05$), pair-wise chi-square comparisons were made with a Bonferroni correction.

Y-maze

We used Y-mazes to examine the choices of *P. cygnus* early-juveniles for the finer components of *Amphibolis* habitat assemblages. This bioassay was designed to test olfactory-mediated responses by removing visual and physical stimuli. The construction of six identical Y-mazes was adapted from the design by Kenning et al. (2015) (Fig. 19). Trials were conducted from August to September 2019 with 70 early-juveniles collected in the same months. Water temperatures of the Y-maze trials reflected ambient ocean temperatures ranging 16.3–19.3 °C. Y-mazes were installed on a levelled, robust platform with an adequate supply of filtered seawater and proximity to the holding tanks. We fixed a flow-meter gauge in the seawater line to ensure uniform flow rates and velocities. The feed lines were connected to gravity-fed water flow systems that held stimulus-infused water containing the scent of each food/habitat type used in the trials. Stimulus water was created by first placing samples of each stimulus in well-lit 150-l holding tubs of seawater. Water supply to the holding tubs were turned off 2 hr before the start of the trials to retain constant concentrations of each stimulus. The respective stimulus-infused water was transferred from the holding tanks to reservoirs that supply inflow into the Y-mazes prior to each trial. The reservoirs held each stimulus for no longer than 20 min. Two stimuli were compared for each trial, giving three potential outcomes which were stimulus A, stimulus B, or no response when the animal made no choice.

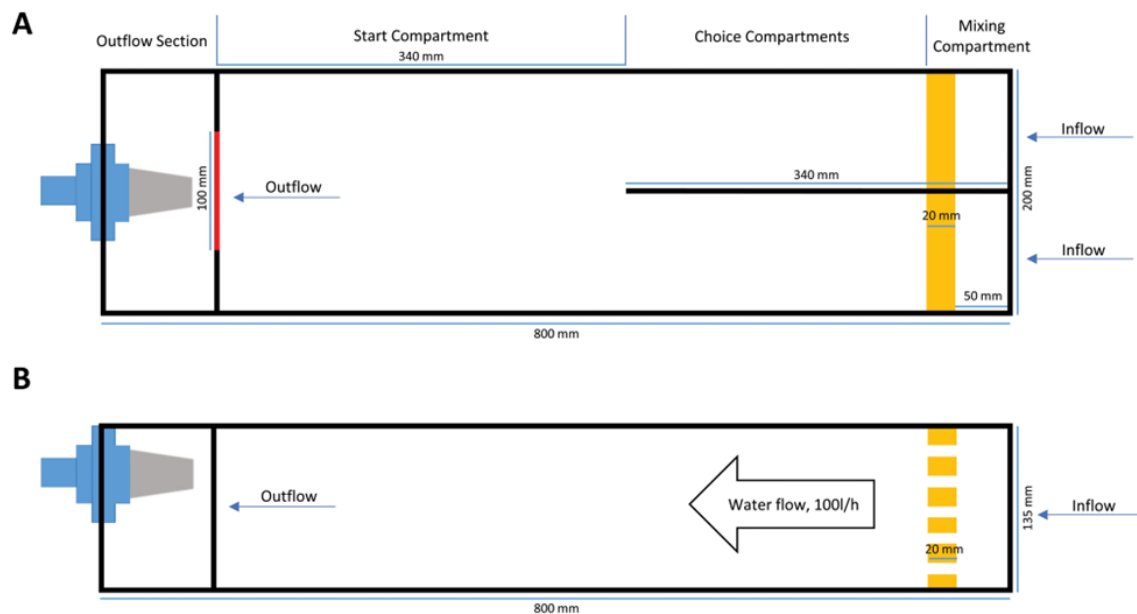


Figure 19 Experimental setup of the Y-maze seen from top (A) and side (B) views, with modified design adapted from Kenning et al. (2015). All walls of the Y-maze were made of PVC except a mesh screen (red line) providing a rough filter for the outflow. Yellow bars indicate perforated PVC sheets to allow water to flow through.

We tested three treatment combinations between two chemical stimuli to examine the choices of early-juvenile for fine-scale components of *Amphibolis*-habitat assemblages. Based on Edgar (1990b), these combinations tested between common prey items, habitat structure, and habitat types within *Amphibolis*. The first treatment combination examined choices between *Amphibolis* fronds and rhizomes (120 replicates with 70 ‘fresh’ individuals, 50 used a second time). We used four *Amphibolis*-assemblage samples to create the stimuli in this combination. The fronds stimulus consisted of all *Amphibolis* stems separated from the rhizomes by cuttings. The second treatment combination tested whether the chemical stimuli of epiphytic algae and epifauna, common prey items in their omnivorous diet (Joll & Phillips, 1984), influenced the habitat selection of early-juveniles (36 trials with 20 individuals used for a second time and 16 for a third time). Epiphytic algae and associated epifauna used in this combination were collected from four *Amphibolis*-assemblage samples. The third treatment combination tested

between *Amphibolis* with or without associated epiphytes (48 replicates with 48 individuals, all used for a third time). Four fresh *Amphibolis* assemblage samples were washed in a flow-through seawater system. The outflow ran through a 100 µm filter sock which removed all epifauna and any dislodged epiphytic material. The remaining epiphytes on *Amphibolis* stems were also scraped with gloved hands and collected into the filter. The *Amphibolis* without epiphytes were used as a stimulus whereas unmanipulated *Amphibolis* samples with additional dislodged epiphytes were used as the other.

Different sample sizes between the treatment combinations were due to different numbers of suitable early-juveniles (10–20 mm CL with no physical damage) available for trials at that time. Early-juveniles were rested for at least two weeks between the three treatment combinations. Within the same treatment comparison, individuals rested for a minimum of 24 h before they were randomly selected to be reused. Early-juveniles were held in different holding tanks, depending on how many times they have been used.

All seawater lines, gravity-fed water tanks, and stimulus feed-lines were flushed with fresh seawater before trials began to avoid mixing stale water with stimulus-infused water. Y-mazes were filled before inflow rates were reduced to 100 l h⁻¹. The flow was left to stabilise for 60 s to ensure laminar flow. Stimulus-feed lines with the desired scents were added to the corresponding mixing compartments with their position alternated every trial. This removed any positional bias and ensured choices were made based on chemical stimuli. A holding panel was placed before the mesh screen to remove physical distractions from early-juveniles.

All trials were performed at 23 °C in darkness and observed under dim red light that is considered insensitive to *P. cygnus* (Cummins et al., 1984). The movements of early-juveniles were recorded using GoPro Hero 3 cameras (GoPro, San Mateo, CA, USA). Six replicate Y-maze trials ran simultaneously. A randomly selected early-juvenile *P. cygnus* was left in a confined chamber made of 90 mm PVC coupling placed in the start compartment of the Y-maze at the start of each trial. Each early-juvenile was left in the PVC coupling to acclimatise for 5 min. The coupling was removed slowly to avoid startling the individual. This initiated the start of the trial. The maximum duration of a trial was 10 min. A choice for a stimulus was recorded when the individual passed the start of the partitioning wall into the respective choice compartments. If the individual moved out of the first choice compartment and into the other, the second choice was also recorded. If no choice was made in 10 min, “no response” was recorded. The early-juvenile was removed and placed in another holding tank. Water in the Y-maze was flushed out and replaced to eliminate any cues left from the previous trial.

Time logs for every trial were created by analysing the recorded videos. This provided a step-by-step record of all movements in each trial with a timestamp. The total time an early-juvenile spent in each mixing compartment with the corresponding stimulus in each trial was pooled. Two-tailed, paired t-tests were conducted in R (R Core Team, 2021) to compare differences in time spent between two treatments by early-juveniles.

Results

Amphibolis and *Posidonia* assemblages

The observed frequencies of early-juvenile *P. cygnus* in *Amphibolis* and *Posidonia* assemblages, and no association (Fig. 20) were significantly different to a uniform distribution across three habitat choices ($\chi^2 = 54.47$, $df = 2$, $P < 0.001$). Early-juveniles were more likely to be found in *Amphibolis* than in *Posidonia* assemblages or have no seagrass association.

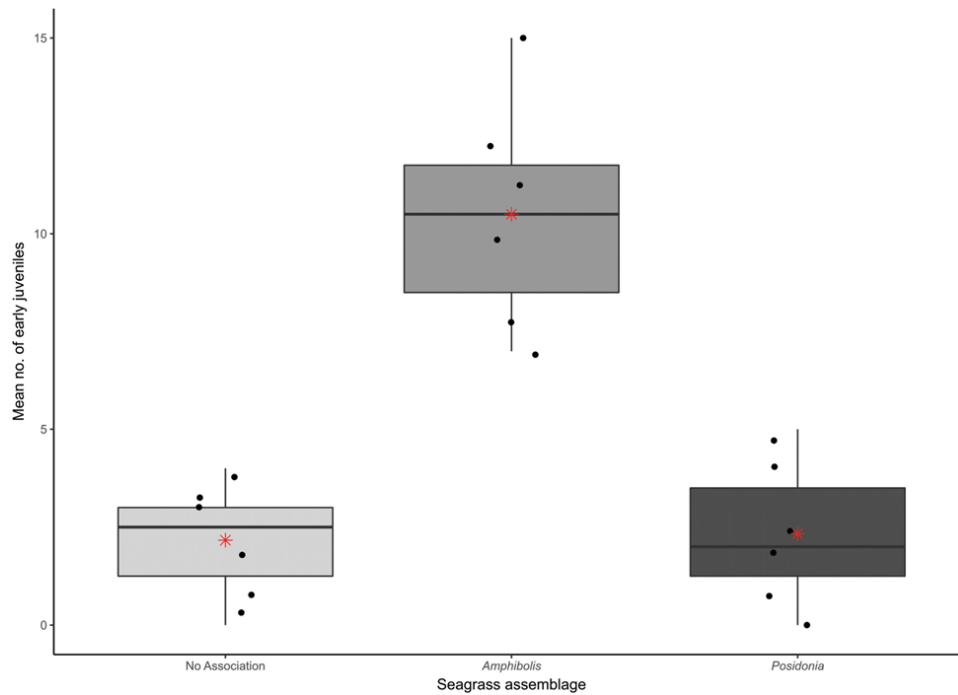


Figure 20 Mean number of early-juvenile *Panulirus cygnus* found in *Amphibolis* and *Posidonia* assemblages, or having no association with either seagrass assemblages, after 24 h in mesocosm trials (N = 6). Dots represent data points. Each box represents the interquartile range (IQR) and length of whiskers is restricted to maximum of 1.5 times of IQR. Dots outside of whiskers interval are outliers. Bold line in each box and the red star represents the median and mean, respectively.

Density of *Amphibolis* stems

Stem density in *Amphibolis* and alternate habitat types (either bare sand or limestone crevices) significantly affected the probabilities of early-juveniles associating with a habitat type (*Amphibolis* assemblage, bare sand, or limestone crevices) instead of having no association at all (Fig. 2, Table 5).

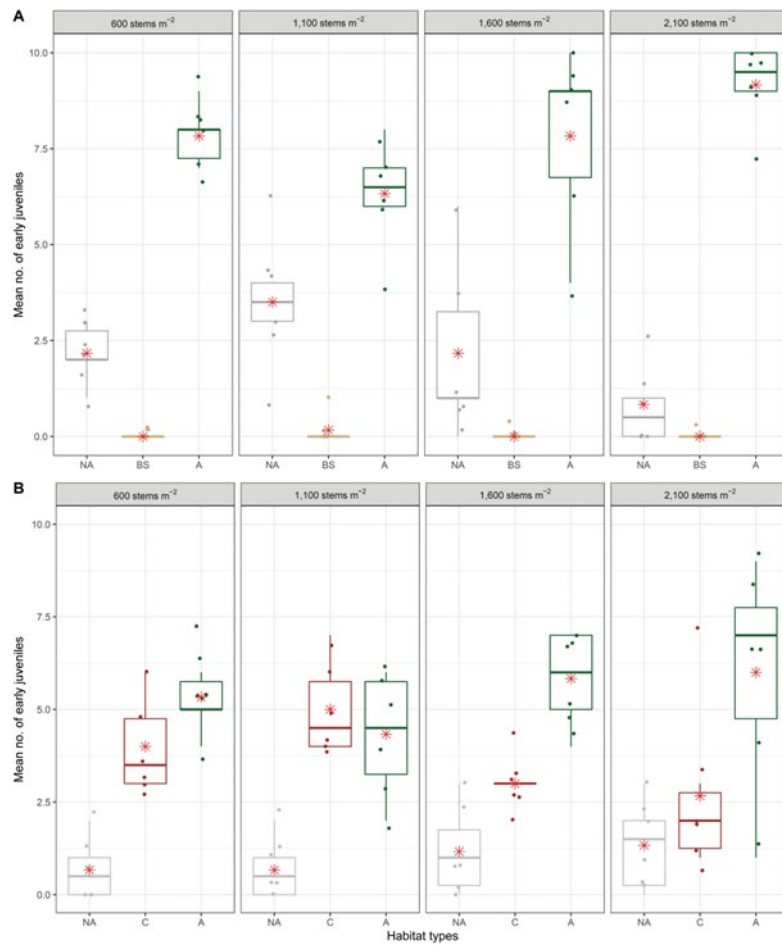


Figure 21 Mean number of early-juvenile *Panulirus cygnus* found in bare sand or *Amphibolis* assemblages (A), limestone crevices or *Amphibolis* assemblages (B), or having no association with habitat types, across four experimental densities of *Amphibolis* in mesocosm trials (N = 6 each treatment) (BS, bare sand; A, *Amphibolis* assemblages; C, limestone crevices; NA, no association). Dots represent data points. Each box represents the interquartile range (IQR) and length of whiskers is restricted to maximum of 1.5 times of IQR. Dots outside of whiskers interval are outliers. Bold line in each box and the red star represents the median and mean respectively.

Table 5 Generalised linear mixed-effects model (GLMM) results for the probability of early-juvenile *Panulirus cygnus* associating with habitat types (*Amphibolis* assemblages, bare sand, or limestone crevices) in response to fixed factors (*Amphibolis* stem density and alternate habitats), random factor (mesocosm Tank) and their interactions. Significant terms ($P < 0.05$) are shown in bold. Coefficients express the difference between each factor level and the intercept. S.E, standard error; *, interaction between the factors.

Term	Coefficient	S.E.	z	p
Intercept (Limestone Crevices)	-2.67	0.54	-4.89	< 0.001
Bare sand	1.3	0.60	2.26	0.02
Stem density (1,100 stems m ⁻²)	0	0.73	0	0.99
Stem density (1,600 stems m ⁻²)	0.61	0.65	0.94	0.34
Stem density (2,100 stems m ⁻²)	0.77	0.64	1.20	0.22
Bare sand*Stem density (1,100 stems m ⁻²)	0.67	0.84	0.81	0.42
Bare sand*Stem density (1,600 stems m ⁻²)	-0.61	0.79	-0.78	0.43
Bare sand*Stem density (2,100 stems m ⁻²)	-1.89	0.85	-2.22	0.02

In the bare sand and *Amphibolis* assemblage trials (Fig. 21A), early-juveniles were more likely to be found within *Amphibolis* assemblages than on bare sand (GLMM: $z = -4.79$, $P < 0.05$; Table 9). Early-juveniles were more likely to not to associate with any habitat types than with bare sand (GLMM: $z = 2.26$, $P < 0.05$; Table 8). High *Amphibolis* stem density and bare sand as an alternate habitat had a significant effect on early-juveniles not associating with any habitat types (GLMM: $z = 2.26$, $P < 0.05$; Table 8).

Table 6. Generalised linear mixed-effects model (GLMM) results for the probability of early-juvenile *Panulirus cygnus* found in either bare sand or limestone crevices in response to fixed factor (alternate habitats), random factor (mesocosm Tank) and their interactions. Significant terms ($P < 0.05$) are shown in bold. Coefficients express the difference between each factor level and the intercept. S.E., standard error.

Term	Coefficient	S.E.	z	P
Intercept (limestone crevices)	-0.38	0.15	-2.52	0.01
Bare sand	-4.85	1.01	-4.79	< 0.001

In the limestone crevices vs. *Amphibolis* trials (Fig. 21B), early-juvenile *P. cygnus* were more likely to be found in *Amphibolis* (GLMM: $z = -4.89$, $P < 0.05$; Table 5) and in limestone crevices (GLMM: $z = -2.52$, $P < 0.05$; Table 6) than have no association regardless of stem density.

Microhabitats within *Amphibolis*

There was a significant association between *Amphibolis* stem density and the frequency of microhabitat associations by early-juveniles ($\chi^2 = 85.06$, $P < 0.01$; Fig. 22). Early-juveniles were significantly more likely to be found in stems and fronds at higher stem density, whereas significantly more early-juveniles were found in *Amphibolis*-associated sand and debris at low stem density (see pair-wise result (Supporting Table 10)).

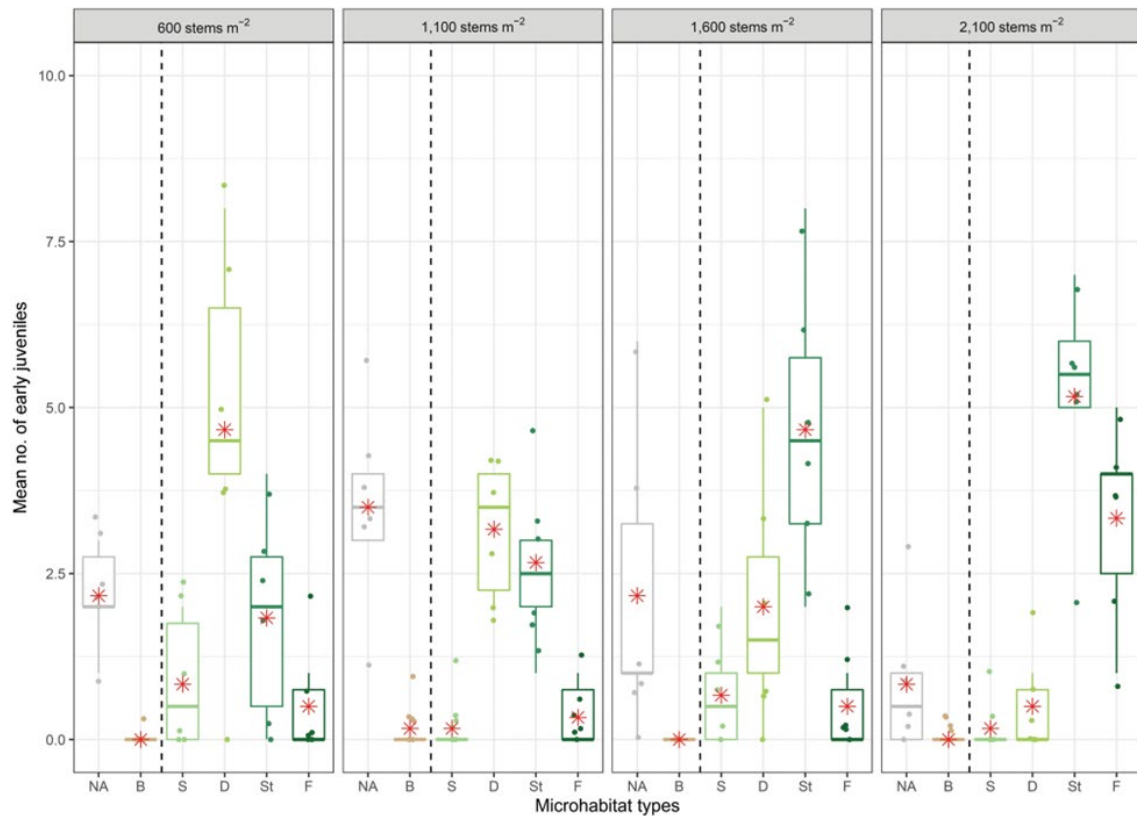


Figure 22 Mean number of early-juvenile *Panulirus cygnus* found in four *Amphibolis* microhabitats across four experimental densities of *Amphibolis* stems in mesocosm trials (F, fronds; St, stems; D, debris; S, *Amphibolis*-associated sand; B, bare sand; NA, no association). Dotted line represents the habitat choices between bare sand (left of line) and the *Amphibolis* assemblage (right). Dots represent data points. Each box represents the interquartile range (IQR) and length of whiskers is restricted to maximum of 1.5 times of IQR. Dots outside of whiskers interval are outliers. Bold line in each box and the red star represents the median and mean respectively.

Y-maze olfaction trials between *Amphibolis* assemblage components

Early-juveniles exhibited no significant choices between any treatment combinations tested in the Y-maze olfaction trials (Table 7). Neither between *Amphibolis* fronds and rhizomes (Fig. 23A), common food items epifauna or epiphytes (Fig. 22B), or between *Amphibolis* with and without epiphytes (Fig. 22C).

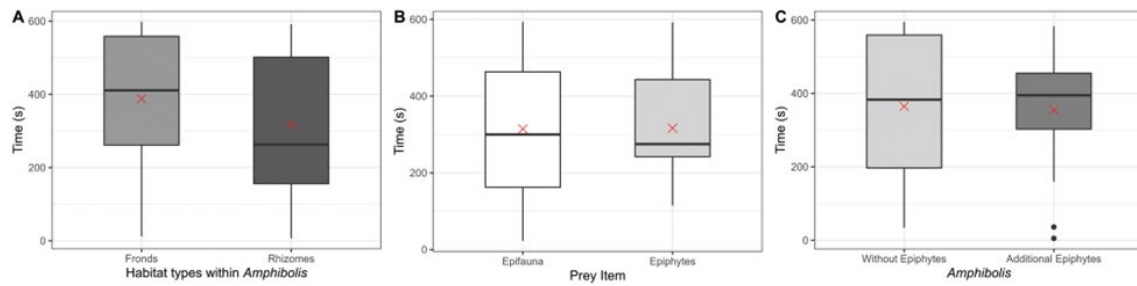


Figure 23 Choices for early-juvenile *Panulirus cygnus* for a chemical stimulus, as defined by total time spent at the end of a chosen Y-maze when presented with scents of habitat assemblages of *Amphibolis* fronds and rhizomes (A), common prey item epifauna and epiphytes (B), *Amphibolis* without and with additional epiphytes (C). Each box represents the interquartile range (IQR) and length of whiskers is restricted to maximum of 1.5 times of IQR. Bold line in each box and the red cross represents the median and mean respectively.

Table 7. Results of paired t-test testing choices of early-juvenile *Panulirus cygnus* for a chemical stimulus using scents of fronds vs. rhizomes of *Amphibolis* (A), epifauna vs. epiphytes (B), and *Amphibolis* without epiphytes vs. with additional epiphytes (C).

	<i>df</i>	<i>t</i> value	<i>P</i>
(A) Habitat types within <i>Amphibolis</i>	62	0.072	0.943
(B) Food items	31	−0.080	0.937
(C) Epiphytes on <i>Amphibolis</i>	37	0.734	0.468

Discussion

Our study demonstrated strong associations of early-juvenile *Panulirus cygnus* (0+ yr, 10–20 mm CL) to *Amphibolis* assemblages over other dominant coastal habitat types in laboratory mesocosm trials. The result of our initial experiment (Fig. 20) reinforced a previous chemosensory study that demonstrated the strong preference for *Amphibolis* over *Posidonia* assemblages (Brooker et al., 2022). The current study thus focused on *Amphibolis* assemblages where we investigated the impacts of changes in *Amphibolis* density on the habitat associations of early-juveniles within mesocosm experiments. We found strong effects of early-juveniles associated with the *Amphibolis* assemblages, suggesting that the characteristics of complete *Amphibolis* assemblages within mesocosms provide a strong physical cue for habitat association of early-juveniles.

The 2010/2011 marine heatwave (MHW) off WA led to the loss of extensive areas of previously dominant shallow-nearshore habitats, including seagrass and macroalgae, and an increase in turf dominated habitats across the centre and north of the fishery (Wernberg et al., 2016). The extensive loss of biotic habitat in the region corresponds with the geographical range of the disjunction seen in the puerulus settlement index and recruitment estimates (Caputi et al., 2019). Our results support evidence that early-juveniles of *P. cygnus* are more associated with seagrass habitats, in particular dense *Amphibolis* assemblages, which suggests that these are possibly critical habitats to the survival and successful recruitment of the species. The results

offer a possible explanation for the reduced recruitment observed in shallow-water fisheries surveys after the MHW (Caputi et al., 2019; de Lestang, unpublished data). This lower-than-expected recruitment was most reduced in near-shore shallow water areas in the northern half of the fishery, where habitats were suspected to be most impacted by the 2010/2011 MHW (Wernberg et al., 2013). The reduced recruitment occurred two years after the heatwave event (Caputi et al., 2019), suggesting an indirect effect rather than direct mortality. With MHW of higher intensity predicted to occur more frequently, impacts on seagrass assemblages are expected to be greater. Early-juveniles in our mesocosm experiment showed stronger associations with *Amphibolis* assemblages over *Posidonia* assemblages, likely due to its higher structural complexity (Gartner et al., 2013). The loss of dense *Amphibolis* meadows during the MHW resulted in fragmentation of the canopy and reduction in structural complexity (Strydom et al., 2020) which may have ecological consequences such as reduced recruitment due to loss of nursery habitat and increased predation risk. The magnitude of damage has also been shown to vary between seagrass species due to different resilience capacities. *Posidonia* meadows showed higher resilience compared to *Amphibolis* meadows, which were more impacted by thermal stress after the 2010/2011 MHW event (Strydom et al., 2020). A loss of preferred habitat could potentially increase mortality in post-settlement early-juvenile lobsters, likely causing reduced recruitment to the fishery. Similar indirect ecological consequences on recruitment have been observed in other invertebrate species to the same MHW event, with a reduction in brown tiger prawn *Penaeus esculentus* Haswell, 1879 recruitment in Exmouth Gulf (Caputi et al., 2019) attributed to loss of seagrass habitat (McMahon et al., 2017).

The early-juveniles of *P. cygnus* are notoriously difficult to detect in the field. Despite numerous attempts, previous in situ studies were unable to find adequate numbers of individuals to conduct robust observations of habitat associations (Jernakoff, 1990; Jernakoff et al., 1994). Our study avoided these limitations by using post-settlement individuals (0+ yr) collected from ongoing monitoring of their post-larval puerulus settlement. Their habitat associations were observed within mesocosms containing contrasting habitats, typical of the nearshore shallow water areas in the northern half of the fishery where settlement and recruitment are suspected to be the greatest (Jernakoff et al., 1994). The results are consistent with previous diver visual surveys of larger juveniles (1+ to 2+ yr, 25–35 mm CL) that found individuals forage at night amongst dense *Amphibolis* beds, rather than other seagrass habitats (Edgar, 1990a; Jernakoff et al., 1993). Jernakoff (1990) also found that large juvenile *P. cygnus* tended to choose holes in artificial limestone reefs overgrown by *Amphibolis* more than crevices in reefs with no cover. Early-juvenile lobsters are suspected to experience high levels of predation during settlement and before recruitment to the fishery (Howard, 1988). It is thus expected of early-juveniles to associate strongly with habitats that provide protection from predators. Field studies of predation found that newly settled individuals (5–15 mm CL) of the Caribbean spiny lobster *Panulirus argus* avoided predation by seeking shelter amongst continuous stands of algae (Smith & Herrnkind, 1992). The dense stems of the *Amphibolis* assemblages most likely provide protection from predators. It is also likely that these upright stems and leaf clusters provide prey, either epiphytic algae or macroinvertebrates, for the early-juvenile *P. cygnus* (Edgar, 1990a, b). Our study nonetheless presents a novel laboratory observation of habitat selection by early-juvenile spiny lobsters towards *Amphibolis* assemblages, where a range of potential cues (e.g. visual, physical, chemical), could have influenced the behaviour of the early-juveniles and their habitat choice. Further studies will be needed to investigate which of these factors is the most influential on habitat choice.

Although adult spiny lobsters are generally thought to be gregarious in nature (Cobb, 1981; MacDiarmid, 1994; de Lestang, 2014), previous observations have suggested that early-juvenile *P. cygnus* (0+ yr, 10–20 mm CL) are asocial and only become gregarious as larger juveniles (> 1+ yr, > 20 mm CL; Jernakoff, 1990; Johnston et al., 2006). We found no evidence of aggregation or social behaviour. There is nevertheless evidence that the early-juveniles (0+ yr) can tolerate

gregariousness to a certain degree when resources are limited, with severe aggression observed only when early-juveniles were in antennal contact with conspecifics while sharing shelter space (Berrill, 1976). Early-juveniles of the spiny lobster *P. argus* were found to be more attracted to the nursery algal habitat with conspecifics than to a habitat without (Baeza et al., 2018). Juvenile *P. argus* were also observed to undergo ontogenetic habitat shift from solitary algal dwelling to aggregation in crevices at a smaller size when food is scarce, predation risk is low, and when conspecifics are present (Childress & Herrnkind, 2001). While this may suggest conspecific attraction, previous studies on lobster *P. argus* (Zito-Livingston & Childress, 2009) and *Jasus edwardsii* (Hutton, 1875) (Butler et al., 1999) found that early-juveniles had no response to conspecific odour. Predation risk reportedly also decreases substantially when juvenile *P. argus* settle in dense algae with distance between conspecifics (Butler et al., 1997). It is possible that early-juveniles actively prefer habitat types with conspecifics in nature to increase survivorship and protection against predation (Butler et al., 1997). We present some of the first steps to understanding the habitat associations of early-juvenile *P. cygnus*, and suggest future studies examine the relationship between proximity to conspecifics, and differences among individuals (Stamps & Groothuis, 2010) to better understand the habitat associations of early-juvenile in the presence of conspecifics.

How microhabitat association varied with seagrass density

Importantly, our mesocosm study found that the early-juvenile *P. cygnus* displayed varied degrees of associations to microhabitat types in response to changing densities of *Amphibolis* stems. Microhabitat use by early-juveniles had been previously studied in various species of spiny lobsters (Marx & Herrnkind, 1985; Yoshimura & Yamakawa, 1988; Butler & Herrnkind, 1991). Our study provides novel observations of the impact of changing seagrass density on the habitat associations of early-juvenile spiny lobsters, providing new insights into the recruitment habitat of an important commercial species. It should be noted that the linear changes in association between habitats (e.g., debris to stems) with linearly increasing stem density could simply be the result of random allocation of individuals between habitats. The non-linear response, however, observed in the association of early-juveniles between *Amphibolis* stems vs. fronds, as the density of stems increases, suggests that other processes rather than random allocation are occurring and we observed behavioural preferences in habitat choice.

Changes in coverage and stem density of *Amphibolis* beds were reported after the 2010/2011 MHW (Fraser et al., 2015; Arias-Ortiz et al., 2018; van Keulen, 2019). Our results suggest active microhabitat association by early-juvenile *P. cygnus*. Fronds and stems of the *Amphibolis* assemblages at higher stem densities make up complex canopy structures (Edgar & Robertson, 1992), which provides shelter from predation and high diversity of trophic resources which are crucial in recruitment (Edgar, 1990a, b; Jernakoff et al., 1993; Heck & Orth, 2006; Gartner et al., 2013). Although the current mesocosm study lacked predators, it is possible that innate predator avoidance behaviours (Cobb, 1981; Howard, 1988) may have driven the strong choices for complex canopy structures. In contrast, early-juveniles displayed stronger associations with surrounding sand shaded by *Amphibolis* stems and leaf debris when *Amphibolis* stem density was low. A manipulative study had found that when *Amphibolis* stem densities were reduced by half, an increase in either mortality or emigration of species associated with more open spaces led to a decrease in the abundance of leaf-associated epifauna (Edgar & Robertson, 1992). With sparse stem density, more open spaces and reduced shelter complexity on the benthos may have led to early-juveniles avoiding *Amphibolis* fronds and stems. They instead seek shelter amongst microhabitats at the sediment surface. Early-juveniles were observed to find refuge by camouflaging against leaf debris and by burrowing into sediment under the layer of debris. This is consistent with the observed behaviour of post-larval American lobster *Homarus americanus* H. Milne Edwards, 1837 burrowing in mud (Dinning & Rochette, 2019) and of the European lobster *H. gammarus* hiding under cobble shelters (van der Meeren & Woll, 2019) when complex habitat

is unavailable. *Amphibolis* leaf debris has additionally been reported to have a distinctive epifaunal assemblage that resembles those of rhizomes of *Posidonia* and *Amphibolis* (Edgar, 1990b). This observation suggests that there could be higher macrobenthic production as leaf debris accumulates, providing both a potential source of food and refuge from predators for early-juveniles.

Early-juveniles in the mesocosm experiments were observed to shift their habitat associations from *Amphibolis* assemblages to limestone crevices as *Amphibolis* stem density decreased. Previous studies highlighted that, at high density and when food resources are limited, post-moult juvenile *P. cygnus* are highly vulnerable to cannibalism from larger conspecifics (Chittleborough, 1970; Moyle et al., 2009). Larger juveniles (30–45 mm CL) have been found aggregating in crevices and under ledges on the same reefs as smaller, early-juveniles (10–20 mm CL; Cobb, 1981). It is thus possible that the early-juveniles are cautious to associate with limestone crevice habitats, where larger conspecifics may occur, as seagrass densities decrease.

The densities of *Amphibolis* stems (600–2,100 stem m⁻²), representative of key sites in the nearshore coastal habitats across the northern half of the fishery, were used in our mesocosm study. The maximum stem density is, however, approximately double to that of typical reported values for *Amphibolis* densities (1,000–1,500 stem m⁻²; Edgar & Robertson, 1992). Our results should therefore be interpreted with caution, but nevertheless suggest that the very high *Amphibolis* stem densities used, which are found at suspected key recruitment sites in the fishery, were demonstrated to be more frequently chosen by early-juveniles and could potentially be important for the survival of this vulnerable life stage.

Y-maze

We found no evidence of early-juvenile *P. cygnus* exhibiting particular choices for various chemical signals when presented with cues for habitat types within *Amphibolis* assemblages or typical prey items in Y-maze bioassays. The early-juveniles have chemosensory receptors (Macmillan et al., 1992), with evidence demonstrating their chemosensory abilities and its importance in habitat selection (Brooker et al., 2022). There is nevertheless little information on the exact properties of chemoreception and its role in active habitat selection of wild *P. cygnus*. Early-juveniles of the Caribbean spiny lobster *P. argus* have been shown to use algal architecture and food abundance as a cue for habitat selection (Herrnkind & Butler, 1986), and early-juveniles of *J. edwardsii* have the ability to detect and respond to habitat-specific acoustic and substrate cues (Stanley et al., 2015). Early-juvenile *P. cygnus* are omnivorous scavengers (Edgar, 1990a). General prey availability may thus be more important than the presence of single prey items in nursery habitats since these early-juveniles have a wide dietary spectrum (Edgar, 1990a). Future studies would be required to investigate the effects of fine-scale components within *Amphibolis* assemblages on choices of early-juvenile *P. cygnus* for the seagrass assemblage.

Obtaining early-juvenile lobsters from existing puerulus collectors is logistically complicated. Lower-than-expected number of early-juveniles were collected during our trials, which necessitated the re-use of individuals. We acknowledge that such re-use led to non-independence within our result, and strongly suggest that future studies attempt to collect adequate numbers of individuals for independent trials. We considered identifying individuals to account for non-independence but due to the very small size (10–20 mm CL) and initial mortality of individuals, it was decided to progress with limited re-use in the current study. We strongly suggest that future studies consider sampling method that enables adequate numbers of individuals to be collected in order to remove the need to re-use test animals.

Although our studies on habitat association in the laboratory have provided insights into potential habitat selection mechanisms, direct detection of early-juveniles in situ is required to confirm *Amphibolis* assemblages as their habitat. The simple mesocosms also lacked predators and larger conspecifics which are likely to be present in natural environments. Future studies should incorporate predation pressure and density-dependent factors for early-juveniles and larger conspecifics in habitat-association experiments to better understand habitat selection by early-juvenile *P. cygnus* in nature. Likewise, the impact of habitat change on the growth and survival of early-juvenile lobsters remains unknown and should be an objective for future research into the impacts of variation in seagrass coverage and density. This study nonetheless corroborate the hypothesis that seagrass habitat loss could be detrimental for *P. cygnus* recruitment to the fishery. Our study suggests that in addition to existing monitoring of puerulus settlement on artificial seagrass collectors (de Lestang et al., 2009) and undersized lobster abundance, seagrass coverage and density could provide useful metrics to estimate both the impacts of future marine heatwaves and the potential of successful recruitment throughout the fishery.

Acknowledgements

We are grateful to Mark Rossbach and Kelvin Rushworth from The Department of Primary Industries and Regional Development, Government of Western Australia (DPIRD) for their help procuring the pueruli and early-juveniles used in the experiments. We also thank Brooke Gibbons, Rob Power, Kye Adams, and Rhei Tan from The University of Western Australia for assisting during field trips to Dongara, and in particular, to K. Adams for providing writing assistance and for proofreading the manuscript. We are always grateful to John and Beth Fitzhardinge for welcoming us to Dongara and for all the conversations on lobster. Lastly, we thank all anonymous reviewers and the Editor-in-Chief for their valuable comments to improve this manuscript. This research was conducted as part of the UWA Marine Ecology Group - Fisheries Research, funded by the Fisheries Research and Development Corporation (Project 2019-099) and the Dr. Keith Sheard Travel Award in Marine Biology (F17/2522).

References

- Arias-Ortiz, A., Serrano, O., Masqué, P., Lavery, P.S., Mueller, U., Kendrick, G.A., Rozaimi, M., Esteban, A., Fourqurean, J.W., Marbà, N., Mateo, M.A., Murrar, K., Rule, M.J. & Duarte, C.M. 2018. A marine heatwave drives massive losses from the world's largest seagrass carbon stocks. *Nature Climate Change*, 8: 338–344.
- Babcock, R.C., Bustamante, R.H., Fulton, E.A., Fulton, D.J., Haywood, M.D.E., Hobday, A.J., Kenyon, R., Mearns, R.J., Plagányi, E.E., Richardson, A.J. & Vanderklift, M.A. 2019. Severe continental-scale impacts of climate change are happening now: extreme climate events impact marine habitat forming communities along 45% of Australia's coast. *Frontiers in Marine Science*, 6: 411 [<https://doi.org/10.3389/fmars.2019.00411>].
- Baeza, J.A., Childress, M.J. & Ambrosio, L.J. 2018. Chemical sensing of microhabitat by pueruli of the reef-dwelling Caribbean spiny lobster *Panulirus argus*: testing the importance of red algae, juveniles, and their interactive effect. *Bulletin of Marine Science*, 94: 603–618.
- Bates, D., Maechler, M., Bolker, B. & Walker, S. 2015. Fitting linear mixed-effects models using lme4. *Journal of Statistical Software*, 67: 1–48.
- Behringer, D.C., Butler, M.J., Herrnkind, W.F., Hunt, J.H., Acosta, C.A. & Sharp, W.C. 2009. Is seagrass an important nursery habitat for the Caribbean spiny lobster, *Panulirus argus*, in Florida?. *New Zealand Journal of Marine and Freshwater Research*, 43: 327–337.
- Bellchambers, L., Mantel, P., Chandrapavan, A., Pember, M. & Evans, S. 2012. Western rock lobster ecology - the state of knowledge (Marine Stewardship Council, principle 2: maintenance of ecosystem). Department of Fisheries, North Beach, WA, Australia.
- Berrill, M. 1976. Aggressive behaviour of post-puerulus larvae of the Western Rock Lobster *Panulirus longipes* (Milne-Edwards). *Marine and Freshwater Research*, 27: 83–88.
- Briones-Fourzán, P. & Lozano-Álvarez, E. 2013. Essential habitats for *Panulirus* spiny lobsters. In: *Lobsters: biology, management, aquaculture and fisheries*, Edn. 2 (B.F. Phillips, ed.), pp. 186–220. Wiley-Blackwell, New York.
- Brooker, M., de Lestang, S., How, J.R. & Langlois, T.L. 2022. Chemotaxis is important for fine scale habitat selection of early juvenile *Panulirus cygnus*. *Journal of Experimental Marine Biology and Ecology*, 553: 151753 [<https://doi.org/10.1016/j.jembe.2022.151753>].
- Butler, M.J. & Herrnkind, W.F. 1991. Effect of benthic microhabitat cues on the metamorphosis of pueruli of the spiny lobster *Panulirus argus*. *Journal of Crustacean Biology*, 11: 23–28.
- Butler, M.J., Herrnkind, W.F. & Hunt, J.H. 1997. Factors affecting the recruitment of juvenile Caribbean spiny lobsters dwelling in macroalgae. *Bulletin of Marine Science*, 61: 3–19.
- Butler, M.J. IV, MacDiarmid, A.B. & Booth, J.D. 1999. The cause and consequence of ontogenetic changes in social aggregation in New Zealand spiny lobsters. *Marine Ecology Progress Series*, 188: 179–191.
- Caputi, N., Kangas, M., Chandrapavan, A., Hart, A., Feng, M., Marin, M. & de Lestang, S. 2019. Factors affecting the recovery of invertebrate stocks from the 2011 Western Australian extreme

marine heatwave. *Frontiers in Marine Science*, 6: 484 [<https://doi.org/10.3389/fmars.2019.00484>].

Childress, M.J. & Herrnkind, W.F. 2001. Influence of conspecifics on the ontogenetic habitat shift of juvenile Caribbean spiny lobsters. *Marine & Freshwater Research*, 52: 1077–1084.

Chittleborough, R.G. 1970. Studies on recruitment in the Western Australian rock lobster *Panulirus longipes cygnus* George: density and natural mortality of juveniles. *Marine and Freshwater Research*, 21: 131–148.

Cobb, J.S. 1981. Behaviour of the Western Australian spiny lobster, *Panulirus cygnus* George, in the field and laboratory. *Marine and Freshwater Research*, 32: 399–409.

Cowen, R.K., Gawarkiewicz, G., Pineda, J., Thorrold, S.R. & Werner, F.E. 2007. Population connectivity in marine systems: an overview. *Oceanography*, 20: 14–21.

Cowen, R.K., Paris, C.B. & Srinivasan, A. 2006. Scaling of connectivity in marine populations. *Science*, 311: 522–527.

Cummins, D.R., Chen, D.-M. & Goldsmith, T.H. 1984. Spectral sensitivity of the spiny lobster, *Panulirus argus*. *Biological Bulletin*, 166: 269–276.

Dinning, K.M. & Rochette, R. 2019. Evidence that mud seafloor serves as recruitment habitat for settling and early benthic phase of the American lobster *Homarus americanus* H. Milne Edwards, 1837 (Decapoda: Astacidea: Nephropidae). *Journal of Crustacean Biology*, 39: 594–601.

Edgar, G.J. 1990a. Predator-prey interactions in seagrass beds. I. The influence of macrofaunal abundance and size-structure on the diet and growth of the Western Rock Lobster *Panulirus cygnus* George. *Journal of Experimental Marine Biology and Ecology*, 139: 1–22.

Edgar, G.J. 1990b. The influence of plant structure on the species richness, biomass and secondary production of macrofaunal assemblages associated with Western Australian seagrass beds. *Journal of Experimental Marine Biology and Ecology*, 137: 215–240.

Edgar, G.J. & Robertson, A.I. 1992. The influence of seagrass structure on the distribution and abundance of mobile epifauna: pattern and process in a Western Australian *Amphibolis* bed. *Journal of Experimental Marine Biology and Ecology*, 160: 13–31.

Feng, M., Caputi, N., Penn, J., Slawinski, D., de Lestang, S., Weller, E. & Pearce, A. 2011. Ocean circulation, stokes drift, and connectivity of Western Rock Lobster (*Panulirus cygnus*) population. *Canadian Journal of Fisheries and Aquatic Sciences*, 68: 1182–1196.

Fraser, M.W., Kendrick, G.A., Statton, J., Hovey, R.K., Zavala-Perez, A. & Walker, D.I. 2015. Extreme climate events lower resilience of foundation seagrass at edge of biogeographical range. *Journal of Ecology*, 102: 1528–1536.

Gartner, A., Tuya, F., Lavery, P.S. & McMahon, K. 2013. Habitat preferences of macroinvertebrate fauna among seagrasses with varying structural forms. *Journal of Experimental Marine Biology and Ecology*, 439: 143–151.

George, R.W. 1962. Description of *Panulirus cygnus* sp. nov., the commercial crayfish (or spiny lobster) of western Australia. *Journal of the Royal Society of Western Australia*, 45: 100–110.

- Haswell, W.A. 1879. On the Australian species of *Penaeus*, in the Macleay Museum, Sydney. In: Proceedings of the Linnean Society of New South Wales, 4: 38–44.
- Heck, K.L. Jr. & Orth, R.J. 2006. Predation in seagrass beds. In: Seagrasses: biology, ecology and conservation. (A.W.D. Larkum, R.J. Orth & C.M. Duarte.), pp. 537–550. Springer-Verlag, Berlin & Heidelberg.
- Herrnkind, W.F. & Butler, M.J. 1986. Factors regulating postlarval settlement and juvenile microhabitat use by spiny lobsters *Panulirus argus*. Marine Ecology Progress Series, 34: 23–30.
- Hope, A.C.A. 1968. A simplified Monte Carlo significance test procedure. Journal of the Royal Statistical Society, Series B, 30: 582–598.
- Howard, R.K. 1988. Fish predators of the Western Rock Lobster (*Panulirus cygnus* George) in a nearshore nursery habitat. Marine and Freshwater Research, 39: 307–316.
- Hutton, F.W. 1875. Descriptions of two new species of Crustacea from New Zealand. Annals and Magazine of Natural History, Series 4, 15: 41–42.
- Jefts, A.G., Montgomery, J.C. & Tindle, C.T. 2005. How do spiny lobster post-larvae find the coast? New Zealand Journal of Marine and Freshwater Research, 39: 605–617.
- Jernakoff, P. 1987. Foraging patterns of juvenile Western Rock Lobsters *Panulirus cygnus* George. Journal of Experimental Marine Biology and Ecology, 113: 125–144.
- Jernakoff, P. 1990. Distribution of newly settled Western Rock Lobsters *Panulirus cygnus*. Marine Ecology Progress Series, 66: 63–74.
- Jernakoff, P., Fitzpatrick, J., Phillips, B.F. & De Boer, E. 1994. Density and growth in populations of juvenile Western Rock Lobsters, *Panulirus cygnus* (George). Marine and Freshwater Research, 45: 69–81.
- Jernakoff, P., Phillips, B.F. & Fitzpatrick, J.J. 1993. The diet of post-juvenile Western Rock Lobster, *Panulirus cygnus* George, at Seven Mile Beach, Western Australia. Marine and Freshwater Research, 44: 649–655.
- Johnston, D., Melville-Smith, R., Hendriks, B., Maguire, G.B. & Phillips, B. 2006. Stocking density and shelter type for the optimal growth and survival of Western Rock Lobster *Panulirus cygnus* (George). Aquaculture, 260: 114–127.
- Joll, L.M. & Phillips, B.F. 1984. Natural diet and growth of juvenile Western Rock Lobsters *Panulirus cygnus* George. Journal of Experimental Marine Biology and Ecology, 75: 145–169.
- Jordà, G., Marbà, N. & Duarte, C.M. 2012. Mediterranean seagrass vulnerable to regional climate warming. Nature Climate Change, 2: 821–824.
- Kendrick, G.A., Nowicki, R.J., Olsen, Y.S., Strydom, S., Fraser, M.W., Sinclair, E.A., Statton, J., Hovey, R.K., Thomson, J.A., Burkholder, D.A., McMahon, K.M., Kilminster, K., Hetzel, Y., Fourqurean, J.W., Heithaus, M.R. & Orth, R.J. 2019. A systematic review of how multiple stressors from an extreme event drove ecosystem-wide loss of resilience in an iconic seagrass community. Frontiers in Marine Science, 6: 455 [[https://doi.org/ 10.3389/fmars.2019.00455](https://doi.org/10.3389/fmars.2019.00455)].
- Kenning, M., Lehmann, P., Lindström, M. & Harzsch, S. 2015. Heading which way? Y-maze chemical assays: not all crustaceans are alike. Helgoland Marine Research, 69: 305–311.

Kennington, W.J., Berry, O., Groth, D.M., Johnson, M.S. & Melville-Smith, R. 2013. Spatial scales of genetic patchiness in the Western Rock Lobster *Panulirus cygnus*. Marine Ecology Progress Series, 486: 213–221.

Keulen, M. van. 2019. Multiple climate impacts on seagrass dynamics: *Amphibolis antarctica* patches at Ningaloo Reef, Western Australia. Pacific Conservation Biology, 25: 211–212 [<https://doi.org/10.1071/PC18050>].

Kilminster, K., Hovey, R., Waycott, M. & Kendrick, G.A. 2018. Seagrasses of Southern and South-Western Australia. In: Seagrasses of Australia: structure, ecology and conservation. (A.W.D. Larkum, G.A. Kendrick, & P.J. Ralph), pp. 61–89. Springer International, Cham, Switzerland.

Koch, M., Bowes, G., Ross, C. & Zhang, X.-H. 2013. Climate change and ocean acidification effects on seagrasses and marine macroalgae. Global Change Biology, 19: 103–132.

Koenigstein, S., Mark, F.C., Gößling-Reisemann, S., Reuter, H. & Poertner, H.-O. 2016. Modelling climate change impacts on marine fish populations: process-based integration of ocean warming, acidification and other environmental drivers. Fish and Fisheries, 17: 972–1004.

Latreille, P.A. 1804. Des langoustes du Muséum national d'Histoire Naturelle. Annales du Muséum national d' Histoire naturelle, 3: 388–395

Lestang, S. de 2014. The orientation and migratory dynamics of the Western Rock Lobster, *Panulirus cygnus*, in Western Australia. ICES Journal of Marine Science, 71: 1052–1063.

Lestang, S. de, Caputi, N. & How, J. 2016.: Resource assessment report: Western rock lobster resource of Western Australia. Western Australian Marine Stewardship Council Report Series No. 9, Department of Fisheries, Perth, WA, Australia.

Lestang, S. de, Caputi, N. & Melville-Smith, R. 2009. Using fine-scale catch predictions to examine spatial variation in growth and catchability of *Panulirus cygnus* along the west coast of Australia. New Zealand Journal of Marine and Freshwater Research, 43: 443–455.

Linnaeus, C. 1758. Systema Naturae per Regna Tria Naturae, Secundum Classes, Ordines, Genera, Species, cum Characteribus, Differentiis, Synonymis, Locis. Vol. 1, Edn. 10. Reformata. Laurentii Salvii, Holmiae [= Stockholm].

MacDiarmid, A.B. 1994. Cohabitation in the spiny lobster *Jasus edwardsii* (Hutton, 1875). Crustaceana, 66: 341–355.

Macmillan, D.L., Phillips, B.F. & Coyne, J.A. 1992. Further observations on the antennal receptors of rock lobsters and their possible involvement in puerulus stage navigation. Marine Behaviour and Physiology, 19: 211–225.

Marx, J. & Herrnkind, W. 1985. Factors regulating microhabitat use by young juvenile spiny lobsters, *Panulirus argus*: food and shelter. Journal of Crustacean Biology, 5: 650–657.

McMahon, K., Statton, J. & Lavery, P. 2017. Seagrasses of the northwest of Western Australia: biogeography and considerations for dredging-related research. Western Australian Marine Science Institution, Perth, WA, Australia.





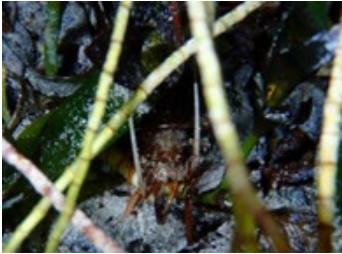


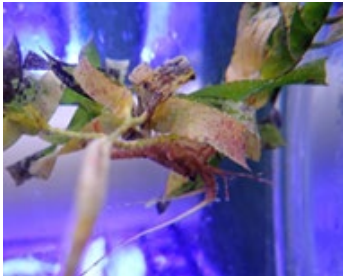
Miller, A., de Lestang, S., How, J., Gibbons, B., Lester, E., Navarro, M., Fitzhardinge, J., Brooker, M. & Langlois, T. 2023. Fine-scale variability in catch and growth rates of Western Rock Lobsters (*Panulirus Cygnus*) show heterogeneous life-history parameters. Marine and Freshwater Research, 74: 335–346.

- Milne Edwards, H. 1837. Histoire Naturelle des Crustacés, Comprenant l'Anatomie, la Physiologie et la Classification de ces Animaux, Vol. 2. Librairie Encyclopédique de Roret, Paris.
- Moyle, K., Johnston, D., Knott, B., Melville-Smith, R. & Walker, D. 2009. Effect of stocking density on the growth, survival, and behavior of postpuerulus Western Rock Lobster, *Panulirus cygnus* (George) (Decapoda: Palinuridae). *Journal of the World Aquaculture Society*, 40: 255–265.
- Oliver, E.C.J., Donat, M.G., Burrows, M.T., Moore, P.J., Smale, D.A., Alexander, L.V., Benthuisen, J.A., Feng, M., Sen Gupta, A., Hobday, A.J., Holbrook, N.J., Perkins-Kirkpatrick, S.E., Scannell, H.A., Straub, S.C. & Wernberg, T. 2018. Longer and more frequent marine heatwaves over the past century. *Nature Communications*, 9: 1324 [<https://doi.org/10.1038/s41467-018-03732-9>].
- Pearce, A.F. & Feng, M. 2013. The rise and fall of the “marine heat wave” off Western Australia during the summer of 2010/2011. *Journal of Marine Systems*, 111-112: 139–156.
- Phillips, B.F. 1972. A semi-quantitative collector of the puerulus larvae of the Western Rock Lobster *Panulirus longipes cygnus* George (Decapoda, Palinuridea). *Crustaceana*, 22: 147–154.
- Phillips, B.F. 1986. Prediction of commercial catches of the Western Rock Lobster *Panulirus cygnus*. *Canadian Journal of Fisheries and Aquatic Sciences*, 43: 2126–2130.
- Phillips, B.F. & McWilliam, P.S. 2009. Spiny lobster development: where does successful metamorphosis to the puerulus occur?: a review. *Reviews in Fish Biology and Fisheries*, 19: 193–215.
- Phillips, B.F., Brown, P.A., Rimmer, D.W. & Reid, D.D. 1979. Distribution and dispersal of the phyllosoma larvae of the Western Rock Lobster, *Panulirus cygnus*, in the south-eastern Indian ocean. *Marine and Freshwater Research*, 30: 773–783.
- Phillips, B.F., Campbell, N.A. & Rea, W.A. 1977. Laboratory growth of early juveniles of the Western rock lobster *Panulirus longipes cygnus*. *Marine Biology*, 39: 31–39.
- Pineda, J., Hare, J.A. & Sponaugle, S.U. 2007. Larval transport and dispersal in the coastal ocean and consequences for population connectivity. *Oceanography*, 20: 22–39.
- R Core Team. 2021. R: A language and environment for statistical computing., R Foundation for Statistical Computing, Vienna [<http://www.Rproject.org>].
- Reid, C., Caputi, N., de Lestang, S. & Stephenson, P. 2013. Assessing the effects of moving to maximum economic yield effort level in the Western Rock Lobster fishery of Western Australia. *Marine Policy*, 39: 303–313.
- Smale, D.A. & Wernberg, T. 2013. Extreme climatic event drives range contraction of a habitat-forming species. *Proceedings of the Royal Society B*, 280: 20122829 [<https://doi.org/10.1098/rspb.2012.2829>].
- Smale, D.A., Wernberg, T. & Vanderklift, M.A. 2017. Regional-scale variability in the response of benthic macroinvertebrate assemblages to a marine heatwave. *Marine Ecology Progress Series*, 568: 17–30.
- Smith, K.N. & Herrnkind, W.F. 1992. Predation on early juvenile spiny lobsters *Panulirus argus* (Latreille): influence of size and shelter. *Journal of Experimental Marine Biology and Ecology*, 157: 3–18.

- Stamps, J. & Groothuis, T.G.G. 2010. The development of animal personality: relevance, concepts and perspectives. *Biological Reviews*, 85: 301–325.
- Stanley, J.A., Hesse, J., Hinojosa, I.A. & Jeffs, A.G. 2015. Inducers of settlement and moulting in post-larval spiny lobster. *Oecologia*, 178: 685–697.
- Strydom, S., Murray, K., Wilson, S., Huntley, B., Rule, M., Heithaus, M., Bessey, C., Kendrick, G.A., Burkholder, D., Fraser, M.W. & Zdunic, K. 2020. Too hot to handle: unprecedented seagrass death driven by marine heatwave in a World Heritage Area. *Global Change Biology*, 26: 3525–3538.
- Thomson, J.A., Burkholder, D.A., Heithaus, M.R., Fourqurean, J.W., Fraser, M.W., Statton, J. & Kendrick, G.A. 2015. Extreme temperatures, foundation species, and abrupt ecosystem change: an example from an iconic seagrass ecosystem. *Global Change Biology*, 21: 1463–1474.
- van der Meeren, G.I. & Woll, A.K. 2019. The cryptic *Homarus gammarus* (L., 1758) juveniles: a comparative approach to the mystery of their whereabouts. In: *Lobsters: biology, behavior and management*. (B.K. Quinn, ed.), pp. 61–120. Nova Science Publishers, New York.
- Wahle, R.A. & Steneck, R.S. 1992. Habitat restrictions in early benthic life: experiments on habitat selection and in situ predation with the American lobster. *Journal of Experimental Marine Biology and Ecology*, 157: 91–114.
- Walker, D.I., Kendrick, G.A. & McComb, A.J. 1988. The distribution of seagrass species in Shark Bay, Western Australia, with notes on their ecology. *Aquatic Botany*, 30: 305–317.
- Wernberg, T., Bennett, S., Babcock, R.C., de Bettignies, T., Cure, K., Depczynski, M., Dufois, F., Fromont, J., Fulton, C.J., Hovey, R.K., Harvey, E.S., Holmes, T.H., Kendrick, G.A., Radford, B., Santana-Garcon, J., Saunders, B.J., Smale, D.A., Thomsen, M.S., Tuckett, C.A., Tuya, F., Vanderklift, M.A. & Wilson, S. 2016. Climate-driven regime shift of a temperate marine ecosystem. *Science*, 353: 169–172.
- Wernberg, T., Smale, D.A., Tuya, F., Thomsen, M.S., Langlois, T.J., de Bettignies, T., Bennett, S. & Rousseaux, C.S. 2013. An extreme climatic event alters marine ecosystem structure in a global biodiversity hotspot. *Nature Climate Change*, 3: 78–82.
- Yoshimura, T. & Yamakawa, H. 1988. Microhabitat and behavior of settled pueruli and juveniles of the Japanese spiny lobster *Panulirus japonicus* at Kominato, Japan. *Journal of Crustacean Biology*, 8: 524–531.
- Zito-Livingston, A.N. & Childress, M.J. 2009. Does conspecific density influence the settlement of Caribbean spiny lobster *Panulirus argus* postlarvae? *New Zealand Journal of Marine and Freshwater Research*, 43: 313–325.

Supplementary materials

Supporting Table 9. Images of early-juvenile *Panulirus cygnus* in microhabitat types of *Amphibolis* in mesocosm trials.

Description of <i>Amphibolis</i> microhabitats		
<p><i>Amphibolis</i> associated sand</p> <p>Defined by one early juvenile body length away from edge of <i>Amphibolis</i></p> <p>Mostly sand with some shelter from <i>Amphibolis</i></p>		
<p>Leaf Debris</p> <p>Leaf pile on sand bed</p> <p>Can be on or hiding below</p>		
<p><i>Amphibolis</i> Stems</p> <p>Early juvenile amongst <i>Amphibolis</i> patch regardless of shoot density</p>		
<p><i>Amphibolis</i> Fronds</p> <p>Up in the leaves of <i>Amphibolis</i></p>		

Supporting Table 10. Results of pairwise chi-square comparisons of choices of *Amphibolis* microhabitat by early-juvenile *Panulirus cygnus* across changing stem density.

Stem density	Microhabitat	2100	1600	1100	600	2100	1600	1100	600	2100	1600	1100	600	2100	1600	1100	600	2100	1600	1100	600	2100	1600	1100	600	2100	1600	1100	600
		Fr	Fr	Fr	Fr	St	St	St	St	De	De	De	De	Sa	Sa	Sa	Sa	BS	BS	BS	BS	NC	NC	NC	NC	NC	NC	NC	NC
2100	Fr																												
1600	Fr	0.444																											
1100	Fr	0.034	-																										
600	Fr	0.341	-	-																									
2100	St	-	0.034	0.034	0.034																								
1600	St	-	0.034	0.034	0.034	-																							
1100	St	-	-	0.409	0.990	-	-																						
600	St	-	-	-	-	0.819	-	-																					
2100	De	0.136	-	-	-	0.034	0.034	-	-																				
1600	De	-	-	-	-	0.921	-	-	-	-																			
1100	De	-	-	-	-	0.546	-	-	-	-	-																		
600	De	-	-	-	-	-	-	-	-	-	-	-																	
2100	Sa	0.034	-	-	-	0.034	0.034	0.102	-	-	0.751	-	0.273																
1600	Sa	0.307	-	-	-	0.034	0.034	-	-	-	-	-	-	-															
1100	Sa	-	-	-	-	0.136	0.751	-	-	-	-	-	-	-	-														
600	Sa	-	0.580	0.102	0.239	-	-	-	-	0.273	-	-	-	0.034	0.887	-													
2100	BS	0.034	-	-	-	0.034	0.034	0.068	-	0.203	0.307	0.273	0.034	-	-	0.955	0.034												
1600	BS	0.034	-	-	-	0.034	0.034	0.034	0.375	-	0.136	0.375	0.102	-	-	-	0.034	-											
1100	BS	0.068	-	-	-	0.034	0.034	0.034	0.171	-	0.819	-	0.239	-	-	-	0.034	-	-										
600	BS	0.034	-	-	-	0.034	0.034	0.068	-	-	0.273	0.205	0.034	-	-	-	0.034	NA	NA	0.425									
2100	NC	0.785	-	-	-	0.034	0.034	-	0.273	-	-	-	-	-	-	-	-	-	-	-									
1600	NC	-	-	-	-	-	-	-	-	-	-	-	-	0.853	-	-	-	0.171	0.068	-	0.239	0.819							
1100	NC	-	0.375	0.034	0.102	-	-	-	-	0.136	-	-	-	0.068	0.273	-	-	0.034	0.034	0.034	0.034	-	-						
600	NC	-	-	-	-	-	-	-	-	-	-	-	-	0.580	-	-	-	0.102	0.136	0.478	0.171	-	-	-					

Study 5 - Disconnect between settlement and fishery recruitment driven by decadal changes in nearshore habitats

Preface

This study brings the components of the study together to examine how long-term changes in nearshore seabed habitats relate to WRL recruitment dynamics across multiple coastal locations throughout the WRLMF. By analysing multidecadal remote sensing data and recruitment indices, we explore how shifts in submerged habitat extent, potentially driven by climate variability and other factors, potentially impact the recruitment of lobster into the fishery.

Disconnect between settlement and fishery recruitment driven by decadal changes in nearshore habitats

Published in: Science of the Total Environment

<https://doi.org/10.1016/j.scitotenv.2025.178785>

Authors and affiliations:

Stanley Mastrantonis^{1,2,3,5}, Simon de Lestang⁶, Tim Langlois^{3,5}, Ben Radford^{1,2,3,4}, Claude Spencer^{3,5}, John Fitzhardinge⁷ and Sharyn Hickey^{1,2,3}

¹School of Agriculture and Environment, The University of Western Australia, Crawley, WA, Australia

²Centre for Water and Spatial Science, The University of Western Australia, Crawley, WA, Australia

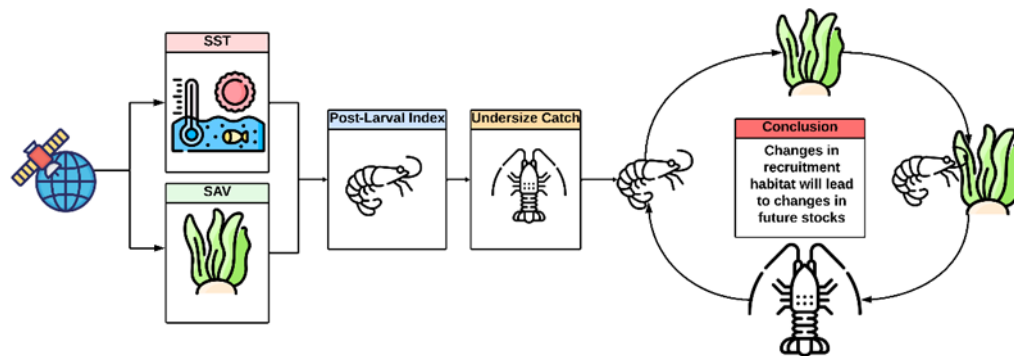
³UWA Oceans Institute, The University of Western Australia, Crawley, WA, Australia

⁴Australian Institute of Marine Science, 39 Fairway, Crawley, Western Australia, Australia.

⁵School of Biological Sciences, The University of Western Australia, Crawley, WA, Australia

⁶Western Australian Fisheries and Marine Research Laboratories, Department of Primary Industries and Regional Development, North Beach, WA, Australia

⁷Dongara Marine, 169 Connell Road, West End, WA, Australia



Abstract

Submerged vegetation is critical to marine ecosystems and can function as recruitment habitats for commercially targeted species, such as the highly valuable Western Rock Lobster *Panulirus cygnus*. The development of vegetation indices for marine remote sensing has made tracking the extent and change of submerged vegetation in space and time possible. Vegetation changes may directly or indirectly affect the recruitment and population dynamics of animals that depend on these habitats. Previous studies have found that extreme climate events, such as marine heatwaves, can cause declines in submerged vegetation extent, but these studies have been limited spatially and temporally. Here, we present multidecadal extents of submerged vegetation and settlement indices for five coastal locations throughout the range of Western Rock Lobster and explore how these vegetation trends relate to an index of recruitment. We found that the correlations of vegetative extent, climate and undersize lobster catch varied significantly between the monitored locations. For some locations, particularly those with a high composition of preferential recruitment habitat (i.e., seagrass), vegetation extent in the previous two years significantly explained variation in undersize catch rates. Regions with a time series of undersize lobster and settlement data combined with consistent remotely sensed imagery allowed for the disentanglement of the influence of habitat change and post-settlement recruitment. Whereas, at locations with poor quality historical data, often due to the combined effect of turbidity and a relatively steep coastal shelf or limited catch data, the recruitment index was not improved by information on submerged vegetation. We have found that decadal changes in nearshore habitats at representative locations have driven the disconnect between settlement and fishery recruitment. We suggest that monitoring marine habitats can complement long-term fishery data collection and coastal management.

Introduction

In addition to the impacts of long-term climatic warming (Reddin et al., 2022), extreme climate events, such as marine heatwaves (MHWs), defined as extensive, persistent and extreme ocean temperature events, can adversely affect coastal ecosystems, including marine invertebrates and primary producers such as Submerged Aquatic Vegetation (SAV; Oliver et al., 2018; Smith et al., 2023). Coordinated research into the mechanisms and ecological impacts of MHWs became prominent after a MHW event across the mid-western Australian coast in 2010/11, from Port Gregory to Mandurah during which the term ‘marine heatwave’ was first used (Holbrook et al., 2020; Fig. 24). Under climate change predictions, MHWs are expected to increase in frequency and extent, leading to increased impacts on submerged vegetation extent and cascading effects on marine ecosystems (Serrano et al., 2021; Straub et al., 2019). Previous research has suggested that the 2010/11 MHW led to significant change in the extent of submerged vegetation, where extreme range contractions of the prominent habitat-forming seaweed *Scytothalia dorycarpa* along the mid-western Australian Coast and an estimated loss of 1,310km² of seagrass *Amphibolis antarctica* and *Posidonia* spp. within the Shark Bay World Heritage Area (Smale et al., 2017; Strydom et al., 2020; Wernberg et al., 2016). Climate-mediated alterations to critical marine habitats, such as SAV, are hypothesised to have flow-on effects on mammals, fishes and invertebrate assemblages (Smith et al., 2023). However, the indirect climate-mediated impact of habitat change on recruitment in invertebrate fisheries has not been systematically quantified across decadal timescales or at regional geographic scales. Despite the relatively recent advent and accessibility of remote sensing imagery, tracking critical fishery habitats across time is challenging and requires historical and standardised marine habitat indices for robust estimates (Study 2; Mastrantonis et al., 2024a).

The West Coast Rock Lobster Managed Fishery (WCRLMF) is Australia’s most valuable single-species fishery, solely focused on the Western Rock Lobster (WRL) *Panulirus cygnus*, and is internationally recognised for its sustainable management practices. The WCRLMF is the world’s first fishery to receive certification for ecological sustainability from the Marine Stewardship Council in 2000 (Caputi et al., 2015). Since the 1960s, management of the WCRLMF has been informed by postlarval (puerulus) settlement indices (PIs) derived from artificial seagrass stations that are monitored lunar-monthly at eight coastal locations across the main geographical range of the species (Phillips and Hall, 1978). The postlarval settlement index has been used to predict subsequent recruitment into the fished population with a three to four-year lag (Fig. 25; Caputi et al., 1995; de Lestang et al., 2009). Following the 2010/11 MHW, previously observed predictive capacity of the PI to undersize recruitment and subsequent commercial catch rates has decreased (de Lestang et al., 2015). Other invertebrate fisheries worldwide have used similar indices to predict recruitment into the fished population and manage stocks sustainably. Indeed, programmes have ‘sought to emulate Australia’s western rock lobster (*P. cygnus*) postlarval index program, both to construct a proper monitoring program for newly settled lobsters and develop an early warning system for future commercial harvest’ (McManus, 2024). Commercial catches of the Caribbean spiny lobsters *Panulirus argus* across Florida were highly correlated with the abundance of pueruli on artificial collectors with an 18-27 month lag (Hutchinson et al., 2024). For the American lobster *Homarus americanus*, annual biomass densities of benthic recruits are used to generate indices of future exploited biomass (White et al., 2024). In a retrospective of the settlement indices to predict catches for the American lobster, McManus (2024) reiterated the importance of the ‘continuous re-evaluation’ of such models, which may be sensitive to the period of data analysed and break down or change over time with additional years of data.

The influence of the environment, especially water temperatures, on the behaviour and biology of WRL has been extensively studied (de Lestang and Melville-Smith, 2012; de Lestang and Caputi, 2015; de Lestang, 2018; Caputi et al. 2019). In general, warmer water temperatures have

been shown to expedite many life history processes, from the timing of moulting, migration, and reproduction to the age at which sexual maturity is attained and the likelihood of a lobster entering a pot. For the American lobster fishery, previous research has shown that adding environmental covariates, specifically bottom temperatures, significantly improved model performance and allowed for better predictions of future landings (Oppenheim et al., 2019). There has also been substantial work published on the habitat choices made by the WRL (Bellchambers et al., 2013; Brooker et al., 2022; Chittleborough, 1970; Oh et al., 2023), with early juveniles exhibiting a preference for seagrass over other habitats, especially the complex sub-canopy structure of *Amphibolis antarctica*. With regard to fisheries outside of Australia, previous research has shown that the Caribbean spiny lobster *Panulirus argus* settles preferentially in macroalgal-covered hard-bottom habitat. However, seagrass is more prevalent across the Caribbean, and lower settlement rates by lobsters within seagrass could still contribute substantially to recruitment (Behringer et al., 2009). Despite the likely importance of benthic habitats for spiny lobster recruitment, such as seagrass and macroalgae, ‘little is known on the potential long-term effect of habitat loss and degradation for *Panulirus* lobsters’ (Briones-Fourzán and Lozano-Álvarez, 2013). Therefore, habitat loss and alteration are particularly concerning as the effects of change on *Panulirus* survival and recruitment could be linear, non-linear or may be linked to undetermined thresholds of loss. Remote sensing offers the potential to track seascape and habitat changes at bioregional spatial scales and has previously been used for fisheries applications (Lan et al., 2017). However, long-term tracking of habitats with remote sensing is challenging, particularly in marine environments. Even with the increased accessibility of aerial imagery and in-situ benthic habitat data worldwide, there remains limited long-term information on habitat and climate change that allows for causal inference on the population dynamics of fisheries species that may rely on shallow-water habitats for recruitment.

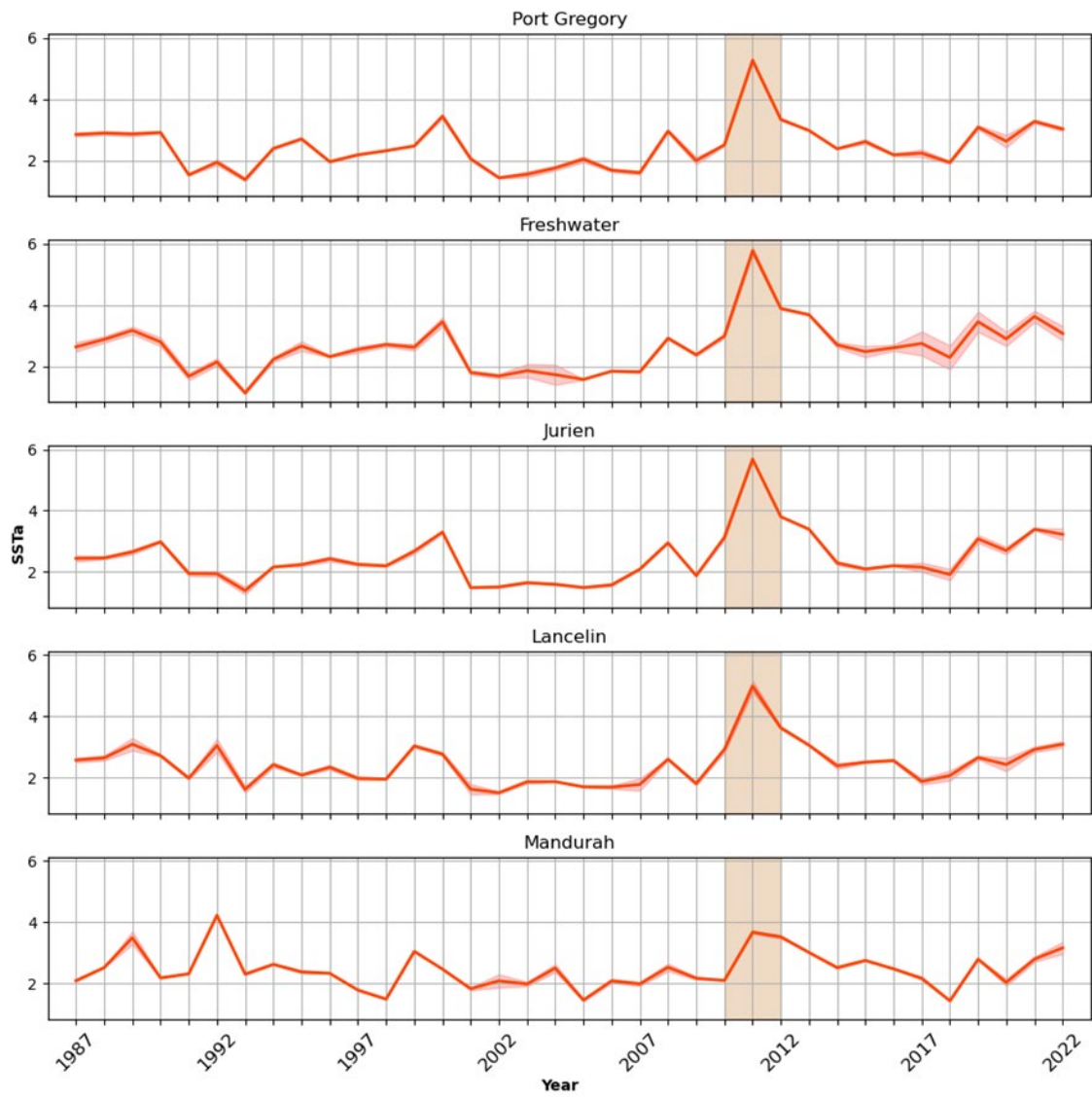


Figure 24 Sea Surface Temperature anomalies (SSTa) for Port Gregory, Freshwater, Jurien, Lancelin, and Mandurah sites from 1987 to 2023. The orange region represents the 2010-/11 Marine Heatwave (MHW). Sea Surface Temperature Anomalies were sourced from NOAA OISST.

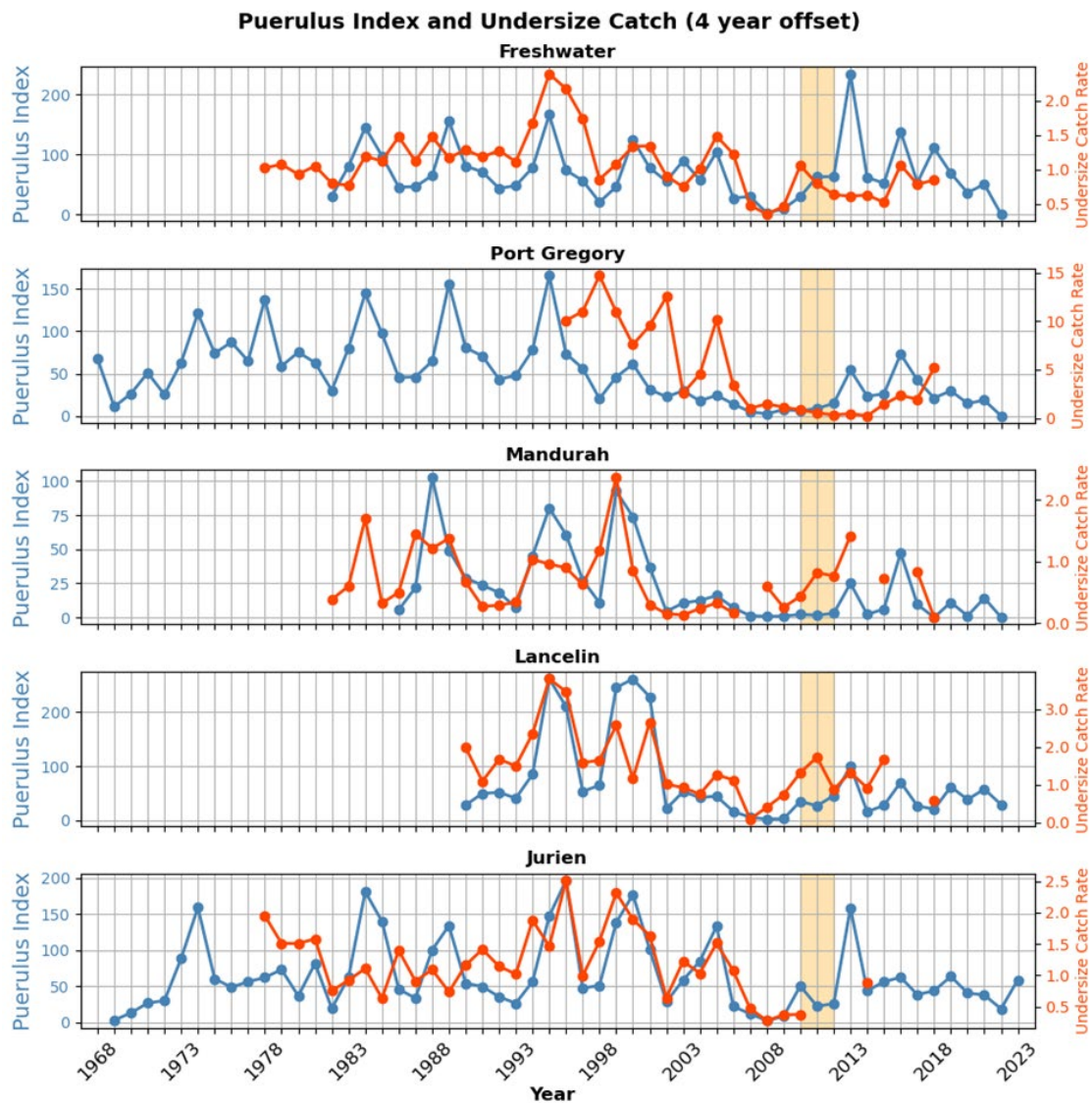


Figure 25 The puerulus Index (PI; blue) and the undersize catch rate with a four-year lag (orange) for Port Gregory, Freshwater, Jurien, Lancelin, and Mandurah from 1968 to 2023. The orange region represents the 2010/11 Marine Heatwave (MHW).

Monitoring changes in WRL recruitment as a response to changes in the extent of recruitment habitat (SAV) or MHWs could be achieved through the use of remote sensing platforms such as Landsat or Sentinel-2 (Study 2; Mastrantonis et al., 2024a). New methods in marine remote sensing allow for the kernelisation of spectral bands, while simultaneously calibrating spectra across space and time (Study 2; Mastrantonis et al., 2024a). Kernelisation and calibration of spectra provide a means to standardise imagery for classification, allowing for robust estimations of SAV extent, even when applied to historical imagery catalogues such as Landsat 5-8 (i.e., 1987-2022).

Here, we investigate changes in the extent and landscape characteristics of SAV since 1987 for five coastal locations on the mid-west Australian coast that have been concurrently monitored for puerulus settlement and standardised undersize catch rate of WRL as a measure of recruitment. Building on decades of research conducted on WRL population dynamics and the influence of climate and habitat change, we investigate how changes in habitat extent affect this commercially valuable species (Penn and Caputi, 1986; Caputi et al., 2013). We model the

relationship between undersize catch rates and the covariates of vegetation change, settlement indices, and long-term climate trends such as Degree Heating Weeks (DHW) and Sea Surface Temperature (SST) anomalies. We hypothesised that undersize catch rates for any given year at the five monitored locations would be significantly affected by changes in puerulus settlement rates and recruitment habitat extent, represented by SAV, or extreme temperatures in previous years. We suggest that nearshore invertebrate fisheries worldwide that model catch from settlement would benefit from integrating long-term habitat metrics to improve predictions and management.

Methods and Materials

Study Location

Five study locations were selected along the west coast of Australia, spanning the major fished area for Western Rock Lobster, and where puerulus settlement is monitored using artificial seaweed stations by the Department of Primary Industries and Regional Development (DPIRD; de Lestang and Roszbach, 2018). The study locations used in this research covered 600 km spanning (North to South) Port Gregory (114.26°E 28.22°S), Freshwater (114.92°E 29.61°S), Jurien Bay (114.99°E 30.26°S), Lancelin (115.29°E 31.01°S) to Mandurah (115.58°E 32.73°S; Fig. 26). The selected locations have a depth range of zero to 30 meters below sea level and predominantly feature brown macroalgae *Ecklonia radiata* and unconsolidated (sandy), consolidated (rocky) substrate and seagrasses present at lower abundance (Fig. 27).

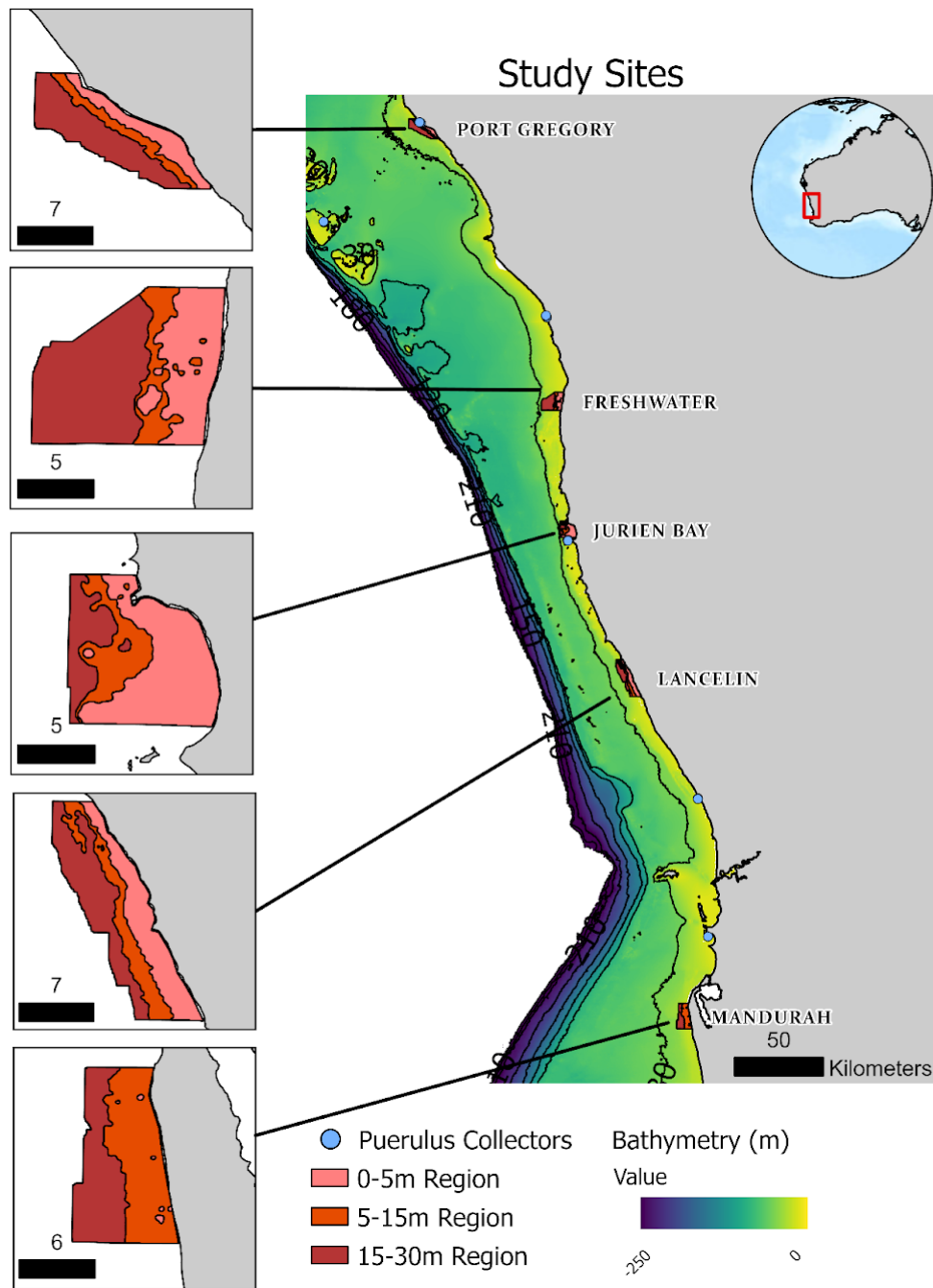


Figure 26 Study locations span the midwest region of Western Australia. Study locations have been shown with 0-5m regions, 5-15m, and 15-30m extents. Bathymetry (m) data were sourced from Geoscience Australia's Bathymetry and Topography Grid (Whiteway, 2009). Contour lines represent 30m depth intervals.

Survey designs

Spatially balanced designs

Sampling of the coastal locations for benthic habitat types was conducted between April 7th and 24th 2021 to generate Ground Truthing Points (GTPs) for SAV model calibration and validation. The survey was designed using Generalised Random Tesselation Stratified (GRTS) sampling, where the study locations were divided into strata using remote sensing imagery and bathymetric LiDAR, and samples were allocated across the stratum in a spatially balanced manner (Stevens and Olsen, 2004). Surveys were conducted using a Benthic Observation Survey System (BOSS) installed on an aluminium frame (<https://drop-camera-field-manual.github.io/>, (Study 1; Langlois et al., 2025). Four cameras were positioned on the frame for horizontal recording, offering a wide-field (~270°) view of the benthos. The BOSS was deployed at each GTP for one to five minutes to ensure that any suspended silt settled for clear footage. Based on the degree of occlusion within the image, the imagery was evaluated ordinally (very poor, poor, moderate, and good); only imagery ranked as good or moderate was included in this investigation. To focus on benthic habitats, picture annotation was limited to the bottom 50% of each image following standard operating procedures (Langlois et al., 2020). A modified version of the Collaborative and Annotation Tools for Analysis of Marine Imagery and Video (CATAMI) schema was used to annotate 80 randomly selected spots for each image (Althaus et al., 2015). Habitats detected across the study sites were macroalgae, seagrass, sandy substrates and consolidated (rocky) substrates, and the average compositions for all camera drops at each site have been summarised (Fig. 27). These habitat summaries only reflect the compositions at discrete points surveyed by the BOSS camera and are not necessarily representative of the habitat compositions at the wider site, but as samples were spatially balanced, there will be some correlation. Using the Scikit-Learn module (Python 3.11.3), a hierarchical clustering method was used to classify the annotated picture into feature labels (Kramer, 2016). Clusters were identified by separating the percentages of each CATAMI class in all underwater images and allocating an unsupervised class to each drop camera point. This resulted in three distinct classes that broadly delineated the data into the seagrass and macroalgae dominated annotations, with the third class grouping the remaining benthic habitats such as sand and consolidated substrates. The seagrass and macroalgae clusters were subsequently grouped into a single class as 'Submerged Aquatic Vegetation' (SAV), while the remaining habitats were classed as 'other' (Study 2 & 3; Mastrantonis et al., 2024a, 2024b).

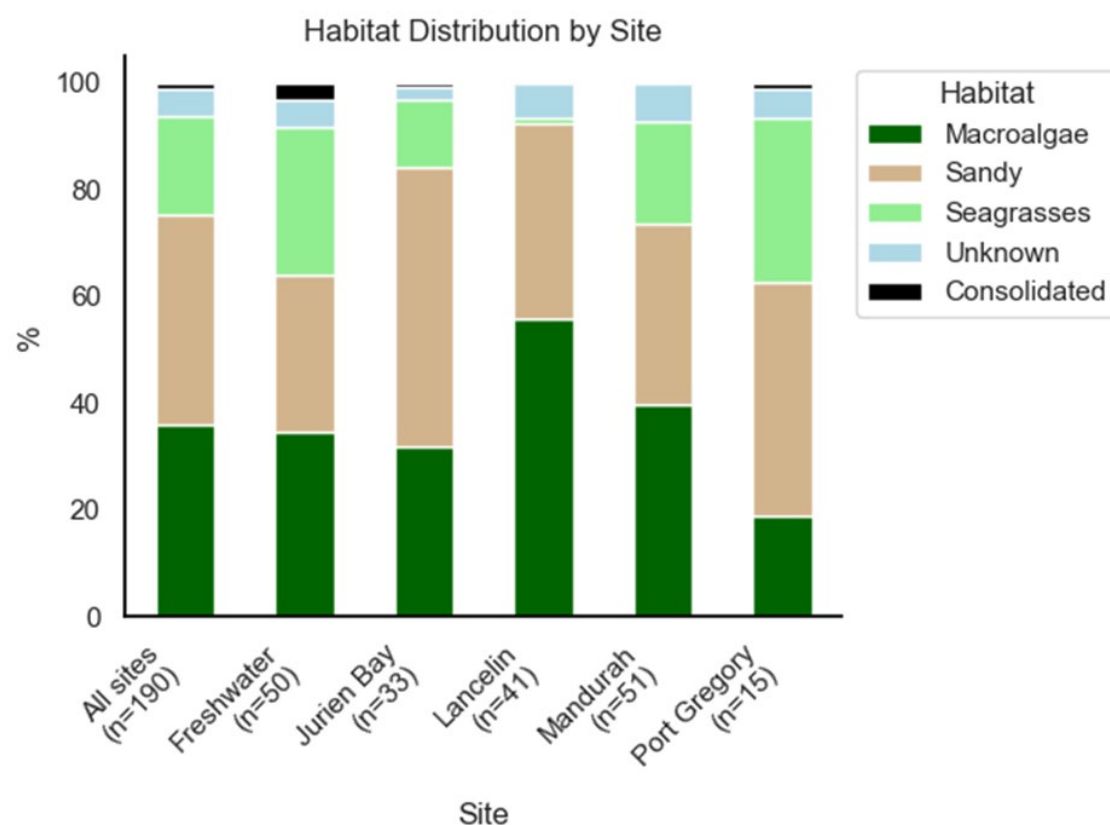


Figure 27 Habitat summaries of the underwater image annotations for each of the study locations. The percent values represent annotations for each habitat in all images for the corresponding location, with the total number of sample points depicted on the x-axis. The stacked bar of 'All locations' represents the average composition of all locations.

Remote sensing imagery, climate and SAV classification

The Landsat 5 and 8 collections were accessed using the Google Earth Engine (GEE) and its Python API (Gorelick et al., 2017). Landsat 7 imagery was deemed unsuitable to use in this study due to the Scan Line Corrector failure that occurred in May 2003 (see USGS website for details: <https://www.usgs.gov/landsat-missions/landsat-7>). Additionally, Landsat 5 data was unavailable for our locations between 1999-2002. A collection of Landsat imagery was generated for each location and year from 1987-2022. Each image in the collection was downloaded and assessed for suitability based on the degree of cloud, turbidity, wind waves and sensor issues (often caused by image calibration and interactions with aerosols in the atmosphere). Only images assessed as being good (i.e., low cloud, low turbidity, low wind waves and no sensor issues) were used in this study (see Supplementary Fig. S16). For turbidity and cloud assessments, images were classed as suitable if occlusion in the image from turbidity and cloud was less than ~10% of the extent of the site. Additionally, much of the good imagery was found to occur in the summer months; thus, only a single image from November to March was selected to keep classifications consistent and avoid any seasonal effects. Using the Blue and Near Infra-red (NIR) bands from each image, the Kernelised Normalised Aquatic Vegetation Index (*k*NDAVI; Study 2) was generated for all locations in all years.

A Random Forest (RF) model in caret (Kuhn, 2008) was trained using *k*NDAVI and the GTP data collected in 2021 and used to classify SAV for all years from 1987-2022 where imagery was available. Model development, calibration and validation were conducted following the procedures communicated in Mastrantonis et al. (Study 2). The RF models were parameterised with 1000 trees and a maximum splitting depth of 4 nodes to avoid overfitting, and the model

was calibrated on Landsat 8 imagery for 2021 (the field survey year). SAV was classified for the full extent of the study locations and 0-5m and 5-15m depth intervals within the study locations (Fig 26). We then calculated the full set of Landscape metrics (Bosch, 2019), including the proportion of the location that was vegetated (%SAV), for the classified data. Historical validation was performed across all the GTPs in the historical Landsat imagery for the same geometries as the 2021 survey year. These historical GTPs were annotated as SAV/Other based on a visual inspection of the corresponding Landsat image, and the classifications were compared to this annotation to derive kappa statistics for the study period at each study site. Climate data, including Degree Heating Weeks (DHW) and Sea Surface Temperature Anomalies (SSTa) were sourced from NOAA for the extent of each location for the study period (Huang et al., 2021). The SAV landscape metric data, climate data, PI and undersize catch rate data were collated for formal statistical analysis.

Puerulus Index

The Puerulus index, used to inform modelling and management of the WRL fishery, is derived from long-term DPIRD monitoring that occurs every five days on either side of every new moon at eight locations along the coast. The lunar-monthly sampling protocol has not changed since the inception of the program. A settlement season spans May to April (a season starting in May 2000 is considered the 2000 season), and the average number of puerulus per collector (five or six collectors deployed per location) is summed over the settlement season to derive an annual index. Some of the puerulus sites are not positioned directly within SAV monitoring sites or undersize catch data regions (see below), but we use this index as wider geographic and temporal proxy of post-larval abundance. For more details, see Kolbusz et al. (2021).

Undersize lobster catch rate index

The undersize lobster catch rate index is derived from data collected by DPIRD staff during the commercial lobster monitoring program and is used to inform modelling and management of the fishery. Staff aim to sample a minimum of 300 lobsters in each of four depth ranges (18m-intervals with the shallowest being 0 – 18m) at every main fishing port (Fremantle, Lancelin, Jurien, Dongara, Kalbarri, Abrolhos) during each month of the fishing season. Not all samples can be obtained if no fishing is occurring in that combination. See de Lestang et al. (2016) for more details on the sampling program. To derive the undersize index, samples are limited to those pots fished in the two shallowest depth categories ($\leq 36\text{m}$) during the non-migratory autumn phase (February - May), with the index being based on the catch rate of lobsters with carapace lengths between 75 and 76.9 mm. This size range is chosen as these lobsters are large enough not to be markedly impacted by the use of escape gaps in the pots (a requirement of the fishery) but not too large to be overly impacted by commercial fishing (minimum legal length is 76 mm). Since the data is based on commercial fishers and its collection is unbalanced between years, it has been standardised using a log-linear model to account for commercial fisher identity, pot soak time, month, depth category (0-18m or 18-36 m) and a fine-spatial index ($\frac{1}{6}^\circ$ latitude), with marginal back-transformed means determined for each year using the emmeans package in R (Lenth, 2024).

Multiple regression and change analysis

A full subsets selection was used to determine which variables should be considered for statistical analysis (Alan Miller, 2020), where the log of the undersize lobster catch rate formed the dependent variable and the SAV landscape metric, climate, and PI data formed the explanatory variables. Data were modelled using multiple linear regressions with statsmodel (Seabold and Perktold, 2010) in Python (3.11.3). Because there is approximately a 3.5 year time

lag between puerulus growing to 76 mm, the explanatory variables were temporally lagged to model the effects of previous years of SAV, climate and PI on undersize WRL catch rates. For example, undersize catch for any given year (t [Feb.-May]) was modelled with the SAV extents for the previous year ($t-1$ [November - March]), two years prior ($t-2$ [November - March]) or three years prior ($t-3$ [November - March]). Models were compared to the models developed by DPIRD to predict catch rates using the PI with three ($t-3$ [May-Apr.]) and four ($t-4$ [May-Apr.]) year lags. Subset selection showed the most important predictors to be the PI at $t-3$ and $t-4$, and SAV at $t-2$. A global model was fit where all data were included in the multiple linear regression, and location, as a factor with five levels, formed an interaction term:

$$\log(\text{Undersize Catch}_{t,s}) = b_0 + b_1 \log(PI_{t-3}) + b_2 \log(PI_{t-4}) + b_s \log(SAV_{t-2})$$

Where $\text{Undersize Catch}_{t,s}$ is the catch in year t at site s and b_s is the site-specific coefficient of the SAV extent effect. Data was also subset for each location to determine local relationships, if any, between undersize catch and SAV. A model was fit to explore any non-linear relationships in the SAV explanatory variable. An additional model was fit using all the available puerulus data and the subset of puerulus data used in the SAV models. Due to the SAV's temporal lags, less data is available for model fitting with the SAV component, and we tested whether there was any discrepancy in relationships between the full and subset data (Supplementary table 1). We performed post hoc regularisation of our liner models using an Elastic Net regression in statsmodel (Seabold and Perktold, 2010). Elastic Net regression combines L1 and L2 regularisation and is useful for understanding how predictors influence a response when there are many potentially correlated predictors, and aids in identifying important features in complex models by shrinking coefficients to avoid overfitting (Zou and Hastie, 2005). Models and summary statistics have been reported for the 0-15m depth ranges at all locations.

Change vector analysis (CVA; Leutner et al., 2017) uses two spectral bands (blue and NIR) to map the magnitude and directions of change in imagery across different dates and has been previously used to map change in forested landscapes with the Landsat inventory (Johnson and Kasischke, 1998). We apply CVA for every year of imagery for each location and aggregate the variation of change for the study period using a Principle Component Analysis (PCA), mapping the magnitude and angle of SAV change from 1987 to 2022. Additionally, we applied Local Indicators of Spatial Association (LISA; Bosch, 2019; Anselin, 1995) to every point in each location, where the magnitude of change is assessed for the associations listed below:

High-High (HH): Locations with change attribute values surrounded by neighbouring locations with high change values.

Low-Low (LL): Locations with low change values surrounded by neighbouring locations with low change values. These locations represent clusters of low values and indicate areas of low concentration or cold spots.

High-Low (HL): Locations with high change values surrounded by neighbouring locations with low change values.

Low-High (LH): Locations with low change values surrounded by neighbouring locations with high change values.

Results

SST & Submerged Aquatic Vegetation

Remote sensing confirmed Port Gregory, Freshwater, Jurien, and Lancelin all experienced unprecedented Sea Surface Temperature anomalies (SSTa) in the summer of 2010-2011, which were more pronounced across Port Gregory, Freshwater and Jurien (Fig. 24). Mandurah, the southernmost location, did not experience any unprecedented SSTa during this period. Remotely sensed measures of Submerged Aquatic Vegetation (SAV) revealed substantial temporal variation across these locations, based on training data collected in 2021 (Fig. 28). However, remote sensing data was not available between 2000-2003 and both during and just after the MHW of 2010-2011. There was also substantial variation in imagery quality over time, with all locations, except Jurien, having substantial gaps in their temporal record, with both Port Gregory to the north and Lancelin to the south missing multiple consecutive years of data due to high turbidity. Moreover, sensing vegetation in deep waters or over relatively steep seabed is challenging, even more so with Landsat, and measures of SAV in the 15-30m depth range and in locations with narrow depth contours should be assessed with a degree of uncertainty. When data was available, the temporal patterns of change in SAV were generally similar for all depth ranges (Fig. 28). The shallow regions (0-5 m) of the Freshwater location were dominated by SAV and showed moderate change over the study period, while SAV measured across deeper water showed a much higher range of variation (Fig. 28). Conversely, SAV at Jurien and Lancelin showed similar patterns of change across time for all depth ranges (Fig. 28). Jurien, with the best record of remote sensing data and was also the sandiest location, showed that SAV in the shallows remained relatively stable for the study period. There is evidence that the 2010-2011 marine heatwave impacted the extent of SAV across several of our study sites (Fig. 29), but the lack of operating sensors during this period obscures the immediate impact of the heatwave on habitats.

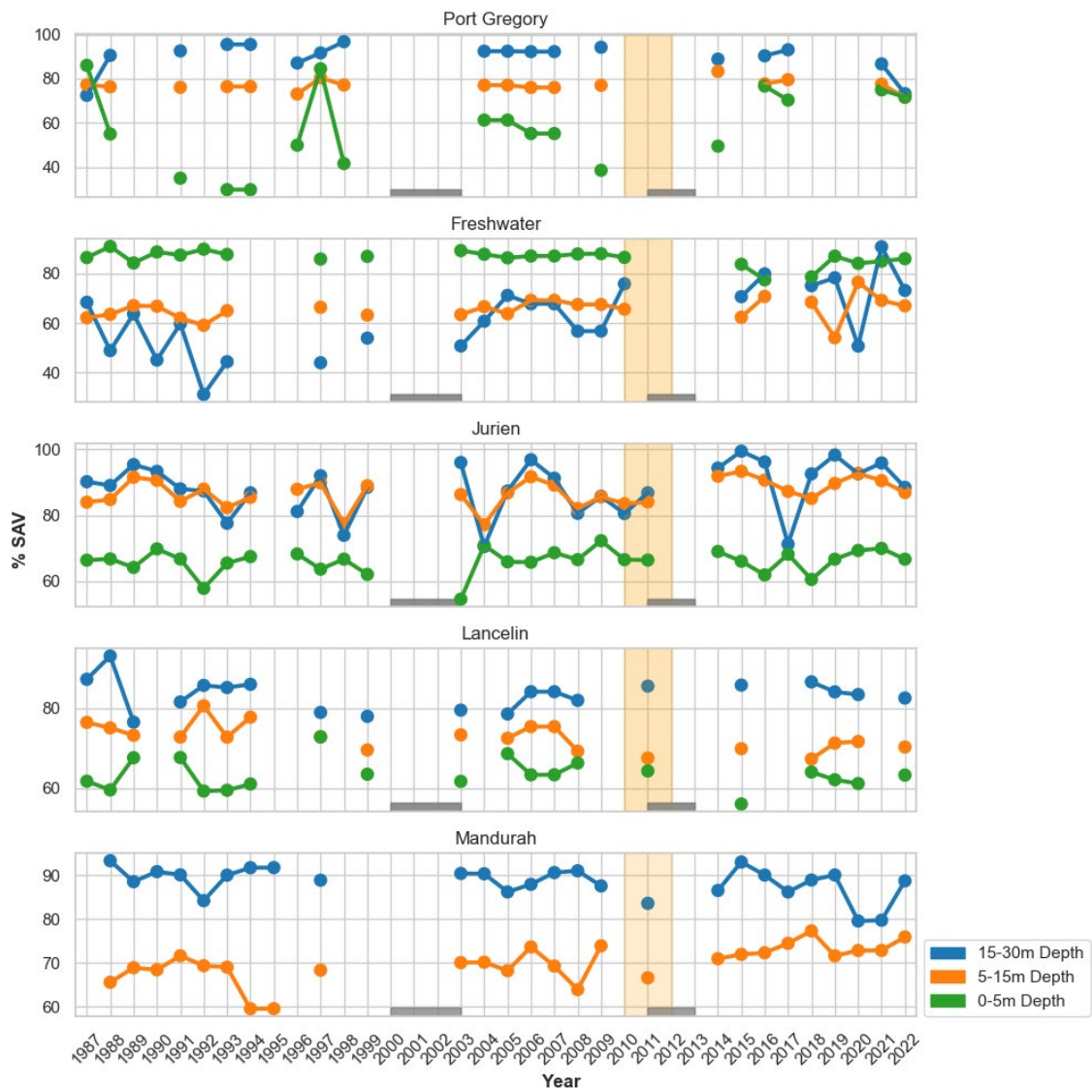


Figure 28 Percent Submerged Aquatic Vegetation (%SAV) for Port Gregory, Freshwater, Jurien, Lancelin, and Mandurah from 1987 to 2023. The %SAV has been depicted for the 15-30m extent (Blue), and for the depth intervals of 5-15 m (orange) and 0-5 m (Green). The pale orange region represents the 2010-2011 Marine Heatwave (MHW), and the grey bars represent years where remote sensing imagery was unavailable.

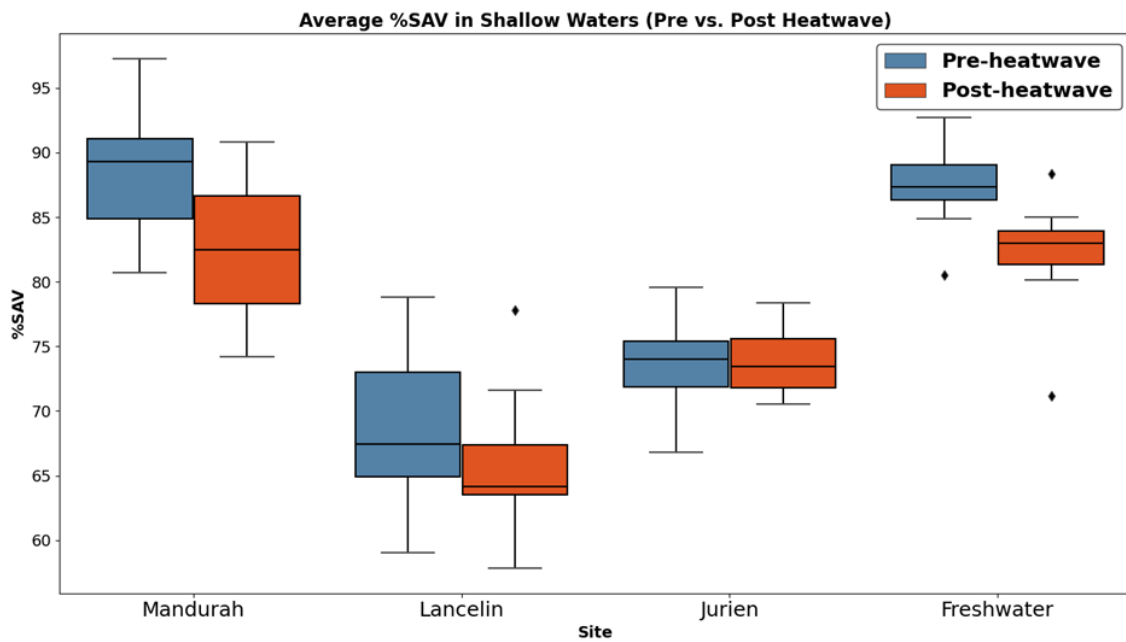


Figure 29 The %SAV five years before and after the 2010-2011 MHW event for Mandurah, Lancelin, Jurien and Freshwater in 0-5 m of water. Port Gregory was not included due to a lack of data, and Mandurah represents the 15-30m depth range as there were few regions at the site shallower than 5m.

Puerulus Index & multiple regression analysis

The results of the full subset selection indicated that the most important variables for formal analysis were the PI in the previous 3 and 4 years (t-3 and t-4) and the %SAV at t-2 and t-3, while SSTa and DHW were not important for modelling future undersize catch rates. The PI at t-3 and t-4 was consistently an important predictor of future under-size catch rate in the WCRLMF, and this is true when predictions are assessed with univariate models and multivariate models that include SAV and temperature (Table. 1). However, there is significant variability in the PI and undersize catch across locations (Fig. 25), and when assessed for all locations (i.e., the global model), the PI index has low predictive power ($R^2 = 0.09$) for future undersize catch but remains significant (Table. 1). When location and habitat are included as controlling factors into the global model, the results are significantly better ($R^2 = 0.42$), where habitat variation and location variation aid significantly in improving model predictions (Table 1). The residuals between the observed estimated and undersize catch rates have been visualised for the history of data where both the PI and undersize catch data were available (Fig. 30). Subsequent to the 2010-2011 MHW, the PI for the northern locations (i.e., Port Gregory, Freshwater and Jurien) showed a trend of overpredicting (i.e., negative residuals) undersize catch (Fig. 30). Conversely, the southern locations (Lancelin and Mandurah), show that the PI is underpredicting undersize catch (Fig. 30).

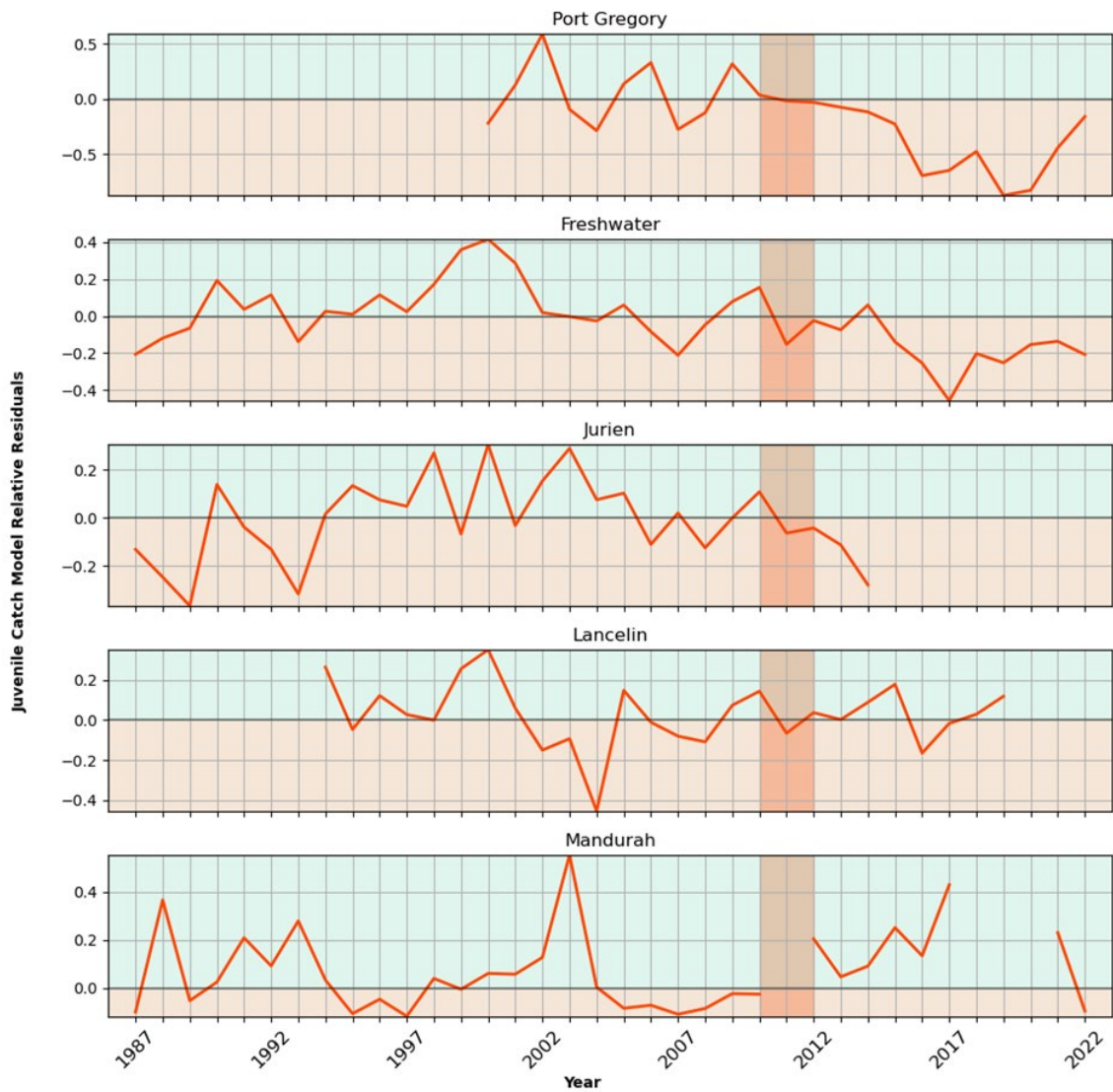


Figure 30 Relative residuals (i.e., the observed undersize catch subtracted from predicted undersize catch and divided by the maximum of the observed catch) between Puerulus-only model predictions and observed undersize WRL catch rates for Port Gregory, Freshwater, Jurien, Lancelin, and Mandurah from 1987 to 2023. The orange region represents the 2010-2011 Marine Heatwave (MHW).

When assessing the effects of vegetation and undersize catch at the location level, the relationship between %SAV (t-2) positively affected the undersize catch rate for Freshwater, Lancelin and Mandurah (Fig. 30), and this relationship was significant for Freshwater, Lancelin and Mandurah (Table 2). For Freshwater in particular, the location that exhibits good quality Landsat imagery and a chronological sequence of undersize catch, the model using the PI at t-3 and t-4 achieved an R^2 of 0.207, while the model that included %SAV at t-2 achieved an R^2 of 0.380 (Table 3). This pattern holds true for Mandurah, with the Freshwater and Mandurah locations having the highest proportion of seagrass habitat. Port Gregory, with its narrow shelf and turbid waters, only achieved 15 moderate or good benthic imagery points and there is not enough data to adequately describe the habitat composition at this location. Nevertheless, SAV variation among the locations with the highest proportion of preferential recruitment habitat (i.e., seagrass) shows strong significant relationships to future undersize WRL catch rates. The Elastic Net regressions showed that the PI (t-3), PI (t-4) and SAV (t-2) features had non-zero effects on the undersize catch, with the PI (t-4) having the greatest influence across all models

(Table 1; Table 3; Supplementary Table 2). The significant effects of SAV for the locations exhibiting good data and high preferential recruitment habitat suggest that we can confirm our hypothesis where the extent of recruitment habitat in previous years influences future catch rates of the WRL. SSTa and DHW have no discernible effects on future WRL catch rates but do seem to impact the extant of SAV, though other factors, such as sedimentation, may also be influencing remotely sensed SAV extents.

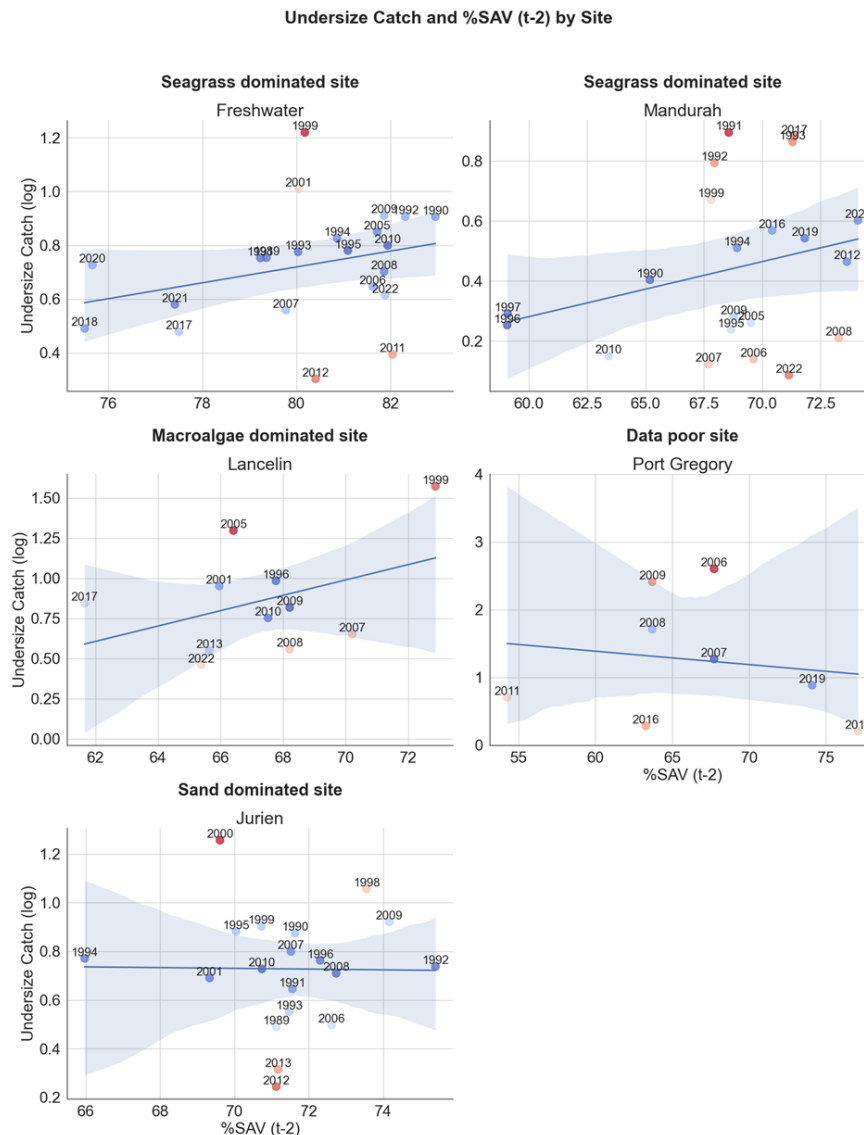


Figure 31 The response of undersize Western Rock Lobster (WRL) catch rates to the percent Submerged Aquatic Vegetation (SAV) with a two-year lag (t-2) at each of the locations. These relationships are representative of the SAV at the 0-15 m depth intervals. Residual points are coloured by the distance to the regression line, where blue is close to the line of best fit and red is far.

Table 8 Global undersize Catch Model Comparison. Numbers outside the brackets represent the effect sizes, while bracketed numbers represent the error estimates. Significant effects are represented by star symbols.

Dependent variable: Undersize Catch			Elastic net	
	PI	PI + SAV	PI	PI + SAV
Intercept	0.312** (0.146)	-0.658 (3.224)	0.101	0.000
PI (t-3)	0.005* (0.047)	0.007 (0.046)	0.048	0.003
PI (t-4)	0.134*** (0.047)	0.165 (0.051)	0.144	0.056
SAV (t-2)		0.186** (0.729)		0.031
Jurien		0.069 (0.148)		
Lancelin		0.214 (0.217)		
Mandurah		-0.011		
Port Gregory		(0.164) 0.765*** (0.204)		
Observations	151	83		
R ²	0.091	0.421		
Adjusted R ²	0.079	0.357		
Residual Std. Error	0.486 (df=148)	0.338 (df=75)		
F Statistic	7.390*** (df=2; 148)	7.61*** (df=7; 75)		
Note:			*p<0.1; **p<0.05; ***p<0.01	

Table 9 Undersize catch models at each location. Numbers outside the brackets represent the effect sizes, while bracketed numbers represent the error estimates. Significant effects are represented by star symbols.

Dependent variable: Undersize Catch					
	Mandurah	Lancelin	Jurien	Freshwater	PG
Intercept	-6.672* (3.626)	-6.243 (8.367)	4.283 (4.579)	-15.044** (6.845)	30.673 (20.443)
PI (t-3)	0.062 (0.050)	0.014 (0.095)	-0.000 (0.052)	0.049 (0.055)	-0.251 (0.502)
PI (t-4)	0.104* (0.054)	0.204** (0.066)	0.164*** (0.050)	0.105* (0.055)	2.202 (1.033)

SAV (t-2)	1.572*	1.484*	-0.982	3.443**	-8.360
	(0.849)	(2.023)	(1.065)	(1.545)	(5.453)
Observations	21	11	21	22	8
R ²	0.376	0.657	0.511	0.380	0.538
Adjusted R ²	0.266	0.510	0.424	0.277	0.191
Residual Std. Error	0.229 (df=17)	0.235 (df=7)	0.189 (df=17)	0.179 (df=18)	0.822 (df=4)
F Statistic	3.414** (df=3; 17)	4.464** (df=3; 7)	5.917*** (df=3; 17)	3.678** (df=3; 18)	1.552 (df=3; 4)
Note: *p<0.1; **p<0.05; ***p<0.01					

Table 10 : Global undersize Catch Model Comparison. Numbers outside the brackets represent the effect sizes, while bracketed numbers represent the error estimates. Significant effects are represented by star symbols.

	Dependent variable: Undersize Catch		Elastic net	
	PI	PI + SAV	PI	PI + SAV
Intercept	0.231 (0.197)	-15.044** (6.845)	0.000	0.000
PI (t-3)	0.001 (0.045)	0.049 (0.055)	0.054	0.061
PI (t-4))	0.120** (0.045)	0.105* (0.055)	0.119	0.085
SAV (t-2)		3.443** (1.545)		0.030
Observations	37	22		
R ²	0.207	0.380		
Adjusted R ²	0.160	0.277		
Residual Std. Error	0.190 (df=34)	0.179 (df=18)		
F Statistic	4.429** (df=2; 34)	3.678** (df=3; 18)		
Note: *p<0.1; **p<0.05; ***p<0.01				

Change analysis

The Change Vector Analysis (CVA) showed that the highest rates of change occurred at the edges or fragmented patches of vegetated regions and regions with typically sandy substrates during the study period (Fig. 32). For all locations, areas of contiguous SAV showed very little change over time for the study period (Fig. 32). Similarly, the Local Indicators of Spatial Autocorrelation (LISA) analysis showed that the highest magnitude of change for neighbourhoods surrounded with a high magnitude of change (HH) was located at the edges and

fragmented patches of SAV (Fig. 33). Regions with low amounts of change, surrounded by neighbourhoods with low change (LL) were those that exhibited contiguous SAV for the study period (Fig. 33).

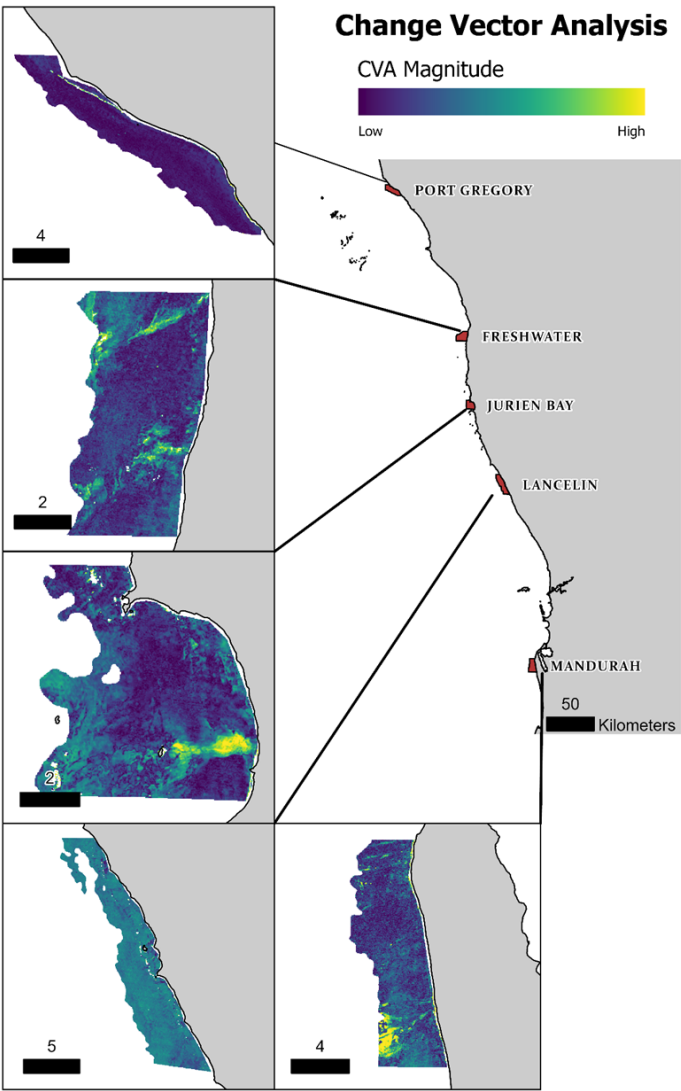


Figure 32 Change Vector Analysis (CVA) results for historical Landsat imagery (1987-2022) for the five regions that have experienced a high magnitude of change for the study period are represented in yellow, while blue represents regions that have remained stable for the study period.

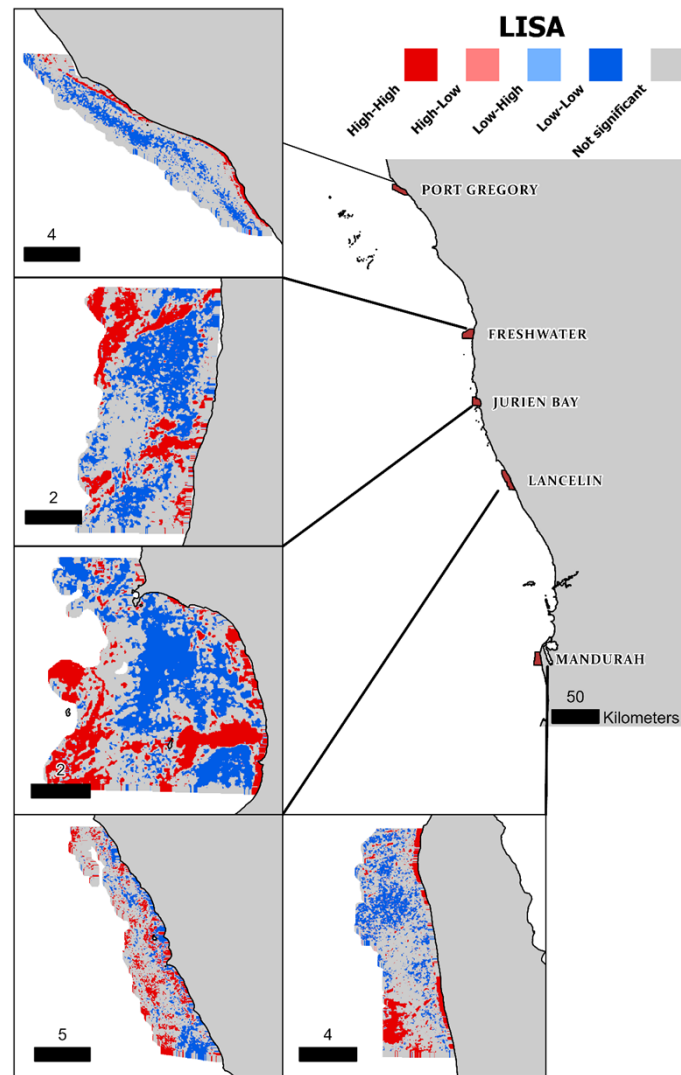


Figure 33 Local Indicators of Spatial Autocorrelation (LISA) results for historical Landsat imagery (1987-2022) for the five locations.

Discussion

At representative locations, we have found a disconnect between settlement and fishery recruitment driven by decadal changes in nearshore habitats. We suggest that remote sensing of change in the extent of marine habitats at appropriate locations can complement long-term fishery data collection. Most of the observed changes in SAV extent have occurred in the shallows and around patches of SAV, and areas of contiguous SAV have remained relatively stable over this 30-year period. For locations like Port Gregory, which are deep and lack a good record of satellite and benthic imagery, creating robust decadal habitat metrics over time was challenging. Nevertheless, for locations with continuous settlement and catch data and large extents of preferential recruitment habitat, the relationship between WRL undersize catch and SAV is strong and significant. These significant relationships suggest that incorporating habitat as a metric will enhance the management of the WCRLMF. The application of nearshore remote sensing for habitat assessments should be considered by other managed fisheries across the world, particularly for invertebrate species whose recruits likely depend on algal or seagrass habitats.

This work demonstrates that monitoring SAV extent using the Landsat inventory is possible and valuable for integrating habitat data into fishery assessment. However, it is important to state that monitoring extent and patch dynamics through Landsat, while representing the longest available time series, may not provide a realistic remote sensing measure of SAV condition or its true response to temperature anomalies. Changes in SAV conditions may occur at spatial scales and spectral resolutions that contemporary remote sensing platforms cannot detect. For example, the density or identity of SAV may change in response to temperature anomalies, but optical imagery is not sensitive enough to monitor the density or phenological traits of SAV (Phinn et al., 2018). There is evidence that the MHW impacted SAV extent (Fig. 29), but the lack of historical remotely sensed imagery obscures this relationship.

Tracking the coastal image quality through the Landsat inventory suggests that much of the intra-annual change in SAV extent occurs after periods of high turbidity observed in the satellite imagery. Much of the turbidity and sediment transport for the midwest coast occurs during the winter months (Supplementary Fig. S16), and locations generally show increasing extents of sand following sediment transport, which gradually returns to SAV during the summer months. This intra-annual change is the primary reason we restricted image classification to the summer months, as the true trends in SAV extent for the study period may have been confounded by sediment transport during the winter. For the same reason, we avoided using composite images in this study, as image composition, though common and useful for correcting cloudy images (White et al., 2014), may mask any true SAV change at our locations. Care needs to be taken when attempting to monitor SAV across time, as changes in SAV extent, true or related to wrack and sediment transport, strongly depend on when and where you look. This has broader implications for any application of environmental ocean accounts to the WCRLMF, where the economic value of seagrass and macroalgae habitats may be linked to fishery output (Cummins et al., 2023). Considering the life cycle of the WRL and the observed correlation between undersized catch and habitat in this study, estimating the true economic value of these habitats for the WCRLMF should integrate these contributions into the overall productivity of the fishery.

Despite the limitations in remotely sensed and undersize catch data, Freshwater, Mandurah and Lancelin showed a significant positive relationship between undersize catch and previous years of SAV. In contrast, Jurien, the most sand-dominated location, and Port Gregory, the location that lacked usable satellite and benthic imagery and catch data, showed no relationship between undersize catch and SAV. Freshwater, in the centre of the fishery, was an ideal location for this work as Landsat imagery was generally of good quality, and the undersize catch data was available for the study period. Freshwater was the location with the highest proportion of seagrass, followed by Mandurah, and the significant relationship between habitat and undersize catch rate in subsequent years for these two locations suggests that WRL population dynamics are closely tied to their recruitment habitats here. Thus, changes to this habitat, regardless of magnitude, could have cascading effects on the future recruitment of WRL into the WCRLMF. Indeed, including SAV extents into predictive models with the PI improves model predictions at locations such as Freshwater and Mandurah, and for the global model, implies that monitoring habitat change over time is useful for future fishery management.

Monitoring using remote sensing is frequently limited by spatial and spectral resolutions of available data, and spatial scale may well be a limiting factor in the work presented here (Hickey et al., 2020). Though our chosen locations cover a significant area (~410km²) of coastline, this only represents a subset of likely available WRL recruitment habitats along the West Australian coast. Whole-coast monitoring of SAV may be necessary to determine the effects of habitat on WRL populations and the fishery as a whole. Careful choice of monitoring locations at fine spatial scales may provide better inference as to the true effects of climate. Future work may be able to identify regions of thermal refugia (Dixon et al., 2022) or regions experiencing extreme

temperature fluctuations where loss or gain of SAV may be directly related to temperature anomalies.

While not incorporated into this study, oceanographic regime-driven settlement likely strongly influences the regional population dynamics of the WRL (Kolbusz et al. 2022). Future work should integrate dispersal, sources and source-sink dynamics, long-term oceanographic models, habitat, and ocean productivity into fisheries models to better determine the WRL's interactions with climate and habitat changes.

Conclusion

Our work demonstrates tracking SAV extent revealed significant effects of habitat on WRL recruitment for several locations on the mid-western coast of Australia. For locations with consistent temporal data and high seagrass composition, such as Freshwater and Mandurah, we found a significantly positive effect of future WRL recruitment to the extent of recruitment habitat (SAV). This represents an important finding for the management of WCRLMF and potentially other managed fisheries around the world, where the historical link of recruitment habitat to catch rates has yet to be quantified. Potentially, critical recruitment habitats can now be monitored at scale using remote sensing, and we have demonstrated this process with the Landsat inventory, an instrument that is less than ideal for monitoring coastal habitats. Current instruments, such as Sentinel-2, and future instruments will provide finer-resolution imagery of coastal habitats that managers and scientists can use to monitor change at better spatiotemporal scales. We suggest that monitoring changes in the extent of marine habitats at appropriate locations can complement long-term fishery data collection and management in Australia and globally.

Acknowledgements

The authors acknowledge the Traditional Custodians of the land, the Noongar and Yamatji peoples, and their connections to the land, sea and community. We pay our respects to their Elders past and present and extend that respect to all Aboriginal and Torres Strait Islander peoples. This research was supported by the Fisheries Research and Development Corporation (FRDC Project Number 2019-099) and the Department of Jobs, Tourism, Science and Innovation on behalf of the Australian Government. The research as part of the ICoAST collaborative project and acknowledges support from the Indian Ocean Marine Institute Research Centre collaborative research fund and partner organisations AIMS, CSIRO, DPIRD and UWA.

References

Alan Miller, Thomas Lumley Based on Fortran Code. 2020. "Leaps: Regression Subset Selection." <https://CRAN.R-project.org/package=leaps>.

Althaus, Franziska, Nicole Hill, Renata Ferrari, Luke Edwards, Rachel Przeslawski, Christine H. L. Schönberg, Rick Stuart-Smith, et al. 2015. "A Standardised Vocabulary for Identifying Benthic Biota and Substrata from Underwater Imagery: The CATAMI Classification Scheme." *PloS One* 10 (10): e0141039.

Anselin, Luc. 1995. "Local Indicators of Spatial association—LISA." *Geographical Analysis* 27 (2): 93–115.

Bellchambers, L. M., S. N. Evans, and J. J. Meeuwig. 2013. "Assessing the Effectiveness of Two Methods of Habitat Characterisation for Understanding Species Habitat Relationships, Using the Western Rock Lobster (*Panulirus Cygnus* George)." *Fisheries Research* 139 (March):5–10.

Behringer, D.C., Butler, M.J., IV, Herrnkind, W.F., Hunt, J.H., Acosta, C.A., Sharp, W.C., 2009. Is seagrass an important nursery habitat for the Caribbean spiny lobster, *panulirus argus*, in Florida? *N. Z. J. Mar. Freshwater Res.* 43, 327–337. <https://doi.org/10.1080/00288330909510003>

Briones-Fourzán, P., Lozano-Álvarez, E., 2013. Essential habitats for *Panulirus* spiny lobsters, in: *Lobsters: Biology, Management, Aquaculture and Fisheries*. John Wiley & Sons, Ltd, Oxford, UK, pp. 186–220. <https://doi.org/10.1002/9781118517444.ch7>

Bosch, Martí. 2019. "PyLandStats: An Open-Source Pythonic Library to Compute Landscape Metrics." *PloS One* 14 (12): e0225734.

Brooker, Michael A., Simon N. de Lestang, Jason R. How, and Tim J. Langlois. 2022. "Chemotaxis Is Important for Fine Scale Habitat Selection of Early Juvenile *Panulirus Cygnus*." *Journal of Experimental Marine Biology and Ecology* 553 (August):151753.

Caputi, N., Brown, R.S., Chubb, C., 1995. Regional prediction of the western rock lobster, *Panulirus Cygnus*, commercial catch in western Australia. *Crustaceana* 68, 245–256. <http://www.jstor.org/stable/20105043>

Caputi, N., Lestang, S., de, Frusher, S., Wahle, R.A., 2013. The impact of climate change on exploited lobster stocks, in: *Lobsters: Biology, Management, Aquaculture and Fisheries*. John Wiley & Sons, Ltd, Oxford, UK, pp. 84–112. <https://doi.org/10.1002/9781118517444.ch4>

Caputi, Nick, Simon de Lestang, Chris Reid, Alex Hesp, and Jason How. 2015. "Maximum Economic Yield of the Western Rock Lobster Fishery of Western Australia after Moving from Effort to Quota Control." *Marine Policy* 51 (January):452–64.

Chittleborough, R. G. 1970. "Studies on Recruitment in the Western Australian Rock Lobster *Panulirus Longipes* Cygnus George: Density and Natural Mortality of Juveniles." *Marine and Freshwater Research* 21 (2): 131–48.

Cummins, G.H., Navarro, M.L., Griffin, K., Partridge, J., Langlois, T.J., 2023. A global review of ocean ecosystem accounts and their data: Lessons learned and implications for marine policy. *Mar. Policy* 153, 105636. <https://doi.org/10.1016/j.marpol.2023.105636>

de Lestang, S., Caputi, N., Feng, M., Denham, A., Penn, J., Slawinski, D., Pearce, A., How, J., 2015. What caused seven consecutive years of low puerulus settlement in the western rock lobster fishery of Western Australia? *ICES J. Mar. Sci.* 72, i49–i58. <https://doi.org/10.1093/icesjms/fsu177>

de Lestang, S., Caputi, N., How, J., 2016. Resource Assessment Report Western Rock Lobster Resource of Western Australia. WA Marine Stewardship Council report series.

de Lestang, S., Caputi, N., Melville-Smith, R., 2009. Using fine-scale catch predictions to examine spatial variation in growth and catchability of *Panulirus cygnus* along the west coast of Australia. *N. Z. J. Mar. Freshwater Res.* 43, 443–455. <https://doi.org/10.1080/00288330909510013>

- Dixon, Adele M., Piers M. Forster, Scott F. Heron, Anne M. K. Stoner, and Maria Beger. 2022. "Future Loss of Local-Scale Thermal Refugia in Coral Reef Ecosystems." *PLOS Climate* 1 (2): e0000004.
- Gorelick, Noel, Matt Hancher, Mike Dixon, Simon Ilyushchenko, David Thau, and Rebecca Moore. 2017. "Google Earth Engine: Planetary-Scale Geospatial Analysis for Everyone." *Remote Sensing of Environment* 202 (December):18–27.
- Hickey, Sharyn M., Ben Radford, Chris M. Roelfsema, Karen E. Joyce, Shaun K. Wilson, Daniel Marrable, Kathryn Barker, et al. 2020. "Between a Reef and a Hard Place: Capacity to Map the Next Coral Reef Catastrophe." *Frontiers in Marine Science* 7. <https://doi.org/10.3389/fmars.2020.544290>.
- Holbrook, Neil J., Alex Sen Gupta, Eric C. J. Oliver, Alistair J. Hobday, Jessica A. Benthuisen, Hillary A. Scannell, Dan A. Smale, and Thomas Wernberg. 2020. "Keeping Pace with Marine Heatwaves." *Nature Reviews Earth & Environment* 1 (9): 482–93.
- Huang, Boyin, Chunying Liu, Viva Banzon, Eric Freeman, Garrett Graham, Bill Hankins, Tom Smith, and Huai-Min Zhang. 2021. "Improvements of the Daily Optimum Interpolation Sea Surface Temperature (DOISST) Version 2.1." *Journal of Climate* 34 (8): 2923–39.
- Hutchinson, E., Matthews, T.R., Renchen, G.F., 2024. Relationships between postlarval settlement and commercial landings of Caribbean spiny lobster (*Panulirus argus*) in Florida (USA). *Fish. Res.* 279, 107137. <https://doi.org/10.1016/j.fishres.2024.107137>
- Johnson, R. D., and E. S. Kasischke. 1998. "Change Vector Analysis: A Technique for the Multispectral Monitoring of Land Cover and Condition." *International Journal of Remote Sensing* 19 (3): 411–26.
- Kolbusz, Jessica, Tim Langlois, Charitha Pattiaratchi, and Simon de Lestang. 2022. "Using an Oceanographic Model to Investigate the Mystery of the Missing Puerulus." *Biogeosciences* 19 (2): 517–39.
- Kolbusz, Jessica, Simon de Lestang, Tim Langlois, and Charitha Pattiaratchi. 2021. "Changes in *Panulirus Cygnus* Settlement Along Western Australia Using a Long Time Series." *Frontiers in Marine Science* 8. <https://doi.org/10.3389/fmars.2021.628912>.
- Kolbusz, Jessica, Charitha Pattiaratchi, Sarath Wijeratne, Tim Langlois, and Simon de Lestang. 2022. "Finding Lobsters: Investigating a Period of Unusually Low Settlement of *Panulirus Cygnus* by Using Larval Dispersal Modelling." *Marine and Freshwater Research* 74 (1): 20–38.
- Kramer, O., 2016. Scikit-Learn, in: Kramer, O. (Ed.), *Machine Learning for Evolution Strategies*. Springer International Publishing, Cham, pp. 45–53. https://doi.org/10.1007/978-3-319-33383-0_5
- Kuhn, M., 2008. Caret package. *Journal of Statistical Software* 28, 1–26.
- Lenth, Russell V. 2024. "Emmeans: Estimated Marginal Means, Aka Least-Squares Means." <https://CRAN.R-project.org/package=emmeans>.
- Leutner, B., Horning, N., Leutner, M.B., 2017. Package 'RStoolbox.' R foundation for statistical computing, Version 0. 1.

Lan, K.-W., Shimada, T., Lee, M.-A., Su, N.-J., Chang, Y., 2017. Using remote-sensing environmental and fishery data to map potential yellowfin tuna habitats in the tropical pacific ocean. *Remote Sens. (Basel)* 9, 444. <https://doi.org/10.3390/rs9050444>

Langlois, Tim, Claude Spencer, Brooke A. Gibbons, Kingsley J. Griffin, Kye Adams, Charlotte Aston, Neville Barrett et al., 2025. "Benthic Observation Survey System (BOSS) for surveys of marine benthic habitats." *Methods in Ecology and Evolution*.

Mastrantonis, Stanley, Ben Radford, Tim Langlois, Claude Spencer, Simon de Lestang, and Sharyn Hickey. 2024. "A Novel Method for Robust Marine Habitat Mapping Using a Kernelised Aquatic Vegetation Index." *ISPRS Journal of Photogrammetry and Remote Sensing: Official Publication of the International Society for Photogrammetry and Remote Sensing* 209 (March):472–80.

Oh, Daphne, Tim J. Langlois, Michael A. Brooker, Hugo Salinas, Jason R. How, and Simon N. de Lestang. 2023. "Observations of the Association by Early-Juvenile Western Rock Lobster *Panulirus Cygnus* with Seagrass Assemblages (Decapoda: Achelata: Palinuridae)." *Journal of Crustacean Biology: A Quarterly of the Crustacean Society for the Publication of Research on Any Aspect of the Biology of Crustacea* 43 (3). <https://doi.org/10.1093/jcbiol/ruad045>.

Oliver, Eric C. J., Markus G. Donat, Michael T. Burrows, Pippa J. Moore, Dan A. Smale, Lisa V. Alexander, Jessica A. Benthuisen, et al. 2018. "Longer and More Frequent Marine Heatwaves over the Past Century." *Nature Communications* 9 (1): 1324.

Oppenheim, N.G., Wahle, R.A., Brady, D.C., Goode, A.G., Pershing, A.J., 2019. The cresting wave: larval settlement and ocean temperatures predict change in the American lobster harvest. *Ecol. Appl.* 29, e02006. <https://doi.org/10.1002/eap.2006>

Penn, J. W., N. Caputi, and S. de Lestang. 2015. "A Review of Lobster Fishery Management: The Western Australian Fishery for *Panulirus Cygnus*, a Case Study in the Development and Implementation of Input and Output-Based Management Systems." *ICES Journal of Marine Science: Journal Du Conseil* 72 (suppl_1): i22–34.

Phillips, B. F., and N. G. Hall. 1978. "Catches of Puerulus Larvae on Collectors as a Measure of Natural Settlement of the Western Rock Lobster *Panulirus Cygnus* George." Report - CSIRO Division of Fisheries and Oceanography (Australia). No. 98. <https://agris.fao.org/search/en/providers/123819/records/64735f3753aa8c89630a18ce>.

Phinn, Stuart, Chris Roelfsema, Eva Kovacs, Robert Canto, Mitch Lyons, Megan Saunders, and Paul Maxwell. 2018. "Mapping, Monitoring and Modelling Seagrass Using Remote Sensing Techniques." In *Seagrasses of Australia: Structure, Ecology and Conservation*, edited by Anthony W. D. Larkum, Gary A. Kendrick, and Peter J. Ralph, 445–87. Cham: Springer International Publishing.

Reddin, C.J., Aberhan, M., Raja, N.B., Kocsis, Á.T., 2022. Global warming generates predictable extinctions of warm- and cold-water marine benthic invertebrates via thermal habitat loss. *Glob. Chang. Biol.* 28, 5793–5807. <https://doi.org/10.1111/gcb.16333>

Rowan, Gillian S. L., and Margaret Kalacska. 2021. "A Review of Remote Sensing of Submerged Aquatic Vegetation for Non-Specialists." *Remote Sensing* 13 (4): 623.

Seabold, Skipper, and Josef Perktold. 2010. "Statsmodels: Econometric and Statistical Modeling with Python," 92 – .

Serrano, Oscar, Ariane Arias-Ortiz, Carlos M. Duarte, Gary A. Kendrick, and Paul S. Lavery. 2021. "Impact of Marine Heatwaves on Seagrass Ecosystems." In *Ecosystem Collapse and Climate Change*, edited by Josep G. Canadell and Robert B. Jackson, 345–64. Cham: Springer International Publishing.

Smale, D. A., T. Wernberg, and M. A. Vanderklift. 2017. "Regional-Scale Variability in the Response of Benthic Macroinvertebrate Assemblages to a Marine Heatwave." *Marine Ecology Progress Series* 568 (March):17–30.

Smith, Kathryn E., Michael T. Burrows, Alistair J. Hobday, Nathan G. King, Pippa J. Moore, Alex Sen Gupta, Mads S. Thomsen, Thomas Wernberg, and Dan A. Smale. 2023. "Biological Impacts of Marine Heatwaves." *Annual Review of Marine Science* 15 (January):119–45.

Stevens, Don L., and Anthony R. Olsen. 2004. "Spatially Balanced Sampling of Natural Resources." *Journal of the American Statistical Association* 99 (465): 262–78.

Straub, Sandra C., Thomas Wernberg, Mads S. Thomsen, Pippa J. Moore, Michael T. Burrows, Ben P. Harvey, and Dan A. Smale. 2019. "Resistance, Extinction, and Everything in Between – The Diverse Responses of Seaweeds to Marine Heatwaves." *Frontiers in Marine Science* 6. <https://doi.org/10.3389/fmars.2019.00763>.

Strydom, Simone, Kathy Murray, Shaun Wilson, Bart Huntley, Michael Rule, Michael Heithaus, Cindy Bessey, et al. 2020. "Too Hot to Handle: Unprecedented Seagrass Death Driven by Marine Heatwave in a World Heritage Area." *Global Change Biology* 26 (6): 3525–38.

Wernberg, Thomas, Scott Bennett, Russell C. Babcock, Thibaut de Bettignies, Katherine Cure, Martial Depczynski, Francois Dufois, et al. 2016. "Climate-Driven Regime Shift of a Temperate Marine Ecosystem." *Science* 353 (6295): 169–72.

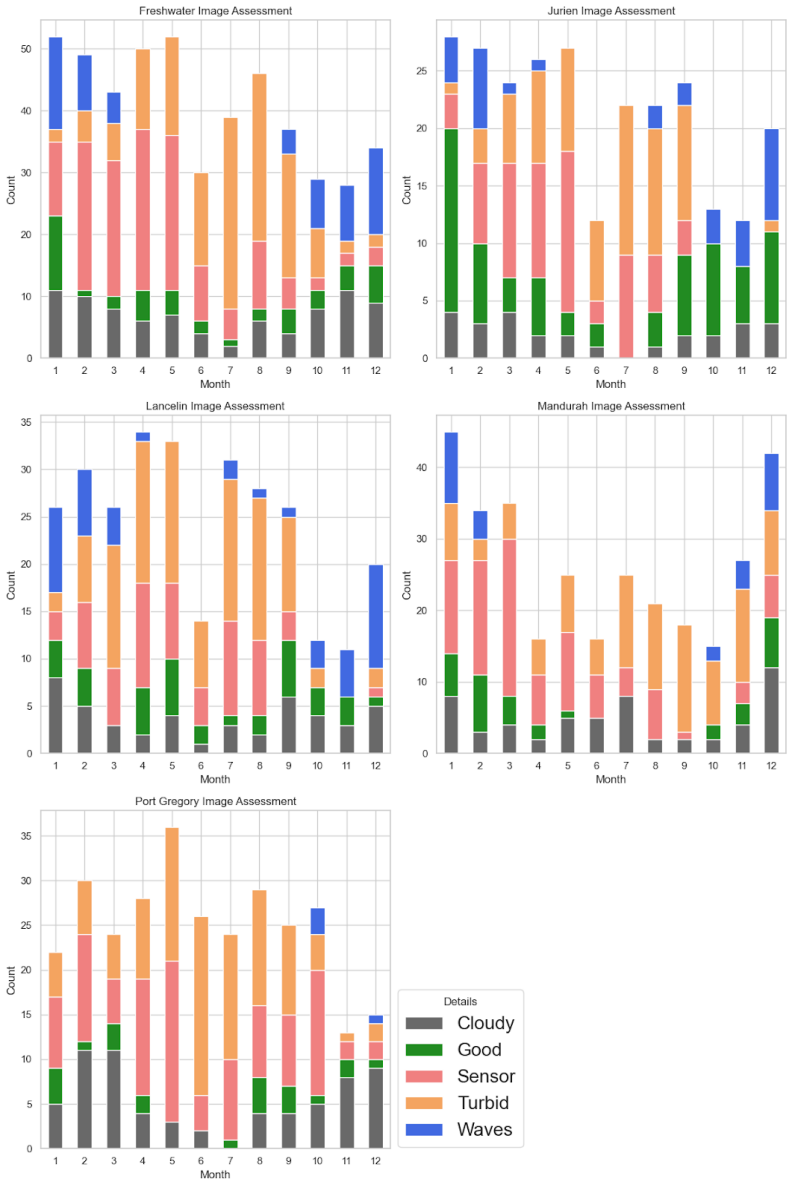
White, J. C., M. A. Wulder, G. W. Hobart, J. E. Luther, T. Hermosilla, P. Griffiths, N. C. Coops, et al. 2014. "Pixel-Based Image Compositing for Large-Area Dense Time Series Applications and Science." *Canadian Journal of Remote Sensing* 40 (3): 192–212.

White, L.M., Sainte-Marie, B., Lawton, P., Rochette, R., 2024. Using benthic recruitment densities to forecast fisheries recruitment of American lobster in Atlantic Canada. *Can. J. Fish. Aquat. Sci.* <https://doi.org/10.1139/cjfas-2023-0277>

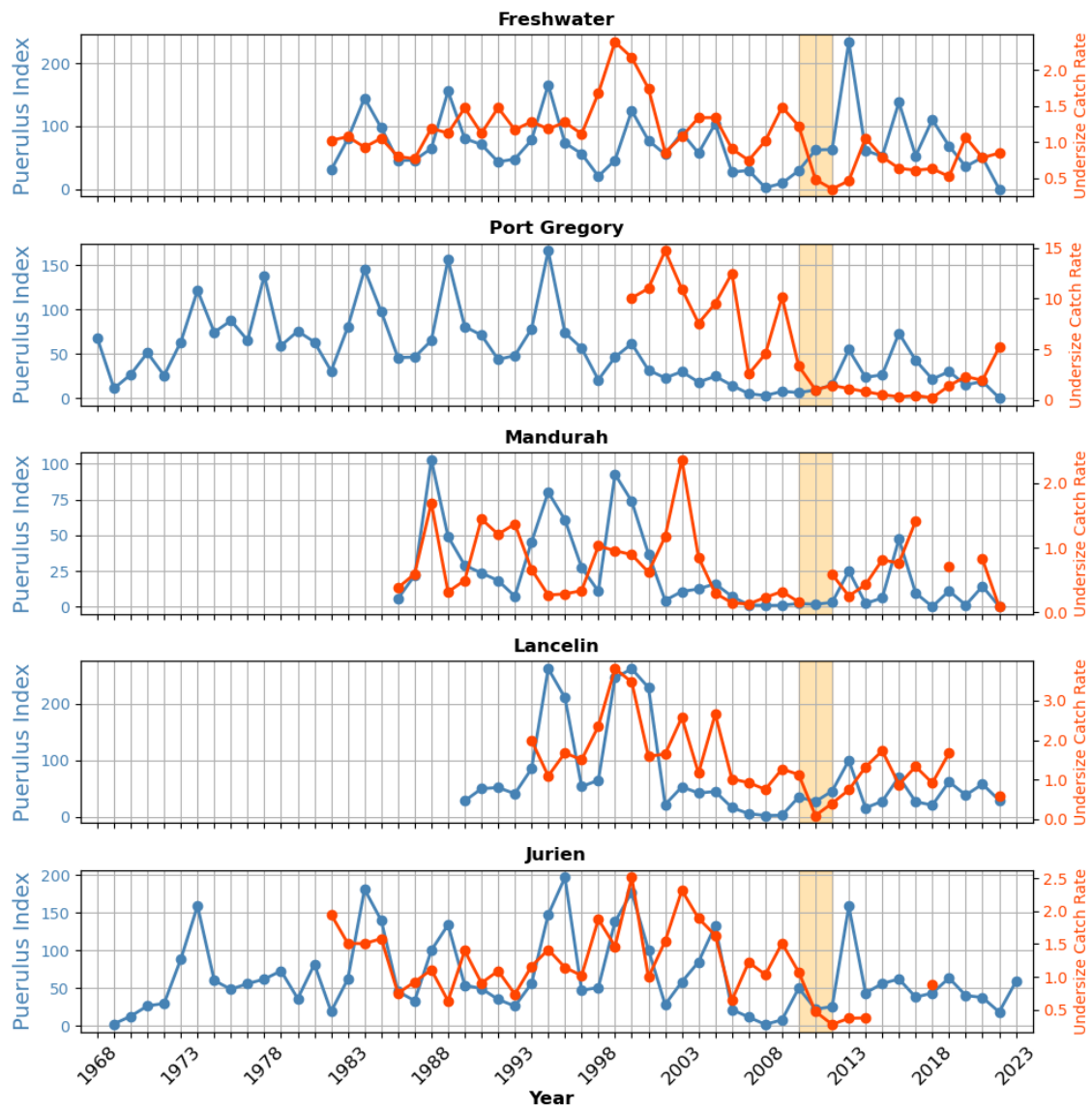
Whiteway, T. 2009. "Australian Bathymetry and Topography Grid, June 2009." <https://doi.org/10.4225/25/53D99B6581B9A>.

Zou, H., Hastie, T., 2005. Regularization and variable selection via the elastic net. *J. R. Stat. Soc. Series B Stat. Methodol.* 67, 301–320.<https://doi.org/10.1139/cjfas-2023-0277>

Supplementary material



Supporting figure 16: The image assessment results, aggregating by month, for the five study sites since 1987-2022.



Supporting figure 17: Undersize catch rates for Port Gregory, Freshwater, Jurien, Lancelin and Mandurah from 1987 until 2022.

Project Conclusions

The need for continuous monitoring of habitat

The ability to cost-effectively monitor coastal habitats that support commercial fisheries at relevant spatiotemporal scales (i.e., regionally across years) has become a possibility with remote sensing (Mellin et al., 2009). However, long term monitoring of habitat, and the quantitative effects of habitat change on fisheries has yet to be adequately explored. The methods and findings presented in this report bridge an important gap in coastal and fisheries monitoring and management.

1. We have developed a robust and efficient approach for ground truthing benthic habitats with the BOSS system (Study 1). This system and study addressed Objective 4 and were essential for developing the spatial index for WRL habitat monitoring (presented in Study 2).
2. We have developed a new spatial vegetation index for accurately monitoring WRL habitat across space and time (Study 2). This index addressed Objective 4 and was critical for mapping WRL habitat across time and understanding how habitat changes impact the WRL's population dynamics (presented in Study 5).
3. We have demonstrated the importance of spatially balanced sampling designs for monitoring coastal habitats (Study 3). To address Objectives 1, 2 and 4, habitat surveys should also be spatially balanced for the future monitoring of the WRL fishery.
4. We have further explored and established the habitat preference of early juvenile WRL for seagrass assemblages (Study 4). Understanding preferential recruitment habitat for the WRL in aquaria experiments provided critical understanding for Objective 3 including understanding the implications of the habitat change revealed by time-series data (Study 5).
5. We have tracked habitat change, at key sites with matching puerulus and undersize monitoring data across the WRLMF to investigate the potential impacts of environmental and climate change related impacts, demonstrating the use of satellite remote sensing of seabed habitats to inform fisheries management via estimates of change in habitat (study 5). The findings addressed Objective 1 and 2 of this study consolidated evidence that the extent of nearshore habitats are critical for understanding recruitment into the fishery.

Recommendations

Further development and future studies

Remote sensing (RS), with appropriate ground truthing, can provide a cost-effective approach to monitoring coastal habitats (Lisboa et al., 2024). Where these habitats are likely to have a key role in fisheries population sustainability (e.g. as recruitment habitats), then systematic remote sensing can provide valuable information to complement more traditional fisheries indices.

Here, we have shown the applications of historical RS imagery for tracking habitat change (Mastrantonis et al., 2024). Potentially critical recruitment habitats can now be monitored at scale using remote sensing, and we have demonstrated this process with the Landsat inventory, an instrument that is less than ideal for monitoring coastal habitats. Current instruments, such as

Sentinel-2, and future instruments will provide finer-resolution imagery of coastal habitats that managers and scientists can use to monitor change at better spatiotemporal scales (Poursanidis et al., 2019). Future fisheries research should consider integrating remotely sensed habitat monitoring into fisheries assessments and we suggest that remote sensing of change in extent of marine habitats at appropriate locations can be a useful complement to long-term fishery data collection.

References

Lisboa, Filipe, Vanda Brotas, and Filipe Duarte Santos. 2024. "Earth Observation—an Essential Tool towards Effective Aquatic Ecosystems' Management under a Climate in Change." *Remote Sensing* 16 (14): 2597.

Poursanidis, Dimitris, Dimosthenis Traganos, Peter Reinartz, and Nektarios Chrysoulakis. 2019. "On the Use of Sentinel-2 for Coastal Habitat Mapping and Satellite-Derived Bathymetry Estimation Using Downscaled Coastal Aerosol Band." *International Journal of Applied Earth Observation and Geoinformation: ITC Journal* 80 (August): 58–70.

Mastrantonis, Stanley, Ben Radford, Tim Langlois, Claude Spencer, Simon de Lestang, and Sharyn Hickey. 2024. "A Novel Method for Robust Marine Habitat Mapping Using a Kernelised Aquatic Vegetation Index." *ISPRS Journal of Photogrammetry and Remote Sensing: Official Publication of the International Society for Photogrammetry and Remote Sensing* 209 (March): 472–80.

Mellin, Camille, Serge Andréfouët, Michel Kulbicki, Mayeul Dalleau, and Laurent Vigliola. 2009. "Remote Sensing and Fish-Habitat Relationships in Coral Reef Ecosystems: Review and Pathways for Multi-Scale Hierarchical Research." *Marine Pollution Bulletin* 58 (1): 11–19.

Project Communication

Workshops, research updates and assessment

July 2022 - Australian Marine Science Association Meeting (AMSA). *A new Marine Submerged Vegetation index for robust and scalable mapping of Shallow Coastal Environments*

October 2023 - The International Conference & Workshop on Lobster (and Crab) Biology and Management (ICWL). *Comparing the predictive accuracy between preferential and spatially balanced sampling designs for modelling aquatic vegetation with remote sensing and machine learning.*

Project media coverage

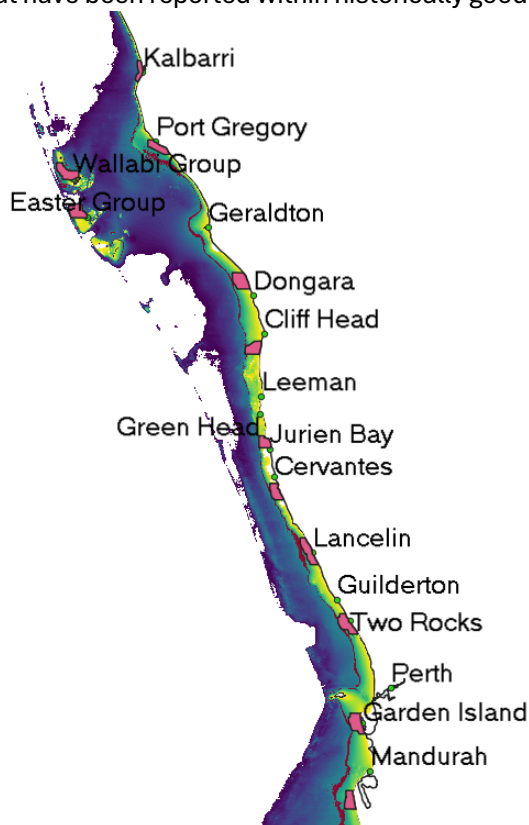
June 2023 - <https://westernrocklobster.org/watching-coastal-habitats-for-the-impact-of-the-ningaloo-nino/>

Watching coastal habitats for the impact of the Ningaloo Niño

Marine heatwaves along the coast of Western Australia, referred to as Ningaloo Niño, have had dramatic impacts on seaweed and seagrass beds over the past decade with potential knock on effect to populations of undersize lobster.

The Western Rock Lobster Council (WRL) in conjunction with the Department of Primary Industries and Regional Development (DPIRD) have developed a new standardised survey to provide an index of undersize lobsters at 12 locations throughout the fishery.

This Independent Shallow Water Survey (ISS) was designed to investigate nearshore areas of low catch that have been reported within historically good shallow fishing grounds.



Independent Shallow Water Survey locations

It is thought the marine heat wave of 2011, driven by a Ningaloo Niño event and unusually strong Leeuwin Current, was responsible for the loss of habitats at key locations, including Kalbarri and Dongara.

To complement the ISS survey the Western Rock Lobster Industry's Partnership Agreement with the Fisheries Research and Development Corporation (FRDC), has funded a study to investigate the use of

satellite imagery to assess and track changes in coastal marine habitats and establish a monitoring program across the West Coast Rock Lobster Managed Fishery.

Dr Stanley Mastrantonis and Dr Sharyn Hickey from the University of Western Australia in collaboration with the Indian Ocean Marine Research Centre's ICoAST program are working to analyse this imagery.

"The most important thing for us to do is ground truth the satellite imagery, and that is where working with experienced fishers has proved invaluable," said Dr Mastrantonis.

John Fitzhardinge, boat builder and fisherman for over 40 years, designed a new panoramic underwater camera system for the project.



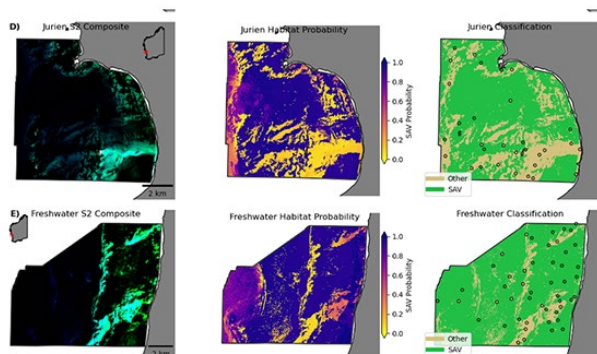
Sebastian Gundling and John Fitzhardinge of Dongara Marine Boat Builders building the underwater camera to be used by fishers.

Now John and the team are working in collaboration with fishers and DPIRD to collect imagery throughout the fishery using this camera system.



PhD student Sam Thompson and Paul Warnock of Dongara Marine Boat Builders testing the underwater camera to be used by fishers.

Stanley has now developed a new spectral analysis to convert composite satellite imagery into an index of Submerged Aquatic Vegetation (SAV), that is performing well to map and track change in habitats across the ISS locations.



Converting composite satellite imagery into an index of Submerged Aquatic Vegetation (SAV) to track changes in coastal habitats.

The next steps in the project are to integrate historical satellite images to map how habitats have changed over time and devise a cost-effective way that the monitoring of recruitment habitat extent can be integrated into monitoring programs across the West Coast Rock Lobster Managed Fishery.

March 2024 - <https://www.uwa.edu.au/news/article/2024/march/new-mapping-method-developed-for-critical-marine-habitat>

New mapping method developed for critical marine habitat

Researchers at The University of Western Australia have led the development of a new technique for accurately mapping shallow and coastal marine habitats.

Dr Sharyn Hickey and Dr Stan Mastrantonis, from UWA's School of Agriculture and Environment, School of Biological Sciences and Oceans Institute, were co-authors of the research published in the [*ISPRS Journal of Photogrammetry and Remote Sensing*](#).

"In an era where critically important coastal ecosystems are threatened by climate change, there is a fundamental need for efficient, reliable mapping and monitoring of marine vegetation," Dr Mastrantonis said.

"Traditional remote sensing methods have struggled to track changes in key underwater flora, such as kelp and seagrass.

"These habitats are foundational to marine ecosystems and vital for the survival and health of commercial fishery species, such as the Western Rock Lobster."

The study, which included researchers from UWA, the Australian Institute of Marine Science and the Department of Primary Industries and Regional Development, spanned a 400km stretch of the Mid West coastline of Western Australia.

Co-author Dr Ben Radford from AIMS said the project explored the limits of satellite remote sensing in the marine and coastal environment.

"By integrating onsite data with information gathered through underwater imagery, and satellite remote sensing, we formulated a novel remote sensing vegetation index," Dr Radford said.

Dr Mastrantonis said the index could be applied across diverse sites, depths, and habitat types.

"It reliably maximises the spectral differences between aquatic vegetation and other types of habitats, making it easier to discriminate compared to other methods," he said.

The mapping method was found to be especially effective in regions dominated by coastal macroalgae, essential for marine life and supporting recreational and commercial fishing activities.

"With seagrass and kelp beds facing alarming rates of decline due to climate-induced change, the urgency for innovative approaches like this has never been greater," Dr Mastrantonis said.

"The method offers a scalable solution for large-scale marine vegetation monitoring and could serve as a universal metric for mapping marine habitats."

The study is part of the Integrated Coastal Analyses and Sensing Technology (ICoAST) project, co-led by Dr Hickey, Dr Radford, Dr Tim Langlois and Dr Simon de Lestang. It is funded by the Indian Ocean Marine Research Centre's partners (UWA, CSIRO, AIMS and DPIRD) and the Western Rock Lobster Industry's Partnership Agreement with the Fisheries Research and Development Corporation.

Satellite tracking reveals key to predicting WA's rock lobster populations

Western Australian scientists have developed a new method to monitor and predict Western Australia's rock lobster populations using satellite technology, in a study that could transform fisheries management worldwide.

Published in *Science of the Total Environment*, the research demonstrated how tracking changes in seagrass and macroalgae habitats can help predict future lobster populations.

The study is part of the Integrated Coastal Analyses and Sensing Technology (ICoAST) project funded by the Indian Ocean Marine Research Centre's partners — The University of Western Australia, CSIRO, Australian Institute of Marine Science and the Department of Primary Industries and Regional Development — and the Western Rock Lobster Industry's Partnership Agreement with the Fisheries Research and Development Corporation and WA Department of Jobs, Tourism, Science and Innovation.

Lead author Dr Stanley Mastrantonis, from UWA's School of Agriculture and Environment, said the Western Rock Lobster fishery, valued at hundreds of millions of dollars annually, had historically relied on monitoring newly settled juvenile lobsters at artificial seagrass stations to predict future populations and set fishing quotas.

"This predictive model became more uncertain after the 2010-2011 marine heatwave, which significantly impacted natural seagrass habitats at some sites along the WA coast," Dr Mastrantonis said.

"While water temperature and environmental conditions are important for lobster growth, their nursery habitat of seagrasses is also critical.

"With climate change increasing the likelihood of extreme weather events, understanding these habitat changes had become crucial for the industry's future."

The study analysed satellite images spanning 600km of coastline from Port Gregory to Mandurah over 35 years, focusing on underwater vegetation crucial for lobster locations, and found satellite data could effectively track vegetation extent, which correlated strongly with lobster gathering in certain regions.

"For locations with high seagrass composition, we discovered that vegetation extent over the previous two years significantly explained variations in juvenile lobster numbers," Dr Mastrantonis said



The study marks the first time long-term satellite monitoring has been used to complement fisheries data collection at this scale, offering a new tool for similar fisheries worldwide to improve their predictive capabilities and sustainability practices.

“Our research provided evidence that tracking habitat is important for fishery assessment models and our hope is that fisheries managers will consider implementing satellite monitoring strategies into their programs as a result,” Dr Mastrantonis said.

“As satellite technology improves the ability to monitor coastal habitats will become even more precise, offering better spatio-temporal monitoring capabilities for fisheries managers globally.”

The study was co-led by UWA researchers Dr Sharyn Hickey, Dr Ben Radford, Dr Tim Langlois and Dr Simon de Lestang.